

ANALYSIS OF CHANGES IN  
MITOCHONDRIAL PROTEINS IN  
SINGLE MUSCLE FIBRES WITH  
DIFFERENT TYPES OF TRAINING

Dr. Elizabeth Reisman

Principal Supervisor:

Prof David J. Bishop

Associate Supervisors: Dr. Cesare Granata & Dr. Nikeisha Caruana

Institute for Health and Sport (IHes)

Victoria University

Melbourne, Australia

Master of Research

Submitted in fulfilment of the requirements of the degree of Master of Research

December 2020

## **Student Declaration**

“I, Elizabeth Reisman, declare that the Master of Research thesis entitled Analysis of Changes in Mitochondrial Proteins with Different Types of Training is no more than 50,000 words in length including quotes and exclusive of tables, figures, appendices, bibliography, references and footnotes. This thesis contains no material that has been submitted previously, in whole or in part, for the award of any other academic degree or diploma. Except where otherwise indicated, this thesis is my own work”.

“I have conducted my research in alignment with the Australian Code for the Responsible Conduct of Research and Victoria University’s Higher Degree by Research Policy and Procedures.”

Signature:



Date: 17<sup>th</sup> December 2020

## Acknowledgements

With its challenges it's been an amazing journey to follow my passion for exercise and research and combine with my knowledge of chemistry to change the path of my future directions.

First, I would like to thank David for offering me the chance, and for constantly providing directions, and feedback through this journey. I really appreciate all the positive constructive feedback while remaining reserved and helping keep my stress levels down. Thanks for all you've done during this time.

And many thanks to Javi Botella for having such a brilliant training study and for allowing me to add to the depth of the research. Also thanks for teaching and providing support with great patience to answer any questions along the way. Additional massive thanks to the rest of the Bishop group, in particular JJ for showing me the ropes around the lab and introducing me to molecular biology techniques which was new to this chemist. Also thanks to Javi-Diaz for handing over the baton as the dot blotting king to me.

Cesare, thanks for getting this project started with such enthusiasm and putting us in contact with Monash Proteomics and Enzo who was a rock and so patient with such a trying sample. Thus a massive thanks goes to Enzo and Iresha, I couldn't have done this project without your help and guidance. Thanks for persisting with this project, teaching me hands on proteomic methods and giving me a great understanding with how it all works. Also big thanks to Nikeisha for jumping on board as a co-supervisor and assisting with the mammoth task of filtering through a tonne of proteomic data when I had limited experience with bioinformatics. Much thanks for your patience and being an amazing sounding board, you've been an absolute legend!

Lastly thanks to my family and closest friends who supported me with my decision to follow my passions and go back to study and research after many years in the workforce. In particular Dad, Sim, Aunty and Jess. Thanks as always for putting up with my trials and tribulations during this time. I'm basically a professional student with the amount of study I've done over the years. Here's to an amazing experience and hopefully a path that combines passions with academia.

## ***First Author Conference Abstracts***

**Reisman, E.,** Botella J., Huang C., Schittenhelm, R. B., Stroud, D. A., Caruana, N., Granata, C. & Bishop, D. J. Quantitative Proteomics to Identify Mitochondrial Proteins in Skeletal Muscle Single Fibres of Healthy Humans. *3rd Annual Victorian Muscle Network Virtual Symposium, October 15<sup>th</sup>, 2020*

**Reisman, E.,** Botella J., Huang C., Schittenhelm, R. B., Stroud, D. A., Caruana, N., Granata, C. & Bishop, D. J. Quantitative Proteomics to Identify Mitochondrial Proteins in Skeletal Muscle Single Fibres of Healthy Humans. *2020 Australian Physiological Society (AuPS) Student and ECR Forum, November 26<sup>th</sup>, 2020*

**Reisman, E.,** Botella J., Huang C., Schittenhelm, R. B., Stroud, D. A., Caruana, N., Granata, C. & Bishop, D. J. Quantitative Proteomics to Identify Mitochondrial Proteins in Skeletal Muscle Single Fibres of Healthy Humans. *Institute for Health and Sport (iHeS) HDR Student Conference, December 10<sup>th</sup>, 2020*

## ***Co-authored Publications***

Diaz-Lara, F. J., Botella, J. & **Reisman, E.,** Are enhanced muscle adaptations associated with carbohydrate restriction regulated by absolute muscle glycogen concentration? *Journal of Physiology*, 1-3, 2019. DOI. 10.1113/JP279076

## *Table of Contents*

<b>Abstract.....</b>	<b>1</b>
<b>Chapter 1 .....</b>	<b>2</b>
<b>1 Role of Mitochondria in Health and Performance .....</b>	<b>3</b>
<b>1.1 Skeletal Muscle and Mitochondria .....</b>	<b>4</b>
<b>1.1.1 Skeletal Muscle .....</b>	<b>4</b>
<b>1.1.2 Mitochondria Distribution in Skeletal Muscle.....</b>	<b>8</b>
<b>1.1.3. Mitochondria Structure .....</b>	<b>8</b>
<b>1.1.4 Fibre-Type Specific Characteristics of Mitochondria in Skeletal Muscle..</b>	<b>9</b>
<b>1.2 Skeletal Muscle Mitochondria and Training .....</b>	<b>15</b>
<b>1.2.1 Mitochondrial Biogenesis .....</b>	<b>15</b>
<b>1.2.2. Influence of Training Characteristics .....</b>	<b>16</b>
<b>1.2.3. Mitochondrial Protein &amp; Exercise Training .....</b>	<b>19</b>
<b>1.3 Mitochondrial Proteins and Training.....</b>	<b>21</b>
<b>1.3.1 Immunoblotting.....</b>	<b>21</b>
<b>1.3.2. Proteomic Approaches .....</b>	<b>32</b>
<b>1.4 Fibre-Specific Protein Responses with Training .....</b>	<b>49</b>
<b>1.4.1. Single-Fibre Immunoblotting .....</b>	<b>51</b>
<b>1.4.2. Single-Fibre Proteomics .....</b>	<b>56</b>
<b>1.5 Conclusions.....</b>	<b>64</b>
<b>Aims .....</b>	<b>65</b>
<b>Contribution to Knowledge .....</b>	<b>65</b>
<b>Statement of Significance.....</b>	<b>65</b>
<b>Chapter 2 .....</b>	<b>66</b>
<b>Conceptual Framework and Methodology.....</b>	<b>66</b>
<b>2.1. Research design overview .....</b>	<b>67</b>

<b>2.2.</b>	<b>Participants.....</b>	<b>68</b>
<b>2.2.1.</b>	<b>Physical Activity and Nutritional Control.....</b>	<b>69</b>
<b>2.3.</b>	<b>Testing.....</b>	<b>70</b>
<b>2.4.</b>	<b>Training .....</b>	<b>70</b>
<b>2.5.</b>	<b>Muscle analysis .....</b>	<b>71</b>
<b>2.5.1</b>	<b>Single Muscle Fibre Isolation .....</b>	<b>71</b>
<b>2.6</b>	<b>Single Muscle Fibre Analysis – Immunoblotting.....</b>	<b>71</b>
<b>2.6.1</b>	<b>Muscle Fibre Typing (Dot Blotting).....</b>	<b>71</b>
<b>2.7</b>	<b>Proteomic-Based Analysis.....</b>	<b>73</b>
<b>2.7.1</b>	<b>SP3 Protein Sample Processing .....</b>	<b>74</b>
<b>2.7.2</b>	<b>S-Trap .....</b>	<b>75</b>
<b>2.7.3</b>	<b>TMTpro Labelling .....</b>	<b>76</b>
<b>2.7.3.1</b>	<b>TMT Labelling Strategy .....</b>	<b>77</b>
<b>2.7.4</b>	<b>Liquid Chromatography and MS .....</b>	<b>79</b>
<b>2.8</b>	<b>Normalisation.....</b>	<b>79</b>
<b>2.9</b>	<b>Statistical analysis.....</b>	<b>80</b>
	<b>Chapter 3 .....</b>	<b>81</b>
<b>3.0</b>	<b>Sample Protein Processing Optimisation .....</b>	<b>82</b>
<b>3.1</b>	<b>Comparison of Methods for Protein Processing of Samples with High Detergent Concentration.....</b>	<b>84</b>
<b>3.1.1</b>	<b>Single-pot, Solid-phase-Enhanced Sample-Preparation (SP3).....</b>	<b>84</b>
<b>3.1.2</b>	<b>Suspension-Trapping (S-Trap).....</b>	<b>86</b>
<b>3.1.3</b>	<b>Sample Preparation assessment.....</b>	<b>87</b>
<b>3.1.3.1</b>	<b>Sample Extraction .....</b>	<b>88</b>
<b>3.2</b>	<b>Validation of Fibre Typing .....</b>	<b>90</b>

<b>3.3</b>	<b>Fibre Pooling</b> .....	<b>93</b>
<b>3.4</b>	<b>Reproducibility</b> .....	<b>94</b>
<b>3.5</b>	<b>Isotopic Labelling</b> .....	<b>97</b>
<b>3.6</b>	<b>Mitochondrial Proteins</b> .....	<b>103</b>
<b>3.7</b>	<b>Conclusions</b> .....	<b>107</b>
	<b>Chapter 4</b> .....	<b>109</b>
<b>4.0</b>	<b>Measuring Fibre Specific Changes in Response to Training by Proteomics</b> .....	<b>110</b>
<b>4.1</b>	<b>Batch Correction</b> .....	<b>110</b>
<b>4.2</b>	<b>Protein Detection</b> .....	<b>112</b>
<b>4.2.1</b>	<b>Detection of Mitochondrial Proteins</b> .....	<b>116</b>
<b>4.3</b>	<b>Fibre Type Differences</b> .....	<b>118</b>
<b>4.4</b>	<b>Training Responses</b> .....	<b>121</b>
<b>4.4.1</b>	<b>Training Responses for Total Single Fibre Proteome</b> .....	<b>121</b>
<b>4.4.2</b>	<b>Training and Fibre-Specific Responses of Mitochondrial Proteins</b> .....	<b>125</b>
<b>4.5</b>	<b>Functional Pathway Responses</b> .....	<b>132</b>
<b>4.5.1</b>	<b>Oxidative Phosphorylation (OXPHOS)</b> .....	<b>133</b>
<b>4.5.2</b>	<b>Individual OXPHOS Protein Trends</b> .....	<b>139</b>
<b>4.5.3</b>	<b>Mitochondrial Ribosomes</b> .....	<b>142</b>
<b>4.5.4</b>	<b>Other Common Functional Pathways</b> .....	<b>143</b>
<b>4.5.4.1</b>	<b>Fatty Acid Oxidation</b> .....	<b>145</b>
<b>4.5.4.3</b>	<b>Tricarboxylic Acid (TCA) Cycle</b> .....	<b>146</b>

<b>4.5.4.4 Glycolysis .....</b>	<b>147</b>
<b>4.6 Conclusions.....</b>	<b>149</b>
<b>Chapter 5 .....</b>	<b>150</b>
<b>5.1 Summary of Key Findings .....</b>	<b>151</b>
<b>5.2 Conclusions &amp; Future Directions .....</b>	<b>153</b>
<b>5.3 Significance and Practical Applications .....</b>	<b>154</b>
<b>References.....</b>	<b>155</b>
<b>Appendices.....</b>	<b>194</b>

# *List of Figures*

## *Chapter 1*

**Figure 1. 1–** a.) Summary of diseases or medical conditions that have been linked to sub-optimal mitochondrial characteristics. b.) Relationship of changes in mitochondrial content (measured by CS activity) to alterations in endurance performance (reported as arbitrary units). Increases in markers of mitochondrial content due to chronic muscle use (e.g. endurance training) lead to improvements in endurance performance. Decrements in markers of mitochondrial content brought about by chronic disuse. Adapted from Irrcher et al. (146)..... 4

**Figure 1. 2–** Mitochondrion Structure (a) Structure of a skeletal muscle fibre. (b) Image of bundle of single muscle fibres, and how they may be represented by different fibre types in a staining image. Transmission electron microscopy high resolution image of a human single muscle fibre showing sub-populations of IMF and SS within a single fibre. (c) Two sub-populations of mitochondria can be found: subsarcolemmal mitochondria (SS) and intermyofibrillar mitochondria (IMF). (d) Transversal illustration of a skeletal muscle fibre. Mitochondria create a reticulum that connects SS and IMF mitochondria (e) Transmission electron microscopy transversal image from a human skeletal muscle biopsy showing the nucleus (N), and the SS and IMF mitochondria. (f) Image of a mitochondrion. High-resolution imaging allows visualization of the densely-packed cristae within a mitochondrion. (g) Image of how a mitochondrion is usually illustrated in textbooks or research articles. Notice how the mitochondrial DNA (mtDNA) and the mitochondrial ribosomes are found in the matrix. The electron transport chain respiratory complexes are located on the IMM, and for the most part in the cristae. (h) Variation in mitochondria size between fibre types (204)..... 14

**Figure 1. 3-** Schematic representation of the definitions used in this review to categorise (a) moderate-intensity continuous exercise or training (MICT) ( $< 75\% \dot{W}_{max}$ ), and high-intensity exercise or training, which includes both (b) high-intensity (HIIT) and (c) sprint-intervals (SIT) ( $> 75\% \dot{W}_{max}$ ) training. Adapted from MacInnis & Gibala (193) (d)

Schematic of blood lactate response to exercise intensity adapted from Jamnick et al (152)  
 (e) Schematic of Phosphocreatine response (157) to exercise intensity (f) Schematic of  
 ADP/ATP ratio and (g) Reactive Oxygen Species (ROS) (307) in response to training  
 ..... 18

**Figure 1. 4** – Representation of pioneering studies demonstrating increase of  
 mitochondrial protein in response to exercise training in both animals (126) and humans  
 (209)..... 19

**Figure 1. 5** – Bergstrom muscle biopsy technique, modified with suction, being  
 performed on the vastus lateralis of a human volunteer ..... 20

**Figure 1. 6**– Overview of the western blotting Procedure 1. Samples are loaded on a  
 Sodium Dodecyl Sulfate–Polyacrylamide Gel Electrophoresis (SDS-PAGE) gel 2.  
 Samples separated on the gel. 3. Transfer of separated proteins onto polyvinylidene  
 difluoride (PDVF) or nitrocellulose membrane. 4. Membranes are blocked with a neutral  
 protein. 5. Incubation with primary antibody specific to target protein. 6. Incubation with  
 secondary antibody. 7. Incubation with chemiluminescent substrate and expose to film.  
 8. Generation of a standard calibration curve..... 22

**Figure 1. 7-** Differentially expressed mitochondrial proteins following exercise training  
 identified in humans and animals by immunoblotting. Created with BioRender.com... 26

**Figure 1. 8-** Overview of LC-MS-based proteomics : Proteomics workflows begin with  
 proteins being extracted from biological samples (i.e. skeletal muscle tissue). In the  
 sample-preparation stage proteins are extracted and digested by a sequence-specific  
 enzyme such as trypsin. Current methods of protein preparation are highly efficient and  
 can be performed in 96-well plates. Peptides are then separated by means of  
 chromatography and ionised, after which they are introduced into the vacuum of a mass  
 spectrometer. Each MS scan results in a mass spectrum, measuring mass to charge ratio  
 (m/z) values and peak intensities. Based on observed spectral information a full spectrum  
 of the peptides is acquired at the MS1 level followed by the collection of as many  
 fragmentation spectra at the MS2 level. Database searching is typically employed to  
 identify the peptides most likely responsible for high-abundance peaks. Finally, peptide  
 information is rolled up to the protein level, and protein abundance is quantified using

either peak intensities or spectral counts (160). A quadrupole–orbitrap mass analyser is depicted. b.) Results are then interpreted using software packages such as MaxQuant. Samples can be multiplexed with tags and the fragment spectra are interpreted. Peptide identities can also be transferred when the peptide is fragmented in only one of the runs but matches precisely the mass and elution time of an aligned peak (known as the 'match between runs' feature in MaxQuant). Peptides/proteins can also be subjected to label-free quantification at the MS2 level. In this case, the fragment-ion intensities that are unique to a specific peptide are used for quantification. In multiplexed shotgun proteomics, up to sixteen samples are labelled differentially so that they release reporter ions that can be distinguished in the MS2 spectra (4). ..... 33

**Figure 1. 9** – a.) Summary of the types of MS-based proteomics methods for training studies. 2DE - two dimensional- polyacrylamide gel electrophoresis, 1DE – 1 dimension gel electrophoresis, 2DIGE - two-dimensional fluorescence difference gel electrophoresis, LC-MS – Liquid Chromatography coupled with Mass Spectrometry. TMT – Tandem Mass Tag Labelling. Adapted from (235). b.) Identification of mitochondrial proteomes over the years looking at the number of differentially expressed mitochondrial proteins identified in response to training in animal and human studies, and the method of proteomic analysis. .... 37

**Figure 1. 10**– (a.) Number of mitochondrial proteins identified as differentially expressed by individual training studies in humans (b. ) Biological processes by gene ontology (GO) enrichment analysis in which the identified proteins are mainly involved. The bars represent  $-\log_{10}(P)$ , where P represents the significance of each GO biological process enriched by the mitochondrial proteins. The P-value was computed using GO enrichment analysis by Protein ANalysis THrough Evolutionary Relationships (PANTHER) (316). (c.) Network model describing cellular processes and interactions of the Differentially Expressed Proteins (DEP) in mitochondria. Colours denotes the study in which the specific protein was identified, and any DEPs mutually identified. Only ATP5A & ATP5B were identified as changing with exercise in all 3 studies. In addition SDHA, ACADVL, ACO2 were common to Holloway and Granata AK3, CKMT2, DLD, FH, HSPE1, MDH2, NDUFA13, SOD2 and TUFM were common to Granata and Egan. FUNDC2, NDUFA2, NDUFS6, ATP5H, ATP5J, SDHA, CHCHD3, IMMT, PARK7 & HSPB1 were common to Granata and Hostrup. Created with BioRender.com ..... 46

**Figure 1. 11** – Publication counts related to “gel-based” and “gel-free” proteomics. The number of publications was taken from PubMed (<https://www.ncbi.nlm.nih.gov/pubmed/>). Adapted from (165)..... 49

**Figure 1. 12**– Recruitment of muscle fibres is dependent on the intensity and duration of contraction. A hierarchal recruitment pattern of type I to IIa to IIx/b occurs as force output of the muscle increases from low to high. During low-intensity exercise, slow-twitch, type I fibres are recruited, which have a high capacity for fat oxidation and a low capacity for glycogenolysis-glycolysis. An increase in contraction intensity results in a proportional increase in the recruitment of type II muscle fibres, which by their intrinsic characteristics generate more ATP from glycolytic pathways (27). ..... 50

**Figure 1. 13**– Modified figure from Wyckelsma et al. (335) demonstrating potential discrepancy in individual protein response between whole muscle and single fibres; in this example, MFN2 is shown as. Each colour used for Pre and Post symbols on the graphs indicates the same participant (consistent across all figures)..... 52

**Figure 1. 14**- Single shot workflow for Single Muscle Fibre Isolation and Analysis adapted from (216) ..... 62

## **Chapter 2**

**Figure 2. 1**- a. General Outline of Research to be Undertaken. b. Single Fibre Analysis and Comparisons by MS on exercise study for groups of Moderate Intensity Training (MICT) and Sprint Interval Training (SIT). ..... 67

**Figure 2. 2**- Flow diagram of the progress through the phases of a parallel randomised trial of MICT and SIT groups..... 69

**Figure 2. 3**- Schematic overview of the timeline of the testing and exercise training session before and after the 8-week period. GXT = Graded exercise test; fam = familiarisation session; 20kmTT = 20 kilometre time trial; 4kmTT = 4 kilometre time trial; submax = submaximal. Two training groups performed the training over the 8 week period. MICT -  $\pm$  10% of the first lactate threshold ( $\sim$  90% of the lactate threshold 1) for 60 – 120 min sessions. SIT – 30 s all out bout for 20 – 40 min per session..... 71

**Figure 2. 4**– Fibre Typing by dot blotting. This example shows membrane images for the identification of fibre types in a single participant. Type I fibres **a.)** presence of MHCI and type II **b.)** presence of MHCIIa ..... 72

**Figure 2. 5**- Workflow for characterisation of single human skeletal muscle fibres 1.) Single fibre preparation and isolation 2.) Fibre pooling 3.) Lysis, reduction, alkylation, and digestion 4.) Check reproducibility 5.) Labelling and MS LC-MS analysis 6.) Data analysis. .... 74

**Figure 2. 6- a.)** Reporter ion interference for 16-plex. **b.)** Sampling strategy for 96 well plate. Samples labelled by participant ID – M (MICT) or S (SIT) and I (Type I fibre) or II (Type II fibre) ..... 79

**Figure 2. 7**- Single Fibre Analysis and Comparisons by MS on exercise study for groups of Moderate Intensity Training (MICT) and Sprint Interval Training (SIT)..... 80

### **Chapter 3**

**Figure 3. 1**- Workflow for characterisation of single human skeletal muscle fibres 1.) Optimise protein processing – including lysis, reduction, alkylation, and digestion 2.) Confirm fibre typing 3.) Optimise fibre pooling 4.) Check reproducibility 5.) Labelling and MS LC-MS analysis 6.) Identify mitochondrial proteins. .... 84

**Figure 3. 2**– Illustration using a simplified protein clean-up scenario with Single-pot, Solid-phase-Enhanced Sample-Preparation (SP3) to provide a simplified platform for the processing of protein samples before MS-based proteomics analysis. The schematic depicts the SP3 workflow for performing clean-up to remove unwanted contaminants from a mixture of proteins. Proteins are bound to magnetic beads via a hydrophilic interaction mechanism. The bound beads are then rinsed to facilitate removal of unwanted contaminants from the proteins. Purified proteins are subsequently eluted for downstream analysis (141)..... 85

**Figure 3. 3 - S-Trap Protocol Schematic** - Proteins are solubilised in SDS, and subsequently reduced and alkylated. Samples are acidified and the S-Trap methanolic buffer is added. The protein suspension is then formed. After the centrifugation, the protein suspension is trapped in the quartz stack. Following washes with the S-Trap buffer and ammonium bicarbonate, a protease is added. After incubation with the protease

enzyme, the S-trap column is washed and peptides captured in the S-Trap are subsequently eluted. Modified from (253). ..... 86

**Figure 3. 4**– Comparison of coverage for the number of proteins identified by S-Trap and SP3 protein processing methods investigated in pilot 1. .... 87

**Figure 3. 5**– Number of proteins observed across all samples. Fibre type is indicated and extra peptide purification step using stage tips with SDB-RPS (Styrenedivinylbenzene-reverse phase sulfonated) discs is indicated by SDB. .... 89

**Figure 3. 6**- Fibre typing by Mass Spectrometry (MS) results a.-d. corresponds to pilot number 1-4 accordingly. e.) represents fibre typing based on Murgia et. al data set for young and old humans (218). Fibres were classified as type I if the relative abundance of MYH7 was > 80%, as type-IIa if MYH2 > 60%, as type-IIx if MYH1 > 60% ..... 92

**Figure 3. 7**– Depth of Coverage in pooled single fibre samples for the number of proteins and peptides identified from pilot 1 & 3..... 94

**Figure 3. 8**– Reproducibility across samples. Here the same sample is analysed in duplicate for fibre type and quantification. a.) Intensity reported by intensity-based absolute quantification (IBAQ) for replicates of type I fibres. Label Free Quantification (LFQ) reliability in replicate samples. **b.)** Type I fibres **c.)** Type II fibres. Core mitochondrial proteins (OXPHOS – NDUFA8, SDHA, URCRC2, COX5B, ATP5B, IDH3B and CKM) are highlighted in yellow addition to sarcomeric proteins (MYH 7 (blue), MYH2 (green), ACTA1(orange)). ..... 96

**Figure 3. 9**– a.) Structure of commercially available TMT (tandem mass tags) b.) The peptide modified by the TMT. c.) TMTpro reagent are available up to 16plex TMTpro - 127C is shown as an example High Collision Dissociation (HCD) Fragmentation d.) TMT are available in up to 16 tags that can be used for labelling practically any peptide or protein sample. TMT makes it possible to multiplex the analysis, providing more efficient use of instrument time and further controls for technical variation. e.) TMT quantification is performed by measuring the intensities of fragment reporter ions released from the labels in the tandem MS mode (MS2) during peptide fragmentation. A further scan in a subsequent MS mode can follow where required in MS3 mode (not shown). Precursor

ions are selected in the full scan mode (MS1). Since ion selection step reduces the noise levels, it is advantageous (182, 259)..... 98

**Figure 3. 10**– Labelling Efficiency of TMTpro-zero. Peptide to TMT ratio is indicated on the x-axis. ---- indicates target threshold of 90% labelling efficiency ..... 100

**Figure 3. 11**- Labelling Efficiency of TMT with and without clean-up in pool of single skeletal muscle fibres. Peptide to TMT ratio is indicated on the x-axis. ---- indicates target threshold of 90% labelling efficiency..... 101

**Figure 3. 12**–Labelling Efficiency of TMT comparing 1 h and Overnight Digestion S-Trap protocols combined with SDB-RPS clean-up. Peptide to TMT ratio was fixed at a ratio of 1:16. ---- indicates target threshold of 90% labelling efficiency. .... 103

**Figure 3. 13**– Number of mitochondrial proteins identified with each pilot study and the corresponding Complex I proteins observed. Proteins were classified as mitochondrial by matched filtration through MitoCarta 2.0 (43). ----- refers to the total of 44 quantifiable complex I subunits..... 105

**Figure 3. 14**– **a.)** The number of mitochondrial proteins involved in cellular processes computed using Gene Ontology (GO) enrichment analysis. MICOS - mitochondrial contact site and cristae organizing system **b.)** Molecular processes in GO analysis in which the identified proteins are mainly involved **c.)** The number of mitochondrial proteins involved in biological processes computed using GO enrichment analysis. GO analysis was performed using Protein ANalysis THrough Evolutionary Relationships (PANTHER) (316) and Database for Annotation, Visualization and Integrated Discovery (DAVID) (137)..... 106

**Figure 3. 15**– Key optimisation findings for protein processing protocol. Highlighted are key finding from each optimisation phase 1 to 6 including, protein processing, fibre typing, fibre pooling, reproducibility, isotopic labelling, and identification of mitochondrial proteins..... 107

## Chapter 4

**Figure 4. 1**– Multidimensional scaling (MDS) plot showing variation among TMT batches following normalisation of raw data. Each colour represents a TMT 16-plex batch, showing complete removal of significant clustering. .... 111

**Figure 4. 2** - Characterisation of the proteome of pooled human single muscle fibres. a.) Proteomic workflow for fibre typing and identifying proteins in single-fibre samples. b.) Venn diagram of quantified proteins i.) *pre* and *post* training and ii.) between fibre types (type I & type II). c.) Protein coverage in muscle fibres. Each bar represents selected GO annotations. The number of corresponding protein-encoding genes in the human genome (calculated DAVID (137)) is considered as 100%. .... 113

**Figure 4. 3**– Number of proteins quantified in the training study dataset by our proteomic workflow in all pooled single-fibre samples. Samples are arranged according to TMT batches (A-H). Samples are labelled according to participant ID, training type (S or M), Training time (pre or post) and Fibre type (I or II) ..... 114

**Figure 4. 4**– Heatmap summarising correlation of all pooled samples in the training study when comparing participants and fibre type. Darkness of the squares reflect the Pearson correlation intensity score..... 115

**Figure 4. 5**- The gene sets for GO terms were visualised using the Cytoscape 3.8.2 Enrichment Map plugin (287). Each node represents a GO biological process term. The node colour indicates the significance of the term's enrichment. The darker colour (red) indicates more significant enrichment. The edges are related to the relationships between the selected terms, which are defined based on the genes that are shared in a similar way. Gene ontology determined using Database for Annotation, Visualization and Integrated Discovery (DAVID) (137)..... 118

**Figure 4. 6**– Multidimensional scaling (MDS) plot showing variation among samples based on fibre type. Each point represents a participant's sample, and the distance between the points correlated to the dissimilarity between the samples. The plot highlights the fibre types and illustrates that there are two distinct clusters showing the separation between fibre types I and II. .... 119

**Figure 4. 7-** Volcano plot of statistical significance against fold change highlighting the most significantly different proteins between type I (blue) and II (red) fibres pre-training (MICT & SIT combined)..... 121

**Figure 4. 8–** Volcano plot of statistical significance (log p) against fold change highlighting the most significantly different proteins between type I (blue) and II (red) fibres a.) Post Moderate Intensity Continuous Training (MICT) b.) Post Sprint Interval Training (SIT)..... 123

**Figure 4. 9–** Venn diagram showing the differentially expressed (DE) proteins when comparing type I to type II fibres. a.) MICT pre and post comparison of overlapping DE proteins. b.) SIT pre and post comparison of overlapping DE proteins. c.) Overall training comparison of MICT and SIT pre and post for overlapping DE proteins. .... 124

**Figure 4. 10-** REViGO Scatterplot of the Enriched GO Cluster Representatives from mitochondrial protein analysis. Fibre type GO enrichment analysis for differentially expressed proteins with adjusted p-value cut off of 0.05 for type I compared to type II fibres. a.) MICT – post b.) SIT – post. GO terms along with their p-values were further summarised by REViGO reduction analysis tool that condenses the GO description by removing redundant terms (306). The remaining terms after the redundancy reduction were plotted in a two dimensional space. using a similarity of 0.7, with SimRel as semantic similarity measure. Colours indicate the p-value (generated from DAVID (137)) of enrichment according to the legend. The size of each bubble reflects the count of each term among the enriched term list. Bubbles of more general terms are larger..... 126

**Figure 4. 11-** Scatterplot showing proteomics data. Points indicate proteins that were differentially expressed (adj. p-value < 0.05) with a positive fold change in type I compared with type II fibres. Mitochondrial proteins that were only identified in POST MICT are labelled..... 129

**Figure 4. 12-** Scatterplot showing proteomics data. Points indicate proteins that were differentially expressed (adj. p-value < 0.05) with a positive fold change in type I compared with type II fibres. Mitochondrial proteins that were only identified in POST SIT are labelled..... 131

**Figure 4. 13– Training and Fibre Type** – Profile plots illustrate the z-score intensity average for all known mitochondrial proteins annotated in type I fibres (blue) and type II fibres (red) for pre and post training for both training types ( $\nabla$  z-score represented by the black line). ..... 132

**Figure 4. 14- Complex I-V** – Profile plots illustrate the z-score intensity average for all known mitochondrial proteins (grey) along with known subunits of complexes I to V (each complex is depicted by a different colour) pre and post training for both MICT (Moderate Intensity Continuous Training) and SIT (Sprint Interval Training) training in both type I and II fibres ( $\nabla$  z-score represented by the black line)..... 134

**Figure 4. 15-** The respiratory chain complexes, showing the cumulative mean z-score intensity change in fibre type for all proteins identified in each complex shown following a.) Moderate Intensity Continuous Training (MICT) and b.) Sprint Interval Training (SIT). For each complex, the changes are reported in type I (blue bar) and type II fibres (red bar). ..... 138

**Figure 4. 16-** Proteomic quantification of individual proteins identified in each complex of the electron transport chain in pooled single human muscle fibres. The expression of the complex subunit is measured by the z-score and subdivided by fibre type (type I & type II) and training type (M/MICT -Moderate Intensity Continuous Training, S/SIT – Sprint Interval Training). Changes are compared from pre and post training. The colour scale represents Z score as indicated. Complexes are labelled from I-V and the names of the mitochondrial subunits are also included. .... 141

**Figure 4. 17– Mitochondrial Ribosomes** –Profile plots illustrate the z-score intensity average for all known mitochondrial proteins (grey) with mitochondrial ribosome proteins annotated in pink ( $\nabla$  z-score - black), pre and post training for both MICT (Moderate Intensity Continuous Training) and SIT (Sprint Interval Training) in both type I and II fibres. .... 142

**Figure 4. 18– Common Functional Pathways** – Profile plots illustrate the z-score intensity average for all known mitochondrial proteins (grey), Fatty Acid Oxidation (black profiles,  $\nabla$  z-score - yellow), Mitochondrial Dynamics (light blue profiles) and the Tricarboxylic Acid (TCA) Cycle (brown profiles), ( $\nabla$  z-score black) pre and post training

for both MICT (Moderate Intensity Continuous Training) and SIT (Sprint Interval Training) in both type I and II fibres. .... 144

**Figure 4. 19 -Glycolysis** –Profile plots illustrate the z-score intensity average for known mitochondrial proteins (grey) with glycolysis proteins annotated in aqua (∇ z-score black) pre and post training for both MICT (Moderate Intensity Continuous Training) and SIT (Sprint Interval Training) in both type I and II fibres..... 148

# *List of Tables*

## *Chapter 1*

Table 1. 1– Fibre Type Description and Characteristics.....	7
Table 1. 2 - Summary of Mitochondrial Proteins Investigated by Immunoblotting in Response to Different Types of Training .....	23
Table 1. 3- A summary of studies that have focused on the proteomic profiling of skeletal muscle in response to exercise training .....	47
Table 1. 4- Summary of Human Single-Fibre Mitochondrial Protein Exercise Training Studies by Immunoblotting .....	55
Table 1. 5- Summary of MS-based Proteomics Studies Using Single Fibres.....	63

## *Chapter 2*

Table 2. 1– Participant Characteristics .....	69
Table 2. 2- Reporter ion interference classification for all TMT batches, specifying the reporter mass tag, the reporter channel within the MS3 scan output and the target channels for primary (+1 Da) and secondary (–1 Da) reporter ion interference.....	78

## *Chapter 3*

Table 3. 1– Results summary from Pilot 1 comparing Suspension Trapping (S-Trap) and Single-pot, Solid-phase-Enhanced Sample-Preparation (SP3) protein processing protocols .....	87
Table 3. 2- Summary of Results from Pilot 2 Comparing the Inclusion of Peptide Purification Step Using Stage-Tips with SDB-RPS (Styrenedivinylbenzene-reverse phase sulfonated) Discs .....	89
Table 3. 3- Results Summary from Pilot 3 and Depth of Proteome Coverage for a Fixed Pooling of 6 Fibre Segments Using S-Trap with SDB-RPS Clean-up and a Protease mix of Trypsin/LysC.....	90
Table 3. 4– Labelling Efficiency and Digestion Results Comparing 1 h and Overnight Digestion S-Trap Protocols combined with SDB-RPS Clean-Up.....	102

**Chapter 4**

Table 4. 1– Most Abundant Mitochondrial Proteins Annotated Across All Samples. 117

Table 4. 2– Summary in Changes in Fibre Types in Mitochondrial Proteins of Single Fibre Samples\* ..... 132

Table 4. 3– Summary in Changes of Functional Pathways in the Mitochondrial Fraction of Single Muscle Fibre Samples\* ..... 143

Table 4. 4 - Summary of Changes of Glycolytic Proteins of Single Muscle Fibre Samples\* ..... 148

## **Abstract**

Mitochondria are involved in many essential cell functions, including the production of energy and cellular metabolism. Hence, a better understanding of how mitochondria adapt to different interventions may have implications for both health and performance. The ability to distinguish fibre-specific changes may help resolve some of the debate concerning the effects of different types of exercise on mitochondrial biogenesis. Skeletal muscle fibres represent a large proportion of cell types in humans, with specialised contractile and metabolic functions that depend on a large number of associated proteins with extensive posttranslational modifications. Many of these skeletal muscle proteins are present in a cell-specific or a fibre-type dependent manner. However, while the size principle has clearly demonstrated the recruitment of different fibre types with exercise of different intensities, the methods for studying mitochondrial protein adaptations have mostly been confined to the analysis for whole-muscle samples that contain a mixture of type I and II fibres. Recent advances in proteomics by mass spectrometry (MS) allow for the quantification of thousands of proteins in small biological samples, providing the potential to analyse changes in mitochondrial proteins in single muscle fibres.

This research describes a proteomic workflow for fibre typing and the subsequent identification of mitochondrial proteins within single human skeletal muscle fibres by MS, even when fibres have been prepared in a high detergent matrix. Fibre types were verified based on the relative abundance of myosin heavy chain (MYH) isoforms, which was determined by dividing the intensity-based absolute quantification of the respective isoform (MYH1, MYH2, MYH4, MYH7) by the sum of the intensities of all four MYH isoforms. This protocol also allows for incorporation of tandem mass tag (TMT) labelling for increased identification of lowly abundant proteins using a TMTpro-16 plex. This permitted a three-tiered comparison of mitochondrial protein content from different fibre types applied to a post *vs.* pre exercise training study design comparing two different types of exercise training performed by 23 men.

The developed proteomic workflow quantified the levels of 536 known mitochondrial proteins, representing more than 45% of the total mitochondrial proteins in single muscle fibres. Analysis of proteins associated with known cellular pathways within the mitochondria demonstrated distinct trends of fibre-type specific protein responses to different types of exercise. This research aims to further the application of proteomic technologies to better understand how specific mitochondrial proteins are altered in response to the stress of exercise at the resolution of single skeletal muscle fibres.

# **Chapter 1**

## **Review of Literature**

### **Training and Mitochondrial Proteins: Current Approaches & Future Perspectives**

## **1 Role of Mitochondria in Health and Performance**

Mitochondria are essential, membrane-enclosed organelles that consist of more than 1100 proteins that allow for many different functions. They have an important role in generating cellular energy, mostly in the form of adenosine triphosphate (ATP). The mitochondria also participate in many other cellular processes, such as the oxidation of carbohydrates and fatty acids and cell-signalling (93, 120, 249). Additionally, mitochondria are a source and target of free radicals, and are involved in programmed cell death (apoptosis) (108). Given the above, it is not surprising that mitochondrial alterations may contribute to some human diseases, such as neurodegenerative disorders, cardiomyopathies, metabolic syndrome, insulin resistance, cancer, and obesity (51, 248, 328) (Figure 1.1a). Mitochondrial characteristics have also been associated with endurance performance (225, 277) (Figure 1.1b). Hence, a better understanding of how mitochondrial proteins adapt to different interventions may provide insights for improving both health and human performance. Although mitochondria are found in most tissues involved in cellular energy generation via oxidation phosphorylation (OXPHOS), they are particularly abundant in skeletal muscle and this will be the main focus of this review.

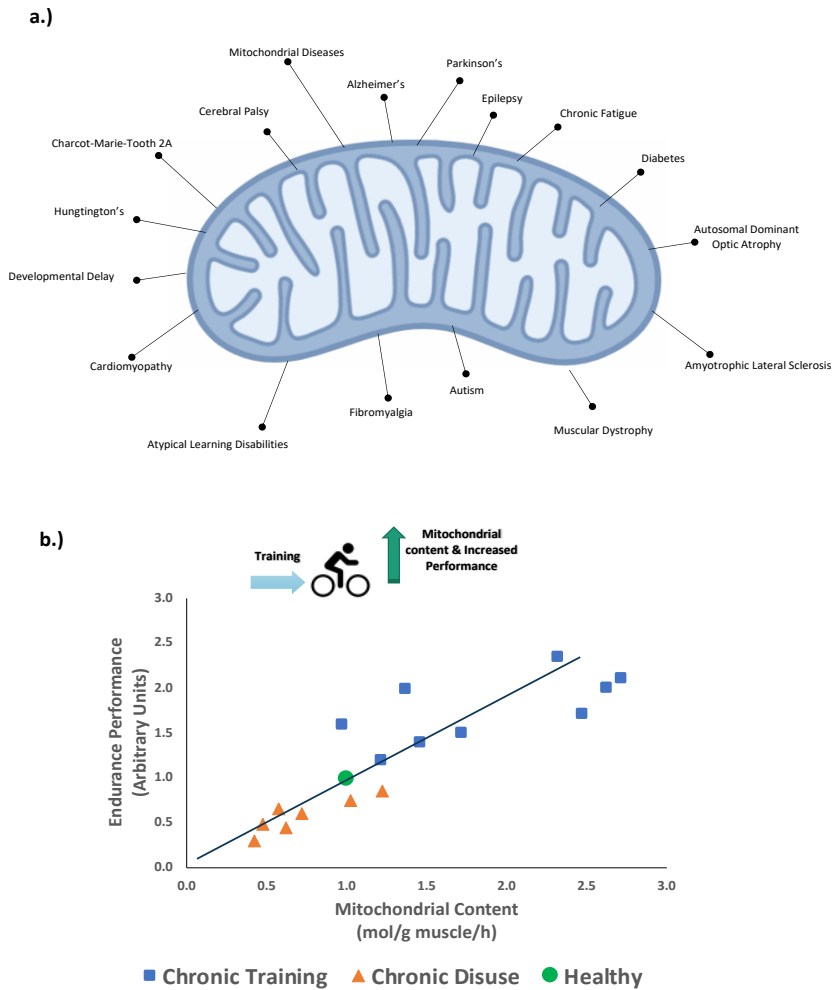


**Figure 1. 1–** a.) Summary of diseases or medical conditions that have been linked to sub-optimal mitochondrial characteristics. b.) Relationship of changes in mitochondrial content (measured by CS activity) to alterations in endurance performance (reported as arbitrary units). Increases in markers of mitochondrial content due to chronic muscle use (e.g. endurance training) lead to improvements in endurance performance. Decrements in markers of mitochondrial content brought about by chronic disuse. Adapted from Irrcher et al. (146).

## 1.1 Skeletal Muscle and Mitochondria

### 1.1.1 Skeletal Muscle

Skeletal muscles are highly specialised tissues with primary roles in locomotion, the maintenance of posture, and metabolism. Skeletal muscles are composed of individual muscle fibres - multinucleated single cells with a diverse range of properties that allows the same muscle to be used for a broad repertoire of functional tasks (Figure 1.2a). Since the first half of the 19th century, scientists have distinguished fibre types on the basis of their colour as red or white (related to myoglobin content) (221) and their contractile properties as fast and slow (Table 1.1). A more complex scheme emerged at the end of the 1960s, when alkali and acid preincubation of muscle fibres combined with histochemical staining for myofibrillar ATPase led to the identification of three major

fibre types in adult human skeletal muscles - type Ia, IIa, and IIb (now referred to as IIx) (14, 37, 77, 236). Based on ATPase staining, it has typically been reported that the vastus lateralis of young, healthy humans contains 25 to 60% type I fibres (180). A parallel classification based on histochemical determination of metabolic enzymes (e.g., SDH and LDH activity) and the analysis of functional properties (e.g., contraction time, fatigue-resistance, etc) produced three analogous fibre types - slow (long contraction time), oxidative, fatigue resistant fibres; fast (short contraction time), oxidative, less fatigue resistant fibres; and fast, glycolytic, quickly fatigued fibres (283). However, while there is correlation between fibre-type determinations based on metabolic properties and myofibrillar ATPase staining, these two classifications are not interchangeable (244, 297, 299). Many studies have reported a wide range of variations of metabolic enzyme activities in each fibre type and a large overlap has been found between fibre types determined via these two classifications (33, 122, 260).

Essentially, fibre-type classification depends on the method used. There are a number of disadvantages with fibre typing based purely on ATPase staining - where there is considerable overlap between all fibre types and, in particular, between type IIa and IIx fibres. (260). Fibre typing based on enzyme activity measurements can also give misleading results (78). With the exception of type I fibres, metabolic properties are loosely coupled with molecular properties of the myofibrillar apparatus but due to pronounced metabolic heterogeneity means that this relationship does not appear to extend beyond the two major groups of fast-twitch and slow-twitch fibres (96). The assessment of metabolic enzyme activity levels has revealed pronounced scattering within and between different fibre types (245). It should be noted, however, that the relative proportion of the different fibre types varies strikingly between species, and in humans shows significant variability between individuals. In contrast to rat and mouse IIx fibres, human IIx fibres have the lowest level of SDH activity compared with all other fibre types. Therefore, it is not justified to extrapolate results from transgenic mice to human muscles assuming that each fibre type has similar properties in different species (281, 283). Furthermore functional and molecular heterogeneity present in human muscle appears different from that described in the muscles of small mammals such as rat or rabbit (33) and greater fibre-type variation exists between mammalian than non-mammalian species (191).

Thus, there is a lack of correlation and distinction for specific fibre types between detection methods. For example, type IIa determined by ATPase or enzyme activity does not necessarily equate to that type II identified by myosin heavy chain (MYH) (246, 261). Therefore, MYH isoforms, rather than typing based ATPase, provide more perspicuous bases for defining type I and type II fibres. Subsequent research has also demonstrated that histochemical ATPase reactivity is based on the presence of specific MYH isoforms, which also determine functional properties such as maximum shortening velocity, maximum power output, and rate of tension redevelopment (298) (245, 296). The evaluation of MYH isoforms has revealed four main muscle fibre types in mammalian muscle, one slow (type I) and three fast (IIa, IIx, and IIb) types (283) (Figure 1.2b). Human muscles lack fast type IIb fibres (although it is present in genes; MYH4); this is the fastest and most glycolytic fibre type that is observed in rodent muscles (64, 283). While each fibre type is characterised by its predominant MYH isoform, there exists a spectrum of fibre types with pure or hybrid MYH composition ( $1 \rightarrow 1/2A \rightarrow 2A \rightarrow 2A/2X \rightarrow 2X \rightarrow 2X/2B \rightarrow 2B$ ) (41). The coexpression of multiple MYH isoforms within a single fibre also occurs under normal conditions (24). The expression of two or more MYHs with the same fibre may help explain why there is a strong correspondence between fibre-type determinations based on MYH content and myofibrillar ATPase staining among most (296, 300), but not all (33, 262), skeletal muscle fibres.

Myosin heavy chain single-fibre studies have demonstrated a relationship between ATP phosphorylation potential and MYH isoform complement (24, 213). This relationship corresponds to different tension costs and provides an additional rationale for the MYH-based fibre type diversity and transitions. Among the two available methods for MYH-based fibre type distinction, single-fibre electrophoresis appears to be superior to immunohistochemistry (24, 213, 214). The electrophoretic separation of MYH isoforms in single fibres is quantitative and, as opposed to immunohistochemistry, yields important information on MYH isoform proportions in hybrid fibres. In addition to differing contractile properties, fibres containing different MYH isoforms also display different surface membrane properties, calcium homeostasis, and mitochondrial characteristics (19, 73, 121, 283). The identification of specific MYH isoforms seems to be a more sensitive, more reproducible, and less subjective method for categorising muscle fibres than ATPase and SDH staining (201, 262). As such, the identification of MYH isoforms appears to be the best choice for fibre type delineation (244, 283, 319).

**Table 1. 1– Fibre Type Description and Characteristics**

Colour	ATPase (pH 4.54)	SDH	MYH	Gene	Protein	Type	Other Characteristics Contraction Time* (milliseconds) Fatigue Resistance^	Mitochondrial Volume* (% of total fibre volume)		
RED				MYH7	MyHC-β/slow	Slow Oxidative Type I	Elongated mitochondria *Slow (90-140) ^ High	6	<b>Humans</b>	<b>Animals</b>
				MYH2	MyHC-2a	Oxidative to glycolytic Type IIa	Elongated mitochondria *Moderately Fast (50-100) ^ Moderately High	4.5		
WHITE				MYH1	MyHC-2x	Glycolytic Type IIx	Punctate mitochondria, *Fast (40-90) ^ Low	3		
				MYH4	MyHC-2b	Glycolytic Type IIb	Punctate mitochondria *Very Fast (20-50) ^ Very Low	0.6		

### **1.1.2 Mitochondria Distribution in Skeletal Muscle**

In skeletal muscle, mitochondria range in size from 0.1 to 5.0  $\mu\text{m}$  in diameter (93) and are classified according to their location. Those situated under the sarcolemma are called subsarcolemmal (SS) mitochondria, whilst those interspersed throughout the myofibrils are termed intermyofibrillar (IMF) mitochondria (Figure 1.2c to f). Intermyofibrillar mitochondria are distributed between myofibrils and sarcomeres within the microfilaments (F-actin) and microtubules (79, 285). The IMF pool embodies approximately 75% of the entire mitochondrial population. There is a close proximity of the majority of mitochondria with the myofilaments, which minimises diffusion distance and enables the efficient conversion of chemical energy to mechanical work. In addition, a reticulum connects SS and IMF mitochondria to provide a pathway for energy distribution along the cell. (267). The two different mitochondrial pools differ in biochemical properties and function, with IMF mitochondria possessing an approximately 3-fold higher maximal respiration rate and ATP production rate compared to their SS counterparts (56). Additionally, the two distinct mitochondrial subpopulations exist as a continuous reticulum in slow (type I) and fast fibres (type IIa, IIx and IIb) with distinct subcellular localisation and morphology. Subsarcolemmal mitochondria show a large, lamellar shape, whereas IMF mitochondria have been shown to be smaller and more compact and located between the myofibrils in close proximity to the triads where calcium is released from sarcoplasmic reticulum (170).

### **1.1.3 Mitochondria Structure**

Mitochondria contain an inner and outer membrane (Figure 1.2f to g) composed of phospholipid bilayers and proteins. The outer mitochondrial membrane (OMM), which encloses the entire organelle, has a protein-to-phospholipid ratio similar to the eukaryotic plasma membrane and contains many integral proteins and enzymes involved in a diverse range of activities. The inner mitochondrial membrane (IMM) contains proteins with four main functions: (1) those that carry out the oxidation reactions of the respiratory chain; (2) ATP synthase, which forms ATP in the matrix; (3) specific transport proteins that regulate the passage of metabolites into and out of the matrix; and (4) mitochondrial protein import mechanisms. The IMM is compartmentalised into numerous cristae, which expand the surface area of the IMM and enhance its ability to generate ATP. The

compartment inside the IMM is defined as the matrix and hosts mitochondrial (mt) DNA, ribosomes, and the enzymes of the tricarboxylic acid (TCA) cycle. The TCA cycle, which includes the enzyme citrate synthase (CS), is the final common pathway for the oxidation of fuel molecules such as carbohydrates, lipids, and amino acids (102). The mitochondrial DNA encodes 37 proteins, of which 13 are essential polypeptides of the electron transport chain (ETC). However, the vast majority of the mitochondrial proteome (>1,100 proteins) consists of nuclear-encoded proteins that are imported via the import machinery into the mitochondria where they combine with those encoded by mtDNA. The import machinery consists of specialised import proteins containing transition pores, such as the translocase of the outer membrane that allow proteins to cross the OMM and the translocases of the inner membrane that allow protein transport within or across the IMM (6, 27, 270).

#### **1.1.4 Fibre-Type Specific Characteristics of Mitochondria in Skeletal Muscle**

Little is known about how mitochondrial proteins differ in different fibre types. However, it has been shown that mitochondrial characteristics, such as volume density, enzymes, respiratory function, and morphology, vary in different skeletal muscle fibre types. These results depend to some degree on the species studied, the age of the individuals, the amount of physical activity of the participants, and whether or not specific fibre types have been considered in the analyses. Nonetheless, key fibre-specific mitochondrial characteristics are highlighted below and provide some insights into potential differences in mitochondrial proteins between fibre types.

##### **a.) *Volume density***

Differences in total mitochondrial protein will be reflected by differences in mitochondrial volume (as determined by TEM), which has been reported to vary within different fibre types. Mitochondrial volume ranges from 5% to 25% of the total fibre volume in rat EDL muscle (282). In human fibres, the mitochondrial volume varies from 6% in type I fibres to 4.5% in type IIa fibres and 2.3% in type IIx fibres (135, 161, 232). Additionally, exercise training has been shown to increase mitochondrial content in all fibre types (as measured by citrate synthase activity and mitochondrial volume) (252).

b.) **Enzymes** – Differences in mitochondrial volume density between fibre types are also reflected by differences in a range of mitochondrial enzymes (proteins that act as biological catalysts) (135, 145, 162). It has been shown in isolated mitochondria from the skeletal muscle of rabbits that the activity of citric acid cycle enzymes (e.g., CS, malate dehydrogenase (MDH), and SDH) is approximately double in type I compared with type II fibres. Furthermore, enzymes of the the mitochondrial carnitine shuttle (e.g., carnitine palmitoyltrans-ferase I (CPT1)) has an obligatory role in  $\beta$ -oxidation by permitting acyl-CoA translocation from the cytosol, and is more highly expressed in type I fibres (163). Lastly, the activity of 3-hydroxy-acyl-CoA dehydrogenase ( $\beta$ HAD), a key enzyme of  $\beta$ -oxidation, is higher in type I than in type II fibres. This work was further validated by a proteomic study of protein expression demonstrating that the entire  $\beta$ -oxidation pathway was upregulated in type I/IIa mitochondria (232).

In contrast, the activity of isocitrate dehydrogenase (an enzyme in the citric acid cycle and regulator of oxidative capacity) was roughly two-fold higher in type II than type I fibres (136, 148). Mitochondrial generation of hydrogen peroxide is two- to three-fold higher in type II fibres than in slow oxidative type I fibres. Further diversity included the high concentration of mitochondrial glycerol-3-phosphate dehydrogenase (GPDH) in type II fibres (148). The GPDH shuttle reveals an important difference between mitochondria of type II and type I fibres; that is, the differential distribution of mitochondrial GPDH, which can be considered as a marker of glycolytic metabolism and is more abundant in type IIx/b fibres and results in decreased expression of oxidative SDH enzyme (242). These enzyme results highlight that the content of individual mitochondrial proteins in different fibre types will likely depend not only on the amount of mitochondria present but also the metabolic properties of the different muscle fibres. However, because mitochondria can comprise less than 3% of skeletal muscle volume density, it is difficult to discern relative mitochondrial protein expression differences from mitochondrial enzyme differences in the whole-muscle samples, leading to the need for single-fibre studies (92).

c.) **Function** – Differences in mitochondrial enzyme activities suggest there are also likely to be differences in the intrinsic respiratory properties of mitochondria from type I and II skeletal muscle fibres, including adenosine diphosphate (ADP) sensitivity and coupling efficiency with ATP stimulated respiration, ATP phosphorylation potential, the regulation of respiration by (ADP), and respiratory capacity in response to the availability of different substrates (247).

**i) ADP Sensitivity**

The greater ADP sensitivity of mitochondria of type I fibres is believed to be due to functional coupling between mitochondrial creatine kinase (CK) and ADP (241, 329). Comparative analysis of human fibre bundles with variable percentages of type II and type I fibres shows that the ADP sensitivity is negatively correlated with type I fibre area and oxidative potential (247).

**ii) Maximal ADP-stimulated respiration.**

Maximal respiratory capacity of mitochondria from predominantly type I and type II fibres has been measured in several species. In general, studies performed on isolated mitochondria have reported little to no fibre-type difference for maximal ADP-stimulated respiration in the presence of substrates feeding the respiratory chain at the level of complex I, complex II, or complex IV (247). In contrast, substantial differences exist between mitochondria from type I and type II muscle fibres with type I having a higher capacity to oxidise fatty acids (206).

**iii) ATP phosphorylation potential**

Type I and II fibres have shown marked diversity in oxygen consumption when maximally stimulated with ADP (247). Studies on single fibres of rabbits rats have revealed a difference in regulation of mitochondrial activity between slow type I and fast type II, where the ATP phosphorylation potential determined by the ratio between ATP to free ADP was higher in type II fibres compared to type I (38, 57, 244). For instance, ATP generation in type I fibres was observed at 6 mmol/kg dw/s, which precisely matches the ATP consumption of type I fibres during maximal isometric contraction. On the other hand, ATP consumption of type II fibres during maximal isometric contraction was observed as more than double ( $17.6 \pm 26.6$  mmol/kg dw/s) (33) and greater than its ability to generate ATP.

#### **iv) Substrate availability**

Substrate availability for mitochondria differs among fibre types. Acetyl-Coenzyme A is provided by two sources: 1) from fatty acids (FA) via activation to acyl-CoA, transfer into the mitochondria via carnitine-acyl-transferase, and degradation to acetyl-CoA via  $\beta$ -oxidation, and 2) from pyruvate, derived from glycolysis via the pyruvate dehydrogenase (PDH) enzyme. The contribution of FA from  $\beta$ -oxidation to the tricarboxylic acid (TCA) cycle is higher in slow than fast fibres, such that type I fibres have greater availability and higher utilisation of free fatty acids than type II fibres. This results in a higher rate of maximal respiration with a fat fuel compared to its counterparts type IIX/IIB which had increased expression of glycolytic substrates (163, 169).

#### **v) Sex Differences**

Sexual dimorphism has been found in the mitochondria of skeletal muscle of rats where females displayed higher mitochondrial DNA (mtDNA) and protein content, OXPHOS machinery and activities of OXPHOS related enzymes (98, 323) compared to male counterparts. Additionally, there were fibre-specific differences inferred by skeletal muscle type comparing gastrocnemius (fast) and soleus (slow) muscles of male (98). In humans, mitochondrial differences in skeletal muscle have been indirectly inferred from results obtained in adipose tissues, where the expression of some mitochondrial genes are higher in women than men (223).

d.) **Morphology** – As mitochondrial function has been strongly linked to mitochondrial morphology (97) the above findings suggest that mitochondrial morphology may also vary between the different fibre types. Studies have observed distinct mitochondrial shape and configuration for human skeletal muscle fibre types (227). Mitochondrial are typically classified in terms of four shapes - networked, rod-like, punctate, or large and round (179). Compared to type II fibres, type I fibres exhibit higher fusion rates and contain elongated mitochondrial networks with more densely packed crista (86, 148). Additionally, type IIA fibres possess a more elongated mitochondria network than type IIX and IIB fibres (204), which have been reported to contain fewer, small,

punctate mitochondria (Figure 1.2h) (167). Structural features of mitochondria in type I and type IIa fibres are similar, but type I fibre mitochondria were found to be more stubby in shape (227). Switching of type IIx fibres (more glycolytic) to IIa type fibres (more oxidative) is associated with elongation of mitochondria, suggesting that mitochondrial fusion is linked to metabolic state (82, 204).

Given the fibre-specific differences in mitochondrial volume, function, and morphology, it is reasonable to hypothesise that mitochondrial proteins might be present in different amounts depending on the specific energy requirements of each muscle fibre type. An *in vivo* study in rats that inhibited complex V activity resulted in fibres with completely fragmented mitochondria having no interconnections, whereas the addition of oxidative media resulted in interconnected, highly tubular mitochondria, suggesting that mitochondrial morphology can dynamically respond to the OXPHOS activity of each individual fibre (82). Similarly, 4 weeks of voluntary running in rodents was accompanied by a 30% increase in type I/IIa (more oxidative fibres), due to a switch from IIx/IIb to IIa fibres, and the “switched” fibres (expressing both the IIa and IIx/IIb markers) exhibited a more elongated mitochondrial morphology (204). Thus, the exercise regimen promoted substantial changes in fibre types that was associated with a significant change in mitochondrial morphology. As interventions that alter the metabolic properties of the different muscle fibres also alter mitochondrial morphology, this suggests that interventions such as exercise may also alter the relative content of individual mitochondrial proteins in different fibre types. However, while it is well known that exercise causes an increase in total mitochondrial protein content, relatively little is known about fibre-specific mitochondrial adaptations following exercise training – especially in humans (219, 335-337).

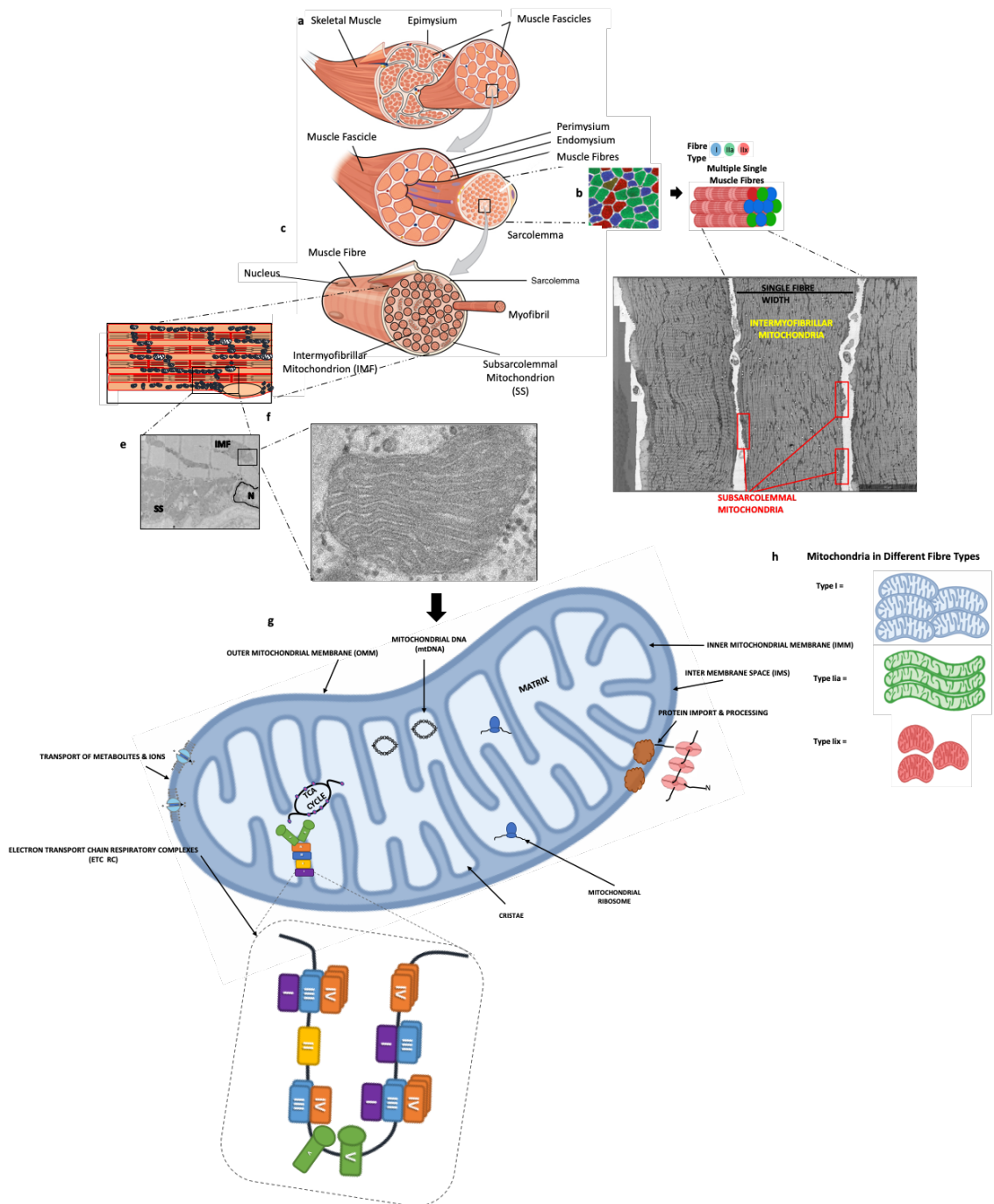


**Figure 1.2– Mitochondrion Structure** (a) Structure of a skeletal muscle fibre. (b) Image of bundle of single muscle fibres, and how they may be represented by different fibre types in a staining image. Transmission electron microscopy high resolution image of a human single muscle fibre showing sub-populations of IMF and SS within a single fibre. (c) Two sub-populations of mitochondria can be found: subsarcolemmal mitochondria (SS) and intermyofibrillar mitochondria (IMF). (d) Transversal illustration of a skeletal muscle fibre. Mitochondria create a reticulum that connects SS and IMF mitochondria (e) Transmission electron microscopy transversal image from a human skeletal muscle biopsy showing the nucleus (N), and the SS and IMF mitochondria. (f) Image of a mitochondrion. High-resolution imaging allows visualization of the densely-packed cristae within a mitochondrion. (g) Image of how a mitochondrion is usually illustrated in textbooks or research articles. Notice how the mitochondrial DNA (mtDNA) and the mitochondrial ribosomes are found in the matrix. The electron transport chain respiratory complexes are located on the IMM, and for the most part in the cristae. (h) Variation in mitochondria size between fibre types (204)

## **1.2 Skeletal Muscle Mitochondria and Training**

### **1.2.1 Mitochondrial Biogenesis**

The term genesis is derived from the Greek word for creation; however, mitochondria are not newly formed but are rather the result of the incorporation of new proteins into pre-existing sub-compartments and protein complexes (271). In this context, mitochondrial biogenesis has been defined as “the making of new components of the mitochondrial reticulum” (27, 203). The outcomes of mitochondrial biogenesis may include changes in mitochondrial content, mitochondrial respiratory function, or other aspects of mitochondrial quality such as increases in cristae density or supercomplex formation (109, 150, 222). The process of mitochondrial biogenesis is complex as mitochondria are composed of proteins derived from both the nuclear and the mitochondrial genomes. The networks of mitochondrial biogenesis has not been completely elucidated, however, the expression of mitochondrial proteins encoded in the nuclear genome have been linked fundamental participation in OXPHOS, mitochondrial protein import, mtDNA transcription and replication, and subsequently regulated by transcription factors and transcriptional coactivators (66).

Exercise-induced mitochondrial biogenesis is believed to be initiated by homeostatic perturbations i.e., changes in muscle energy turnover, reactive oxygen species, and metabolite accumulation. It is then thought these homeostatic disturbances are sensed and initiate a unique series of intracellular signalling events, including the activation of exercise-responsive kinases and transcription factors, which then coordinate the transcription of nuclear and mitochondrial genes (203). The messenger RNA (mRNA) is then translated into specific mitochondrial proteins, followed by the assembly of the multi-subunit protein complexes that contribute to the numerous and diverse functions of the mitochondria (130, 292). Measurements of individual changes in mitochondrial proteins allow researchers to better understand the events underlying mitochondrial biogenesis in response to exercise training.

Common signalling proteins measured in exercise studies include the activation/phosphorylation of AMP kinase (AMPK) (171, 318), p38 mitogen-activated protein kinase (MAPK) and Ca<sup>2+</sup>/Calmodulin-dependent kinases II (CaMKII) (130, 332). When it comes to monitoring regulators and/or co-activators of exercise -induced

mitochondrial biogenesis it is common to measure members of the PGC-1 family, which consists of peroxisome proliferator-activated receptor  $\gamma$  co-activator 1 $\alpha$  (PGC-1 $\alpha$ ), PGC-1 $\beta$ , and PGC-1-related coactivator (PRC). PGC-1 $\alpha$  transcript is the most widely studied of the three and is expressed in many tissues, with the highest abundance found in oxidative tissues such as skeletal muscle (280). PGC-1 $\alpha$  is a transcriptional coactivator that has been shown to regulate mitochondrial content and respiration in muscle cells (334) and also metabolic control in rat skeletal muscle (164). Subsequent studies in humans have shown that exercise training leads to an increase in PGC-1 $\alpha$  protein content in the nucleus (186, 332). PGC-1 $\alpha$  has emerged as a principal coordinator through the coactivation of nuclear transcription factors encoding mitochondrial proteins (130, 184). It therefore plays a pivotal role in the adaptive response to exercise and the modulation of mitochondrial biogenesis (230, 254). The tumour suppressor p53 has also been shown to be an important regulator of mitochondrial biogenesis (275) and via regulation of downstream targets p53 can control mitochondrial function by modulating the balance between glycolytic and oxidative pathways (200, 327). It is assumed/suggested that regular and repeated activation of these pathways leads to increases in mitochondrial size, structure and function (193).

Synthesis rates of individual mitochondrial proteins remains in its infancy, but has previously been investigated *in vivo* in both animal and human skeletal muscle to understand the translational and transcription regulation of genes with the highest synthesis rates observed in a mitochondrial compared to contractile proteins (151, 266). Thus, the relatively rapid rate at which mitochondria respond to different types training permits studies of mitochondrial protein adaptations to different types of exercise training in humans.

### **1.2.2 Influence of Training Characteristics**

Physiological responses to exercise are mediated by characteristics of the exercise stimulus, and are primarily determined by exercise volume and intensity (152). Although there are many different ways to characterise exercise, for the purpose of this review exercise training has been characterised as moderate-intensity continuous training (MICT), high-intensity interval training (HIIT), or sprint interval training (SIT) (Figure 1.3). MICT has been defined for this purpose as consisting of continuous exercise

performed at an intensity below 75%  $\dot{W}_{max}$  (though there is a lack of consensus on a strict intensity for this training type). The term moderate-intensity continuous training (MICT) is used for comparative purposes to describe exercise that is performed in a continuous manner and at lower intensities than HIIT. HIIT is defined as ‘near maximal’ efforts generally performed at an intensity that elicits  $\geq 75\%$  (but often 80–95%) of maximal heart rate. In contrast, SIT is characterised by efforts performed at intensities equal to or greater than the pace that would elicit maximal oxygen uptake ( $\dot{V}O_{2peak}$ ) and includes ‘all-out’ or ‘supramaximal’ efforts. Additionally, these training types can be characterised by specific oxygen uptake kinetics and blood lactate responses (152).

Cellular stress occurs in proportion to exercise intensity (75), and higher intensities of exercise elicit greater metabolic perturbations than moderate intensities (80, 322). For example, phosphocreatine response has been observed to decline during moderate-intensity exercise but is attenuated in the moderate-to-heavy exercise condition (157, 268). Increased contractile activity also results in an increased ADP/ATP ratio (117) (Figure 1.3f). Reactive Oxygen Species (ROS) are produced within the mitochondria during the production of ATP and have been shown to follow a similar pattern to ADP/ATP ratio following increased exercise intensity (307) (Figure 1.3g). Higher exercise intensities are associated with greater improvements in mitochondria respiration (especially relative to training duration) (27). In contrast, training volume has been suggested to be a primary determinant of the exercise-induced increase in mitochondrial content in humans (29) – although, this is currently a topic of ongoing scientific debate (28). However, there is little information on the relationship between training characteristics and changes in mitochondrial proteins.

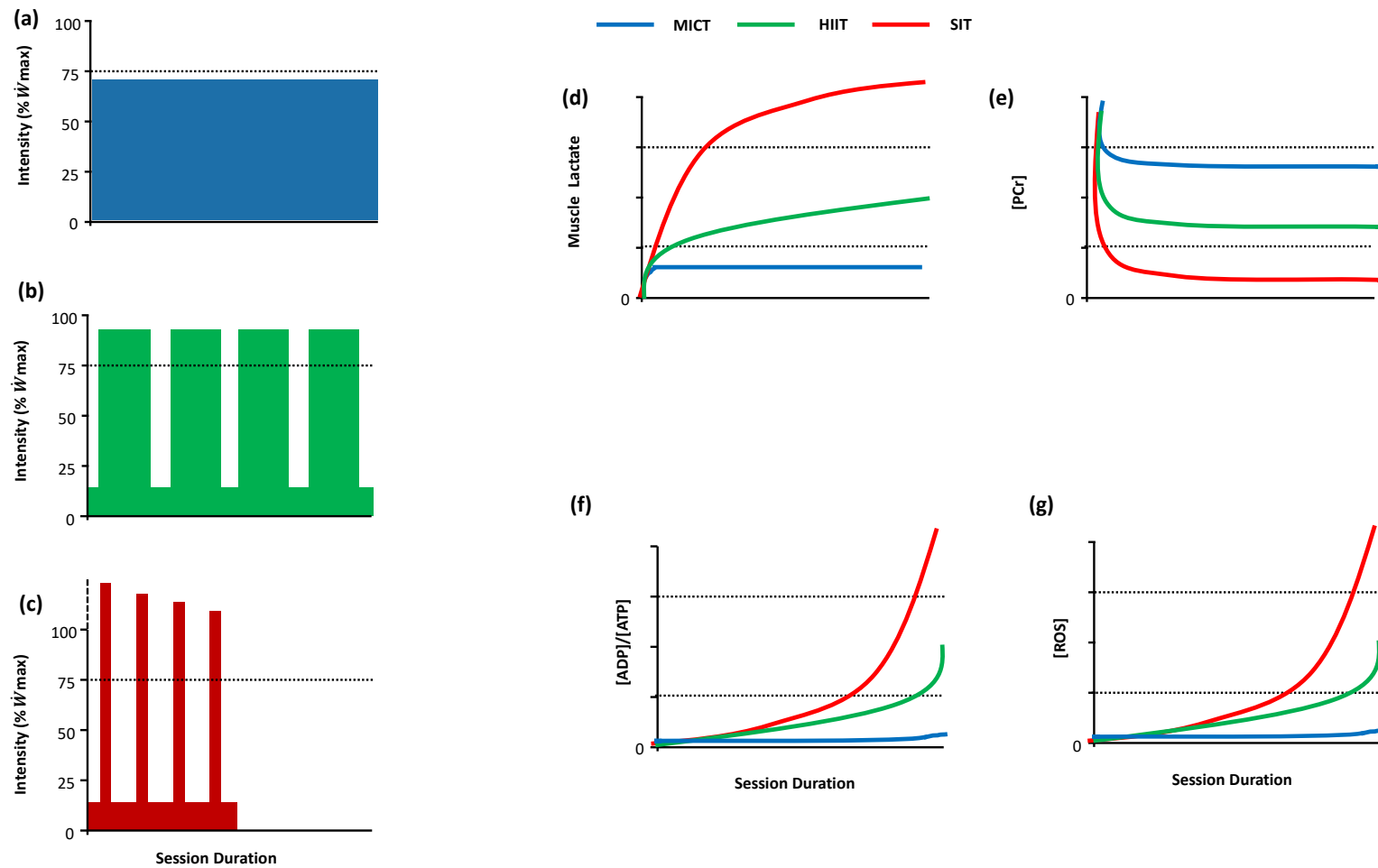


**Figure 1. 3-** Schematic representation of the definitions used in this review to categorise (a) moderate-intensity continuous exercise or training ( $< 75\% \dot{W}_{max}$ ), and high-intensity exercise or training, which includes both (b) high-intensity (HIIT) and (c) sprint-intervals (SIT) ( $> 75\% \dot{W}_{max}$ ) training. Adapted from MacInnis & Gibala (193) (d) Schematic of blood lactate response to exercise intensity adapted from Jamnick et al (152) (e) Schematic of Phosphocreatine response (157) to exercise intensity (f) Schematic of ADP/ATP ratio and (g) Reactive Oxygen Species (ROS) (307) in response to training

## 1.2.3 Mitochondrial Protein & Exercise Training

### 1.2.3.1 Animal Studies

Based on observations of early work in the 1950s, which revealed a strong relationship between the ability of a muscle to perform prolonged submaximal exercise and its content of respiratory enzymes (i.e., throughout Cytochrome c oxidase) (126), Holloszy hypothesised that total mitochondrial protein content might also be linked to the level of habitual muscle contractile activity (126). To test this hypothesis, male Wistar rats performed an intense program of treadmill running with a combination of MICT and SIT (120 min of continuous exercise, with 12 sprints at 42 m per min, each lasting 30 seconds, interspersed at intervals through the workout, 5 days per week for 12 weeks). An increase in skeletal muscle mitochondrial protein content was observed (see Figure 1.4) (126). This increase in mitochondrial protein was associated with a parallel increase in the ability to produce ATP and prolonged endurance running time after training (126). Similar increases in mitochondrial protein content in rats (94, 95, 127) and also in guinea pigs (15) were observed in subsequent studies following exercise training.

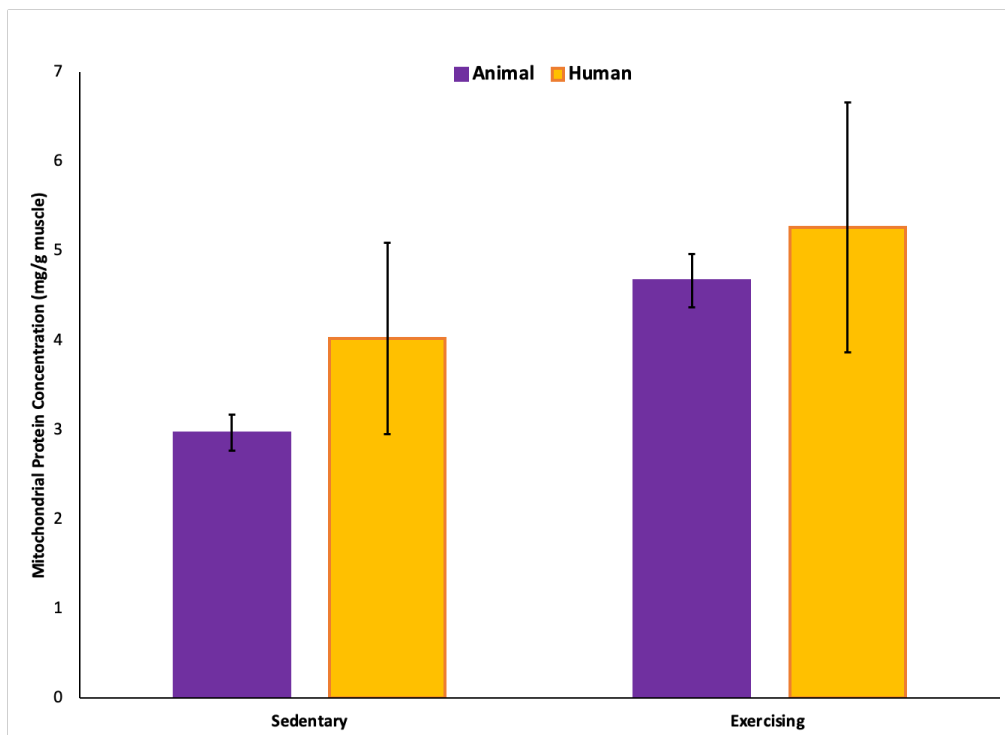


**Figure 1.4** – Representation of pioneering studies demonstrating increase of mitochondrial protein in response to exercise training in both animals (126) and humans (209).

### 1.2.3.2 Human Studies

While early studies on changes in mitochondrial proteins with exercise training were limited to research performed on animals, the introduction of the Bergström muscle biopsy technique (21, 22) (Figure 1.5) paved the way for researchers to investigate whether exercise training induced similar changes in mitochondrial protein content in humans. Morgan et al. (209) was one of the first to validate changes in mitochondrial proteins in human skeletal muscle after endurance exercise training. In agreement with previous animal studies (126), they observed a similar fold change of 1.31 in humans compared to 1.57 in rats. Similarly, a later study by Granata et al. (106) investigating the effects of training volume observed a 1.42-fold increase with training compared to baseline and a further increase of mitochondrial protein content of 2.21 fold compared to baseline with increased training volume. Evidence shows that training volume is an important determinant of increases in skeletal muscle mitochondrial content (106, 132). While these studies established that endurance exercise training can increase total mitochondrial protein, they don't tell us how individual proteins respond to training. Recent research has indicated that mitochondrial proteins may respond differently to nuclear proteins (286), where a systematic upregulation of nuclear and mitochondrial genes targeted by peroxisome proliferator-activated receptor  $\gamma$  coactivator 1 (PGC-1) was not observed following different intensities of exercise training.



**Figure 1. 5** – Bergstrom muscle biopsy technique, modified with suction, being performed on the vastus lateralis of a human volunteer

## **1.3 Mitochondrial Proteins and Training**

### **1.3.1 Immunoblotting**

The traditional approach to assess changes in individual proteins is the western blot technique. With this technique, proteins from a sample are denatured, separated on a gel, and then transferred onto a membrane (Figure 1.6). The presence of a certain protein is then determined by using putatively specific antibodies for the proteins of interest. The density of the detected band reflects the relative abundance of the protein in the sample, when the system is calibrated (220). The application of the western blot technique to skeletal muscle and exercise physiology has increased since its introduction in the early 1980's. This method has been extensively applied to detect mitochondrial proteins in whole-muscle samples (summarised in Table 1.2 & Figure 1.7). For the purpose of this review, we have defined a protein as mitochondrial if it is listed as part of The Integrated Mitochondrial Protein Index (IMPI) (293, 294) and/or MitoCarta 2.0 (43, 258) - a list of all the genes and proteins that make up the mammalian mitochondrion. IMPI identifies 1626 genes in humans, with 1184 known mitochondrial and 442 predicted from experimental data, whereas MitoCarta 2.0 provides an inventory of 1158 human genes encoding proteins with strong support of mitochondrial localisation.

Fundamental to western blotting success are a number of important considerations associated with sample fractionation, sample loading amount, calibration, and antibody specificity. In particular, the antibody must only detect a single species as output readings are unable to indicate whether they are reflecting single or multiple species. Typically, antibody datasheets do not provide tissue-specific data, or comprehensive sample preparation information, and it is imperative that researchers undertake their own antibody validation work on their particular protein and tissue of interest, which unfortunately is often overlooked (16, 88). Western blotting outcomes can also be influenced when either the density of proteins detected lie within a nonproportional region of a standard curve or a standard curve is not taken into account for data analyses, which is based on the underlying assumption that a directly proportional relationship exists between the amount of sample loaded and the density obtained for the protein band(s) of interest. At times there is a possibility of true changes being overlooked through the simple mistake of using band density alone and/or through analysing too much sample (207). This linearity is most likely to hold true within a narrow detection range between calculated density and protein loaded. Proportionality optimisation of standard curves is

crucial to improve the quantitative nature of western blotting, which is typically considered semiquantitative at best (90, 220). In order to determine lowly expressed proteins, it has been shown that many of these may be better detected by dramatically reducing the amount of sample loaded - as is the case with a single cell (fibre). This has the ability to detect proteins in small samples of 5 to 10  $\mu\text{g}$  total muscle mass (1 to 3  $\mu\text{g}$  total protein), which is an order of magnitude less than often used (220). In the following sections some key training studies that have utilised western blotting to investigate specific mitochondrial proteins in response to exercise are highlighted.

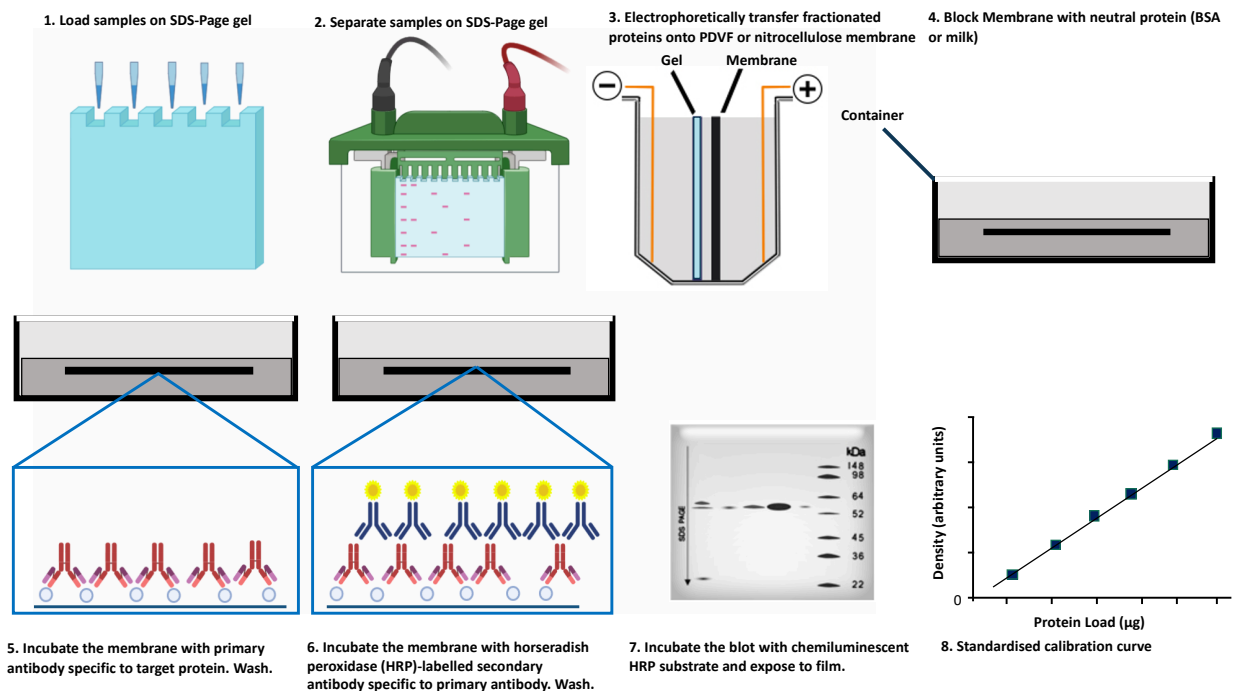


**Figure 1. 6**– Overview of the western blotting Procedure 1. Samples are loaded on a Sodium Dodecyl Sulfate–Polyacrylamide Gel Electrophoresis (SDS-PAGE) gel 2. Samples separated on the gel. 3. Transfer of separated proteins onto polyvinylidene difluoride (PDVF) or nitrocellulose membrane. 4. Membranes are blocked with a neutral protein. 5. Incubation with primary antibody specific to target protein. 6. Incubation with secondary antibody. 7. Incubation with chemiluminescent substrate and expose to film. 8. Generation of a standard calibration curve.

**Table 1. 2 - Summary of Mitochondrial Proteins Investigated by Immunoblotting in Response to Different Types of Training**

	Downregulated	No Significant Change	Upregulated			
Mitochondrial Protein	Training Type			Animal	Human	Reference
	MICT	HIIT	SIT			
ACAD1				✓		(63)
ACSL1				✓		(303)
ACSL4				✓		(303)
ACSL5				✓		(303)
ACSL6				✓		(303)
ACOT				✓		(166)
AIF					✓	(106) (3, 104)
ALAS1				✓		(158, 332)
ATP5A1 (CV)				✓	✓	(48, 55, 134, 339)
				✓	✓	(106) (48, 52, 109, 133, 340)
ATP5B (CV)					✓	(74, 133)
BAX				✓	✓	(23, 80)
BCL2				✓	✓	(23, 80)
BNIP3					✓	(81)
CAT					✓	(34)
CISD1				✓		(340)
CISD2				✓		(340)
CKMT2				✓	✓	(52, 339)
COXI (CIV)				✓	✓	(34, 49)
COXII (CIV)				✓	✓	(49, 106, 134, 144, 185, 276, 339)
COXIV (CIV)				✓	✓	(3, 34, 49, 52, 55, 58, 80, 81, 89, 112, 133, 158, 169, 187, 193, 199, 239, 274, 279, 301, 311, 332)
				✓		(48)
COXVI (CIV)					✓	(276)
CPT1				✓	✓	(52, 311)
CS				✓	✓	(106, 112, 134, 279, 332)
CYCS				✓	✓	(32, 58, 158)
						(58)
DHPR					✓	(133)

Mitochondrial Protein	Training Type			Animal	Human	Reference
	MICT	HIIT	SIT			
DRP1					✓	(80, 81, 158, 208)
FABP1					✓	(311)
					✓	(239)
FIS1				✓	✓	(168, 199, 208)
				✓		(158)
					✓	(11)
GAPDH				✓	✓	(208, 332)
				✓		(175)
HADHA					✓	(133)
HADHB					✓	(112)
HK2					✓	(63)
HSPA9				✓		(3, 9, 205)
HSP27					✓	(211)
HSP60					✓	(211, 276)
HSP70					✓	(81, 211, 276)
IDH					✓	(81)
LC3B				✓	✓	(23, 76, 80)
LCAD					✓	(63)
LONP1					✓	(199)
MCT1					✓	(239)
MCT2					✓	(239)
MDH					✓	(74)
MFN1					✓	(185)
MFN2				✓	✓	(48, 63, 81, 106, 158, 199, 208, 335)
				✓	✓	(48, 80)
MIEF1				✓		(340)
MT-COI (CIV)				✓	✓	(109, 205, 340)
MTIF2				✓		(340)
MTIF3				✓		(340)
NDUFA5 (CI)					✓	(74)
NDUFA8 (CI)				✓	✓	(52, 63, 81, 106, 133, 134, 144, 339, 340)
				✓		(48)
NDUFA9 (CI)				✓	✓	(109, 186, 193, 194, 313)
OGG1					✓	(3)
				✓		(324)
OMA1					✓	(11)
OPA1				✓	✓	(11, 80, 158, 205)

Mitochondrial Protein	Training Type			Animal	Human	Reference
	MICT	HIIT	SIT			
PARK					✓	(11) (208)
				✓		(49, 158)
PDH				✓	✓	(63, 133)
PDK4				✓		(313)
PINK				✓		(208)
						(158)
RRF2				✓		(340)
SCO2					✓	(106) (3)
SDHA (CII)					✓	(109)
SDHB (CII)				✓	✓	(48, 52, 81, 133, 134, 158, 194, 313, 340)
				✓	✓	(48, 339)
SIRT3				✓		(52, 237)
SLC25A19				✓		(166)
SLIRP				✓		(166)
SOD2					✓	(3, 34, 74, 211, 272)
				✓		(175)
TACO1				✓		(340)
TFAM				✓	✓	(106) (3) (49, 199, 272)
TOMM20					✓	(3)
TRAP1				✓	✓	(9, 276)
UCP3					✓	(80, 81, 272) (81, 143)
UQCRC2 (CIII)				✓	✓	(52, 81, 134, 143, 215, 339, 340)
					✓	(48)
VDAC1				✓		(84, 339)
VDAC2				✓		(339)
VDAC3				✓		(339)

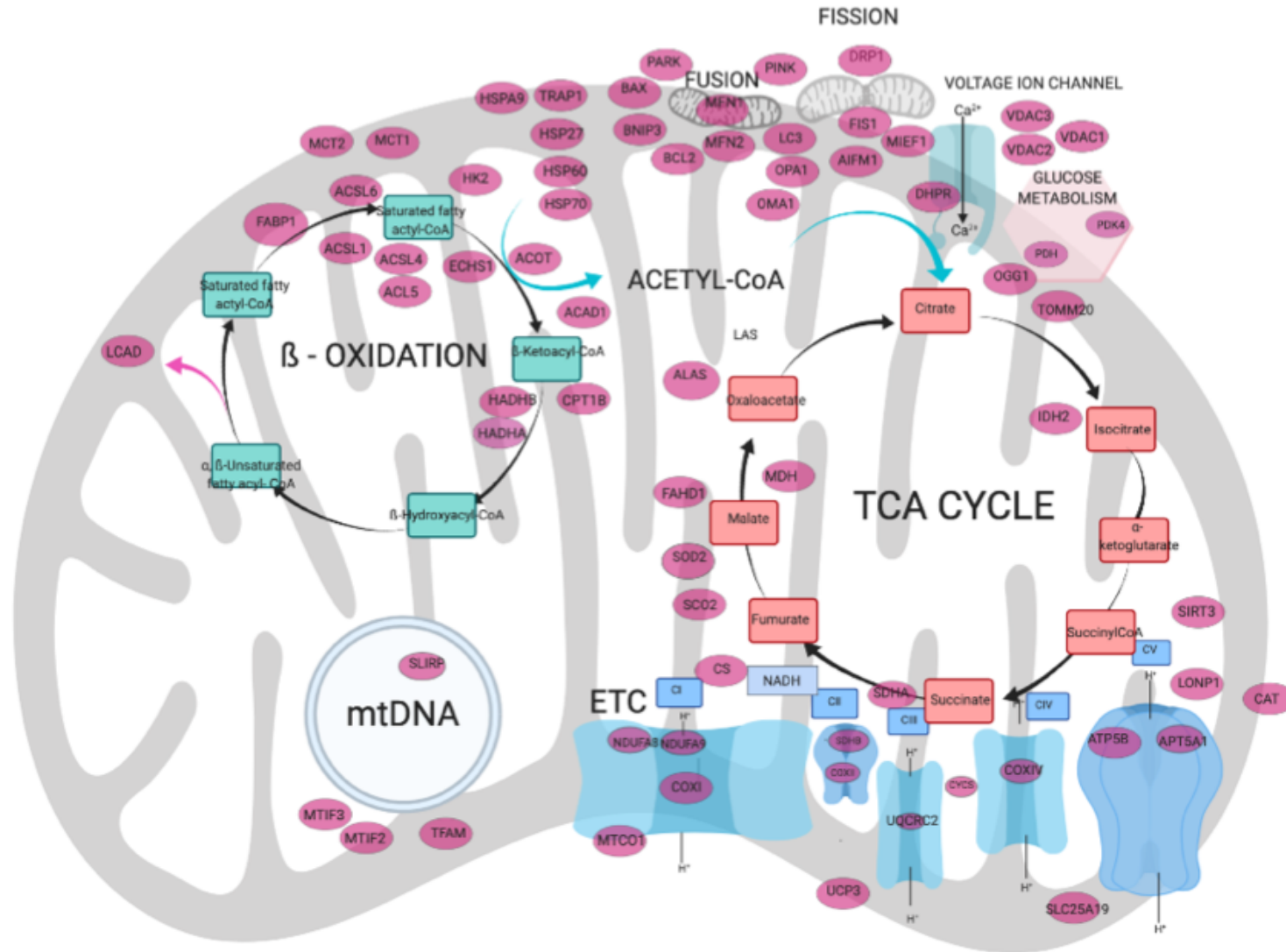


**Figure 1. 7-** Differentially expressed mitochondrial proteins following exercise training identified in humans and animals by immunoblotting. Created with BioRender.com

### 1.3.1.1 Animal Studies

The protein content of selected subunits of the five complexes of the ETC is routinely used as a biomarker of changes in mitochondrial content following a training intervention (177). Consistent with the previously reported increase in total mitochondrial protein following exercise training (Figure 1.4), studies have reported increases in subunits of the mitochondrial electron transport chain complexes (Table 1.2). This is consistent amongst training types, although SIT has not been performed with animal species. The complex IV (cytochrome oxidase, COX) subunits play a crucial role in aerobic respiration by catalysing the transfer of electrons from reduced cytochrome c to molecular oxygen (274). In particular, cytochrome c oxidase subunit 1 (COXI) has been investigated as it is a common protein in skeletal muscle and has been shown to result in rapid increases in its protein content following exercise (performed by rats) (332). The most common subunit investigated in response to training is subunit IV (COXIV), which has repeatedly been shown to increase in response to training (63, 199, 272, 313). While most studies reported increases in respiratory chain subunits (c.f. Table 1.2), one study comparing training types in mice found a different response in these subunits with significantly greater increases in all respiratory chain subunits for the HIIT compared to the MICT cohort (48). This suggests that mitochondrial proteins may respond differently to varying volumes and intensities of training

Further studies have used a variety of exercise protocols to challenge mouse muscle in order to determine the impact on specific mitochondrial proteins involved in the assembly and organisation of mitochondria and mitochondrial dynamics. For example, training resulted in increases in mitochondrial organisational proteins, such as 5-aminolevulinate synthase (ALAS) (332) and a similar increase was observed for mitochondrial import receptor subunit TOM22 and the mitochondrial transcription initiation complex - Transcription factor A (TFAM) (272) was also observed. Markers of mitochondrial dynamics have been looked at where regulators of mitochondrial fission, mitochondrial fission 1 protein (FIS1) and Dynamin related protein 1 (DRP1) were all upregulated following MICT (208). Additionally, muscle expression of the internal mitochondrial membrane cristae remodelling regulator OPA1 was increased in conjunction with increases in general markers of mitophagy and autophagy such as PTEN Induced Kinase

1 (PINK1) (208). Conversely, expression of outer mitochondrial membrane fusion markers (MFN1 and MFN2) were unchanged by exercise training in mice (48, 208).

While most mitochondrial proteins increased in response to training, some decreased or remained unchanged providing evidence that not all mitochondrial proteins respond the same way to the stress of exercise. The key finding from protein specific analysis by western blot is that it began to give evidence of different responses to different proteins, giving new insights beyond total mitochondrial protein analysis. Though similarities exist between animals and humans, literature has shown differences in contractile properties of skeletal muscle (281, 283) and thus it is important to expand this research to determine possible alterations in mitochondrial proteins responses in humans.

### **1.3.1.2 Human Studies**

Following on from animal studies, many studies have used the western blotting technique to investigate changes of mitochondrial proteins in human skeletal muscle in response to exercise training. These studies have focused on specific proteins contributing to OXPHOS, mitochondrial dynamics (including markers of mitofission and mitofusion), the TCA cycle, and fatty acid  $\beta$ -oxidation. Overall, many of the proteins observed to change in animals have also been observed in humans (even though in humans this is on mixed fibre samples). Some of these findings are highlighted below, but this research in humans has extended evidence that different mitochondrial functional classes respond differently to exercise training.

Increases in subunits of complex I-V have been reported in several studies though a variable response were observed depending on training type in complex V (Table 1.2). Studies investigating changes in contrasting training types, types, such as MICT and SIT, have revealed similar increases in complex IV subunits (COXII and COXIV) with reported increases of up to 126% (89, 168). Complex II; succinate dehydrogenase (SDH) has shown training induced increases of up 52% suggesting differences in specific mitochondrial ETC subcomplex protein responses (161). Additionally, complex I subunit NDUFA8 has been shown to increase with all training types (81, 105, 133, 144), though a discrepancy in response to SIT was observed for subunit NDUFA9, which increased in other modes of training (186, 193, 194, 313). Complex III subunit, ubiquinone,

(UQCRC2) reported increases in all training types in humans (81, 133, 143), which was contrary to a finding in mice (48) (cf Table 1.2).

Additionally, training volume may be a critical factor affecting changes in mitochondrial content, whereas relative exercise intensity is an important determinant of changes in mitochondrial respiratory function. While associated changes in mitochondrial content and mitochondrial respiration are typically reported, a dissociation between these two parameters has been observed in numerous studies (106, 150) whereby higher training statuses were associated with relatively larger values of mass-specific mitochondrial respiration than CS activity. For example sprint interval training induced an increase in mass-specific respiration despite no change in mitochondrial content (as assessed by CS activity). Conversely, moderate training did not change mass-specific mitochondrial respiration (29). Thus, an improvement in mitochondrial function of human skeletal muscle can take place independently of changes in mitochondrial content.

To a slightly lesser extent, mitochondrial proteins involved in the TCA cycle and fatty acid oxidation have been investigated. Citrate synthase, a TCA precursor that is involved in the subpathway that synthesises isocitrate from oxaloacetate, has been shown to increase by up to 102% in response to MICT (168). Conversely, isocitrate dehydrogenase (IDH) was found to not change with SIT (81).  $\beta$ -subunit (HADHB), a mitochondrial protein that is required for  $\beta$ -oxidation of fatty acids in mitochondria, increases in response to MICT (112) as does Carnitine palmitoyltransferase 1 (CPT1), which catalyses the first step in long-chain fatty acid import into mitochondria. Differing responses to HIIT have been found with fatty-acid binding protein (FABP1), with either increases or no significant change to training (239, 311).

It has also been shown that stress applied in the form of exercise can affect the abundance of proteins associated with mitophagy, fission and fusion within the skeletal muscle (190, 233, 275). Markers of mitofusion (MFN1, MFN2) and mitofission (FIS1) have been shown to increase with MICT providing insight on mitochondrial dynamics within human skeletal muscle to suggest mitochondrial adaptations with increases in the range of 41 to 55 % for mitofusion proteins and up to 117% for fission (168). These adaptations to MICT were also observed by Axelrod et al. (11) for the same proteins that influence mitochondrial dynamics, in addition to increases in protein expression of Dynamin-like

120 kDa protein (OPA1) and metalloendopeptidase (OMA1) which contribute to mitochondrial quality control. However, a decrease in the expression of Parkin protein and FIS1 was observed (~50%). In response to HIIT Granata et al (106) found no significant changes to MFN2 or DRP1. While the regulation of mitochondrial protein Apoptosis Inducing Factor (AIF) showed consistent findings in differing training types with no change in the protein content of AIF observed following MICT (3) or after both high and reduced volume HIIT. Thus there are contrasting results in regard to changes in the different mitochondrial remodelling proteins and further research is needed to better determine the effects of different types of exercise on these proteins.

Chaperone and transport proteins that typically result in the greater import of matrix precursor proteins into mitochondria (310) have also been investigated in human training studies with varying responses to heat shock proteins which have revealed in most cases no significant changes with training types (3, 80, 81, 205). Uncoupling protein, UCP3, an anion carrier and important mediator of thermogenesis responds differently to training type, with increases to MICT and decreases with SIT interventions. While transporter protein, monocarboxylic acid transporter (MCT1 and MCT2) that allows lactic acid to enter the mitochondria increases in response to HIIT (239). Additionally, the protein import machinery composed primarily of the translocases of the outer membrane (TOM complex) including receptor proteins such as TOM20 has been shown to increase in response to chronic contractile activity; however, research also showed MICT showed did not alter the response of TOM20 but did evoke a 1.4-fold increase in mitochondrial heat shock protein 70 (HSP70) (3).

In many cases, changes in mitochondrial proteins between animal in humans are similar with training. Some discrepancies appear to exist in protein responses with SIT studies. Comparisons of SIT in humans and animals models have many limitations as animals (i.e., rodents) do not have the ability to do higher intensity training in a controlled manner. Additionally, this may indicate increases in some individual mitochondrial protein responses may differ between species and training types. Furthermore, some evidence suggests volume and/or intensity affects changes in mitochondrial proteins, but this has only been done for a select few mitochondrial proteins.

Despite obvious successes and the convenience of western blotting as a method (which was developed decades ago) for protein detection, limitations still exist with this method. For instance, the use of western blotting is semiquantitative at best and available antibodies can be of poor specificity (90). Antibody reagents are poor or non-existent for many proteins (196). Therefore, it is imperative that researchers undertake their own antibody validation for tissue specific analysis (220). A more fundamental limitation of this method lies in its targeted nature. Using *a priori* antibody selections, researchers can only find what they look for. Thus, unexpected effects in proteins will often go undiscovered. As a result, the cell is not seen as a whole system and researchers explore the same coverage repeatedly. For example, of the studies highlighted in Table 1.2, only a small fraction (less than 60, or only approximately 5 %) of the more than 1100 proteins collated in the MitoCarta inventory for mitochondrial proteins have been reported (43). Another limitation is that these analyses are typically done on whole muscle and therefore we make assumptions and don't truly know the changes relative to changes in total mitochondrial protein at a fibre-specific level.

The increasing use of proteomic approaches, which allow the large-scale study of proteins, has the potential to increase our understanding of the breadth and complexity of changes in mitochondrial protein following exercise training. In most cases, proteomics will reveal more changes than previously anticipated and provide greater scope for a greater array of new scientific findings. It is important to take advantage of recent advancements in proteomic techniques to give a more accurate representation and move beyond the measurement of a few proteins to measure training-induced changes in hundreds to thousands of mitochondrial proteins in skeletal muscle fibres (218, 234, 284).

### 1.3.2 Proteomic Approaches

Powerful mass spectrometry (MS)-based technologies now provide unprecedented insights into the composition, function, and control of the proteome, shedding light on complex biological processes – including the effects of exercise training on mitochondrial proteins. Proteomics is essentially the large-scale study of proteins. Virtually every mass spectrometry-based proteomic workflow consists of three distinct stages:

(i) Protein samples are isolated from their biological source and optionally fractionated. The final protein sample is then digested, and the resulting peptide sample is further fractionated and typically separated by chromatography (when using liquid chromatography based mass spectrometry - LC-MS).

(ii) The peptides are subjected to qualitative and quantitative mass-spectrometric analysis. Fundamentally, MS measures the mass-to-charge ratio ( $m/z$ ) of gas-phase ions. Mass spectrometers consist of an ion source that converts analyte molecules into gas-phase ions, a mass analyser that separates ionised analytes based on their  $m/z$  ratio, and a detector that records the number of ions at each  $m/z$  value. The mass analyser is central to MS technology, and for proteomics research the common types of mass analysers are quadrupole, ion trap, and time-of-flight mass analysers. They vary in their physical principles and analytical performance. “Hybrid” instruments have been designed to combine the capabilities of different mass analysers (114). In tandem MS (MS/MS), selected LC-MS peaks are analysed by a collision-induced dissociation (CID) and a second MS scan recorded.

(iii) In the analysis of LC-MS/MS data, the relative abundance of species in a sample is generally quantified by the spectral count or some measure of the species' ion abundance derived from an analysis of its feature peak signature in LC-MS space. The large data sets generated are then analysed by suitable software tools to deduce the amino acid sequence and, if applicable, the quantity of the proteins in a sample. The peptide identity is assigned to the tandem mass spectrometry (MS/MS) spectra through database searching and a subsequent statistical analysis of the search results is performed (160) (Figure 1.8).

The data acquisition is typically categorised into two forms, either data dependent acquisition (DDA) or data independent acquisition (DIA). In MS, DIA is a method of molecular structure determination in which all ions within a selected  $m/z$  range are fragmented and analysed in a second stage of tandem mass spectrometry. In DDA, a fixed number of precursor ions are selected and analysed by tandem mass spectrometry (110).

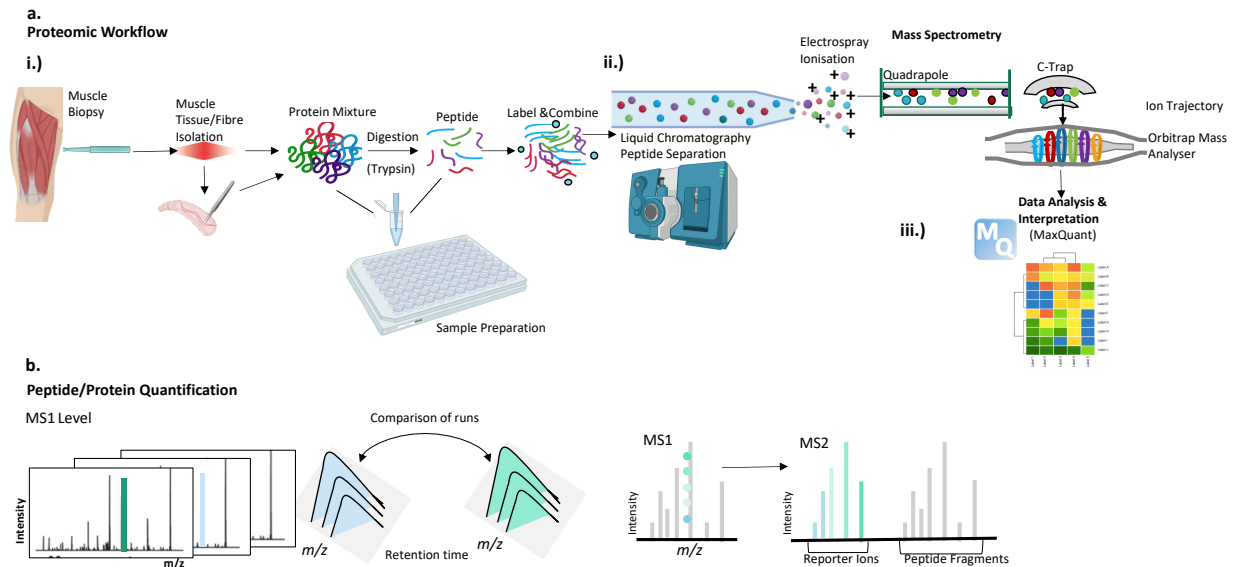


**Figure 1.8-** Overview of LC-MS-based proteomics : Proteomics workflows begin with proteins being extracted from biological samples (i.e. skeletal muscle tissue). In the sample-preparation stage proteins are extracted and digested by a sequence-specific enzyme such as trypsin. Current methods of protein preparation are highly efficient and can be performed in 96-well plates. Peptides are then separated by means of chromatography and ionised, after which they are introduced into the vacuum of a mass spectrometer. Each MS scan results in a mass spectrum, measuring mass to charge ratio ( $m/z$ ) values and peak intensities. Based on observed spectral information a full spectrum of the peptides is acquired at the MS1 level followed by the collection of as many fragmentation spectra at the MS2 level. Database searching is typically employed to identify the peptides most likely responsible for high-abundance peaks. Finally, peptide information is rolled up to the protein level, and protein abundance is quantified using either peak intensities or spectral counts (160). A quadrupole–orbitrap mass analyser is depicted. b.) Results are then interpreted using software packages such as MaxQuant. Samples can be multiplexed with tags and the fragment spectra are interpreted. Peptide identities can also be transferred when the peptide is fragmented in only one of the runs but matches precisely the mass and elution time of an aligned peak (known as the 'match between runs' feature in MaxQuant). Peptides/proteins can also be subjected to label-free quantification at the MS2 level. In this case, the fragment-ion intensities that are unique to a specific peptide are used for quantification. In multiplexed shotgun proteomics, up to sixteen samples are labelled differentially so that they release reporter ions that can be distinguished in the MS2 spectra (4).

Fundamental explanations behind the achievement of mass spectrometry in proteomics incorporate its intrinsic specificity to identify the nature of the proteomics workflow and its potential for extreme sensitivity that theoretically could identify down to a single ion. Practically, it has been challenging for researchers to reach the full potential of the technique; however, innovative ways of implementing mass spectrometry as a widespread detector of protein identity, abundance, precise chemical state, and cellular

context are continually being devised. At present, no single mass-spectrometry-based system or method can determine by itself these diverse dimensions for proteome data (4). Here the main proteomic approaches that have been utilised for the analysis of skeletal muscle are highlighted.

Historically, gel-based proteomics was one of the most commonly used methods for separating protein complexes. Among these methods, two-dimensional-polyacrylamide gel electrophoresis (2-DE) was one of the first and most popular methods used to simultaneously separate, identify, and quantify proteins when subsequently coupled with mass spectrometric identification. Although 2-DE was first introduced more than three decades ago, several challenges and limitations to its efficacy still exist. Quantitation of proteins using 2-DE has been limited due to the lack of robust and reproducible methods for detecting, matching, and quantifying spots, as well as some physical properties of the gels.

2-DE consists mainly of two steps of separation. In the first dimension, protein molecules are separated depending on their isoelectric point (pI) under a pH gradient. In the second dimension, proteins are further separated by mass, this can result in low reproducibility, and different types of proteins can often be missed due to the difficulty in separating membrane-bound, hydrophobic proteins. Notably, highly acidic or basic proteins are neither easily extracted nor solubilised. This difficulty in extraction relies mainly on the solubilisation power of the buffer used (195). Additional sources of error in the gel analysis is unequal precipitation of the proteins between gels. Thus, horizontal or vertical shifts can be seen in two-dimensional (2D) gels, necessitating alignment of all the gels to a reference gel. After gel alignment, spot detection and removal is performed, which may introduce further errors. The excised gel plugs are then transferred to microplates or other vessels for proteolytic digestion and further MS analysis. Mismatched spots compromise the ability to detect differentially expressed proteins since different proteins are mistakenly grouped together for the analysis, causing analysis challenges and introducing potential bias.

Two-dimensional difference gel electrophoresis (2D-DIGE) is a modified form of 2-DE that allows one to compare two or three protein samples simultaneously on the same gel. The proteins in each sample are covalently tagged with different colour fluorescent dyes

that are designed to have no effect on the relative migration of proteins during electrophoresis. Proteins that are common to the samples appear as “spots” with a fixed ratio of fluorescent signals, whereas proteins that differ between the samples have different fluorescence ratios. A limitation of 2D-DIGE is the fact that proteins without lysine cannot be labelled, and additionally the method requires special equipment for visualisation and fluorophores tend to be very expensive (325). As with 2-DE, extracted proteins are identified by subsequent MS analysis.

A LC-MS-based proteomic experiment requires several steps of sample preparation. Complex mixtures of proteins are first subjected to lysis to break cells membrane using a lysate buffer followed by enzymatic cleavage using a proteolytic enzyme. The resulting peptide products are analysed using a mass spectrometer as previously mentioned. A standard experiment has the following key steps (i) extraction of proteins from a sample, (ii) fractionation to remove contaminants and proteins that are not of interest, (iii) digestion of proteins into peptides, (iv) post-digestion separations to obtain a more homogeneous mixture of peptides, and (v) analysis of ionised proteins by MS. In LC-MS/MS, for example, the most abundant peptides are selected in the first MS step for further fragmentation in the following MS step, and only peptides selected for further fragmentation have a chance to be identified (160). The two fundamental challenges in the analysis of MS-based proteomics data are then the identification of the proteins present in a sample, and the quantification of the abundance levels of those proteins. There are a host of informatics tasks associated with each of these challenges. With MS, no individual method is able to identify all proteins. Additionally, matrix-assisted laser desorption/ionization (MALDI) and electrospray ionisation (ESI) do not favour identification of hydrophobic peptides and basic peptides (47) (Figure 1.8). Significant technological progress that was made in MS over the last decade has substantially improved the quality of proteomics data. Of many possible instrument configurations, quadrupole–orbitrap analysers dominate DDA proteomics. With the Orbitrap analyser the ion motion is determined by an electrostatic field, providing higher resolving power, detection limits, dynamic range, and speed of analysis, which also lends itself to multiplexing techniques (345). This has now been applied to extremely complex biological samples with challenging dynamic ranges, such as skeletal muscle tissues. The ability to apply a single shotgun (a typical term for bottom-up proteomics referring to identification of proteins by proteolytic digestion prior to MS analysis) experiment for

the detection of functionally important low-abundant proteins in addition to thousands of other proteins has been a significant development in understanding the breadth and complexity of proteins at the cellular level in skeletal muscle. The key to this application is using a simple and controlled sample preparation protocol (47).

Notwithstanding some of the limitations described above, proteomics techniques enable researchers to undertake more comprehensive investigations and provide a pragmatic approach to discovering novel changes at the protein level. Recent publications have described the skeletal muscle proteome (270) and the changes that occur during development (61), ageing (61, 218, 228), obesity (123), and type 2 diabetes (46), or in response to experimental interventions such as denervation (40) and chronic low-frequency stimulation (70, 71). Early proteomic studies identified that most of the proteins of skeletal muscle are localised in the sarcomere (i.e., myosins, actins, troponins, tropomyosins, and auxiliary proteins of sarcomeric units), representing about 55–60% of the total proteins. Mitochondrial proteins constitute around 6% of the total proteins found in skeletal muscle (258), confirming its importance in muscle for energy metabolism. Many of these sarcomeric, glycolytic, and mitochondrial proteins exist in different isoforms, which may also affect the functionality and protein synthesis in skeletal muscle (100).

The application of proteomics to investigate the effect of exercise training on mitochondrial proteins is in its infancy, with only four studies in animals (31, 40, 166, 338) and only four studies in humans (74, 107, 129, 134) have been published in the area of exercise training. A summary of proteomic training studies is presented in Table 1.3. These studies have evolved from gel-based proteomics in both animals and humans, with their previously discussed limitations, to the adoption of shotgun in-solution proteomics coupled with LC-MS in human training studies (Figure 1.9a). The evolution of the use of proteomic methods to investigate responses to training and exercise over the past decades is presented in Figure 1.9b. Studies investigating changes in the mitochondrial proteome in response to exercise have increased, though limited and even fewer studies have delved into long-term training effects. Over time, the ability to identify differentially expressed mitochondrial proteins has provided novel insights into the process of muscular plasticity and placed key importance on the development of exercise-based strategies in the

prevention and therapy of many chronic inflammatory and degenerative diseases that are accompanied by muscle deconditioning.

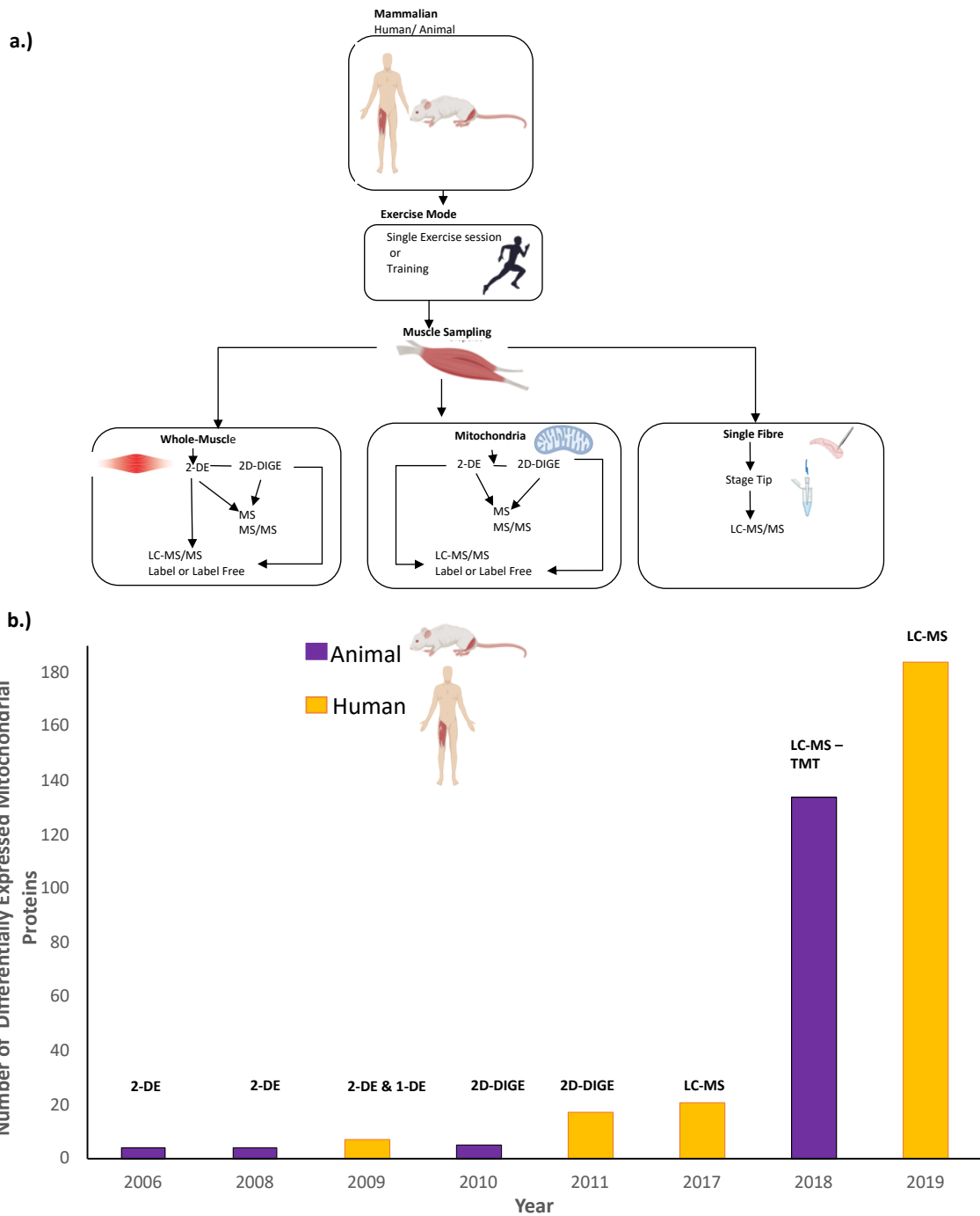


**Figure 1.9** – a.) Summary of the types of MS-based proteomics methods for training studies. 2DE - two dimensional- polyacrylamide gel electrophoresis, 1DE – 1 dimension gel electrophoresis, 2DIGE - two-dimensional fluorescence difference gel electrophoresis, LC-MS – Liquid Chromatography coupled with Mass Spectrometry. TMT – Tandem Mass Tag Labelling. Adapted from (235). b.) Identification of mitochondrial proteomes over the years looking at the number of differentially expressed mitochondrial proteins identified in response to training in animal and human studies, and the method of proteomic analysis.

### 1.3.2.1 Animal Studies

Although an earlier study utilised proteomics to investigate mitochondrial protein changes in rodent cardiac muscle in response to aerobic training (31), only three studies in rodents have investigated these changes in skeletal muscle (40, 166, 338). Burniston (40) was the first to progress from cardiac to skeletal muscle. Animals in the exercise group trained for 30 minutes at 70 to 75% of their  $\dot{V}O_{2\text{peak}}$  for 4 days/week for 5 weeks. The study identified 187 gel spots corresponding to 40 unique proteins by 2-D gels and 11 identified by MS that were differentially expressed after training. Changes were observed in four mitochondrial proteins. The only protein consistent with the earlier study in cardiac muscle (31) was TPI1, a protein associated with glucose metabolism that was also increased in skeletal muscle. However, two other glycolytic proteins were reported to decrease (lactate dehydrogenase A and  $\beta$ -enolase). Exercise-induced increases in aconitase (ACO2), which had not previously been observed were also reported. Mitochondrial ACO2 is important in the catalysis of the reversible conversion of citrate to isocitrate in the TCA cycle.

Another study (338) had rats perform daily HIIT over 5 days (14 x 20-s swimming bouts, 10 s rest). Using 2-DIGE, they identified 800 detected matched spots and 13 proteins with altered expression after HIIT. Of these, five were mitochondrial including three OXPHOS proteins (two complex I subunits NDUF51 and NDUF52 and one complex V, ATP synthase b-subunit (ATP5B)). There was also two TCA proteins - oxoglutarate dehydrogenase (OGDH) and mitochondrial malate dehydrogenase (MDH). This is the first report to show that exercise training induces NDUF5 protein expression, which catalyse NADH oxidation with concomitant ubiquinone reduction and proton export out of mitochondria. While up-regulation of ATP5B after HIIT was detected by 2D-DIGE analysis, this was not shown to significantly differ when validated with western immunoblot analysis. These discrepancies could be attributed to unsatisfactory specificity of the antibodies to these proteins (88, 250). The combination of proteomic technology and a training protocol previous utilised in another study (315) that had shown increases in citrate synthase following HIIT revealed new information on mitochondrial proteins not previously investigated by other analysis techniques.

It's worth noting that in these early proteomic studies many proteins that would be expected to change based on earlier studies investigating mitochondrial protein responses to training using classical immunoblotting techniques were not observed (e.g. CS, COXIV, NDUFA8 and MFN1/2; Table 1.2). In addition, these studies using 2-DE tend to resolve a high abundance of myofibrillar proteins, and glycolytic enzymes, and yet only relatively few mitochondrial proteins. This was further observed in a later 2DE proteomic study of MICT in mice where only 5 mitochondrial proteins were observed to be differentially expressed including ATP5A which is inherently related to the regulation of creatine kinase (CKMT2), glucose and pyruvate metabolism related PDHA1, TCA cycle related MDH2, and previously reported ACO2 (45). The lack of overlap between the 2-D and 2DIGE studies raises further questions regarding the sensitivity of the two methods. This highlights an important consideration regarding the reporting of 2-D gel and 2-DIGE analyses. Clearly, when a gene product is present as multiple 2-D gel spots, it is misleading to report a change in expression of an individual spot as being indicative of a change in the expression of the entire gene product. A more appropriate approach would be to report which gene products are present as multiple spots and which of these spots were altered by the experimental intervention. While all these early studies launched the field of proteomics in exercise sciences, confirming some data obtained from transcriptomic studies, it should be noted that the use of gel electrophoresis methods is limited to the analysis of abundant and soluble proteins. Many variables can interfere with the results observed in studies using 2-DE, including the protein extraction protocol, the *pI* and molecular mass ranges used to separate the proteins, the immobilised pH gradient (IPG) strip length, how missing values are addressed, and even the particular statistical analysis used.

More recently, a study of mice eating various diets, which trained for 20 weeks for 6km/day found an increased number of 134 differentially expressed proteins (DEP) using a sensitive LC-MS coupled with tandem mass tagging (TMT) labelling technology. The study found significantly enriched mitochondrial proteins in endurance-trained chow-fed mice related to OXPHOS (36 DEP), fatty acid metabolism (19 DEP), and mitochondrial transport (17 DEP) (166).

### 1.3.2.2 Human Studies

Two studies have used gels and MS to investigate training-induced mitochondrial proteins in human skeletal muscle. Similar to the animal studies, changes in relatively few mitochondrial proteins were identified. The first application of proteomic techniques to human muscle investigated the impact of six weeks of interval training (6 x 1-min bouts at 90–100%  $VO_{2max}$ , interspersed by 4 min at 50%  $VO_{2max}$ ) for 30 minutes three times per week (129). Protein expression profiling was performed using differential analysis of 2-DE gels, complemented with quantitative analysis of tryptic peptides from 1-DE gel lane-segments. Using a false discovery rate (FDR) of 10%, they observed 20 gel spots that were significantly changed (from 256 spots detected). The gene products differentially expressed after interval training were categorised as metabolic enzymes, myofibrillar proteins, heat shock proteins, and transport proteins. Yet again, due to the high abundance of myofibrillar proteins and glycolytic enzymes, relatively few mitochondrial proteins were resolved using broad-range 2-DE. However, using 1-DE combined with LC-MALDI and iTRAQ they confidently identified increases in the expression of seven mitochondrial proteins involved in oxidative phosphorylation (complex I subunit NDUFV1, complex II SDHA, and complex V ATP synthase  $\alpha$  and  $\beta$  subunits (ATP5A1 & ATP5B)), fatty acid metabolism (ACADVL & HADHA), and the TCA cycle (ACO2); the latter was consistent with the findings by Burniston in animals (40). Training significantly increased the expression of succinate dehydrogenase ubiquinone flavoprotein (SDHA), which has previously been reported as a marker of mitochondrial density (65, 135, 145, 162). Interval training also increased the expression of proteins that catalyses the last three steps in the  $\beta$ -oxidation of fatty acids -hydroxyacyl-CoA dehydrogenase (HADHA) and acyl-CoA dehydrogenase (ACADVL). The increased expression of this enzyme suggests a greater capacity to oxidise fatty acids, which aligns with findings of previous studies (39).

A subsequent study examined the effects of two weeks of short-term endurance training (60 min per session at the target exercise intensity of 80%  $VO_{2peak}$  on 14 consecutive days) on the mitochondrial proteome in the skeletal muscle of sedentary participants (74). Mitochondria-enriched protein fractions were obtained from skeletal muscle biopsies at baseline and following training. It should be noted that the use of the mitochondrial fraction of the skeletal muscles may assist in reducing issues associated with the large

amount of myofibrillar proteins. The samples were subjected to 2-D Difference Gel Electrophoresis (2-DIGE) analysis with subsequent MS followed by database interrogation to identify the proteins of interest. Thirty-one proteins were identified as differentially expressed after either 7 or 14 days of training, and 17 of these were mitochondrial proteins. These proteins included subunits involved in OXPHOS, enzymes of the TCA cycle, as well as chaperone and mitochondrial transport proteins. Notably, differential expression of proteins involved in the TCA cycle (malate dehydrogenase 2, (MDH2) and Fumarase (FH)) were observed. An increase in the expression of mitochondrial transport Adenylate Kinase 3 (AK3) was also observed. Additionally, chaperone proteins (10 kDa Heat Shock Protein; mitochondrial (HSPE1) and protein disulfide isomerase A3 (PDIA3) were found to increase, while  $\alpha$ -Crystallin B chain (CRYAB)) protein was found to decrease. These are proteins that have been less notable in classical training studies. There were also changes in associated malate-aspartate shuttle protein glutamic-oxaloacetic transaminase (GOT2) and manganese superoxide dismutase (SOD2) protein, which binds to the superoxide by-products of oxidative phosphorylation and converts them to hydrogen peroxide and diatomic oxygen. Only two mitochondrial proteins, both subunits of ATP synthase (ATP5A1 & ATP5B), were commonly expressed by Egan's (74) and Holloway's (129) study. It should be noted, however, that both studies utilised different gel separation techniques and also performed different types of training (HIIT vs MICT). There was an additional overlap of ATP5B with an animal study using HIIT (338). A novel observation in this proteomic research was the reduction in the abundance of the complex IV subunit COX5A, which was not previously observed but its analogous protein is repeatedly reported to increase with training when analysed by western blot (3, 187, 193, 199, 272, 274, 301, 311, 333). An increase in COX complex activity has also classically been observed in response to exercise training (126). Classical immunoblotting studies have repeatedly reported increases in complex I proteins following both HIIT and MICT, whereas the application of proteomics has shown there is differentiation between training type and functional pathways (c.f. Table 1.2). The application of proteomics to humans began to reveal additional proteins either typically seen with immunoblotting analysis or those that are known to be part of functional pathways but not targeted in training studies.

As noted earlier, while providing important new information, there are limitations to gel-based approaches. The use of more sensitive methods was required to counter some of

the limitations and led to the development of state-of-the-art proteomic strategies such as gel-free mass spectrometry-based methods, including shotgun proteomics linked to label-free or stable isotope-based relative quantifications. When applied to exercise studies, this unlocked a transition from “*blind proteomics*”, which creates databases as resources for further biological follow-up, to *specific-driven proteomics*, in which proteomics is based on clearly defined biological questions in an integrative perspective and proteins are identified from an ever increasing database of mitochondrial proteins (43, 85).

Granata et al. investigated how different training volumes influence mitochondrial proteins. Ten healthy participants performed HIIT during three consecutive training phases of normal-volume training, followed by high-volume training and 2 weeks of reduced-volume training. Using LC-MS, the study quantified the relative abundances of 1411 proteins from an enriched mitochondrial fraction, including 721 known mitochondrial proteins across all participants and timepoints. The study readily detected cytoskeletal proteins associated with the mitochondria, and their levels had a strong inverse correlation with the relative abundances of mitochondrial proteins. The study overcame this via structural remodelling *in-silico*, allowing the identification of 184 mitochondrial proteins differentially regulated in response to different volumes of exercise training. Highlights include a temporary repression of oxidative phosphorylation and an increase in amino acid degradation with an initial training volume, followed by increases in tricarboxylic acid cycle and mitochondrial biogenesis proteins with additional training. As seen in Figure 1.10, many of the differentially expressed mitochondrial proteins observed in Granata’s study correspond with typical findings of all recent immunoblotting studies (c.f. Table 1.2). In addition, a further 173 mitochondrial proteins that have not previously been studied with the targeted nature approach of immunoblotting techniques were observed. Novel observations by Granata include the ability to observe an unprecedented number of mitochondrial proteins that respond to training. In particular, changes were observed for a host of mitochondrial ribosomal proteins (i.e., MRPS5, MRPS22, & MRPL4 mitochondrial ribosomal protein S5, mitochondrial ribosomal protein S22, and Mitochondrial Large Ribosomal Subunit Protein 4). Of note, the study identified differentially expressed mitochondrial proteins related to the following GO and KEGG pathways; 42 proteins involved with OXPHOS (12 complex I, 2 complex 2, 5 complex III, 2 complex IV, 5 complex V) and respiratory chain processes including novel cytochrome c-heme lyase (HCCS) which links

covalently the heme group to the apoprotein of cytochrome c, 49 proteins with TCA cycle & other metabolism, 29 mitochondrial proteins associated with fatty acid oxidation, 15 mitochondrial proteins associated with pyruvate metabolism and ubiquinone synthesis, 18 mitochondrial proteins associated with protein import and organisation and an additional 32 mitochondrial proteins associated with cristate formation and various cellular functions. This included metaxin-1 and metaxin-2 (MTX1 and MTX2), which were also observed as being differentially expressed in single-fibre proteomic studies with denervation (174).

The crossover of proteins identified in the early human training studies is shown in Figure 1.10a. There is limited cross over in the proteins identified and there has been an increasing number of proteins identified in the latter years with the advancement of proteomic technologies. In all three human studies, ATP synthase subunits  $\alpha$  &  $\beta$  were the only mitochondrial proteins consistently identified as upregulated. This is not surprising given its role in skeletal muscle, with contractile activity being directly dependent on the supply of adenosine triphosphate (ATP) to three ATPases. This analysis highlighted a training-related proteome signature characterised by the up-regulation of the capacity for ATP generation. In addition SDHA, ACADVL, ACO2 were common to Holloway and Granata, and AK3, Creatine Kinase Mitochondrial 2 (CKMT2), dihydrolipoamide dehydrogenase (DLD), FH, HSPE1, MDH2, NADH:Ubiquinone Oxidoreductase Subunit A13 (NDUFA13), SOD2 and TUFM were common to Granata and Egan. These proteins belong to a mixture of pathways associated with the tri-carboxylic acid (TCA) cycle, complexes essential for the breakdown of molecules to produce energy in cells, mitochondria organisation and transport, fatty acid beta-oxidation, and cristae formation, representing proteins that are not typically targeted by western blot training studies, highlighting the discovery potential of MS.

In addition, prior to Granata's work some recent studies utilising proteomic technologies have investigated the influence of HIIT in conjunction with various treatments (134, 142). A study using gel-free based proteomics observed dominantly upregulated pathways that were related to the mitochondria, in particular proteins associated with oxidative phosphorylation, which represented 57% of the total number of proteins upregulated, as well as metabolic pathways, including glycogen metabolism. Of the 486 proteins identified as human skeletal muscle proteins, training upregulated the expression of 26

proteins and downregulated the expression of 6 proteins (134); of these, 21 were mitochondrial and 10 were in common with the work of Granata et al. This included complex I subunits NDUFA2 and NDUFS6 and complex V subunits ATP5H and ATP5J. Additionally, 2DE proteomic analysis of the response of type 2 diabetes participants with HIIT have shown alterations of 13 mitochondrial proteins involved in energy metabolism via glycolysis, the TCA cycle, OXPHOS, or  $\beta$ -fatty acid oxidation. Of these, common to Granata and other proteomic training studies there were changes in MDH2, mitochondrial creatine kinase (CKMT2), isoform 1 of succinyl-CoA ligase (ADP-forming) subunit beta (SUCLA2), isoform cytoplasmic of fumarate hydratase (FH), trifunctional enzyme subunit alpha (HADHA), and complex subunit V ATP5A1. In a similar manner to training, the power of physical activity to alter mitochondrial proteins was demonstrated in another proteomic study employing isotopic labelling techniques. The study focused on assessing the association of daily physical activity with the muscle proteome in healthy individuals and found that high levels of physical activity were coupled with an overrepresentation of 102 mitochondrial proteins, including those in the TCA cycle and chaperone proteins (320). This analysis identified 27 mitochondrial proteins in common with Granata's training study.

The key findings of proteomic studies investigating the response to human training is presented in Figure 1.10b, which provides insight into the numerous cellular processes identified. Further to this, the biological processes represented by the 203 differentially expressed mitochondrial proteins in these four training studies were examined by performing enrichment analysis of Gene Ontology (GO) biological processes using the Protein ANalysis THrough Evolutionary Relationships (PANTHER) classification system (316). This analysis has highlighted processes significantly ( $P < 0.05$ ) represented by the mitochondrial proteome and includes those processes associated to mitochondrial functions in skeletal muscles such as oxidative phosphorylation (OXPHOS), glycolysis, the tricarboxylic acid (TCA) cycle, mitochondrion organisation/ transport, fatty acid beta-oxidation, and cristae formation.

The lack of common differentially expressed proteins identified in each of the training studies leads to the question as to why there is a lack of commonality. Can this be attributed to the type of training performed or is it a matter of technology and methodology with increased capacities of more current MS instrumentation in addition

to the preparation of samples? Indications from several immunoblotting studies have shown that mitochondrial proteins can respond differently to training type (c.f. Table 1.2). Furthermore, as previously stated, the use of 2D-DIGE and 1D & 2D gels require the gels to be excised and then digested for loading into the MS instrumentation. More recent methodologies perform lysis, alkylation, and digestion in the one vessel decreasing the likelihood of sample loss. In the early era of proteomics, gel electrophoresis was a dominant technique of sample preparation for mass spectrometry analysis. Particularly, 2D electrophoresis provided high-resolution proteome separation, and was regarded as the standard methodology for the separation of proteomes from a wide-range of tissue types. However, gel electrophoresis turned downwards in its application due to the progress of other separation techniques, including liquid chromatography and ionisation techniques, with resulting gel-free proteomics finally becoming dominant players at present. Analysis of publication counts related to “gel-based” and “gel-free” proteomics (quoted from PubMed, <https://www.ncbi.nlm.nih.gov/pubmed/>) reveal a rapid decline in gel-based approaches from 2009, whereas, in contrast, gel free approaches that can handle highly complex peptide mixtures without gel-separation have seen a steady increase from that point in time (165) (Figure 1.11).

These various methods for studying mitochondrial protein adaptations in skeletal muscle represent analysis have been confined to the analysis of whole-muscle samples, where the results may be confounded by changes in a mixture of type I and II fibres. Integrating recent advances in proteomic techniques and MS with the study of single fibres could provide new information regarding mitochondrial protein changes that are divergently regulated in type I and II fibres in response to exercise training.

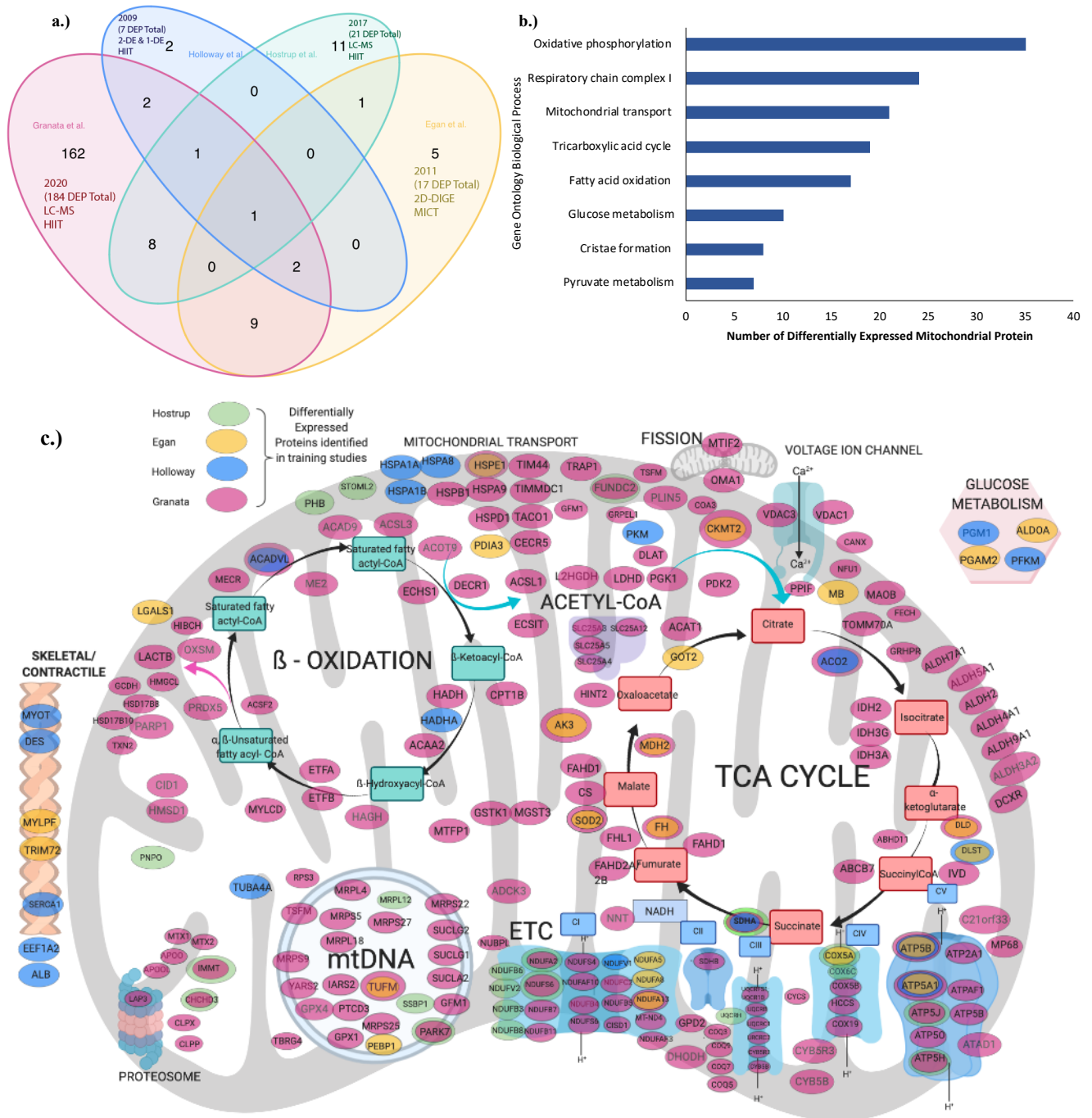


**Figure 1. 10**– (a.) Number of mitochondrial proteins identified as differentially expressed by individual training studies in humans (b.) Biological processes by gene ontology (GO) enrichment analysis in which the identified proteins are mainly involved. The bars represent  $-\log_{10}(P)$ , where P represents the significance of each GO biological process enriched by the mitochondrial proteins. The P-value was computed using GO enrichment analysis by Protein ANalysis THrough Evolutionary Relationships (PANTHER) (316). (c.) Network model describing cellular processes and interactions of the Differentially Expressed Proteins (DEP) in mitochondria. Colours denotes the study in which the specific protein was identified, and any DEPs mutually identified. Only ATP5A & ATP5B were identified as changing with exercise in all 3 studies. In addition SDHA, ACADVL, ACO2 were common to Holloway and Granata AK3, CKMT2, DLD, FH, HSPE1, MDH2, NDUFA13, SOD2 and TUFM were common to Granata and Egan. FUNDC2, NDUFA2, NDUFS6, ATP5H, ATP5J, SDHA, CHCHD3, IMMT, PARK7 & HSPB1 were common to Granata and Hostrup. Created with BioRender.com

**Table 1. 3- A summary of studies that have focused on the proteomic profiling of skeletal muscle in response to exercise training**

Year (Reference)	Exercise Training Protocol	Species (tissue)	Volume a. total duration b. volume x intensity	Protein Separation	Detection	Number of Differentially Expressed Mitochondrial Proteins	Results
2006 (31)	Training - six weeks of progressive treadmill training 5 days/wk, 1 h in duration (n=30)  5 days/week. 5 min runs at 33 m/min were alternated with 5-min in which the speed was incrementally increased each minute to a maximum of 66 m/min The total duration was 10 min for the first week and was increased 2 min each day thereafter	Rats (heart - left ventricular free wall)	a. 225 min b. 180	2-DE	MALDI-TOF/TOF MS	4	<ul style="list-style-type: none"> <li>• 2-fold increase, in TCA associated DLST (dihydrolipoamide S-succinyltransferase) protein, &amp;</li> <li>• 2-fold increase in associated glucose metabolism proteins triosephosphate isomerase 1 (TPI1) and glyceraldehyde-3-phosphate dehydrogenase (GAPDH)</li> <li>• OXPHOS related ATP synthase D-chain (ATP5D) decreased by 60%</li> </ul>
2008 (40)	Moderate intensity exercise study 4 days/wk, over 5 weeks. (n = 12)  Animals in the exercise group trained for 30 min at 70–75% of their $\dot{V}O_2$ peak, which equated to a treadmill speed of 12 m/min	Rats (Skeletal Muscle - plantaris)	a. 600 min b. 450	2DE	MALDI-TOF	4	<ul style="list-style-type: none"> <li>• Changes in related glucose metabolism proteins lactate dehydrogenase A and <math>\beta</math>-enolase</li> <li>• Decrease in TCA associated aconitase (ACO2)</li> <li>• Increase in in associated glucose metabolism protein TPI1.</li> </ul>
2010 (338)	HIIT (Swimming) - For 5 days, rats performed HIIT, which consisted of 14 20-s swimming exercise bouts carrying a weight (14% of the body weight), and 10-s pause between bouts. (n=4)	Rats (Skeletal Muscle - epitrochlearis muscle)	a. 20 s bouts, total bouts unspecified b. n/a	2D-DIGE	MALDI-TOF/TOF MS	5	<ul style="list-style-type: none"> <li>• Altered expressions in OXPHOS proteins in complex I subunits NDUFS1 and NDUFS2 and complex V ATP synthase b-subunit (ATP5B)</li> <li>• Changes in TCA proteins oxoglutarate dehydrogenase (OGDH) and mitochondrial malate dehydrogenase (MDH),</li> </ul>
2018 (166)	MICT – 20 weeks, 6 km/day	Mice (gastrocnemius)	a. unspecified b. n/a		LC-MS with TMT labelling	134	<p>Significantly enriched mitochondrial proteins in endurance trained chow-fed mice related to:</p> <ul style="list-style-type: none"> <li>• OXPHOS (36 DEP),</li> <li>• fatty acid metabolism (19 DEP), and</li> <li>• mitochondrial transport (17 DEP)</li> </ul>

Year (Reference)	Exercise Training Protocol	Species (tissue)	Volume a. total duration b. volume x intensity	Protein Separation	Detection	Number of Differentially Expressed Mitochondrial Proteins	Results
2009 (129)	HIIT - six weeks of progressive treadmill training 3 days/week, 30 min duration (n=5).  Session – 6 x 1-min bouts at 90–100% VO <sub>2peak</sub> , interspersed by 4 min at 50% VO <sub>2peak</sub> .	Human (Skeletal Muscle - vastus lateralis)	a. 540 min b. 324	2-DE & 1-DE	LC-MALDI-TOF/TOF MS with iTRAQ labelling	7	Interval training increased: <ul style="list-style-type: none"> <li>OXPHOS proteins - Complex I - NDUFV1, complex II SDHA and complex V ATP synthase a- and b-chains (ATP5A1 &amp; ATP5B)),</li> <li>Greater expression of in fatty acid metabolism proteins (ACADVL &amp; HADHA)</li> <li>Increase in TCA associated ACO2</li> </ul>
2011 (74)	MICT for 60 min per session at the target exercise intensity of 80% VO <sub>2peak</sub> on 14 consecutive days (n=8)	Human (Skeletal Muscle - vastus lateralis)	a. 840 min b. 672	2D-DIGE	LC-MS	17	Extensive remodelling of the mitochondrial proteome occurring after just 7 days of exercise training. Including alterations in: <ul style="list-style-type: none"> <li>OXPHOS complex I units NDUFA13, NDUFA5, NDUFA8 and complex V ATP subunits ATP5A1, ATP5B, and associated by-product manganese superoxide dismutase (SOD2) protein</li> <li>Increases in TCA proteins malate dehydrogenase 2, (MDH2) , Fumarase (FH))</li> <li>Increases in mitochondrial transport and chaperone proteins (Aspartate aminotransferase (AK3), 10 kDa Heat Shock Protein; mitochondrial (HSPE1), protein disulfide isomerase A3 (PDIA3), and α-Crystallin B chain (CRYAB)</li> <li>Increase Glucose metabolism associated protein Glutamic-oxaloacetic transaminase (GOT2)</li> </ul>
2017 (134)	HIIT - four weeks of 3 days/week, 30 min duration (n=5).  Session – 3 x 10-min bouts at 85% VO <sub>2peak</sub> , with 30 s all out sprint at the end	Human (Skeletal Muscle - vastus lateralis)	a. 360 min b. 672		LC-MS	21	Dominated by training response in OXPHOS proteins including: <ul style="list-style-type: none"> <li>OXPHOS complex I units NDUFA2, NDUFS6, NDUFB6, NDUFB3, &amp; NDUFB8, complex II unit SDHA, complex III URCRH subunit, complex IV subunit COX5A, COX6C and complex V ATP subunits ATP5H, &amp; ATP5J</li> <li>Increase responses in 7 other related mitochondrial proteins, and a decrease in 2 mitochondrial proteins including a decrease in PARK7 which plays an important role in cell protection against oxidative stress</li> </ul>
2019 (unpublished) (107)	High-intensity interval training during 3 consecutive training phases of normal-volume training (4 weeks – 3/wk), followed by 20 d of high-volume training and 2 weeks of reduced-volume training (n=10).	Human (Skeletal Muscle - vastus lateralis)	a. 2296 min b.307		LC-MS	184	184 differential expression mitochondrial proteins were identified in response to training, relating to the following pathways: <ul style="list-style-type: none"> <li>42 proteins involved with OXPHOS and respiratory chain</li> <li>49 proteins with TCA cycle</li> <li>29 proteins with fatty acid beta oxidation</li> <li>15 mitochondrial proteins associated with pyruvate metabolism and glucose metabolism, &amp; another metabolism and additional</li> <li>78 mitochondrial proteins associated with various other cellular functions.</li> </ul>

2-DE - two dimensional- polyacrylamide gel electrophoresis, 1-DE – 1 dimension gel electrophoresis, 2D-DIGE - two-dimensional fluorescence difference gel electrophoresis, LC-MS – Liquid Chromatography coupled with Mass Spectrometry.

MALDI - matrix-assisted laser desorption/ionisation. TOF -Time of Flight

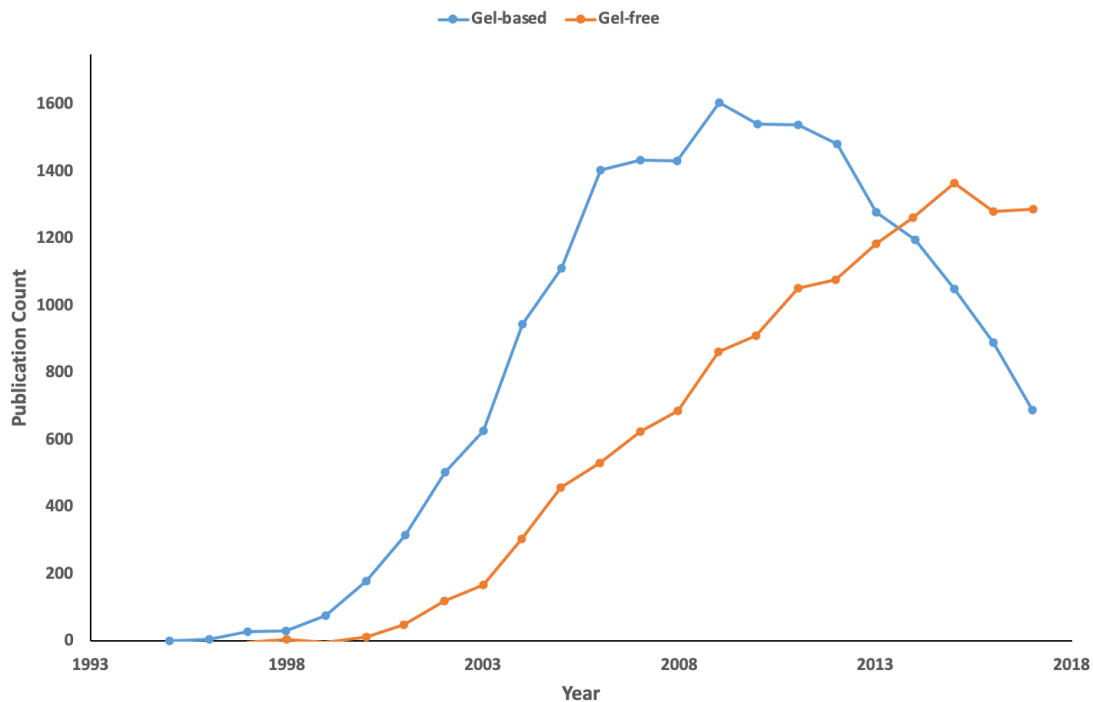


**Figure 1. 11** – Publication counts related to “gel-based” and “gel-free” proteomics. The number of publications was taken from PubMed (<https://www.ncbi.nlm.nih.gov/pubmed/>). Adapted from (165).

#### 1.4 Fibre-Specific Protein Responses with Training

The size principle states that under load, motor units (a motor neuron and all of the skeletal muscle fibres it innervates) are recruited from smallest to largest. In practice, this means that slow-twitch fibres (type I), which have a lower threshold of activation, will be utilised at lower exercise intensities, whereas fast-twitch fibres (type IIa and IIx), which have a higher recruitment threshold, will be recruited at higher intensities (Figure 1.12). Skeletal muscle fibre recruitment is therefore related to exercise intensity (273, 326), and it has been hypothesised that higher exercise intensities might stimulate greater adaptations in type II fibres relative to lower exercise intensities (118, 119, 202). This highlights that one of the main limitations of analysing of changes in mitochondrial proteins in whole-muscle lysates is that observations may be confounded by the heterogenous nature of a typical muscle sample composed of a mixed-fibre population (i.e., a variable proportion of type I and type II fibres), which consequently may mask the changes occurring in individual fibre types.

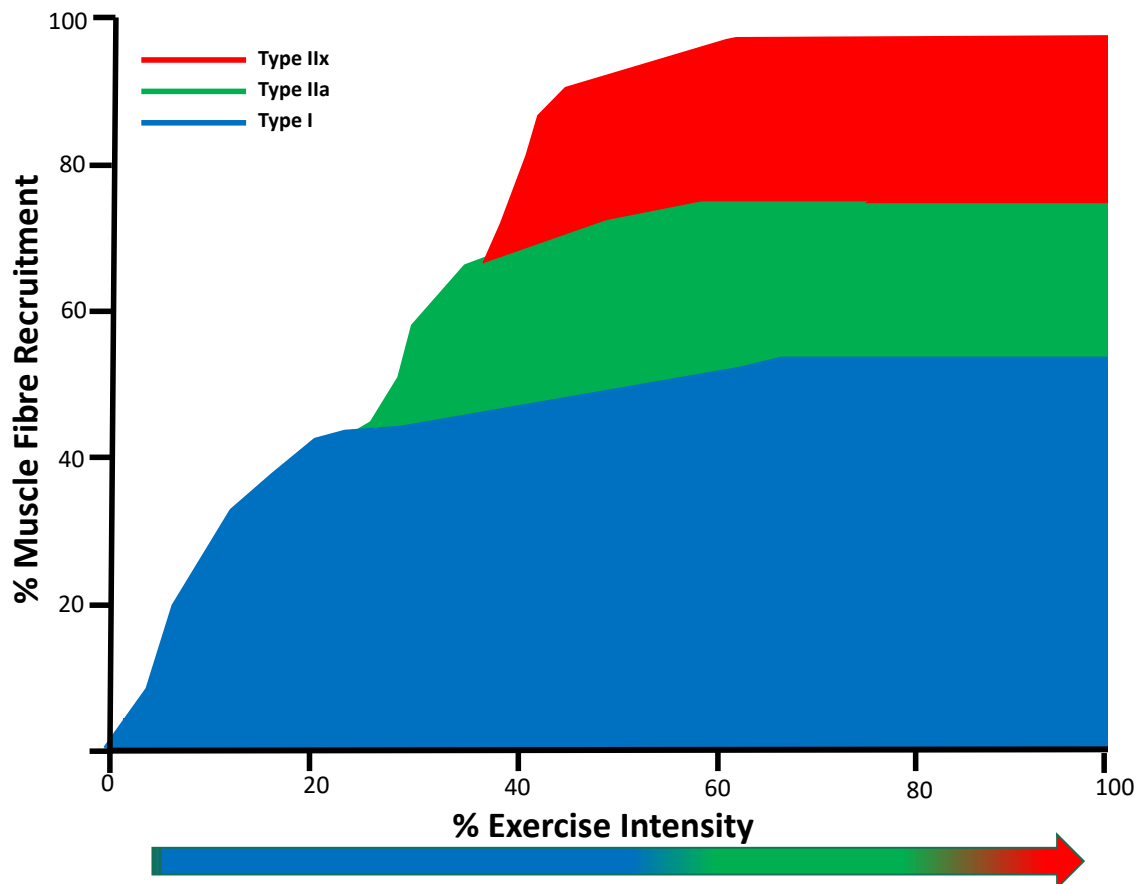


**Figure 1.12**– Recruitment of muscle fibres is dependent on the intensity and duration of contraction. A hierarchal recruitment pattern of type I to IIa to IIx/b occurs as force output of the muscle increases from low to high. During low-intensity exercise, slow-twitch, type I fibres are recruited, which have a high capacity for fat oxidation and a low capacity for glycogenolysis-glycolysis. An increase in contraction intensity results in a proportional increase in the recruitment of type II muscle fibres, which by their intrinsic characteristics generate more ATP from glycolytic pathways (27).

The ability to isolate, identify, and accurately quantify proteins in individual fibres could overcome these shortcomings, providing enhanced understanding of the adaptive response to training compared with typically performed whole-muscle analyses. Current technologies now enable a single human muscle fibre segment to be quantitatively analysed for targeted proteins by western blotting techniques. These advances have identified fibre-specific abundances of proteins related to the contractile apparatus (i.e., myosin heavy chains) (219, 220).

Nonetheless, aside from initial findings by Murphy (219) and Christensen et al. (53) looking at a few mitochondrial proteins, there has been little research investigating the mitochondrial proteins of different fibre types in humans. Evidence from rodent studies suggests that mitochondrial adaptations to exercise occur in a fibre type-specific manner

(72, 314); however, the interaction between fibre type and exercise intensity has received less attention in humans, as most studies examine adaptations at the whole-muscle level. Fibre-specific changes may contribute to some of the debate concerning the effects of different types of exercise on mitochondrial biogenesis. Given the fibre-specific mitochondrial characteristics, it seems reasonable to hypothesise that mitochondria adaptations will be fibre-specific. There is evidence of this being shown in rats; however, there is little research on fibre-specific mitochondrial adaptation to training in humans.

#### **1.4.1 Single-Fibre Immunoblotting**

One of the first studies assessing protein changes in single fibres by western blotting was Kristensen et al. (171). These authors observed that most measured proteins were equally affected in type I and II fibres following a single moderate-intensity exercise session (30 min at 70 %  $VO_{2peak}$ ), whereas there was a fibre-specific regulation of some proteins (e.g., AMPK phosphorylation) following high-intensity exercise (6 × 1.5-min bouts 95%  $VO_{2peak}$  interspersed by 2.5 min at 40%  $VO_{2peak}$ ) (171). Since then, only three studies have specifically investigated the adaptability of mitochondrial proteins to exercise training in single muscle fibres taken from humans (Table 1.4) (194, 312, 337). Due to the limited starting material, these studies only probed for three proteins representative of OXPHOS and mitochondrial dynamics (i.e., COXIV, NDUFA9, MFN2). All three studies utilised slight variations of HIIT and reported increases in COXIV protein in whole-muscle; however, only two reported similar increases of this protein in type I and type II fibres.

Wyckelsma et al. (337) investigated the effects of HIIT in older adults on the abundance of mitochondrial proteins (COXIV, NDUFA9, and MFN2) in whole-muscle homogenates and pools of single muscle fibres using immunoblotting techniques. There was a higher abundance of the mitochondrial respiratory chain subunits COXIV and NDUFA9 in type I compared with type II fibres at rest, and these results were similar in the older and younger cohorts. Following 12 weeks of HIIT, older adults exhibited an increase in mitochondria content in whole-muscle homogenates (assessed by CS activity). When examined in pooled single fibres, there were increases in COXIV in both type I and II fibres and NDUFA9 in type II fibres, while there was a decline of MFN2 in type II fibres. The results suggest fibre-specific differences for training-induced changes in proteins of

the respiratory chain and mitochondrial dynamics. An in-depth analysis of individual results, however, reveals that in some individuals there was an increase of MFN2 in whole-muscle lysates and yet a decline in both fibre types. Given the fibre type ratio of the cohort was roughly 50:50 of type I and type II fibres, such a discrepancy in individual protein response between whole muscle and single fibres is difficult to explain (Figure 1.13). As such, caution is needed when interpreting the results of immunoblot analyses of single fibres.

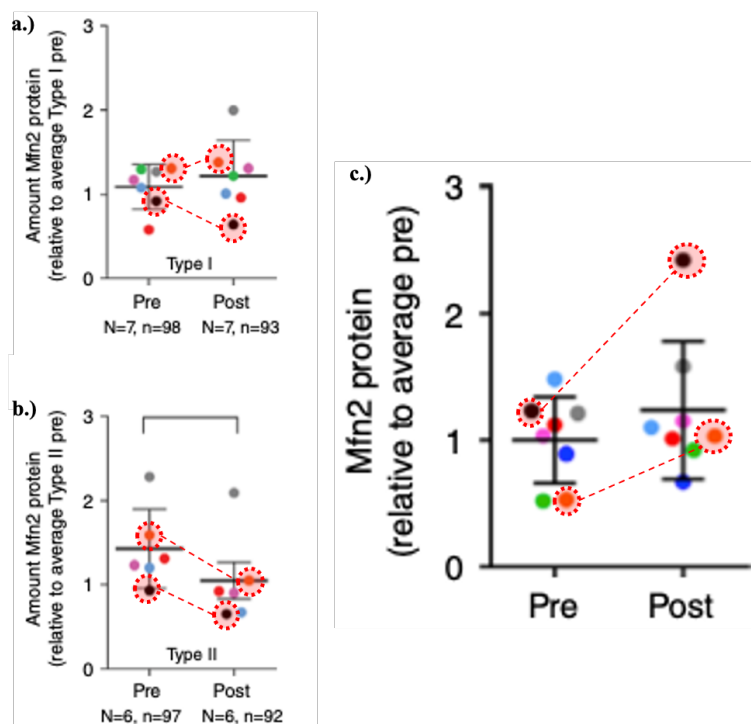


**Figure 1. 13**– Modified figure from Wyckelsma et al. (335) demonstrating potential discrepancy in individual protein response between whole muscle and single fibres; in this example, MFN2 is shown as. Each colour used for Pre and Post symbols on the graphs indicates the same participant (consistent across all figures).

Similarly, MacInnis et al. (194) examined the role of exercise intensity and/or the pattern of muscle contraction on the regulation of skeletal muscle adaptations in whole-muscle samples and pooled single fibres with the same immunoblotting protocol. The protein content of COXIV, NDUFA9, and MFN2 increased in both training groups (i.e., HIIT and MICT) in whole muscle. While COXIV and NDUFA9 were more abundant in type I than type II fibres, training did not increase the content of COXIV, NDUFA9, or MFN2 in either fibre type (194). This again indicates that fibre-specific alterations following training do not always correspond with the results obtained in whole-muscle

homogenates. Training was conducted only over a two-week period, and perhaps longer training periods are required to observe fibre-specific changes. While the abundance of respiratory chain complexes in the two fibre types was consistent with the earlier study by Wyckeslma (335), they did not see a similar training effect as was observed with 12 weeks of training. Conversely, research by Tan et al. (312), investigating the influence of HIIT on fibre-type-specific adaptations in overweight women, also revealed higher COXIV protein intensity in type I compared to type II fibres, but found that training increased the content of COXIV in both fibre types. There was a greater response in type II fibres compared to type I (27% and 46% increase in COXIV protein content in type I and type II fibres from baseline fibre type response, respectively). At the whole-muscle level, there was a ~27% increase in COXIV protein content following HIIT. This 6-week training protocol showed parallel responses to the observations by Wyckeslma. In general, these studies showed correlations in fibre-type differences for mitochondrial protein in respiratory chain complexes of COXIV and NDUFA9, while there were discrepancies in the studies for training responses. These studies provided new insights into fibre-specific responses of mitochondrial proteins to training, but also highlight the complexity and importance of sample preparation when analysing small protein amounts in single fibre. Considering that around 80% of the total cellular pool of muscle fibres consists of myofibrillar proteins, it is difficult to accurately analyse the less abundant mitochondrial proteins. A centrifugation step is often undertaken to remove the myofibrillar proteins; however, this can result in a significant loss of up to 80% of the sarcoplasmic reticulum. This can consequently have adverse effects for investigations of skeletal muscle mitochondria enrichment with potential disruption of the intracellular organelles and critical protein–membrane interactions (220).

Little is known about biological variation stemming from the percutaneous muscle biopsies in heterogeneous skeletal muscle. A recent study has that shown variability in fibre-type distribution increased when fewer than 150 muscle fibres were quantified. This helped prompt an evolution of the single-fibre immunoblotting technique, from research based on a single fibre with limited starting material to utilising a combination of dot blotting to identify fibre types and the pooling of single fibres to increase starting material and protein content (16). A study by Christiansen et al. (16) reported that the greatest between-run variabilities were seen with single fibres, where the linear regression slopes were statistically different for SERCA1 and AMPK $\beta$ 2 protein content, but not for total

protein. As groups of single fibres increased to four pooled single fibres, variability was reduced and the greatest decrease in variability was seen with groups of 10 or 20 fibres. Based on this, pooling a minimum of 10 fibres may give the best representation for western blot analysis. This would also allow more proteins to be analysed. Given the heterogeneity of fibre types in whole-muscle lysates in western blotting, the need to reduce variability in single fibres should be paramount to the ability to detect differences in fibre-specific responses. Also to be taken into consideration is the method of fibre typing for immunoblotting studies, which is based on MYH. Proteomic investigations have shown that even in individual fibres there can still be multiple isoforms of MYH, and thus a single fibre type should be based on the purity (i.e. percentage of the dominant MYH isoform) (216).

The main insight obtained from single-fibre studies is that we begin to see fibre-specific differentiations in the response to training, which to date has focussed on a small number of respiratory chain sub-units. Although overall, training-induced changes in very few mitochondrial proteins in single fibres have been analysed thus far (COXIV, NDUFA9 and MFN2 – only three of the more than 1100 of mitochondrial proteins). Recent advances in single-fibre proteomics have the potential to discover changes in a greater range of mitochondrial proteins at the single-fibre level. This approach is complicated by the fact that the low amount of proteins in individual muscle fibres compromises in-depth proteome analysis and thus comes with its own challenges, which is discussed in subsequent sections.

**Table 1. 4- Summary of Human Single-Fibre Mitochondrial Protein Exercise Training Studies by Immunoblotting**

Reference	Participant Characteristics	Training Protocol	Training Volume a. Total volume b. volume x intensity	Detection Method	Findings
Wyckelsma et al. 2017 (335)	<ul style="list-style-type: none"> <li>n= 8 (2 females, 6 males)</li> <li>Age - 69.9 ± 3.8 years</li> <li>BMI - 75.1 ± 12.8 kg m<sup>-2</sup></li> <li>VO<sub>2</sub> peak 25.1 ± 6.1 L.mL kg<sup>-1</sup> min<sup>-1</sup></li> </ul>	36 sessions of HIIT (4 x 4 min cycling intervals at 90–95% of the HR <sub>max</sub> , interspersed by 4 min of recovery where at 50–60% HR <sub>max</sub> ) over 12 weeks	<b>a.</b> 1008 min <b>b.</b> 806.4	Single fibre was fibre-typed using the dot blotting and western blotting Pooling: type I and type II consisted of 4–11 fibres	<ul style="list-style-type: none"> <li>COXIV and NDUFA9 greater in type I vs type II fibres</li> <li>↓ Mfn2 in type II fibres of older adults following training and ↑COXIV protein content in both type I and type II fibres were observed. No significant change in type I NDUFA9 but ↑ in type II fibres were observed</li> <li>no fibre type difference between the older adults and young groups with training</li> </ul>
MacInnis et al. 2017 (194)	<ul style="list-style-type: none"> <li>n = 10 (male)</li> <li>Age - 23 ± 1 years</li> <li>BMI - 25 ± 1 kg m<sup>-2</sup></li> <li>VO<sub>2</sub> peak 2.6 ± 0.2 L.mL kg<sup>-1</sup> min<sup>-1</sup></li> </ul>	6 sessions of unilateral leg exercise protocol with HIIT [4 × (5 min at 65% W <sub>peak</sub> and 2.5 min at 20% W <sub>peak</sub> )] or MICT (30 min at 50% W <sub>peak</sub> ), were performed 10 min apart on each day, in an alternating order. The work performed per session was matched for MICT and HIIT over 2 weeks	<b>a.</b> 180 min <b>b.</b> 173 HIIT, 90 MICT	Single fibre was fibre-typed using the dot blotting and western blotting Pooling : type I 7.0 ± 2.9 and type II 9.0 ± 5.2	<ul style="list-style-type: none"> <li>COXIV and NDUFA9 greater in type I vs type II fibres</li> <li>training did not increase the content of COXIV, NDUFA9 or MFN2 in either fibre type</li> <li>No difference in MICT vs HIIT for either fibre type</li> </ul>
Tan et al., 2018 (312)	<ul style="list-style-type: none"> <li>n = 13 (female)</li> <li>Age: 26 ± 7 years;</li> <li>BMI: 30 ± 4 kg. m<sup>-2</sup></li> <li>VO<sub>2</sub> peak: 2.16 ± 0.45 L mL kg<sup>-1</sup> min<sup>-1</sup></li> </ul>	18 sessions of HIIT (10 × 60-sec cycling intervals at ~90% HR <sub>max</sub> , interspersed by 60 s of recovery) over 6 weeks	<b>a.</b> 360 min <b>b.</b> 252	Fibre typing by immunohistochemical analysis and western blotting for analysis Pooling: type I and type II consisted of 25 fibres	<ul style="list-style-type: none"> <li>COXIV greater in type I vs type II fibres</li> <li>training ↑ COXIV protein content in both type I and type II fibres</li> </ul>

## 1.4.2 Single-Fibre Proteomics

Whole-muscle analysis is confounded by the influence of other tissues such as connective tissue, blood vessels, and nerves (218, 229). Nonetheless, despite the power of proteomics techniques, there continues to be an absence of data on protein changes occurring in type I and II fibres in response to exercise and training. In part, this can be attributed to the adverse dynamic range caused by highly abundant sarcomeric proteins that account for over 50% of total signal, with myosin heavy chain ranking highest (216). Proteins from all other muscle compartments, including the mitochondria, are confined to the lower half of the MS-signal range (216). Additionally, single-muscle fibres contain very limited protein amounts compared to typical starting amounts in proteomic projects (tens to hundreds of times less). This limits the capabilities of the MS to fragment the more low abundant proteins (64, 229).

To overcome these difficulties, Murgia et al. (207) devised a single-step sensitive workflow to describe the proteome of mouse single muscle fibres and to describe the contractile and metabolic features of single muscle fibre types (see Figure 1.12). Their workflow began with the establishment of a deep skeletal muscle proteome for whole-muscle samples digested using the filter-aided sample preparation (FASP) method and with the resulting peptide mixture then separated into 12 fractions by isoelectric focusing (138, 330). This procedure was able to identify approximately 6500 proteins. They then developed a workflow for single-muscle fibre proteome analysis, which is performed in a single vessel to reduce sample loss using the method of Kulak et al. (173). The analysis of this workflow was initially applied to mice (216) and then to ageing human skeletal muscle (218) to identify proteins in specific fibre types. The deep proteome workflow was combined with MaxQuant analysis software and employed its ‘match between runs’ (MBR) feature (60). Briefly, the MBR algorithm assesses each identified peak in a MS1 spectrum from an LC–MS/MS run and compares its retention time to unidentified peaks in another. An identification is transferred if an unidentified peak with the same properties (e.g.,  $m/z$ ) is found within a specified retention time window. As retention time is critical for the algorithm to function, the MBR algorithm first realigns compared chromatograms before attempting to transfer identifications. Thereby, identifications through peptide-spectrum matches (PSMs) from one run can be transferred to peaks having no tandem

MS information in another run (183). In this case, MaxQuant was used to transfer peptide identifications from the deep muscle proteome, where a given peptide is much more likely to have been fragmented, to a single fibre, where often only the intact peptide has been measured. The benefits using MBR is that it assists in achieving higher precision and fewer missing values in protein quantification.

To perform fibre type assignment by MS in a reproducible manner, the MYH isoforms were assigned based on having more than 80% sequence identity using the relative abundance of MYH isoforms. Type IIa and IIx fibres tended to have a higher degree of heterogeneity than type I and IIb fibres. Virtually all single fibres express two or more MYH isoforms at low levels; thus, fibres were classified as type I if their relative abundance was over 80% of MYH7, IIb if containing over 80% of MYH4, and, due to the greater heterogeneity, IIa if containing over 60% of MYH2, and IIx if containing > 60% MYH1 (Figure 1.14). This discovery provided an unprecedented method for fibre-type-specific analysis, making the prospect of analysing proteins in single muscle fibres possible at the proteomic level. To quantify the variability of the muscle fibre proteome among different donors, median protein abundances across all individuals and samples were compared using the MaxQuant label-free quantification (LFQ) algorithm (59). Despite the limitations identified above, this new workflow allows for not only qualification of proteins in different fibre types but also quantification (216).

The limited number of single-fibre studies employing proteomics is summarised in Table 1.5, which includes only two studies in mice and two in humans. In their initial mouse study, Murgia et al, identified that different fibre types have differing capacities for substrate utilisation (218) and revealed an unexpected diversity and specialisation in the metabolic properties of individual fibre types (216). Their single-fibre proteomic study detected a total of 654 proteins annotated as mitochondrial, with an average of more than 270 quantified in individual fibres. The majority of the components of the respiratory chain and TCA cycle were quantified in each fibre. By normalising the mitochondrial content (using cytochrome c or succinate dehydrogenase as indicators of mitochondrial quantity), they found notable differences in major pathways of OXPHOS, fatty acid beta-oxidation, and the TCA cycle at a fibre-specific level. Similar pathway observations have been seen prior to single-fibre proteomics in fibre types (92) with single-fibre research providing further evidence for the existence of distinct subsets of mitochondrial proteins

in specific fibre types that may not have been observed by whole-muscle analysis. OXPHOS proteins were typically more abundant in type IIa fibres. With respect to fatty acid beta oxidation, type I fibres had higher protein levels for enzymes involved in this pathway, including ACADL, HADHA, the ETFA and ETFB complex, and ETFDH. Also more prevalent in type I than type II fibres were proteins located in the mitochondrial outer membrane involved in the conversion of fatty acids to fatty acyl-CoA esters via ACSL1, and proteins involved in fatty acid import at the inner mitochondrial membrane (e.g., CPT2A). The same held true for proteins involved in ketone body metabolism, such as OXCT1- an enzyme responsible for acetoacetyl-CoA production from acetoacetate, and ACAT1 - which converts acetoacetyl-CoA into acetyl-CoA. Conversely, proteins associated with the regulation of glucose and pyruvate dehydrogenase (PDH) metabolism and the TCA cycle show greater abundance in type IIX fibres. The protein Pyruvate Dehydrogenase Phosphatase Catalytic Subunit 1 (PDP1), a protein involved in pyruvate metabolism, was more than two-fold more abundant than in other fibre types. Additionally, isocitrate dehydrogenase 3 (IDH3), a member of the TCA cycle, displayed higher abundances in type IIX fibres, whereas it was lowest in IIb fibres. Further findings related to pyruvate metabolism and TCA pathways were significant variations in Mitochondrial Pyruvate Carrier 1 (MPC1) and MPC2, which are located in the mitochondrial inner membrane and had not previously been investigated in skeletal muscle. The ratio of the two subunits differed in the two fibre types, with MPC2 more abundant in type I, IIa, and IIX fibres, whereas MPC1 had higher levels in type I compared to IIX and IIb fibres. The most noteworthy consideration we begin to see with this first proteomics study at a single-fibre level is the array of mitochondrial proteins that are observed to differ at a fibre-specific level, along with their associated functional pathways, which had previously remained overlooked via the analysis of whole-muscle samples and with the *a priori* nature of immunoblotting techniques.

The hundreds of mitochondrial proteins identified in the four fibre types revealed a multifaceted picture that clearly established that mitochondria differ in the various muscle fibre types not only quantitatively but also qualitatively. This supports the notion of metabolic specialisation that is finely tuned to the physiological properties of muscle fibres. With further streamlining of the technology, similar experiments could now be performed to explore changes in mitochondrial proteins as a function of muscle use or disease perturbations. An animal study by Lang et al (174) investigated fibre-type protein

remodelling after denervation leading to muscular atrophy. More than 200 mitochondrial proteins were detected across all fibre types, with a slight decrease in the number of mitochondrial proteins in type IIa fibres of the soleus and type IIb fibres of the EDL after denervation compared with type-I fibres from the soleus after denervation. Common observation to animal studies was fibre-specific substrate utilisation in the TCA cycle. Lang reported that TCA proteins IDH3B and IDH3G, and D-beta-hydroxybutyrate dehydrogenase (BDH1), and the mitochondrial ribosomal protein S36 (MRPS36), were still more abundant in type-IIa fibres than in type-I fibres after denervation, which was consistent with the findings of Murgia et al. (216). The mitochondrial contact site and cristae organising system (MICOS) that modulate respiratory complexes was another complex that exhibited heterogeneous regulation. Although most members were significantly downregulated after denervation, metaxin-2 (MTX2) was upregulated in both type I and type IIa fibres. This has potential implications for cristate formation and protein import into mitochondria because it is localised at the outer mitochondrial membrane. Analysis of the OXPHOS complexes (I–V) revealed downregulation of complex III and IV in type-IIa and -IIb fibres after denervation, whereas these proteins were less affected in type-I fibres. The results of this study highlight the need to investigate fibre-type-specific changes of mitochondrial proteins in response to different stressors (e.g., activity and inactivity).

Murgia et al. went on to further apply their workflow to the first study on human single muscle fibres. This combination led to the quantification of more than 60,000 peptides and 5400 proteins in 152 single human muscle fibres across eight donors; on average they obtained 2,100 proteins per single muscle fibre. The fibre-type-specific analysis of the cohort still revealed variability among individuals (in terms of the number of proteins and fibre type composition between samples), but this was outweighed by functional similarity between their fibre types. There was a correlation between the proteins identified in fibre types of donors ranging from 0.85 to 0.95 for the least to the most similar individuals. When compared to pooling fibres, they found Pearson correlation coefficient were higher with a median of 0.93. The power of this method is shown by the ability to identify 757 mitochondrial protein across all donors. Unique donors had between 300 to 500 mitochondrial proteins, where, for instance, analysis of a select donor revealed 589 mitochondrial proteins in a single type I fibre and 359 mitochondrial proteins in a selected type II fibre.

Common amongst the small number of single-fibre proteomics studies is greater abundance of mitochondrial proteins associated with OXPHOS in respiratory chain complexes in type I fibres, a known feature of human muscle (131). This was also common in human single-fibre immunoblotting studies that showed greater amounts of COXIV protein (194, 312, 335). In contrast, type II fibres tended to have a greater content of proteins involved in the TCA cycle and OXPHOS. Contrary to this was the findings in single fibre mice studies, which revealed more abundant OXPHOS proteins in type IIa fibres and a greater abundance of beta-oxidation proteins in type I fibres. The other notable fibre-type difference in mice is for the TCA protein isocitrate dehydrogenase, in which IDH3 is significantly higher in type IIx fibres. In human muscle, there is a higher abundance of IDH2 than IDH3 in type II fibres.

In response to aging, Murgia et. al (218) saw a decrease in mitochondrial protein content in both type II and type I fibres; this observation is in line with many previous studies (154). Intriguingly, this was associated with an increase in the mitophagy pathway and a decrease in the fusion machinery - two mechanisms that may at least partly explain age-related mitochondrial defects (218). Amongst this information there was complete quantification of all five respiratory chain complexes, comprising both the nuclear- and mitochondrial-encoded subunits, that clearly shows that OXPHOS respiratory chain proteins are more abundant in type I than in type IIa fibres, though content did reduce with age. GO-annotated mitochondrial proteins showed no age-related changes in type IIa fibres. Further to this, mitochondrial pathways related to aging and linked to type 2 diabetes were also identified by these analyses with the expression of proteins involved in mitochondrial dynamics such as MFN2 and OPA1 strongly declining with age. Additional differential response in glycolysis during aging and fibre types were observed with increased expression in type I old fibres and a decrease in type II compared to their young counterparts. Specifically, there was a several-fold decrease of MAOA in type I fibres, which is a protein that stimulates glucose uptake in skeletal muscle by acting on GLUT4 translocation (218). This study hints to the power and capacity of proteomics to identify many proteins and mitochondrial mechanistic pathways related to fibre types in a single shot. The only other human single-fibre proteomic study investigating mitochondrial disease showed a correlation with a decline in OPA1 in aging muscle (217). This study also revealed that complex IV subunits of the respiratory chain were more abundant in COX+ stained fibres (representative of cytochrome c oxidase to succinate

dehydrogenase ratio (COX/SDH) staining with linked functioning electron transport to complex IV) that are associated with type I fibres. Defective fibres also showed greater abundance of fatty acid oxidation proteins in type I but not type II muscle fibres. However, a key observation in most of these studies is the small sample size used for analysis (n=8 and 18–20 single fibres per donor). Additionally, it could be speculated that key mitochondrial changes observed in aging may exhibit opposite changes with exercise. Thus, further studies are required to investigate the effects of exercise on mitochondrial proteins in single fibres.

While the single-fibre studies summarised in Table 1.5 demonstrate good coverage of structural and metabolic features of the muscle fibre proteome, the challenge of dominating signals of sarcomeric proteins remains with an average identification of 60% of proteins annotated to the sarcolemma and 70% of sarcoplasmic reticulum proteins in single fibres observed. Murgia's (216-218) work employs Label Free Quantification (LFQ), which has a relatively simple workflow suitable for numerous sample matrices; however, given that low abundant proteins generate a limited set of peptides with ion signal for quantification making them generally difficult to quantify, LFQ can typically be subject to limitations of the maximal number of samples than can be easily analysed without introducing batch effects (36, 238). Non-biological experimental variation or such "batch effects" are commonly observed across multiple batches of microarray experiments, often rendering the task of combining data from these batches difficult. The ability to combine microarray data sets is advantageous for researchers to increase statistical power to detect biological phenomena from studies where logistical considerations restrict sample size or in studies that require the sequential hybridisation of arrays (5). Thus, the ability to use labelling techniques such as Tandem Mass Tags (TMT) has the advantage of potentially providing extensive pre-fractionation that can be performed with approaches to minimise batch effects and a possible alternative to LFQ proteomics to detect low-abundant mitochondrial proteins in single muscle fibres. Additionally, the use of MBR in this research typically increases the peptide identification (183, 226). This strength can also represent the primary difficulty in assessing the accuracy of MBR, in this case resulting in increased observation of mitochondrial proteins. Nonetheless, these single-fibre studies have presented the ability to discover in excess of 5000 proteins and 250 to 750 mitochondrial proteins in a single-shot experiment with the potential of further application to exercise training.

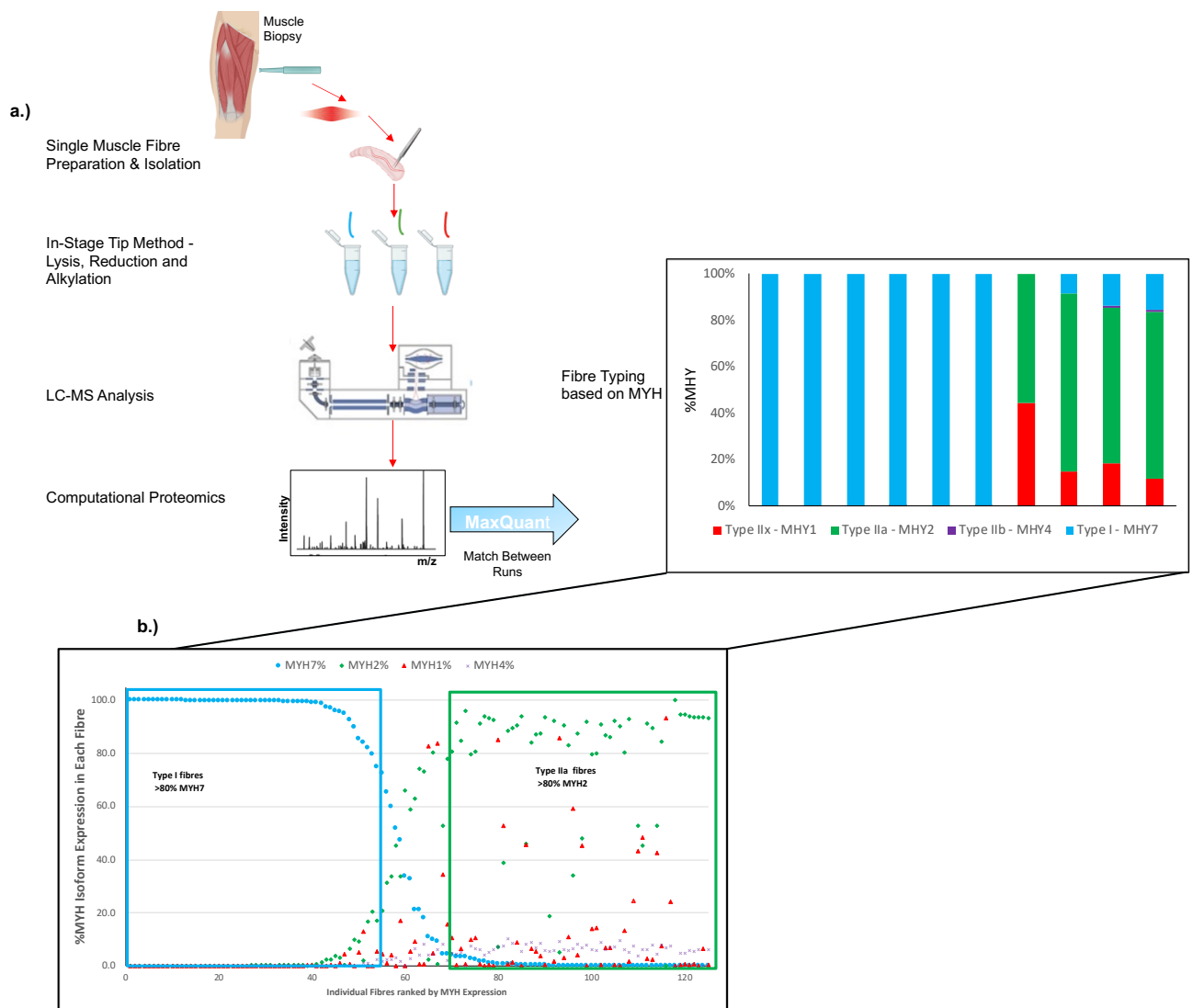


**Figure 1. 14-** Single shot workflow for Single Muscle Fibre Isolation and Analysis adapted from (216)

- Single fibre isolation followed by lysis, reduction and alkylation and MS analysis to acquire mass/charge data and converted by MaxQuant for protein analysis and fibre typing.
- MS-based quantification of MYH isoforms reveals pure-type fibres and different combinations of mixed-type fibres. The scatter graph shows the percent expression of the four adult isoforms of MYH in all analysed fibres, distributed along the x axis. Fibres from older donors have a black contour. Fibres were ordered and ranked based on the prevalence of expression of MYH7 (blue diamonds), MYH2 (green squares), and MYH1 (grey triangles) isoforms. MYH4 (cross) which are essentially not expressed in humans.

**Table 1. 5- Summary of MS-based Proteomics Studies Using Single Fibres**

Reference	Sample Type	Preparation Method	Detection Method	Analysis Method	Number of Mitochondrial Proteins Identified	Findings
2015 (216)	Mice (n=10)	Single shot for single fibres & Filter-aided sample preparation (FASP) followed by isoelectric focusing for whole muscle	LC-MS (linear quadrupole Orbitrap MS)	MaxQuant with match between runs	654	<ul style="list-style-type: none"> <li>• OXPHOS proteins &gt;in Type IIa fibres.</li> <li>• Beta &gt; in Type I fibres ( ACADL, HADHA, ETFA and ETFB)</li> <li>• Fatty acid conversion and ketone metabolism proteins &gt; in Type I fibres ( ACSL1, CPT2A., OXCT1)</li> <li>• In TCA cycle IDH2 &gt; in Type I fibres and &lt; in Type IIx/b fibres</li> <li>• IDH3 &gt;in Type II fibres</li> </ul>
2017 (218)	Human Sex =Male (n = 8, 4 young/4 old).	Single shot for single fibres	LC-MS (linear quadrupole Orbitrap MS)	MaxLFQ with match between runs	757	<ul style="list-style-type: none"> <li>• OXPHOS proteins in Type I &gt; Type IIa fibres.</li> <li>• &lt; in MFN2 &amp; OPA1 in Type I with ageing</li> </ul>
2018 (217)	Human (n=6, 3 control, 2 mitochondrial disorder) Sex = Male 18 single fibres	Single shot for single fibres	LC-MS (linear quadrupole Orbitrap MS)	MaxQuant with match between runs	217	<ul style="list-style-type: none"> <li>• &lt; the OPA1 in type I fibres</li> <li>• &gt;fatty acid oxidation proteins occur in defective type I but not type II muscle fibres</li> <li>• Complex IV subunits were more abundant in type I fibres (associated with COX+)</li> </ul>
2018 (174)	Mice (n=3) 150 pooled single fibres	In silico grouping of fibre types. Stop and Go (C18 stage tip) for peptide extraction	LC-MS/MS (QExactive MS)	MaxQuant LFQ with Andromeda	672	<ul style="list-style-type: none"> <li>• Type-I fibres &gt;in proteins than type-IIa fibres of soleus and type-IIb fibres of the EDL after denervation</li> <li>• IDH3 &gt;in Type II fibres after denervation</li> <li>• Beta-hydroxybutyrate dehydrogenase (BDH1), and the mitochondrial ribosomal protein S36 (MRPS36) in type IIa &gt;type-I fibres after denervation</li> </ul>

## 1.5 Conclusions

During the past two decades, the application of molecular techniques to exercise biology has led to the identification of multiple molecular pathways with key roles in promoting training-induced mitochondrial biogenesis. However, linking many of these signals to defined metabolic responses and specific changes in protein expression in skeletal muscle that occur as a consequence of exercise has proved more difficult. This is because many of these pathways are not linear but are instead part of a complex network, with feedback regulation and transient activation (116). The advances of various proteomic approaches, can be used in combinations with computational approaches to resolve the complex biological interactions associated with diverse exercise responses (343).

Future research in the field of exercise science requires increasingly sophisticated approaches to understand the critical nodes of energy homeostasis and how these pathways are upregulated in response to exercise training and disrupted in a number of disease-related disorders. The development of MS-based proteomics has provided us this sophistication and decisively improved our understanding of physiological changes in skeletal muscle. The successful miniaturisation of the proteomic workflow has provided the mechanism by which we can now perform single cell proteomics of different fibre population leading to a comprehensive coverage of the skeletal muscle proteome. The results of such research in not only skeletal muscle but muscle fibre types will hopefully spark the advent of individualised exercise prescription for enhanced health and performance (240).

## **Aims**

1. To investigate training-induced changes in mitochondrial proteins in single muscle fibres from humans.
2. To elucidate how different types of training affect mitochondrial proteins in different fibre types.

### ***The hypothesis of this proposed research project was:***

That different types of exercise would induce fibre-specific changes to some mitochondrial proteins given that the types of training chosen should require very different skeletal muscle fibre recruitment. It is hypothesised that MICT will elicit mitochondrial protein changes related to type I fibres and oxidative pathways. Whereas, SIT will have greater expression of proteins related to type II fibres and glycolytic pathways.

### **Contribution to Knowledge**

This study will contribute further evidence of the effects of different types of exercise (moderate and high-intensity exercise) on fibre-specific mitochondrial adaptations.

### **Statement of Significance**

It is known that mitochondria play a key role in skeletal muscle function and health. Through a better understanding of how to target specific adaptations within the mitochondria, and subsequently differently fibre types, it may be possible to add valuable information for optimising the exercise prescription to enhance skeletal muscle mitochondrial adaptations to improve health and performance.

## **Chapter 2**

### **Conceptual Framework and Methodology**

## 2. Conceptual Framework and Methodology

### 2.1 Research design overview

An overview of the study design can be seen in Figure 2.1. In brief, the study was conducted as part of a larger study on muscle samples that had already been collected by Javier Botella as part of his PhD (HRE17-075). A summary of the training design can be found in Figure 2.3. The study consisted of an 8-week training intervention, where participants were randomly divided into two groups that performed either moderate-intensity training or sprint-interval training. These two types of training were chosen as they should require very different skeletal muscle fibre recruitment. Single muscle fibres from muscle biopsies collected pre and post training from the vastus lateralis muscle were analysed for this study.

a.

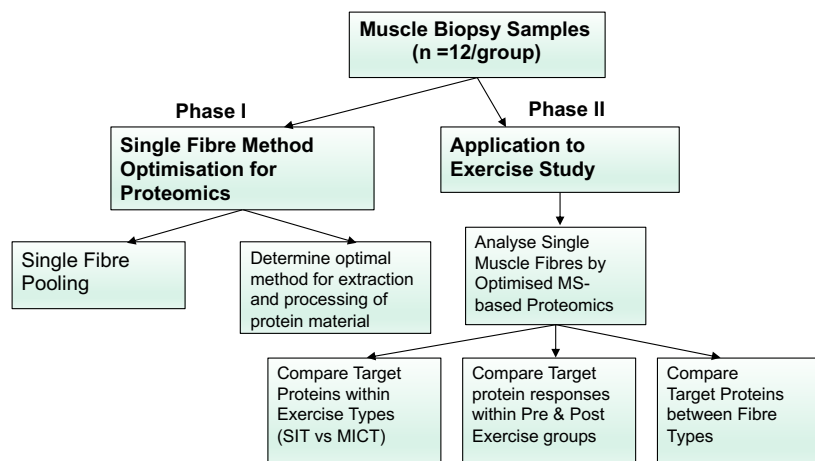


**Figure 2. 1-** a. General Outline of Research to be Undertaken. b. Single Fibre Analysis and Comparisons by MS on exercise study for groups of Moderate Intensity Training (MICT) and Sprint Interval Training (SIT).

The first phase of this masters' project focused on the method optimisation for the digestion of single muscle fibres and obtaining suitable amounts of protein for identification by MS-based proteomics in single muscle fibres. The second phase of the project was directed towards the application of this optimised single-fibre method to the training study and quantification of mitochondrial proteins in type I and type II muscle fibres pre and post training.

## 2.2 Participants

Prior to this study commencement, participants were provided with enough written and oral information as needed before voluntarily signing the informed consent form. Samples were collected according to an approved ethics application, which conformed to the standards set by the latest revision of the Declaration of Helsinki (Application ID: HRE17-075). Selection criteria for the study were based on recruiting participants considered physically active, but not conducting any systematic training (more than 3 sessions per week) for the previous 3 months.

The sample size (n) required to reach a significant level of 0.05 with a sufficient power of 80% was calculated for the following variables: mitochondrial volume, mitochondrial cristae density, and mitochondrial respiration. This was based on studies with a lower training volume or duration than the present study, and previous research has shown that differences between groups are likely. Based on this a sample size of 8-14 per group was suggested as sufficient to reach the level of significance required.

A total of 28 participants were recruited and their characteristics are summarised in Table 2.1. After initial screening and testing, they were matched by the power attained at the lactate threshold (WLT) and randomly assigned to the moderate-intensity-continuous-training (MICT) (n=14) or sprint-interval-training (SIT) (n=14) group. Twenty-three participants completed the study, whilst five (two from the MICT and two from the SIT group) withdrew from the study due to time constraints and one was excluded from analysis as the sample was too fibrotic (Figure 2.2). There was no significant difference between groups for baseline characteristics (i.e., age, BMI,  $VO_{2\text{ max}}$ , or  $W_{\text{peak}}$ ).

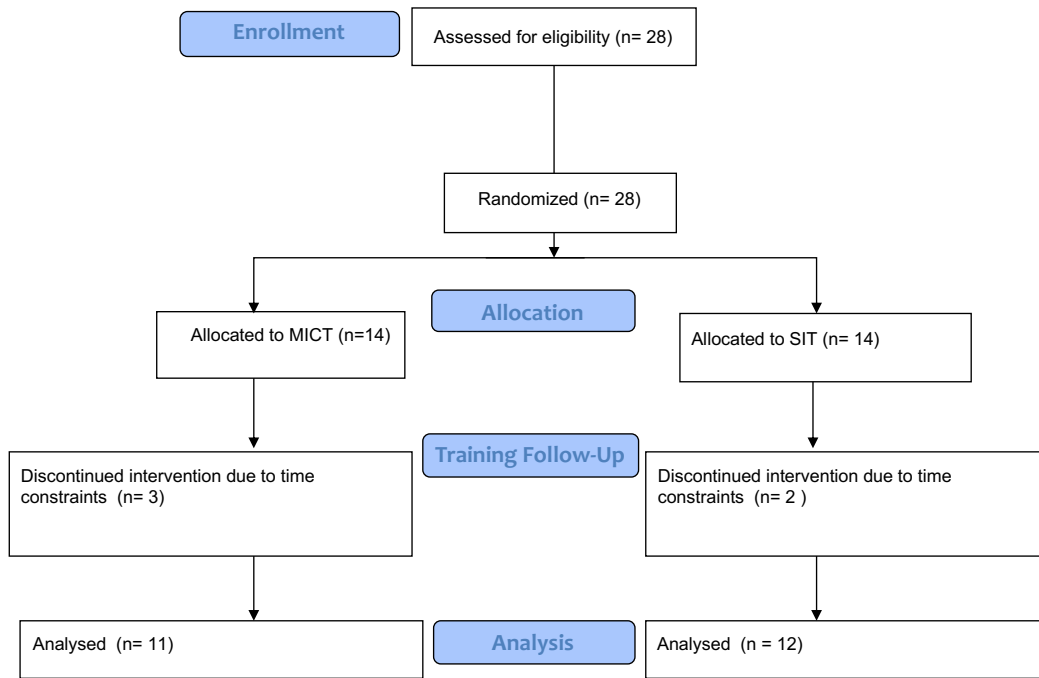


**Figure 2. 2-** Flow diagram of the progress through the phases of a parallel randomised trial of MICT and SIT groups.

**Table 2. 1– Participant Characteristics**

<i>Measurement</i>	<i>MICT group (n= 11)</i>	<i>SIT group (n = 12)</i>
<i>Age (years)</i>	26.4 ± 5.8	27.5 ± 5.3
<i>Body Mass (kg)</i>	73.6 ± 10.1	75.5 ± 9.7
<i>Height (m)</i>	1.80 ± 0.1	1.80 ± 0.1
<i>BMI (kg/m<sup>2</sup>)</i>	23.7 ± 2.9	23.5 ± 2.9
<i>W<sub>peak</sub> (W)</i>	301 ± 46	320 ± 70
<i>VO<sub>2max</sub> (mL/min/kg)</i>	52.0 ± 76.8	51.7 ± 7.1

MICT: Moderate intensity continuous training; SIT: sprint interval training;  $\dot{V}O_{2max}$ : maximal oxygen uptake. All values are mean ± SD

### 2.2.1 Physical Activity and Nutritional Control

Participants were requested to maintain a normal dietary pattern and physical activity throughout the study. To minimise the variability in muscle metabolism, participants were provided with a standardised dinner (55 kJ/kg of body mass (BM), providing 2.1 g carbohydrate/kg BM, 0.3 fat/kg BM, and 0.6 g protein/kg BM) and breakfast (41 kJ/kg BM, providing 1.8 g carbohydrate/kg BM, 0.2 g fat/kg BM, and 0.3 g protein/kg BM) to be consumed 15 h and 3 h before the biopsies. Furthermore, participants were requested to keep a nutrition diary in which they record the last 3 meals before each performance test (i.e., GXT and 20-km Time Trial), and were asked to replicate this post-testing.

### **2.3 Testing**

Before and after training, participants were assessed for various measures of aerobic fitness. The maximal oxygen uptake ( $VO_{2max}$ ) and lactate threshold (LT), obtained from a graded exercise test (GXT), incorporating stages of 3 min in duration, followed by a  $VO_{2max}$  confirmation bout. Moreover, a 20-km time trial (20-km TT) was conducted to obtain a direct measure of endurance performance (26, 106). To reliably measure these parameters, participants underwent a familiarisation session of each test, spread over the two weeks preceding the start of the baseline testing. Previous research by our group has shown that 1 familiarisation trial is sufficient to obtain reliable measures of these parameters. In addition, oxygen consumption ( $VO_2$ ), rating of perceived exertion (RPE), heart rate (HR), and blood lactate (La) were sampled during the testing and during selected training sessions (i.e., the experimental day, and the first exercise session of the 4th, 8th and 12th week).

### **2.4 Training**

The training was based on previous research within our group (104, 106), and the polarised training approach (304), and followed a classical periodisation model (4-week mesocycles composed of 3 weeks of progressive overload followed by a week of reduced load). Both groups trained 3 to 4 days/week for 8 weeks (Figure 2.3). Training intensity for the MICT group was established at 10% less than the first lactate threshold (90% of the lactate threshold 1 (LT1) for 60-120 min, 3-4/wk over 8 wk). The sprint interval training group (SIT) group involved 4 to 8 sprints of 30-second “all-out” cycling bouts against a resistance set at 0.075 kg/kg body mass, interspersed with a 4-min recovery period between sprints (91, 104). Training sessions and load distribution was done in the same way as the MICT group (3-4/wk, over 8 wk). Due to the nature of this type of training, it was not possible to match the work completed by the MICT group.

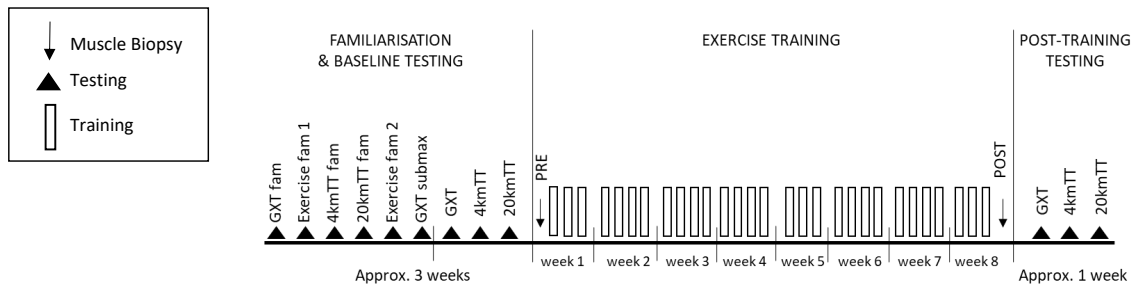


**Figure 2. 3-** Schematic overview of the timeline of the testing and exercise training session before and after the 8-week period. GXT = Graded exercise test; fam = familiarisation session; 20kmTT = 20 kilometre time trial; 4kmTT = 4 kilometre time trial; submax = submaximal. Two training groups performed the training over the 8 week period. MICT -  $\pm 10\%$  of the first lactate threshold ( $\sim 90\%$  of the lactate threshold 1) for 60 – 120 min sessions. SIT – 30 s all out bout for 20 – 40 min per session.

## 2.5 Muscle analysis

### 2.5.1 Single Muscle Fibre Isolation

Skeletal muscle biopsies (50 to 100 mg in total, divided into smaller segments) were obtained under local anaesthesia (lidocaine hydrochloride, 5 mg/mL) from the *vastus lateralis* pre and three days post training. One piece of muscle was placed in RNALater (ThermoFisher) on the biopsy day and stored at 4 degrees, and then separated on ice into single fibres within a few days. Forty fibres were individually isolated, and cut into half, with one half of the fibre stored in RNALater™ (ThermoFisher) and the remaining fibre halves were placed in a Laemmli solution (a solubilising buffer) (219). The Laemmli solution was composed of; 4% (v/v) sodium dodecyl sulfate (SDS), a thiol agent of 10% (v/v)  $\beta$ - mercaptoethanol, 20% (v/v) glycerol, 0.125 M tris-hydroxymethyl-aminomethane (tris)-HCl; and 0.015 % (v/v) bromophenol blue, pH 6.8. Each fibre was diluted with 5  $\mu$ L of 3x the solubilising buffer 2:1 (v/v) with 10  $\mu$ L of 1x Tris-Cl (pH 6.8) (219, 337). These fibre segments were then immediately frozen in liquid nitrogen and stored at  $-80^{\circ}\text{C}$ .

## 2.6 Single Muscle Fibre Analysis – Immunoblotting

### 2.6.1 Muscle Fibre Typing (Dot Blotting)

To assess muscle fibre types, PVDF membranes were activated in 95% ethanol for 15 to 60 s and then equilibrated for 2 min in transfer buffer (25 mM Tris, 192 mM glycine, pH 8.3 and 20% methanol). The wet membrane was then placed on a stack of filter paper (one to two pieces soaked in transfer buffer on top of one dry piece). The single fibre samples in the Laemmli solution were then thawed and vortexed, but not centrifuged to

avoid pelleting and hence loss of any of the skeletal muscle protein (219). Samples were spotted to a specific part of the membrane in aliquots equating to 1/8 of a fibre segment (i.e., 1  $\mu$ L) using a multi-channel pipette. This was repeated twice, once for type I detection and another time for type II. After complete absorption of samples, the membrane was placed on top of a dry piece of filter paper to dry for 2 to 5 min before being reactivated in 95% ethanol for 15 to 60 s and equilibrated in transfer buffer for 2 min. After three quick washes in Tris-buffered saline-Tween (TBST), the membrane was blocked in 5% non-fat milk in TBST (blocking buffer) for 5 min at room temperature. Following blocking, the membrane was rinsed with TBST and then incubated in MHCIIa (#A4.74, Developmental Studies Hybridoma Bank [DSHB]) or MHCI (#A4.840, DSHB) antibody overnight at 4 degrees with gentle rocking. On the second day, membranes were washed in TBST and then incubated in secondary antibody IgG (MHCIIa, #A32723, ThermoFisher Scientific) or IgM (MHCI, # Cat # A-21042 4, ThermoFisher Scientific) at room temperature for 1 h with rocking. Lastly, membranes were washed in TBST and then exposed to Clarity enhanced chemiluminescence reagent (BioRad, Hercules, CA, USA), imaged (ChemiDoc MP, BioRad), and analysed for signal density (ImageLab 5.2.1, BioRad). Using images of all the membranes, it was possible to determine the fibre type of each sample (I and IIa) or if no MHC protein was present (54), which would indicate unsuccessful collection of a fibre segment (Figure 2.3). Samples with signal density in both type I and IIa membranes were discarded (i.e., I/IIa hybrid, 2 different fibres in the same sample).

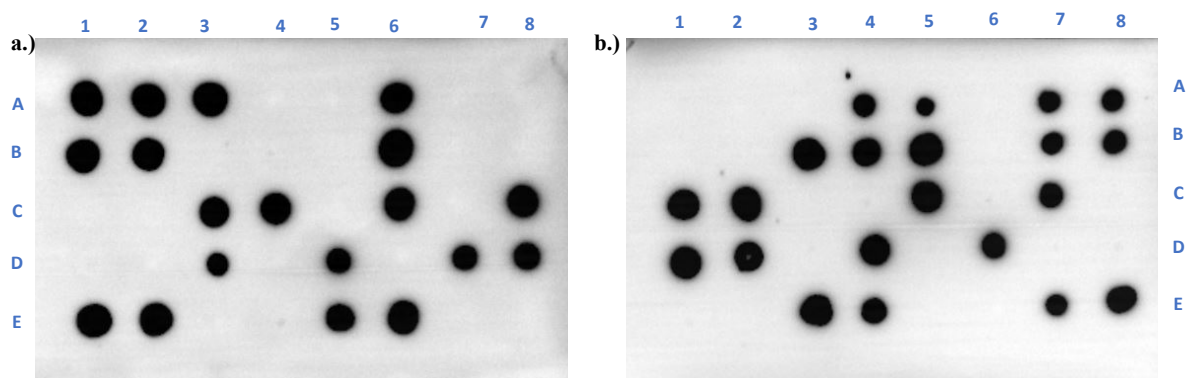


**Figure 2. 4**– Fibre Typing by dot blotting. This example shows membrane images for the identification of fibre types in a single participant. Type I fibres **a.)** presence of MHCI and type II **b.)** presence of MHCIIa

## 2.7 Proteomic-Based Analysis

Liquid chromatography-mass spectrometry (LC-MS/MS) based proteomics was used to elucidate how different types of training affect fibre types. The analysis protocol followed the steps summarised in Figure 2.4, requiring single fibre isolation and pooling, lysis, reduction, and alkylation performed via a protein processing method that was determined in the optimisation phase (see Chapter 3). Once fibre type is confirmed by dot blotting, volumes of individual lysates of the same fibre types are pooled together for further analysis. The optimal number of fibre segments to be pooled is described in section 3.3, this was determined to be 6 fibre segments following optimisation. This method differed from the in-stage tip method previously used by Kulak et al. (173) and Murgia et al. (216), as the single fibre samples were prepared in a Laemmli buffer for fibre type determination by dot blotting. Quantitative multiplexed labelled MS analysis was performed at Monash Proteomic and Metabolomic Facility and the protein identification was derived from values of all known mitochondrial proteins identified in the mitochondrial proteome (MitoCarta 2.0 and/or IMPI ) database.

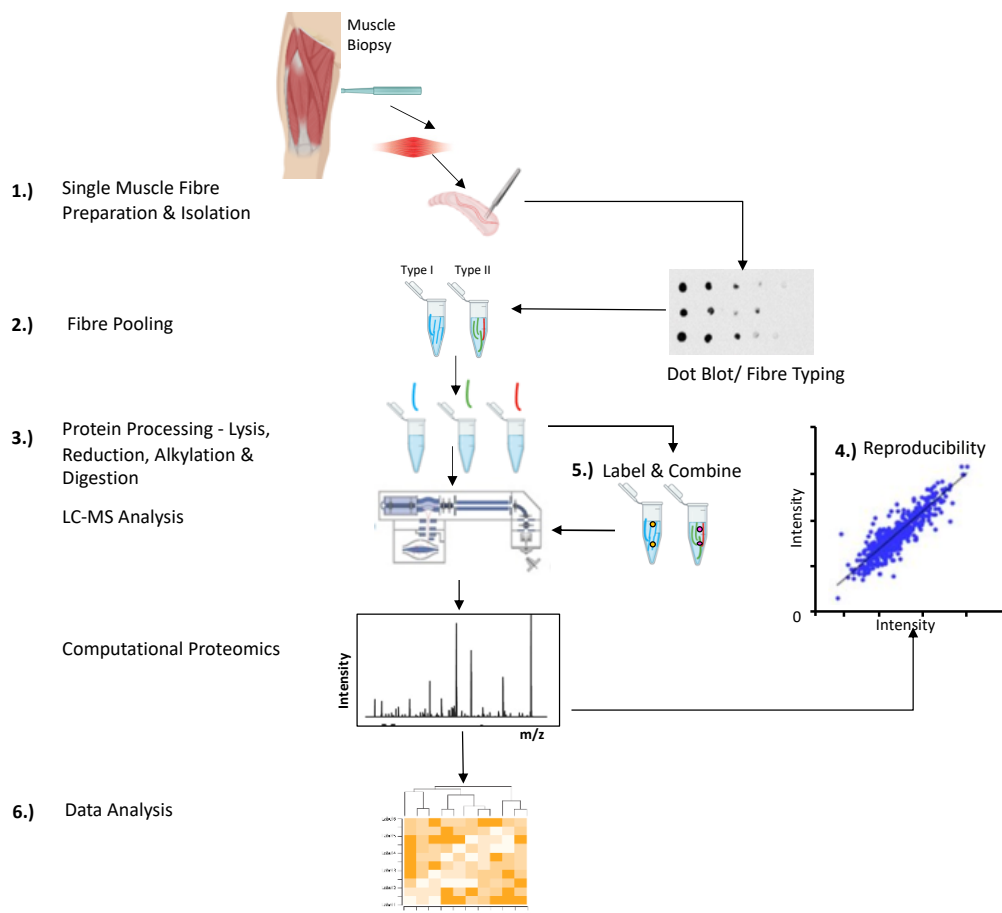


**Figure 2. 5-** Workflow for characterisation of single human skeletal muscle fibres 1.) Single fibre preparation and isolation 2.) Fibre pooling 3.) Lysis, reduction, alkylation, and digestion 4.) Check reproducibility 5.) Labelling and MS LC-MS analysis 6.) Data analysis.

### 2.7.1 SP3 Protein Sample Processing

Fibres were prepared in 5  $\mu$ L of a 2x SDS solubilising buffer (0.125 M Tris·Cl, pH 6.8, 4% SDS, 10% glycerol, 4 M urea, 5% 2-mercaptoethanol, 0.001% bromophenol blue) diluted 2 times (vol/vol) with 1 x Tris·Cl, pH 6.8. Fibres immersed in the SDS buffer were then pooled according to fibre type and further lysed with heating at 95°C for 10 min. Following, pooled fibres were sonicated for 20 min (Bioruptor, Diagenode, 20 cycles of 30 s). Samples were then diluted to 1% SDS with 100 mM HEPES (4-(2-hydroxyethyl)-1-piperazineethanesulfonic acid) buffer. Samples were then alkylated with chloroacetamide (475 mM CAA, Sigma) (the concentration was dependent on the concentration of 2-mercaptoethanol). Twenty  $\mu$ L of beads ((Seramag Speedbead carboxyl Beads (GE Life Sciences) – 1:1 mix of hydrophilic (Cat No. 45152105050250) and hydrophobic (Cat No. 65152105050250) beads in liquid chromatography (LC) grade H<sub>2</sub>O at 10mg/mL of each bead type (20 mg/ml beads total)), were added to the samples. Samples were shaken at room temperature for 8 min using a thermo mixer at 1600 rpm and subsequently placed on place on magnet (Invitrogen™ DynaMag™-2 Magnet, FisherScientific). The lysis buffer was discarded, and the protein was bound to the beads. Beads were then washed beads with 3 x 1 mL of 80% (v/v) ethanol and 50  $\mu$ L of digestion Buffer is added (10% trifluoroethanol, CF<sub>3</sub>CH<sub>2</sub>OH, in 100 mM HEPES, pH 8.5) and shaken for 2 min. 200 ng/5  $\mu$ L of LysC was added to each sample and incubated at 37°C for 1-2 hours with shaking 1500 rpm. Following 200 ng/5  $\mu$ L of trypsin was added and incubated overnight at 37°C with shaking at 1500 rpm. Peptide purification was performed the following day where 2x SDB-RPS (Styrenedivinylbenzene-reverse phase sulfonated ) discs stage tips (68, 257) were prepared by equilibration by centrifuging at 500 g for 3 min in the following order: i) 50  $\mu$ L of acetonitrile (CH<sub>3</sub>CN) ii) 50  $\mu$ L of 30% methanol (CH<sub>3</sub>OH) containing 0.2% Trifluoroacetic acid, CF<sub>3</sub>CO<sub>2</sub> (TFA) iii) 50  $\mu$ L of 0.2% TFA. Following to the stage-tips, 150  $\mu$ L of 1% TFA was added and the peptides were loaded onto the stage-tips containing the 1% TFA. Peptides were then centrifuged through the column at 1000 g, for 2-3 min. Stage tips were washed with 2 x 100  $\mu$ L of 0.2% TFA, then with 40  $\mu$ L of 90% isopropanol (C<sub>3</sub>H<sub>8</sub>O) containing 1% TFA. Peptides were then eluted by adding 60  $\mu$ L of 80% acetonitrile containing 5% ammonium

hydroxide. Samples were vacuum centrifuged for 45-50 min at 45°C and reconstituted in 20  $\mu$ L of loading buffer (0.1% formic acid,  $\text{CH}_2\text{O}_2$ , 2% acetonitrile) for subsequent LC-MS/MS analysis.

### 2.7.2 S-Trap

Fibres were placed into 5  $\mu$ L of a 2x SDS solubilising buffer (0.125 M Tris·Cl, pH 6.8, 4% SDS, 10% glycerol, 4 M urea, 5% mercaptoethanol, 0.001% bromophenol blue) diluted 2 times (vol/vol) with 1 x Tris·Cl, pH 6.8. Fibres were pooled according to fibre type and further lysed with heating at 95°C for 10 min. Following, pooled fibres were sonicated for 20 min (Bioruptor, Diagenode, 20 cycles of 30 s). Reduction and alkylation of disulfides was performed by adding chloroacetamide (40 mM, CAA, Sigma) and further incubated for 30 min at 50°C. The SDS lysate is acidified with 12% aqueous phosphoric acid at 1:10 for a final concentration of ~1.2% phosphoric acid and mixed. This step was essential as the proteins are filtered at this pH. The high percentage of methanol can then precipitate the protein out, which will be retained on top of the S-trap. Following 350  $\mu$ L of S-Trap buffer (90% Methanol (MeOH), 100 mM triethylammounium bicarbonate (TEAB),  $\text{C}_7\text{H}_{17}\text{NO}_3$ ) was added to the acidified lysis buffer (final pH 7.1). A colloidal protein particulate was instantly formed in this step. With the S-Trap micro column in a 1.7 mL tube for flow through, the acidified SDS lysate/MeOH S-Trap buffer mixture was added into the micro column. The micro column was then centrifuged at 6500 rpm for 30 s until all SDS lysate/S-Trap buffer had passed through the S-Trap column. Protein was then trapped within the protein-trapping matrix of the spin column. The captured protein was then washed with 350  $\mu$ L S-Trap buffer; with centrifugation and washing repeated three times. The spin column was then transferred to a fresh 1.7 mL tube (this aided in preventing contamination of the digestion). For best results, the S-Trap micro column was rotated 180 degrees between the centrifugations washes. The S-Trap micro column was then moved to a clean 1.7 mL sample tube for the digestion where the protease (trypsin and LysC) 1:50 in 125  $\mu$ L of 50 mM digestion buffer is added a (1:50 wt:wt) into the top of the micro column. Sample was then centrifuged at low speed at 1000 rpm for 30 s and any solution that passes through is returned to the top of the column. (The protein-trapping matrix is highly hydrophilic and will absorb the solution, however, it was important to ensure there was no bubble at the top of the protein trap). The column was transferred to a fresh tube and

incubated at 37°C overnight (~16 hours). For 96-well plates the protease combination was added at 1:25 in 125 µL of 50 mM digestion buffer and incubated for 1 hour at 47°C.

Peptides were eluted with 80 µL each of digestion buffer (50mM TEAB) and then 0.2% aqueous formic acid to the S-trap protein trapping matrix centrifuged at 3600 rpm for 60 s for each elution. Hydrophobic peptides were recovered with an elution of 80 µL 60% (v/v) acetonitrile containing 0.2% formic acid and then centrifuged at 6500 rpm for 60 s. Elutions were pooled.

Further peptide purification was performed as required with 2x SDB-RPS discs stage tips are prepared and sample is loaded onto the stage-tip. Peptides are then centrifuged through the column at 1500 g for 3 min. Stage tips are washed with 100 µL of 90% isopropanol (C<sub>3</sub>H<sub>8</sub>O) containing 1% TFA and then washed again with 0.2% TFA in 5% acetonitrile and centrifuged for 4 min following each wash. Peptides are then eluted by adding 100 µL of 60% acetonitrile containing 5% ammonium hydroxide and centrifuged for 4 min to collect elution. Samples are lyophilised down to dryness with the SpeedVac (CentriVap Benchtop Centrifugal Vacuum Concentrator, # 7810038, VWR) and reconstituted for labelling and subsequent MS analysis.

### **2.7.3 TMTpro Labelling**

TMTpro Label Reagents (ThermoFisher) were equilibrated to room temperature and 20 µL of anhydrous acetonitrile is added to each tube. Dried samples were reconstituted in 0.5 M HEPES buffer, pH 8.5. The desired amount of TMTpro label was added and incubated at 20 °C for 1 h with shaking (1000 rpm). Following the reaction is quenched by adding a final concentration of 0.25% of hydroxylamine to peptide and TMT mixture, and further incubated at 20 °C for 30 min. Samples are lyophilised down to dryness with the SpeedVac and reconstituted in loading buffer. Each sample was fractionated into 16 fractions using basic pH reverse phase C18 liquid chromatography. Peptides were subjected to basic-pH reverse-phase high pressure liquid chromatography (HPLC) fractionation. Labelled peptides were solubilised in buffer A (10 mM ammonium hydroxide) and separated on an Agilent HpH Poroshell120 C18 column (2.7 µm particles, 2.1 mm i.d., and 5 cm in length).

### 2.7.3.1 TMT Labelling Strategy

Multiplexing techniques have recently extended from 11 to 16 plex, which not only increases sample throughput but accommodates complex experimental designs such as this training study which provided the ability to label 16 samples in one go and then merge as one sample through the LC-MS. A 16-plex allows for an expanded number of treatments such as replicates, and dose-response or time-course measurements can be analysed in the same experiment with basically no missing values across all samples extending the statistical power across the entire system (182). The main study used TMTpro 16-plex version with a different reporter and mass normaliser than earlier TMT versions (i.e., TMT-6 plex). A limitation of tag-based proteomic strategies is ion interference-related ratio distortion resulting from fragmentation and analysis of background ions co-isolated with those of interest. Each sample is differentially labelled such that when pooled, the signal-to-noise values of sample-specific reporter ions represent the relative abundance of each protein. As such, the degree of ion interference by the level of TMT signal detected in channels where a specific protein should be absent can be assessed (36). To best accommodate for possible reporter ion interferences, the following sampling strategy to be performed in a 96-well plate was used (see Figure 2.6). Reporter ion interference (RII) targets were classified according to a typical product data sheet for 16-plex TMTpro Label Reagents from ThermoFisher Scientific, as summarised in Table 2.2.

**Table 2. 2- Reporter ion interference classification for all TMT batches, specifying the reporter mass tag, the reporter channel within the MS3 scan output and the target channels for primary (+1 Da) and secondary (-1 Da) reporter ion interference**

Mass tag	Reporter channel	-1Da (secondary RII)	+1Da (primary RII)
TMTpro <sup>16</sup> -126	1	–	127C
TMTpro <sup>16</sup> -127N	2	126	128N
TMTpro <sup>16</sup> -127C	3	126	128C
TMTpro <sup>16</sup> -128N	4	127N	129N
TMTpro <sup>16</sup> -128C	5	127C	129C
TMTpro <sup>16</sup> -129N	6	128N	130N
TMTpro <sup>16</sup> -129C	7	128C	130C
TMTpro <sup>16</sup> -130N	8	129N	131N
TMTpro <sup>16</sup> -130C	9	129C	131C
TMTpro <sup>16</sup> -131N	10	130N	132N
TMTpro <sup>16</sup> -131C	11	130C	132C
TMTpro <sup>16</sup> -132N	12	131N	133N
TMTpro <sup>16</sup> -132C	13	131C	133C
TMTpro <sup>16</sup> -133N	14	132N	134N
TMTpro <sup>16</sup> -133C	15	132C	134C
TMTpro <sup>16</sup> -134N	16	133N	135N

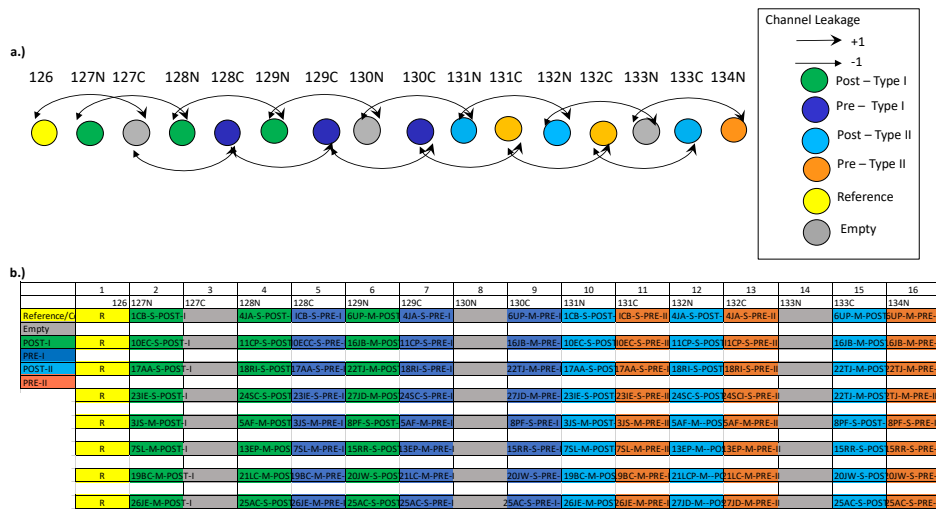


**Figure 2. 6-** a.) Reporter ion interference for 16-plex. b.) Sampling strategy for 96 well plate. Samples labelled by participant ID – M (MICT) or S (SIT) and I (Type I fibre) or II (Type II fibre)

## 2.7.4 Liquid Chromatography and MS

Peptides were loaded onto a 2 cm PepMap trap column (ThermoFisher) and separated using a PepMap 75  $\mu\text{m} \times 50$  cm column (ThermoFisher) with a gradient of 2–30% MeCN containing 0.1% FA over 120 min at 250 nL/min at 40 °C. The Orbitrap Fusion mass spectrometer was operated with the following parameters: an MS1 scan was acquired from 375–1575 m/z (120,000 resolution, 2e5 AGC, 50 ms injection time) followed by MS2 data-dependent acquisition with collision-induced dissociation (CID) and detection in the ion trap (4e3 AGC, 150 ms injection time, 30 NCE, 1.6 m/z quadrupole isolation width, 0.25 activation Q). To quantify TMTpro reporter ions, a synchronous precursor selection MS3 scan was performed higher-energy collisional dissociation (HCD) and detection in the orbitrap (120 to 750 m/z, 1e5 AGC, 250 ms injection time, 60 NCE, 2.5 m/z isolation width). The total cycle time was set to 2.5 s. The acquired raw data was analysed with Proteome Discoverer 2.4 (ThermoFisher) and the non-normalised protein reporter intensity was exported to Excel and further analysed in R.

## 2.8 Normalisation

Normalisation was performed using a combination of trimmed mean of M values (TMM), sample loading (SL), and ComBat methods(155, 189, 251, 264). When normalising for SL, the loading amount for the MS is adjusted so that the amount of peptide per sample is as equivalent as possible. The TMM method uses the average or median signal and is typically applied to use a single multiplicative factor to further adjust the samples to each

other. Further to this, ComBat allows users to adjust for batch effects in datasets where the batch covariate is known, using methodology described in Johnson et al. (155).

## 2.9 Statistical analysis

Statistical analysis was performed using the R package Limma (295) to conduct the differential expression analysis on the relative protein abundances after first performing normalisation technique as described in section 2.8. Differential expression values were determined by comparing the expression of samples against the average expression of all other samples (background) by fitting data to a linear model. The resulting differential expression values were then filtered for an adjusted p-value of  $< 0.05$ .

To focus on proteins specifically associated fibre type, the differential expression results from Limma were first filtered to include only those proteins that were significantly differentially expressed in the type I fibres than in the type II fibres for each training condition (MICT and SIT) and time (pre and post) (adjusted p value  $< 0.05$ ;  $\log_2$  fold change  $> 1$ ). The comparisons were made according to the hierarchy in Figure 2.7. Mitochondrial proteins were identified by annotation using both the Integrated Mitochondrial Protein Index (IMPI) and Mitocarta 2.0 databases (43), which has recently updated to version 3.0 (258).

To better characterise the proteomics changes, gene ontology and enrichment analysis were performed by investigating non-random associations between proteins and over-represented Gene Ontology (GO) conducted using Database for Annotation, Visualization and Integrated Discovery (DAVID) (137) and Protein ANalysis THrough Evolutionary Relationships (PANTHER) to classify proteins (316).

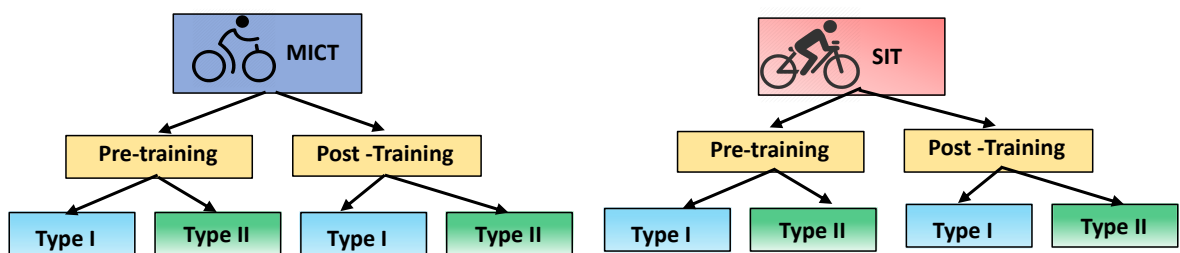


**Figure 2. 7-** Single Fibre Analysis and Comparisons by MS on exercise study for groups of Moderate Intensity Training (MICT) and Sprint Interval Training (SIT).

## **Chapter 3**

### **Methodological Optimisation**

#### **Optimisation of Proteomic Processing Method for Single Muscle Fibre Analysis**

The aim of this study was to develop an optimised protein processing protocol capable of confirming fibre typing and pooling of single fibres by immunoblotting, and thus a further capacity identify an increased depth of protein coverage of single muscle fibre cells in a high detergent matrix. Part of this work has been presented at Victorian Muscle Network Symposium for Students and ECR – Australia, 2020.

### 3.0 Sample Protein Processing Optimisation

For discovery proteomics, sample preparation procedures should comprehensively and reproducibly capture the protein inventory with minimal artifactual modification, degradation, or contamination (10). Furthermore, it is ideal to eliminate complications arising from interference with downstream processes (e.g., digestion, labelling reactions, and ionisation) (10). Simultaneous cell lysis and protein solubilisation is typically achieved by combining physical and chemical (detergent) methods. In-solution digestion is often more efficient than using digestion incorporating gels (see Chapter 1), and peptide extraction from a gel matrix is limited by diffusion kinetics whereas in-solution digestion produces greater peptide yields and can enhance peptide coverage. However, virtually all detergents cause interferences with mass spectrometry (MS) and require removal to the highest degree possible. Achieving such a comprehensive preparation strategy can be a tedious and challenging task when dealing with single-cell samples with minimal amounts of protein. Often, there is no ideal detergent for all applications and results often vary for the same application. The efficacy of detergents for extracting and solubilising proteins can be further refined by additives, such as chaotropes (urea and thiourea), and trial and error is typically the best strategy to find the optimal extraction method (10). The choice of detergent and buffer was predetermined in this research as fibre type was first determined via dot blotting of fibres in Laemmli buffer prior to the pooling of fibres for MS analysis.

The high concentrations of detergents (0.5 to 4%) associated with the Laemmli buffer used in this research is typically required for protein membrane extraction and efficient solubilisation of an array of proteins for western blotting but is often incompatible with downstream processes involved with gel free proteomic approaches. These detergents can inhibit trypsin activity (important for the digestion of proteins), suppress MS electrospray ionisation, compromise chromatographic separation, and generate high-abundance ions that interfere with MS analysis (321). Hence, their elimination is as crucial for subsequent analytical manipulations as the removal of inherent interfering compounds (lipids, nucleic acids, phenolic compounds, carbohydrates, proteolytic and oxidative enzymes, and pigments) (111). While dilution can minimise the adverse effects of those detergents on proteolysis, these efforts can become problematic when working with minute amounts of protein such as single-fibre muscle cells. To minimise protein modifications and

proteolysis arising from such interfering compounds, the purification method should also be considered, such as utilising solid-phase extraction techniques for the digested peptides. Efforts to optimise protein sample preparation from single muscle fibres in this study encompassed: a) optimising cell lysis with chemical and physical methods, b) comparison of two protein processing methods to handle high-detergent concentrations and c) a further purification method for use in conjunction with multiplexing techniques using isotopic labels. The optimisation process also aimed at determining the optimal number of pooled fibres with respect to protein abundance and proteome coverage (in particular mitochondrial proteins) (Figure 3.1). In addition, fibre typing by dot blotting was verified via MS analysis. The optimised protocol presented in this work entails a one-step extraction method utilising an optimal lysis method followed by purification with reverse phased membranes. This work presents a significant step towards implementation of efficient proteome analysis of single muscle fibres that can be used in conjunction with immunoblotting techniques.

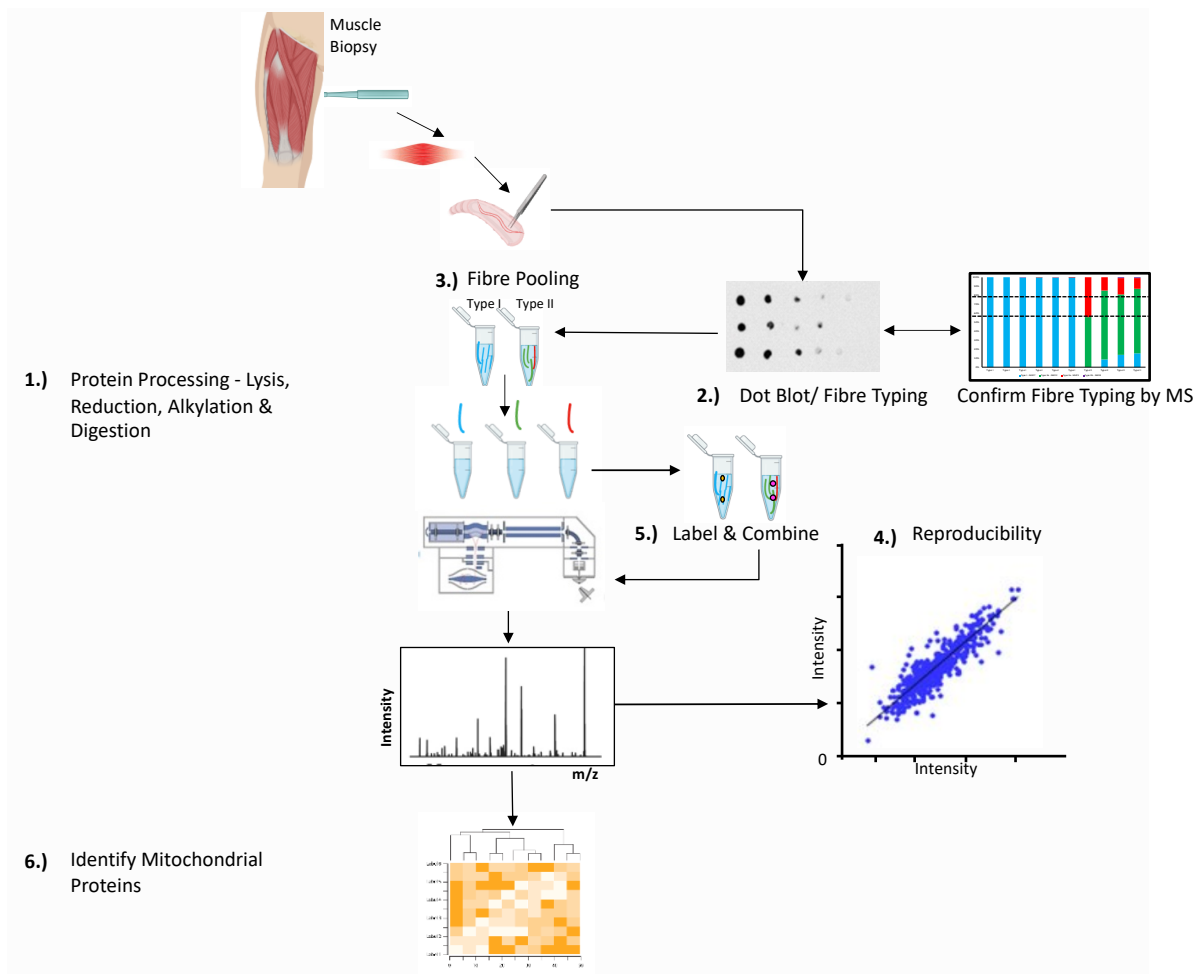


**Figure 3. 1-** Workflow for characterisation of single human skeletal muscle fibres 1.) Optimise protein processing – including lysis, reduction, alkylation, and digestion 2.) Confirm fibre typing 3.) Optimise fibre pooling 4.) Check reproducibility 5.) Labelling and MS LC-MS analysis 6.) Identify mitochondrial proteins.

### 3.1 Comparison of Methods for Protein Processing of Samples with High Detergent Concentration

#### 3.1.1 Single-pot, Solid-phase-Enhanced Sample-Preparation (SP3)

A critical step in proteomics analysis is the optimal extraction and processing of protein material to ensure the highest sensitivity of downstream detection. Achieving this requires a sample-handling technology that exhibits unbiased protein manipulation, flexibility in reagent use, and virtually lossless processing. Two common methods for protein processing were trialled to address these needs. The first was the single-pot, solid-phase-enhanced, sample-preparation (SP3) technology (Figure 3.2). SP3 is a paramagnetic bead-based approach for rapid, robust, and efficient processing of protein samples for proteomic analysis, which uses a hydrophilic interaction mechanism for exchange or removal of components that are necessary to facilitate cell or tissue lysis, protein

solubilisation, and enzymatic digestion (e.g., detergents, chaotropes, salts, buffers, acids, and solvents) before downstream proteomic analysis. SP3 has previously been used as an efficient method to accommodate the different requirements imposed by various tissue types, including skeletal muscle (67, 159, 212).

The fibre samples in this study were originally prepared in a Laemmli buffer for the western blot analysis needed to perform the fibre typing. Thus, one of the key issues to be addressed when selecting a protein processing method for subsequent proteomic analysis was the use of a protocol that could manage high detergent-based samples. The SP3 protocol consists of non-selective protein binding and rinsing steps that are enabled through the use of ethanol-driven solvation capture on the surface of hydrophilic beads and elution of purified material in aqueous combining compatibility with a substantial collection of solution additives. It has been reported to result in minimal losses and recovery of proteins in large or small amounts across numerous organisms (140, 141, 159, 290) and thus was a good candidate for investigation in this single-fibre study. The SP3 protocol is simple and efficient and can be easily completed by a standard user in ~30 min, including reagent preparation. To date, there has been minimal research utilising the benefits of SP3 to facilitate examination complex protein mixtures such as skeletal muscle (17, 159). Figure 3.1 describes the steps involved in performing SP3 in bottom-up proteomics, using a simplified protein clean-up scenario (141).

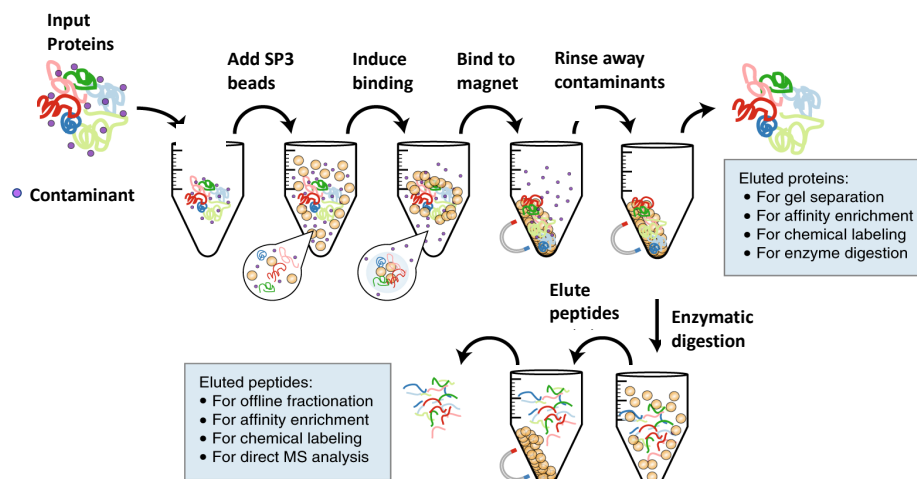


**Figure 3. 2**– Illustration using a simplified protein clean-up scenario with Single-pot, Solid-phase-Enhanced Sample-Preparation (SP3) to provide a simplified platform for the processing of protein samples before MS-based proteomics analysis. The schematic depicts the SP3 workflow for performing clean-up to remove unwanted contaminants from a mixture of proteins. Proteins are bound to magnetic beads via a hydrophilic interaction mechanism. The bound beads are then rinsed to facilitate removal of unwanted contaminants from the proteins. Purified proteins are subsequently eluted for downstream analysis (141).

### 3.1.2 Suspension-Trapping (S-Trap)

The alternative protein processing method investigated was the suspension trapping (S-Trap™) method, which combines the advantage of efficient SDS-based protein extraction with rapid detergent removal, reactor-type protein digestion, and peptide clean-up (344). This protocol is specific for proteins solubilised in strong SDS (~ 5%), as was the case for our Laemmli buffer (~ 3.3% SDS). The sample is acidified and introduced into the suspension trapping tip, incorporating a depth filter and hydrophobic compartments, filled with the neutral pH methanolic solution. The instantly formed fine protein suspensions were trapped in the depth filter stack, which is a crucial step aimed at separating the particulate matter in space. SDS and other contaminants are removed in the flow-through, and a protease is introduced. Following the digestion, the peptides are cleaned up using the tip's hydrophobic part. The methodology allows processing of protein loads down to the low microgram/submicrogram levels (344). The typical protein concentration of a single muscle fibre has previously been indicated to be in the range of 1.2 to 2.7 µg (54, 219); however, given the very small amount of tissue in the samples used in this study, it was not possible to assess the muscle weight or total protein in absolute terms. A further benefit of the S-Trap™ is that it dissolves even poorly soluble proteins (like membrane proteins), which are often left behind in the pellet. Reduction and alkylation are also performed in high SDS precluding any precipitation at this step (see Figure 3.3).

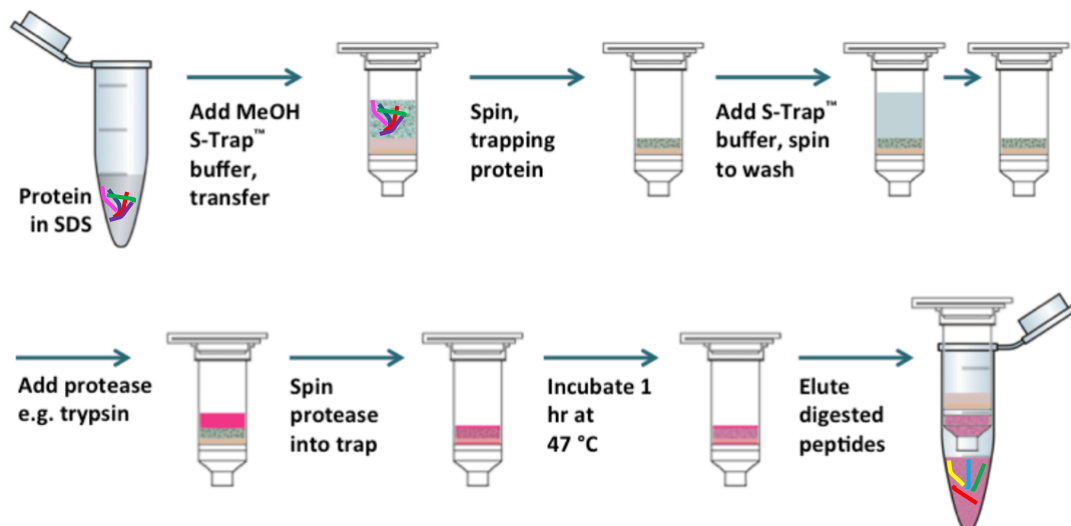


**Figure 3.3 - S-Trap Protocol Schematic** - Proteins are solubilised in SDS, and subsequently reduced and alkylated. Samples are acidified and the S-Trap methanolic buffer is added. The protein suspension is then formed. After the centrifugation, the protein suspension is trapped in the quartz stack. Following washes with the S-Trap buffer and ammonium bicarbonate, a protease is added. After incubation with the protease enzyme, the S-trap column is washed and peptides captured in the S-Trap are subsequently eluted. Modified from (253).

### 3.1.3 Sample Preparation assessment

The first pilot study investigated two protein processing methods. As shown in Table 3.1 and Figure 3.4, both processing methods were able to successfully extract and identify proteins on varying pools of fibres (note that the number of fibres refers to a fibre segment, as described in section 2.5.1, which was approximately half a single muscle fibre). While both methods were able to identify many proteins on as few as two pooled fibres, the S-Trap method was able to identify more proteins. For example, when eight fibres segments were used 840 proteins were identified with SP3 and 1247 proteins identified with the S-Trap.

**Table 3.1– Results summary from Pilot 1 comparing Suspension Trapping (S-Trap) and Single-pot, Solid-phase-Enhanced Sample-Preparation (SP3) protein processing protocols**

<i>Sample Processing Method</i>	<i>Number of Fibre segments</i>	<i>Peptide Conc. (mg/mL)</i>	<i>#Proteins</i>	<i>#Peptides</i>	<i>Fibre Type</i>
SP3	2	0.021	386	1119	2
SP3	4	0.036	721	2785	1
SP3	8	0.069	840	4233	2
SP3	16	0.082	917	4157	1
S-Trap	2	0.994	786	4702	2
S-Trap	8	1.372	1247	9027	2

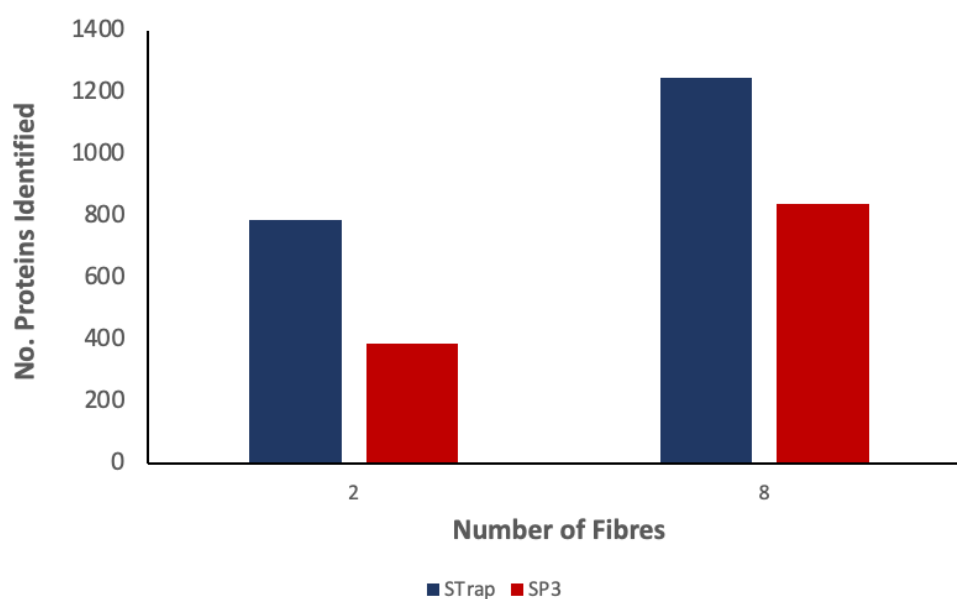


**Figure 3.4– Comparison of coverage for the number of proteins identified by S-Trap and SP3 protein processing methods investigated in pilot 1.**

Given the increased number of proteins identified by the S-Trap method compared to SP3, it appeared to be the optimum candidate to move forward as the method of choice for the study and further testing. To further strengthen the selection of the S-Trap method, an additional consideration was the detection of mtDNA-encoded proteins. These proteins are typically difficult to detect as they are very hydrophobic (44) and they were only detected with the S-Trap method. Of the 13 possible mtDNA-encoded proteins, only 5 were detected with 8 fibre segments (MTATP6, MT-ND1, MT-ND5, MT-CO1 and MT-CO2) and only 1 was detected with 2 fibres (MT-CO2). Another approach to gauge the strength of a method is by looking at abundant core proteins such as complex V subunits, of which 13 (ATP5A1, ATP5B, ATP5C1, ATP5D, ATP5I, ATP5J2, ATP5L, USMG5, ATP5F1, ATP5H, ATP5J, ATP5O, and ATP5F) of the possible 20 subunits (25, 156) were observed with both the S-Trap and SP3 method. Nonetheless, given the increased proteome coverage of the S-Trap method and greater efficiency it was chosen as the preferred method.

### **3.1.3.1 Sample Extraction**

Following the first pilot study, the next phase investigated the S-Trap protocol with an extra peptide purification step using stage tips with SDB-RPS (Styrenedivinylbenzene-reverse phase sulfonated) discs. The discs are typically used for purification and concentration of analytes for analysis to reduce analytical interferences. The Stage-tip is produced by punching a plug out of a disc made from Empore™ C18-SDB-RPS extraction disc with a syringe needle, which is then directly placed and tightly stuffed into the narrow end of a 200 µL pipette tip. Sometimes these filters are known to leak if not packed correctly and this can be tested with a buffer; however, this was not performed at the time of the experiment (83).

To further assist with cell lysis and protein extraction additional sonication to improve the protein coverage was incorporated with Bioruptor sonication. Samples were lysed in the Laemmli buffer, with additional sonication via a Bioruptor that uses state-of-the-art ultrasound technology to efficiently disrupt and homogenise tissues. The S-Trap protocol was then repeated to ensure sufficient protein extraction and additional replicates to observe the effect of peptide purification with the SDB-RPS stage tips. Results are shown in Table 3.2. The additional cell lysis produced a similar depth of protein coverage to that

observed in the initial pilot. Furthermore, additional peptide purification did not have a significant effect ( $p = 0.42$ ) on the number of proteins observed (Figure 3.5).

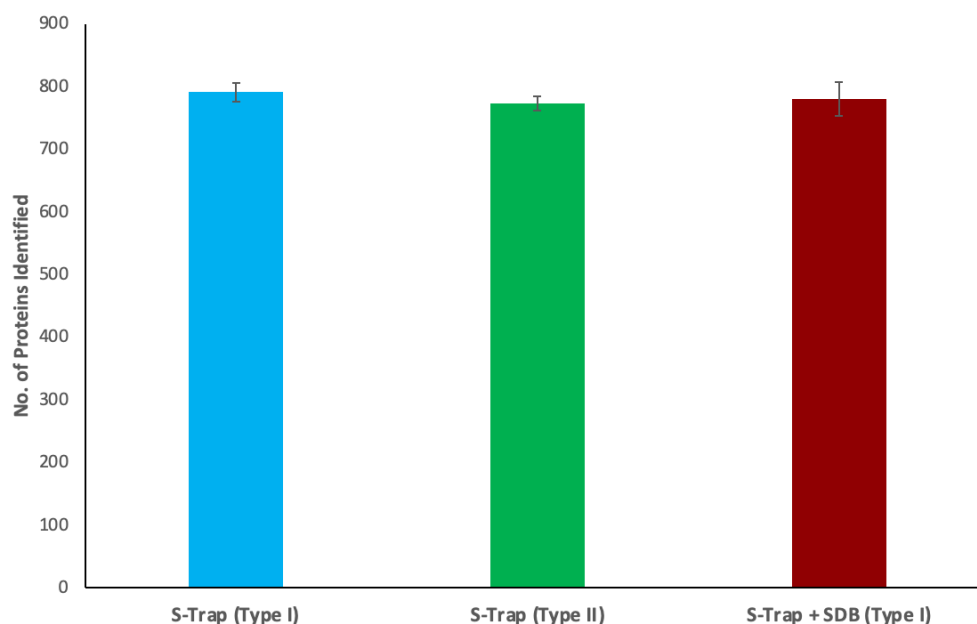


**Figure 3. 5**– Number of proteins observed across all samples. Fibre type is indicated and extra peptide purification step using stage tips with SDB-RPS (Styrenedivinylbenzene-reverse phase sulfonated) discs is indicated by SDB.

**Table 3. 2- Summary of Results from Pilot 2 Comparing the Inclusion of Peptide Purification Step Using Stage-Tips with SDB-RPS (Styrenedivinylbenzene-reverse phase sulfonated) Discs**

<i>Sample Processing Method</i>	<i>Number of Fibre Segments</i>	<i>Conc. Peptide (mg/mL)</i>	<i>#Proteins</i>	<i>#Peptides</i>	<i>Fibre Type</i>
<i>S-Trap</i>	4	0.192	781	7141	1
<i>S-Trap + SDB</i>	4	0.06	761	6368	1
<i>S-Trap</i>	4	0.25	764	7623	2
<i>S-Trap</i>	4	0.199	802	7699	1
<i>S-Trap + SDB</i>	4	0.069	799	7268	1
<i>S-Trap</i>	4	0.184	765	7623	2

An additional consideration for optimisation is the use of a protease. Trypsin is the most popular protease used in MS due to its high proteolytic activity and cleavage specificity. Trypsin comes with its own limitations, as digestion with trypsin is rarely complete and tightly folded proteins can often resist proteolysis (278). Also, as previously discussed, reagents with high detergent concentrations in protein preparation can inhibit trypsin activity. Supplementing trypsin with Lys-C can often address these shortcomings, and

when used in combination to digest proteolytically resistant proteins this has been shown to provide an increased number of identified peptides and proteins, higher analytical reproducibility, and more accurate protein quantitation (278, 309). While using trypsin alone can miss a number of cleavage sites, analysis of various protein samples has shown that the use of a trypsin/Lys-C mix can increase the number of identified proteins by up to 20% and the number of identified peptides by up to 40% (278). In pilot 3, a mixture of LysC & trypsin as the protease was trialled, which slightly enhanced the number of proteins observed for 6 fibre segments (Table 3.3); there was an average of 1029 proteins  $\pm$  65 for all samples in pilot 4. A regression analysis of fibre segments and proteins identified in previous pilots with just trypsin predicted that 6 fibres should identify approximately 969 proteins; thus a 6% improvement was observed with a mixture of proteases. In addition, it is worth noting that the number of proteins in type I and type II fibres were similar ( $p = 0.47$ )

**Table 3. 3- Results Summary from Pilot 3 and Depth of Proteome Coverage for a Fixed Pooling of 6 Fibre Segments Using S-Trap with SDB-RPS Clean-up and a Protease mix of Trypsin/LysC**

<i>Sample Number</i>	<i>Number of Fibre Segments</i>	<i>#Proteins</i>	<i>#Peptides</i>	<i>Fibre Type</i>
1	3	882	7453	1
2	6	1037	8635	1
3	6	1089	9923	1
4	6	937	8677	2
5	6	1051	9451	2
6	9	1135	10744	Mix

### 3.2 Validation of Fibre Typing

The fibre type of single fibres was determined by dot blotting using myosin (MYH) antibodies (53) and fibres of the same type were then pooled. This method was chosen to reduce biological variability between participants by enabling the pooling of fibres prior to MS analysis. The validity of using dot blotting to accurately determine fibre type prior to pooling for MS analysis was a critical consideration in the current study, as antibodies can be cross-reactive or non-specific resulting in false positives (53). The accuracy of the fibre typing was therefore validated using the results of the MYH isoforms detected via MS. Following the data processing methods for determining fibre types in the papers by Murgia (218), fibre types were assigned based on the abundance of myosin heavy chain

(MYH) isoforms. The relative amount of each MYH isoform was determined by dividing the intensity-based absolute quantification (IBAQ) of the respective isoform (MYH1, MYH2, MYH4, MYH7) by the sum of the intensities of all four MYH isoforms. Fibres were classified as type I if the relative abundance of MYH7 was  $> 80\%$ , as type-IIa if MYH2  $> 60\%$ , as type-IIx if MYH1  $> 60\%$  (Figure 3.6a-d). Using this approach results compare well to the classification of human single muscle fibres reported by Murgia (218) (Figure 3.6e), and there was a good correspondence between fibre typing determined via dot blotting and proteomics all in experiments ( $p > 0.05$ ). This provided good confidence to proceed with the pooling of fibres according to the dot blotting method so as to reduce biological variability and increase protein coverage.

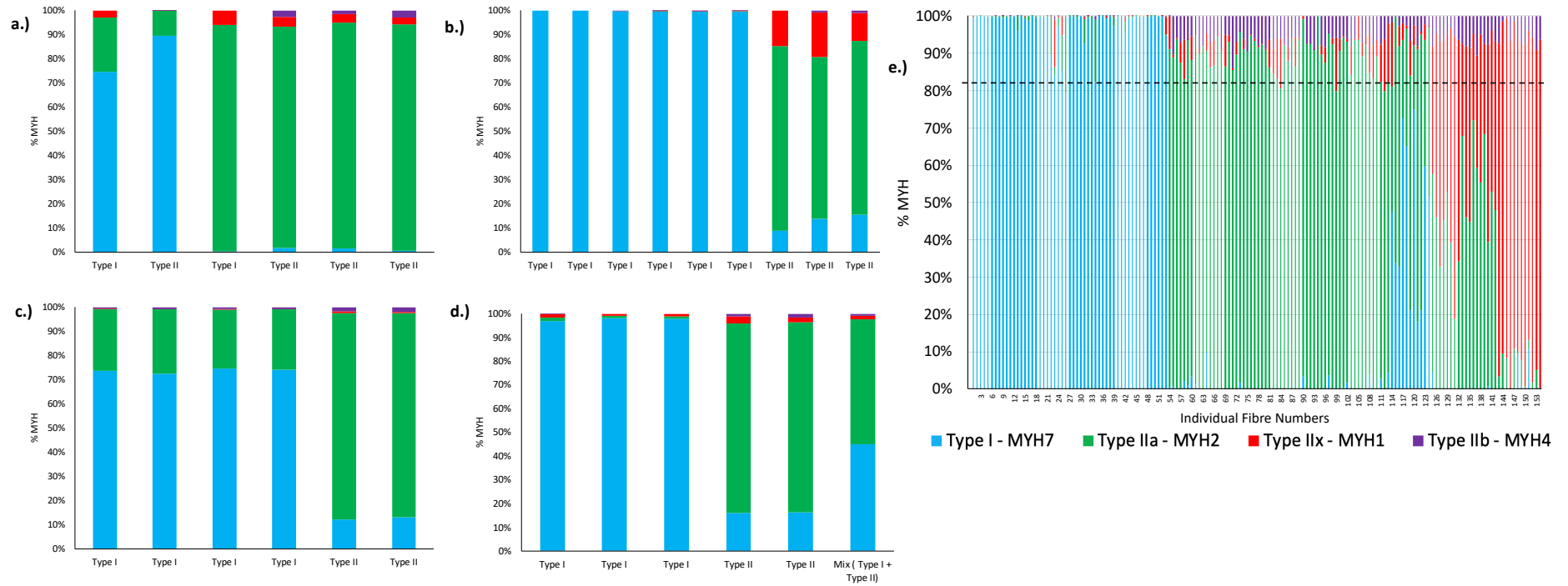


**Figure 3. 6-** Fibre typing by Mass Spectrometry (MS) results a.-d. corresponds to pilot number 1-4 accordingly. e.) represents fibre typing based on Murgia et. al data set for young and old humans (218). Fibres were classified as type I if the relative abundance of MYH7 was > 80%, as type-IIa if MYH2 > 60%, as type-IIx if MYH1 > 60%

### 3.3 Fibre Pooling

A study by Christiansen et al. (54) reported that the greatest between-run variabilities were seen when performing immunoblotting with single skeletal muscle fibres, where the linear regression slopes were statistically different for SERCA1 and AMPK $\beta$ 2 protein content but not for total protein. This variability was attributed to the difficulty in isolating single fibres of the same size, where fibre size is weighted heavily on fibre radius and less on fibre length (54). As groups of single fibres increased to four pooled single fibres, variability was reduced and the greatest decrease in variability was seen with groups of 10 or 20 fibres. Based on this, it was suggested that pooling a minimum of approximately 10 fibres may give the best representation for western blot analysis. An additional benefit of fibre pooling is that it provides sufficient reference material for use in many experiments (259). The pooling of samples is also recommended for proteomic analysis, as it provides a representative proteome of all of the samples that are detected in comparative samples and is needed for reliable quantification (69). However, it is not known how many fibres are needed to obtain a representative pool of single muscle fibres and to optimise the number of proteins detected.

The initial examination of how the number of proteins changed with increasing pooling is shown in Figure 3.7, where an increasing number of proteins and peptides identified was observed with the increased number of pooled fibres. However, there was not much difference from 6 to 9 fibre segments with the number of proteins identified appearing to plateau beyond 6 fibres. Based on this, a fixed fibre pooling of 6 fibre segments was chosen for the main training study to allow for sufficient protein coverage and to provide reduced heterogeneity with the same number of pooling across all samples. In addition, this was the minimum number of a single fibres for each fibre type for a particular participant (Appendix 1).

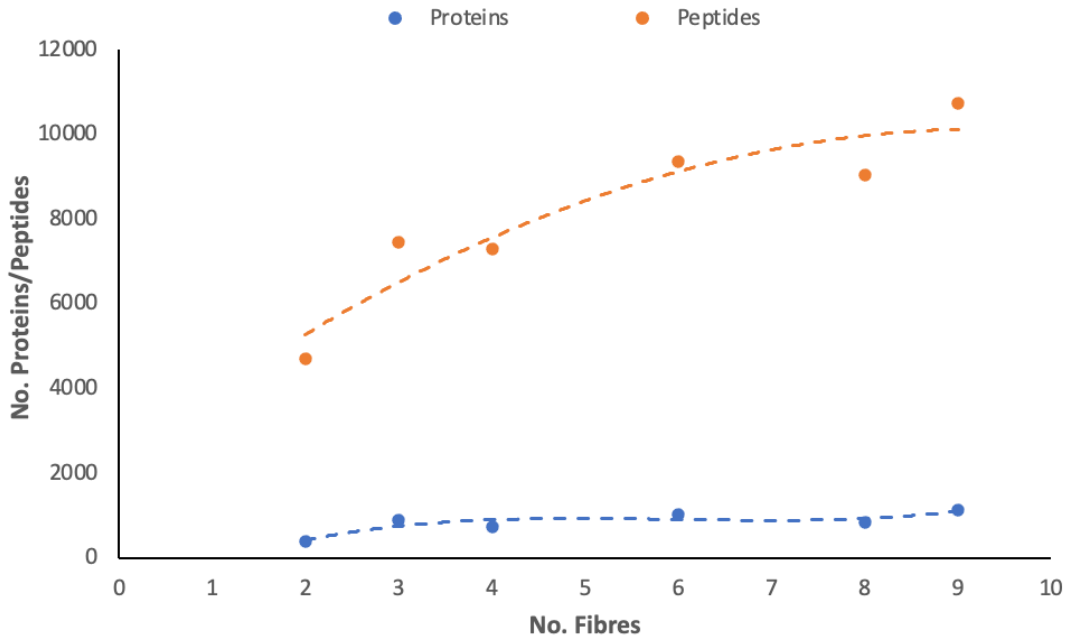


**Figure 3. 7**– Depth of Coverage in pooled single fibre samples for the number of proteins and peptides identified from pilot 1 & 3.

### 3.4 Reproducibility

Following this, the reproducibility of the protein processing protocol across 6 samples (this included 3 replicates from the same participant) of pooled fibres was analysed. Reproducibility was assessed by comparison of the presence of proteins and their corresponding IBAQ or label free quantification (LFQ) intensity among replicates. As shown in Figure 3.8a, there was a strong correlation between samples ( $R^2 = 0.9545$ ). Additionally, there was a high dominating presence of sarcomeric proteins of type I myosin heavy chain (MYH) 7 and type II MYH 2, in addition to actin (ACTA1). As previously highlighted, MS analysis of muscle tissue is often challenging due to these highly abundant sarcomeric proteins. Given single muscle fibres contain very limited protein amounts compared to typical starting amounts in whole muscle, it was promising to see the range of proteins observed. Applying LFQ intensity, by which MaxQuant computes protein intensities as the sum of all identified peptide intensities to normalise globally across all samples, an increase was observed in the correlation coefficient to 0.9991 strengthening support for the reproducibility of the protein processing protocol. Core mitochondrial proteins of OXPHOS and TCA cycle were also repeatedly identified across samples (Figure 3.8). Interestingly, there appears to be an order in the intensity of electron transport chain complexes, which corresponds to a previous proteomic study of

mitochondria, that observed a highly ordered mitochondrial architecture involving electron transport chain proteins rather than a random unorganised protein pool based on the protein abundances (188). Good reproducibility was also observed among replicates of fibre types, where the most abundant protein along the line of identity of samples pooled for type I fibres was MYH7 (Figure 3.8b) and whereas the most abundant protein in the samples pooled for type 2 fibres was MYH2 (Figure 3.8c). Notably, the presence and abundance of key mitochondrial proteins remains consistent among fibre types.

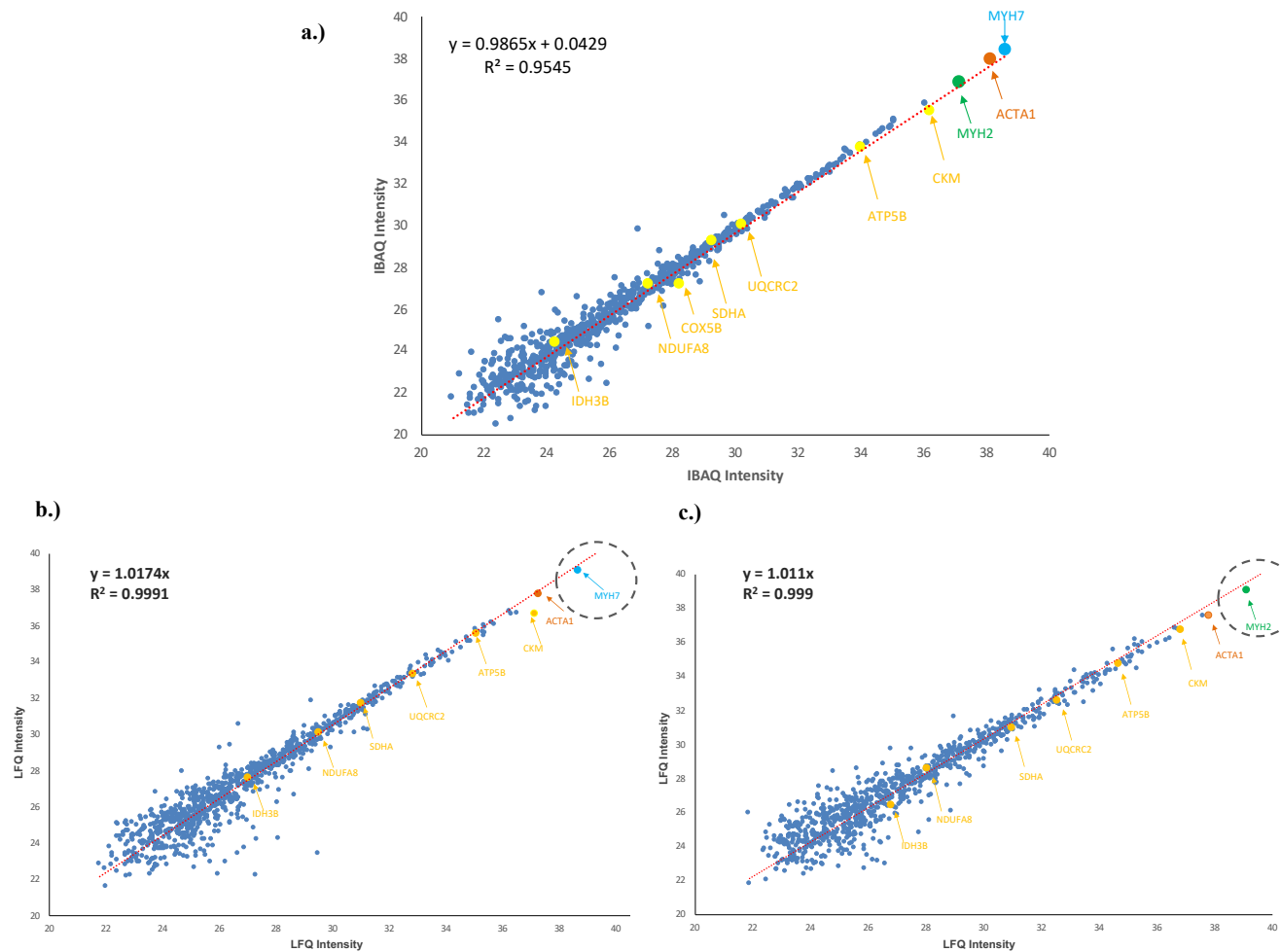


**Figure 3. 8**– Reproducibility across samples. Here the same sample is analysed in duplicate for fibre type and quantification. **a.)** Intensity reported by intensity-based absolute quantification (IBAQ) for replicates of type I fibres. Label Free Quantification (LFQ) reliability in replicate samples. **b.)** Type I fibres **c.)** Type II fibres. Core mitochondrial proteins (OXPHOS – NDUFA8, SDHA, URCRC2, COX5B, ATP5B, IDH3B and CKM) are highlighted in yellow addition to sarcomeric proteins (MYH 7 (blue), MYH2 (green), ACTA1(orange)).

----- Line of identity  
 ----- Highlighting most abundant protein

### 3.5 Isotopic Labelling

To cope with the challenges arising from the analysis of a large number of biological samples in proteomics, strategies have been developed to allow for multiple samples to be analysed in parallel through multiplexing isotopically tagged peptides. The most widely used MS multiplexing method is tandem mass tagging (TMT) (317). Multiplexing by TMT provides the ability to increase sample throughput in proteomics studies and reduce the “missing values” problem (proteins that are not identified in all samples) that arises from the random sampling methods common in data-dependent acquisition (DDA) proteomics (8, 238). Another major advantage is the inherent high reproducibility between samples due to the samples being combined after labelling and co-analysed. In addition labelling can assist in reducing the MS signal drift for a number of samples that can often translate to subsequent batch effects with high sample volume numbers. Further, the precision of the quantification within a multiplexed TMT batch is high (12, 36, 181).

TMT reagents are composed of an amine-reactive group, a mass normalisation group, and a reporter ion group. The amine-reactive group can label peptides. The reporter ion provides the abundance of a peptide upon MS analysis in individual samples being mixed (62). Thus, labelled peptides simultaneously elute as a single composite peak with the same  $m/z$  value in an MS1 scan and further fragmentation of the labelled peptides during the subsequent MS2 or MS3 scans generates reporter ion peaks of differing mass enabling quantification across large samples numbers (182, 259) (Figure 3.9).

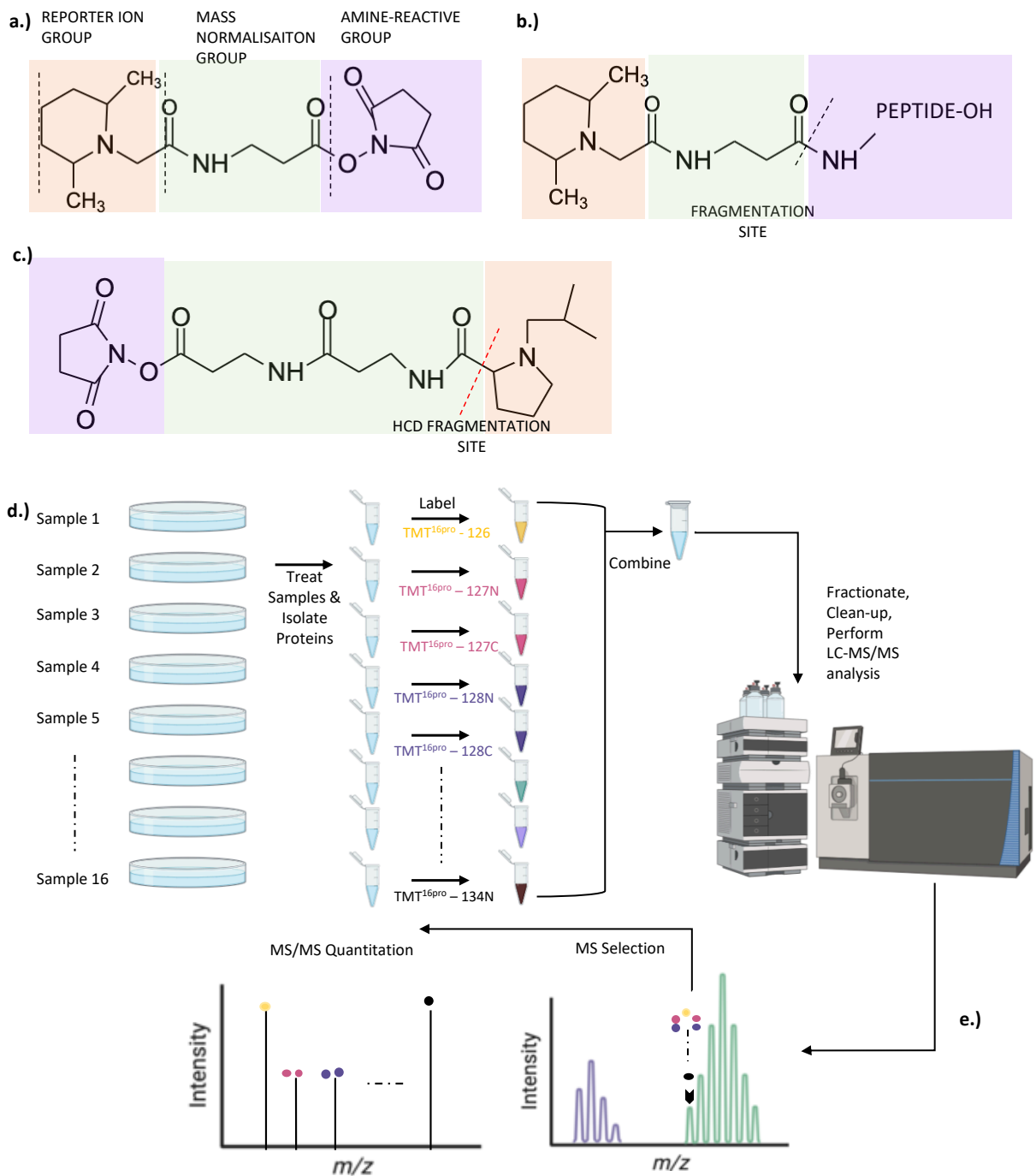


**Figure 3.9**– a.) Structure of commercially available TMT (tandem mass tags) b.) The peptide modified by the TMT. c.) TMTpro reagent are available up to 16plex TMTpro -127C is shown as an example High Collision Dissociation (HCD) Fragmentation d.) TMT are available in up to 16 tags that can be used for labelling practically any peptide or protein sample. TMT makes it possible to multiplex the analysis, providing more efficient use of instrument time and further controls for technical variation. e.) TMT quantification is performed by measuring the intensities of fragment reporter ions released from the labels in the tandem MS mode (MS2) during peptide fragmentation. A further scan in a subsequent MS mode can follow where required in MS3 mode (not shown). Precursor ions are selected in the full scan mode (MS1). Since ion selection step reduces the noise levels, it is advantageous (182, 259).

Labelling is usually very efficient; however, when primary amino groups are present elsewhere in the sample they may interfere with the labelling reaction since they can react with the amine-reactive isobaric mass tags (50, 259). Hence, proper sample preparation is imperative for the success of an isobaric labelling-based quantification technique and includes either avoiding the use of primary amine-containing buffers such as tris and ammonium bicarbonate or performing sample clean-up prior to the isobaric labelling reaction (259, 341). Additional influences can come from the choice of alkylating agents that may interact with the buffers. For example, the alkylating agent chloroacetamide (CAA) possesses a free amine for exchange, whereas a less frequently used alternative of N-(tert-butyl)-2-Iodoacetamide does not possess a free amine (172). Furthermore, various factors including ratio compression and reporter ion dynamic range can cause an underestimation of changes in relative abundance of proteins across samples, reducing the ability of the isotopic labelling. Thus, it is imperative to optimise ratios and labelling in ideal combinations for experimental design and optimal data acquisition to increase the precision and accuracy of the measurements (259).

To improve detection limits and achieve a reliable estimate of quantification, it is recommended that the labelling efficiency be determined for each isobaric labelling experiment. The labelling efficiency can be ascertained by searching the data separately against protein databases using TMT modifications as variable instead of fixed modifications. Using these parameters both labelled and unlabelled peptides can be identified and used to calculate labelling efficiency, which is defined as the percent of labelled peptides among all identified peptides (259) and where ideally all peptides are fully labelled (7).

The efficiency of the TMT labelling was investigated as a strategy to be utilised in the main study to multiplex large sample numbers. As with any protein processing strategy, completeness of reaction and elimination of side reactions are a primary concern. One of the first studies utilising TMT-zero and TMTpro-zero on trypsinised human cell lysates was able to achieve small fractions of unlabelled peptides (231), with labelling efficiencies of 95.4% (TMT-zero) and 97.6% (TMTpro-zero) (182). However, taking into consideration that trypsin digests arginine and lysine (231), while TMT labels free amine (N-terminus and lysing) (182, 259), if a peptide with blocked N-terminus (e.g., acetylation) and ends with arginine, it can result in the peptide not being labelled,

reducing the reaction yield and labelling efficiency. Consequently, this required serious consideration for a complex matrix as was the case with samples prepared in Laemmli buffer. Additionally, post-translational modification on the N-terminus or lysine makes them inaccessible to labelling and potential low confidence in peptide identification needs to be excluded. Thus, while a previous study reported > 95% labelling efficiency, a target of at least 90% labelling efficiency consistently across all samples was selected as a reasonable aim for this study provided consistency was achieved across all samples.

As seen in Figure 3.10, a poor labelling efficiency was initially observed with the use of TMTpro-zero at varying TMT to peptide ratios. This was suspected to be predominantly a consequence of the low pH in the dried sample and/or due to possible interfering compounds in the Laemmli buffer, such as the primary amine tris and  $\beta$ -mercaptoethanol (259, 341). Mercaptoethanol is used for disulfide bridge reduction to reduce fragmenting of disulfide-linked peptides; however, tris(2-carboxyethyl-phosphine (TCEP) and dithiothreitol (DTT) are typically used in proteomic experiments as they are more stable and often prevent further disulfide scrambling (308, 342).

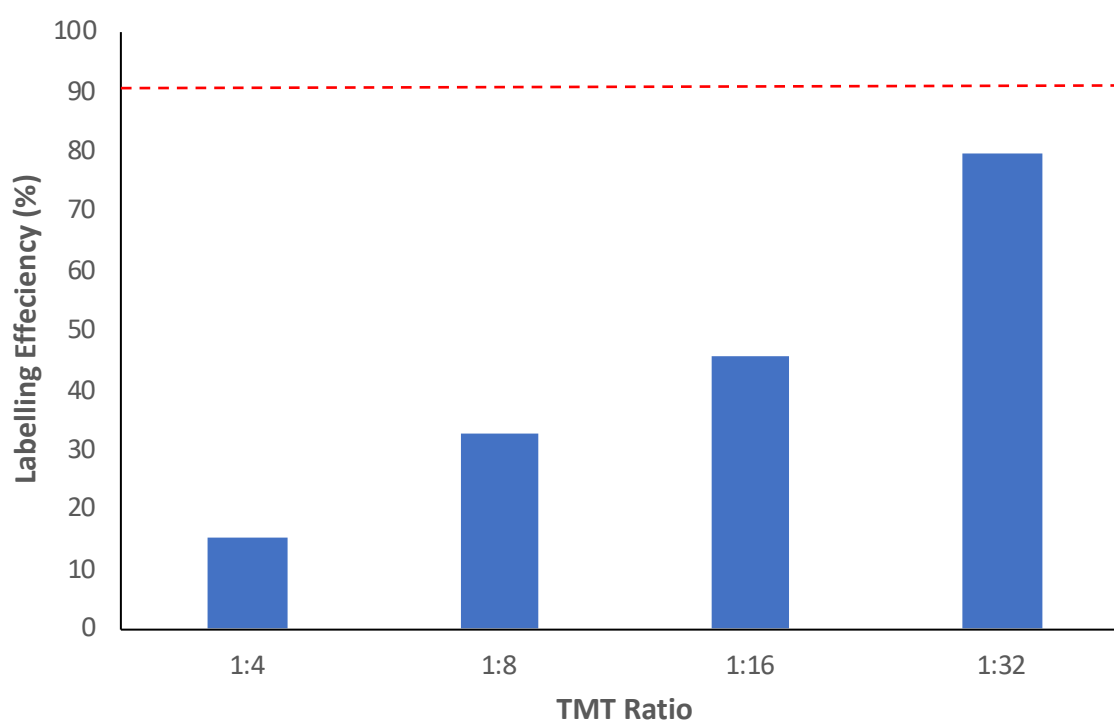


**Figure 3. 10**– Labelling Efficiency of TMTpro-zero. Peptide to TMT ratio is indicated on the x-axis. --- indicates target threshold of 90% labelling efficiency

In the earlier pilots, SDB stage-tips were initially tested in the proteomic workflow (c.f. section 3.1.3.1). Given they did not enhance the number of proteins identified in a label free environment, the use of SDB-RPS stage-tips was deemed an extra time consuming step. However, to achieve greater than 90% labelling efficiency, it appeared that a further clean-up of the samples before TMT labelling was required. Thus, the use of SDB-RPS stage-tips to remove the amine-containing buffers and any residual  $\beta$ -mercaptoethanol was reintroduced into the workflow to be trialled in combination with TMT labelling. Samples were also reconstituted in a stronger concentration of HEPES to ensure pH was not too acidic and the labelling reaction was allowed to proceed for 1 h, as suggested by the manufacturer. These modifications to the protocol increased labelling efficiency to > 90% when a ratio of 1:16 or 1:32 of peptide to TMT was used (Figure 3.11). It can be seen that without effective sample clean-up measures the labelling efficiency was compromised, possibly affecting N-terminal residues where the percentage of labelled amino acids dropped to below 50% (259).

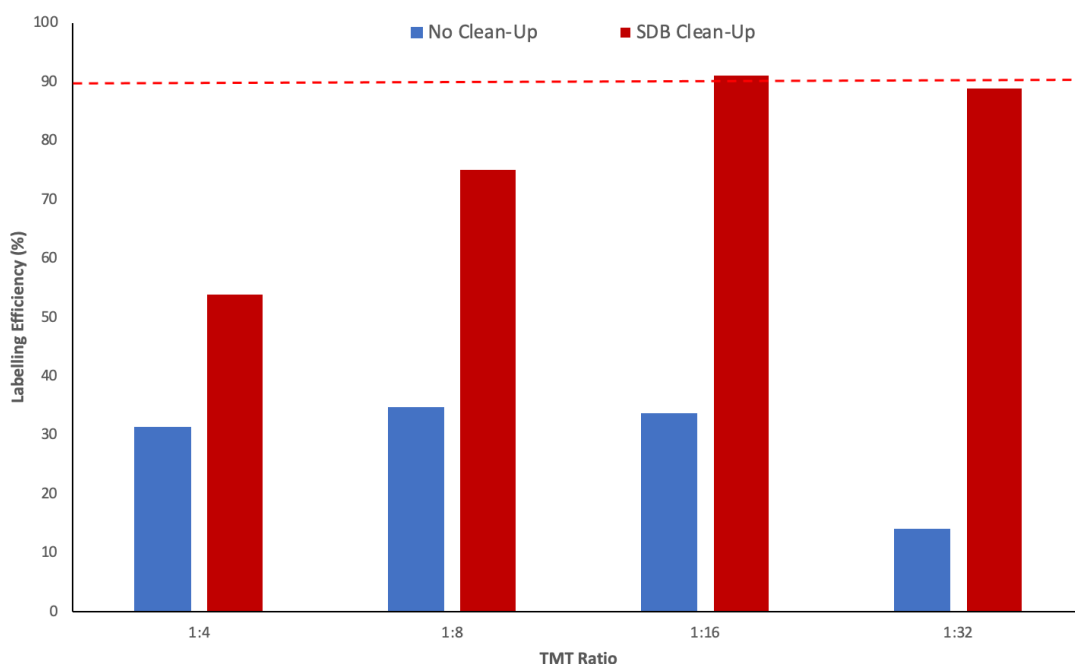


**Figure 3. 11-** Labelling Efficiency of TMT with and without clean-up in pool of single skeletal muscle fibres. Peptide to TMT ratio is indicated on the x-axis. --- indicates target threshold of 90% labelling efficiency

Ideally, the goal is to achieve optimal labelling efficiency without diluting the sample excessively or having an overabundance of TMT label. Thus, a labelling ratio of 1:16 peptide to TMT was selected as the optimal condition for the main study and this was

further assessed in subsequent tests to validate the 1:16 peptide to TMT ratio in conjunction with proteolytic S-Trap digestion of 1 h for increased sample throughput. Using this streamlined protocol, overnight digestion achieved 99% ± 2.3 labelling efficiency. This is comparable to that previously observed by Li et al. (182). However, a shorter digestion period of 1 h was preferred to enable a shortened experimental protocol and to allow for sample processing of a large sample-set within a week. It was found that using a short digestion period of 1 h at a higher temperature of 47 °C (compared to an overnight digestion at 37 °C) was able to achieve sufficient number of peptides (Table 3.4) and labelling efficiency (> 90%) to meet the previously recommended criteria (182) (Figure 3.12). This became the selected parameters for the adapted streamlined-TMT-based protocol combined with S-Trap protein processing technique of 96 samples in the main training study. Thus, the final protein processing protocol employed cell lysis with Bioruptor sonication and SDS detergent in the Laemmli buffer followed by protein extraction with S-Trap using 1 h of digestion with a combination of Trypsin and LysC and further peptide purification with SDB-RPS stage tips. This was followed by efficient TMT labelling of samples.

**Table 3. 4– Labelling Efficiency and Digestion Results Comparing 1 h and Overnight Digestion S-Trap Protocols combined with SDB-RPS Clean-Up**

<i>Description</i>	<i>Peptide:TMT Ratio</i>	<i>*Number of Fixed modifications</i>	<i>*Number of Variable modifications</i>	<i>*No modifications</i>	<i>Labelling Efficiency (%)</i>
<i>SDB- Overnight Digestion</i>	1:16	5924	5887	-	100.0
<i>SDB- Overnight Digestion</i>	1:16	7226	7425	-	97.3
<i>SDB-1h Digestion</i>	1:16	7010	7781	-	90.1
<i>SDB-1h Digestion</i>	1:16	6192	6854	-	90.3
<i>SDB-1h Digestion</i>	No TMT	-	-	8081	-
<i>SDB-1h Digestion</i>	No TMT	-	-	8256	-

\*Number of peptides observed

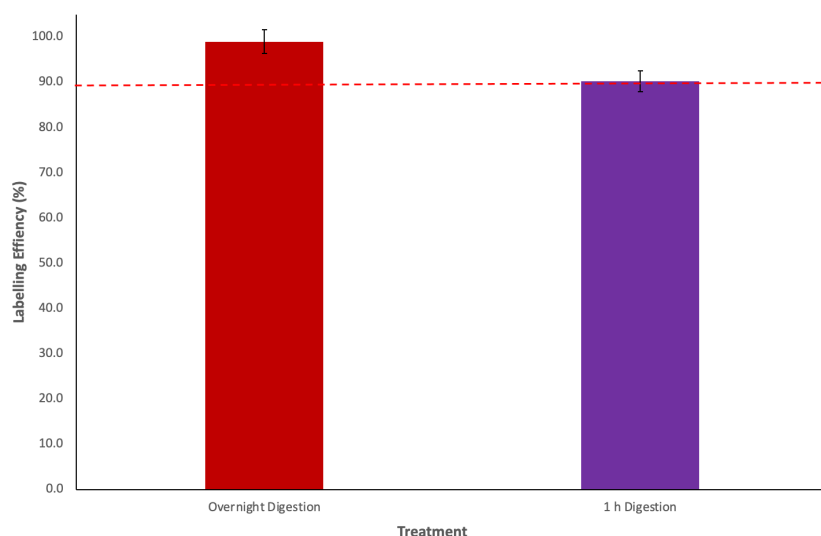


**Figure 3. 12**–Labelling Efficiency of TMT comparing 1 h and Overnight Digestion S-Trap protocols combined with SDB-RPS clean-up. Peptide to TMT ratio was fixed at a ratio of 1:16. ---- indicates target threshold of 90% labelling efficiency.

### 3.6 Mitochondrial Proteins

As previously highlighted, the mitochondrion houses not only pathways for energy metabolism, such as OXPHOS and the TCA cycle, but many additional pathways, such as heme biosynthesis, fatty acid/amino acid oxidation, pyrimidine biosynthesis, calcium homeostasis, and apoptosis. Of the estimated 1158 proteins in the mitochondrial proteome (MitoCarta 2.0 (43)), approximately 300 have no known function and an additional 300 have only domain annotations based on similarity from analysis by various researchers (43, 44). These proteins could be new components of well-studied pathways or, alternatively, represent components of pathways not previously appreciated to even reside in mitochondria.

The most complete mitochondrial catalogue is the MitoCarta catalogue, which contains 1158 gene loci that encode mitochondrial proteins. The MitoCarta catalogue is estimated to be 85% complete. Based on a Bayesian probabilistic model that incorporates run-through data and a prior probability that 7% of all mammalian genes are mitochondrial, it has predicted that there are 1050 to 1400 genes that encode mitochondrial proteins and have a dynamic range of abundance. Recent MS/MS analysis supports the high abundance of these proteins. Based on rough estimates of protein abundance across muscle tissues, the three most abundant mitochondrial proteins are ATP5A1, ATP5B, and ACO2 (44).

Given the focus of the current study is on mitochondrial protein changes, I also investigated the coverage of mitochondrial proteins observed across the pilot studies. The number of mitochondrial proteins was analysed by filtering through the MitoCarta 2.0 database (43). In general, good coverage of mitochondrial proteins is seen across the pilots. In all pilot studies, the three most abundant mitochondrial proteins were observed (i.e., ATP5A1, ATP5B and ACO2). The strength of the protein processing protocol can further be assessed by looking at dominant subunits of the electron transport complexes. Analysing complex I subunits in the first trial, there were 39 of 44 detected; this was similar to that observed by deep fractionated proteomics for HeLa cells, which was promising (305). On average, we were able to identify in the range of 200 to 360 mitochondrial proteins, which was found to represent greater than 35% of the total quantified proteins in single skeletal muscle fibres. Additionally, in pilot three we observed 36 complex I proteins without further fractionation (Figure 3.13). Given the complex starting matrix in this study (required to pool fibres), this compared well to one of only two other single skeletal muscle fibre proteomic studies in humans (218). The aforementioned study prepared single fibres with the more stable DTT, and lysed the fibres in sodium deoxycholate (SDC) for further sample processing, and were able to identify 300 to 500 mitochondrial proteins in single skeletal muscle fibres (218). Thus, the results in the protocol optimisation provide a solid baseline to move forward and observe differentially expressed mitochondrial proteins as a consequence of training in single skeletal muscle fibres.

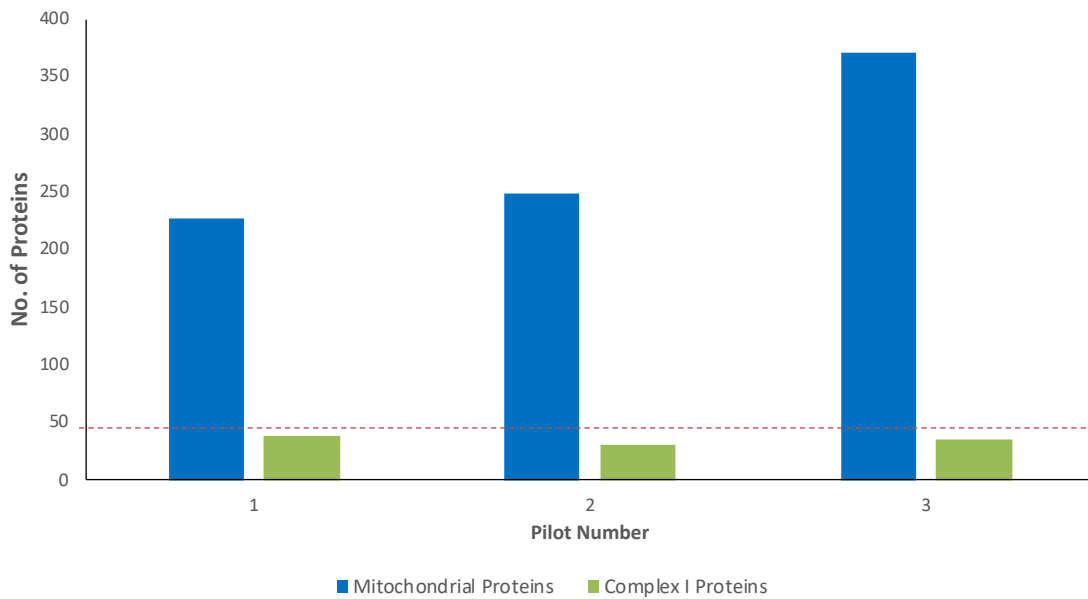


**Figure 3. 13**– Number of mitochondrial proteins identified with each pilot study and the corresponding Complex I proteins observed. Proteins were classified as mitochondrial by matched filtration through MitoCarta 2.0 (43). ----- refers to the total of 44 quantifiable complex I subunits.

Further to this, I explored the functionality of the mitochondrial proteins identified and how these proteins are spread across these functions. An examination of the cellular processes represented by the > 300 mitochondrial proteins identified in all the pilot studies was performed using enrichment analysis of Gene Ontology (GO) biological processes through Protein ANalysis THrough Evolutionary Relationships (PANTHER) (316) and Database for Annotation, Visualization and Integrated Discovery (DAVID) (137). This identified that detected mitochondrial proteins were included in processes associated with mitochondrial functions in skeletal muscles, such as oxidative phosphorylation (OXPHOS), glucose metabolism, the tri-carboxylic acid (TCA) cycle, mitochondrion transport,  $\beta$ -oxidation, and cristae formation (Figure 3.14 a-c). At a cellular component level, mitochondrial proteins appear to dominate within the inner membrane, with the highest proportions belonging to the respiratory chain complexes, followed by the outer member and the intermembrane space.

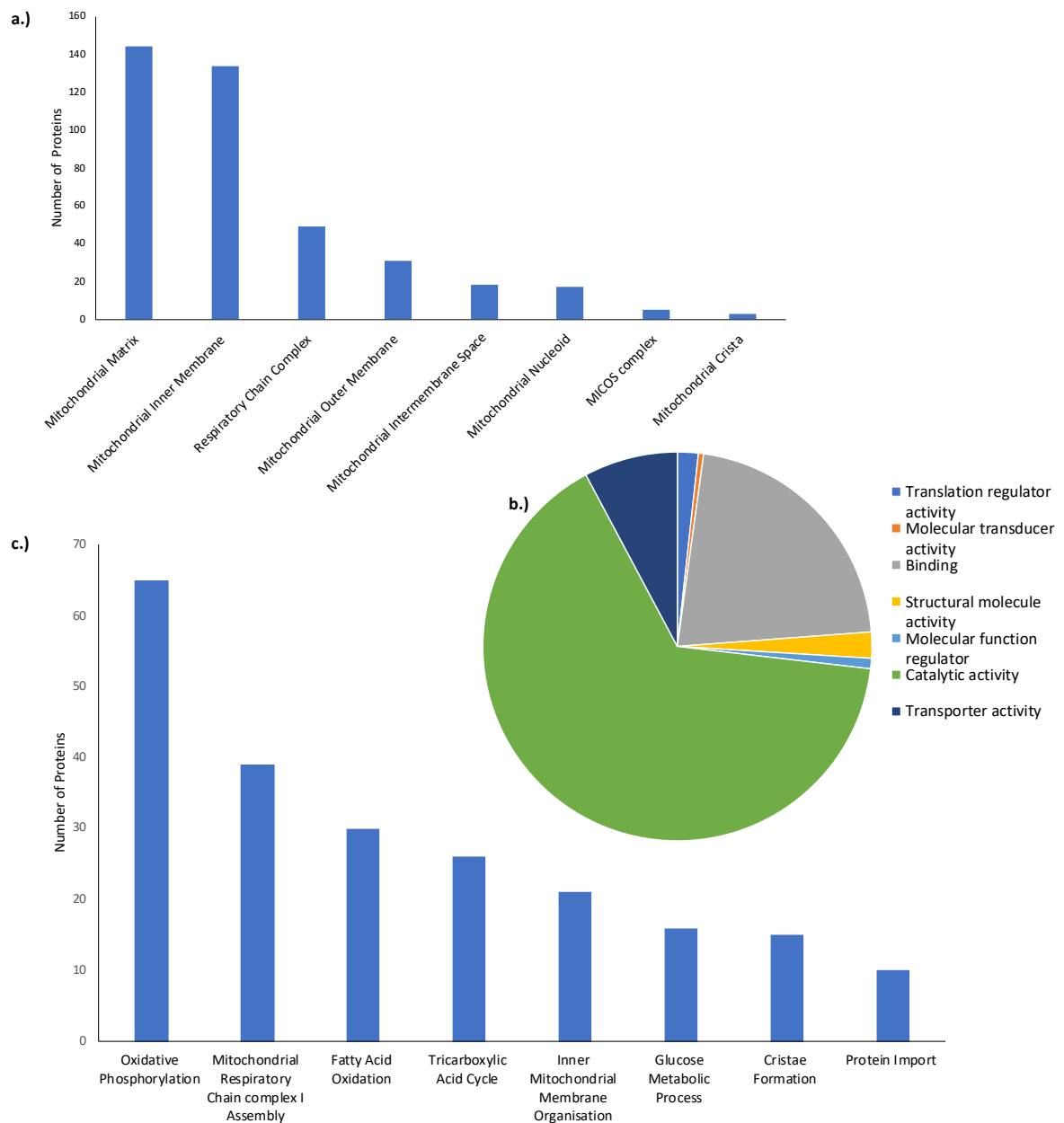


**Figure 3.14– a.)** The number of mitochondrial proteins involved in cellular processes computed using Gene Ontology (GO) enrichment analysis. MICOS - mitochondrial contact site and cristae organizing system **b.)** Molecular processes in GO analysis in which the identified proteins are mainly involved **c.)** The number of mitochondrial proteins involved in biological processes computed using GO enrichment analysis. GO analysis was performed using Protein ANalysis THrough Evolutionary Relationships (PANTHER) (316) and Database for Annotation, Visualization and Integrated Discovery (DAVID) (137).

### 3.7 Conclusions

Mitochondrial biology has been studied extensively for decades using traditional biochemical and molecular approaches. The comprehensive characterisation of its protein inventory opens up exciting new opportunities for the system-level analysis of this organelle in health and disease. The optimisation data presented in this chapter provided a new methodology for the combination of dot blotting for fibre typing and the analysis of single fibres in a high detergent matrix. This allows the application of this methodology to the analysis of training adaptations in the mitochondrial proteome in single skeletal muscle fibres. The key optimisation findings are summarised in Figure 3.15, which included a reproducible method utilising S-Trap protein extraction for sample processing in combination with SDB peptide clean-up to observe over 1000 proteins in pools of 6 fibres segments with a TMT labelling efficiency of > 90% when using a 1-h trypsin/LysC digestion combination. This research also highlights that optimal extraction and processing of protein material is crucial to ensure the highest sensitivity for the downstream detection of proteins in complex matrices, such as skeletal muscle.

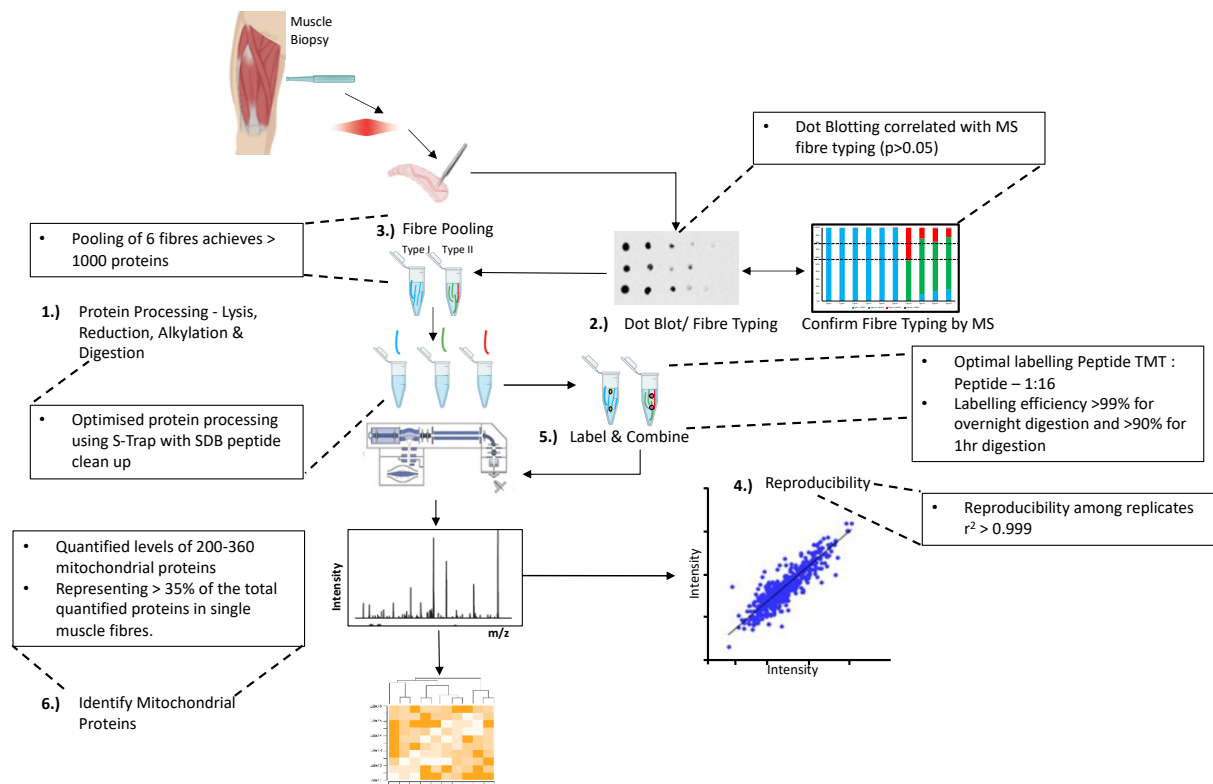


**Figure 3. 15**– Key optimisation findings for protein processing protocol. Highlighted are key finding from each optimisation phase 1 to 6 including, protein processing, fibre typing, fibre pooling, reproducibility, isotopic labelling, and identification of mitochondrial proteins.

It is anticipated that mitochondrial proteomics applied to exercise and training will be a fast-moving area in the coming years, as we can see the advantage of being able to identify thousands of proteins in a single experiment compared to traditional immunoblotting techniques. This research hopes to be at the forefront of improved understanding of how mitochondrial proteins function together in pathways and complexes in single fibres in response to training and possibly the localisation within the mitochondrion. It may be possible for hundreds of currently uncharacterised mitochondrial protein responses to training to be linked to functions as a consequence of the utilisation of proteomic technology.

## **Chapter 4**

### **Training and Mitochondrial Protein Responses in Single Muscle Fibres**

The aim of this chapter is to explore the mitochondrial protein responses in single muscle fibres following 8 weeks of training. In the previous chapter, an optimised protein processing protocol capable of fibre typing and handling single muscle fibres in a high detergent matrix was described. This method was then used to elucidate which mitochondrial proteins are regulated in different fibre types following 8 weeks of moderate-intensity or sprint interval training. Part of this work has been presented at Australian Physiological Society Student and ECR Forum – Australia, 2020.

#### **4.0 Measuring Fibre Specific Changes in Response to Training by Proteomics**

For many years, different analysis techniques have been used to investigate physiological adaptations induced by exercise training in skeletal muscle. This includes investigating changes in specific proteins, which was dominated by immunoblotting techniques. Among the new trends in exercise physiology research is quantitative proteomics by mass spectrometry (MS), which plays a key role in allowing quantitative comparisons of changes in protein expression and post-translational modifications after perturbations such as exercise. The limitations of gel-based methods have been addressed via the development of gel-free techniques based on in-solution separation and digestion, protein labelling, peptide fragmentation, and high throughput MS instruments to improve reproducibility and depth of coverage of proteome data acquisition (243, 259).

Due to the heterogeneity of mammalian samples and their wide range of protein content, there are some important sample preparation considerations (as discussed in Chapter 3) that have to be taken into account to ensure successful proteomic analysis. Optimal protein identification data by gel-free methods often depends on successful tissue harvesting, cell lysis, and protein extraction procedures, followed by protein quantification (243). Using a combination of suspension-trapping, peptide purification (using SDB-RPS, Styrenedivinylbenzene-reverse phase sulfonated), TMT labelling, and further fractionation with LC-MS/MS, we compared the protein abundance of isolated single muscle fibres pooled by fibre type, obtained from 23 healthy male individuals before and after two types of training (Moderate Intensity Continuous Training; MICT and Sprint Interval Training; SIT).

#### **4.1 Batch Correction**

There are numerous factors that can make data analyses challenging in experiments where more than one set of isobaric tag reagents are used. Our study required numerous 16-plex reagent labelling sets to permit a three-tiered comparison of treatment groups (training), time, and fibre type. To help ensure the sources of measured differences between groups were due to the biological variations, normalisation is required to remove unwanted batch effects that may result from other unwanted sources of variation such as inaccuracies in protein assays and pipetting errors. Applying normalisation to make samples similar, without removing or affecting biological differences, improves the power and precision

across all batches and is a critical component of the processing pipeline for proteomic analyses (36). After conducting a very large-scale proteomics analysis across multiple TMT 16-plex batches, it was essential to be aware of the potential for batch variation to affect data quality and to normalise accordingly in an objective manner (264). Figure 4.1 shows that appropriate normalisation of 8 TMT sets incorporating 92 biological replicates with 4 technical replicates was able to appropriately remove batch effects. The multidimensional scaling (MDS) plot demonstrates complete removal of any substantial clustering. Here we used ComBat methodology (155), which allows users to adjust for batch effects in datasets using a known batch covariate (see Chapter 2). This data underlines the importance of normalising for batch effects, within each TMT batch. This allowed for objective data normalisation to minimise the batch effects, as has been reported (36, 155). Data normalisation can be found in the Appendix 2.

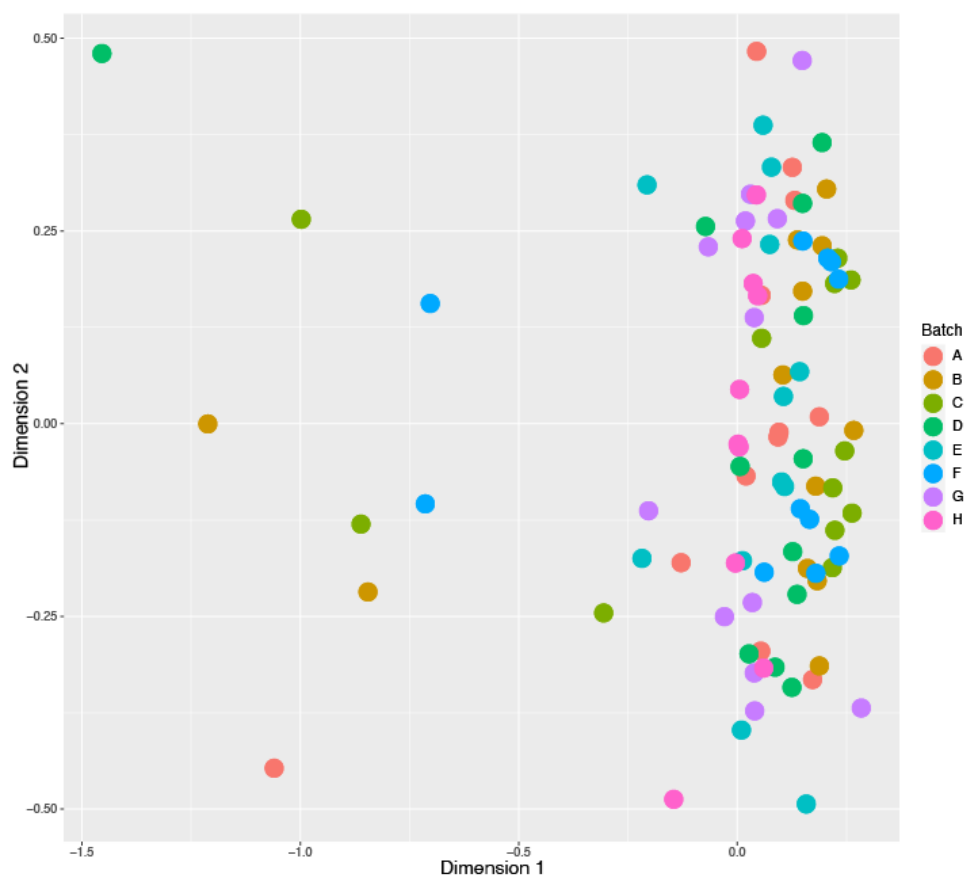


**Figure 4. 1**– Multidimensional scaling (MDS) plot showing variation among TMT batches following normalisation of raw data. Each colour represents a TMT 16-plex batch, showing complete removal of significant clustering.

## 4.2 Protein Detection

Utilising the optimised proteomic workflow described in Chapter 3 (Figure 4.2a) enabled a total of 3141 proteins to be identified in all samples, with 81% (2534 proteins) of these identified with high FDR confidence. Of these 2534 proteins, 66% were identified in over 70% of the total samples - with any extra missing data being imputed with a kNN (k-nearest neighbour) imputation. This ensured the data is robust and provides a stringent cut off in which to assess the biological difference within the data. The variability of the muscle fibre proteome is demonstrated in Figure 4.2b, which compares differences in proteins identified pre and post training and between fibre types. Almost all proteins were quantified in both fibre types (98%) and at both times (98%). The strong overlap between the conditions of time and fibre type further supports the strength of the developed methodology to reduce variability amongst samples. Thus, the variability amongst individuals and the length of fibres isolated is outweighed by similarities within the muscle proteome.

Gene Ontology (GO) analysis (Figure 4.2c) demonstrates good coverage of structural and metabolic features of the muscle fibre proteome, including contractile, sarcomeric, ribosomal, and mitochondrial proteins. This included greater than 50% of proteins annotated to the sarcolemma and contractile proteins in pooled single fibre samples. The sensitivity of the method is also demonstrated by good coverage of proteins in less abundant compartments such as the mitochondrion and ribosome. The highest ranked proteins in terms of abundance detected in individual samples was dominated by sarcomeric proteins.

On average, 1832 of total proteins per sample were quantified in pooled single fibres reflecting approximately 60% of the total quantified proteins measured in all 96 samples. Individual number of proteins quantified per samples is shown in Figure 4.3, demonstrating any variability amongst individual samples prior to normalisation. Following normalisation and removal of outliers, an average of 1516 total proteins were annotated per sample.

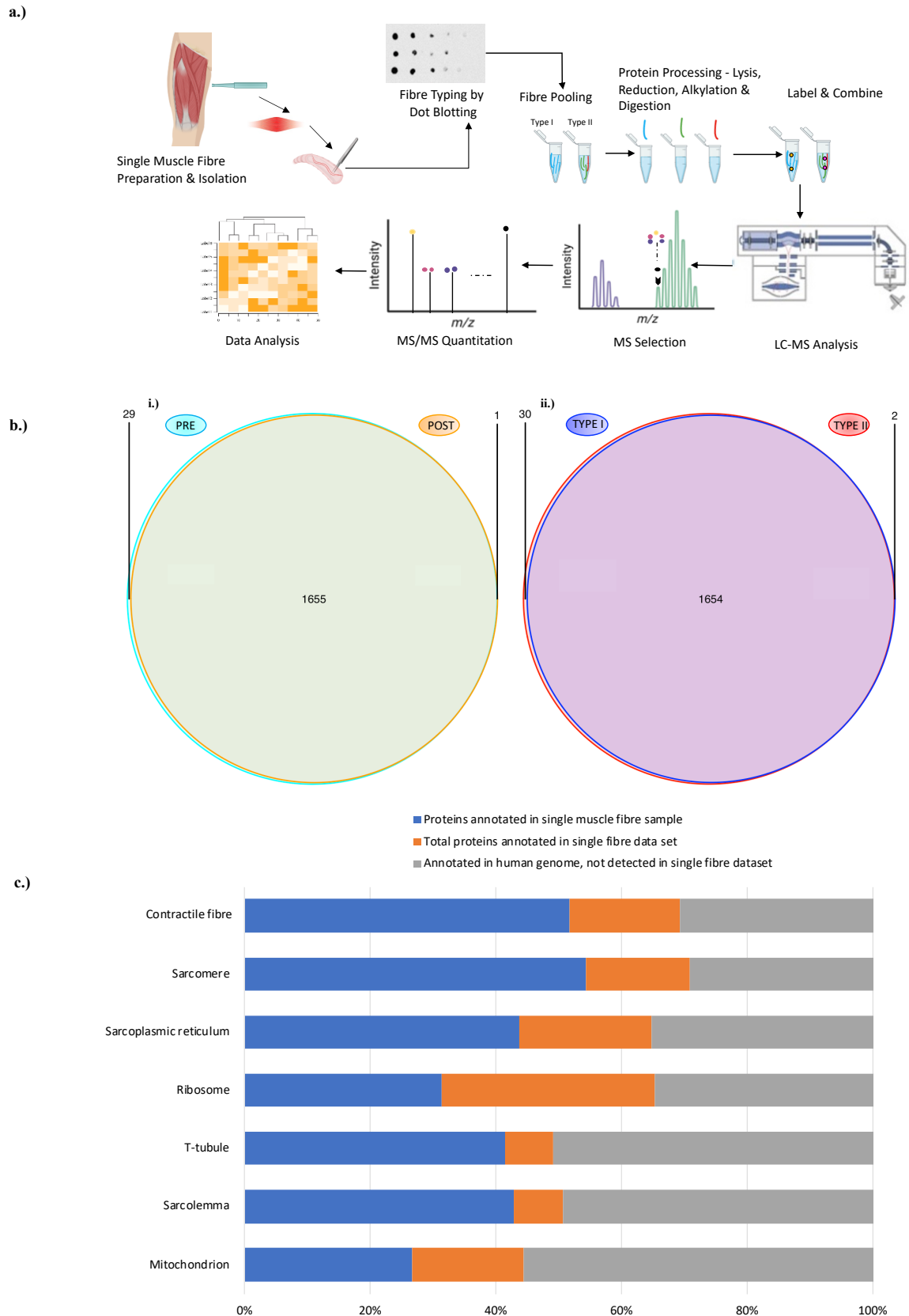


**Figure 4. 2** - Characterisation of the proteome of pooled human single muscle fibres. a.) Proteomic workflow for fibre typing and identifying proteins in single-fibre samples. b.) Venn diagram of quantified proteins i.) *pre* and *post* training and ii.) between fibre types (type I & type II). c.) Protein coverage in muscle fibres. Each bar represents selected GO annotations. The number of corresponding protein-encoding genes in the human genome (calculated DAVID (137)) is considered as 100%.



To further quantify the variability of the muscle fibre proteome among different participants and fibre types, we compared protein identification across all individuals and report correlation coefficients between each variable and other individuals. Most similar samples are reflected by a darker red colour. According to the correlation matrix, proteins identified in samples labelled as type I fibres were highly correlated with each other in terms of the presence of proteins identified when derived from different participants for both pre and post training conditions, as were type II fibres (Figure 4.4). This indicates functional similarities between fibre type despite biological variability amongst individuals.

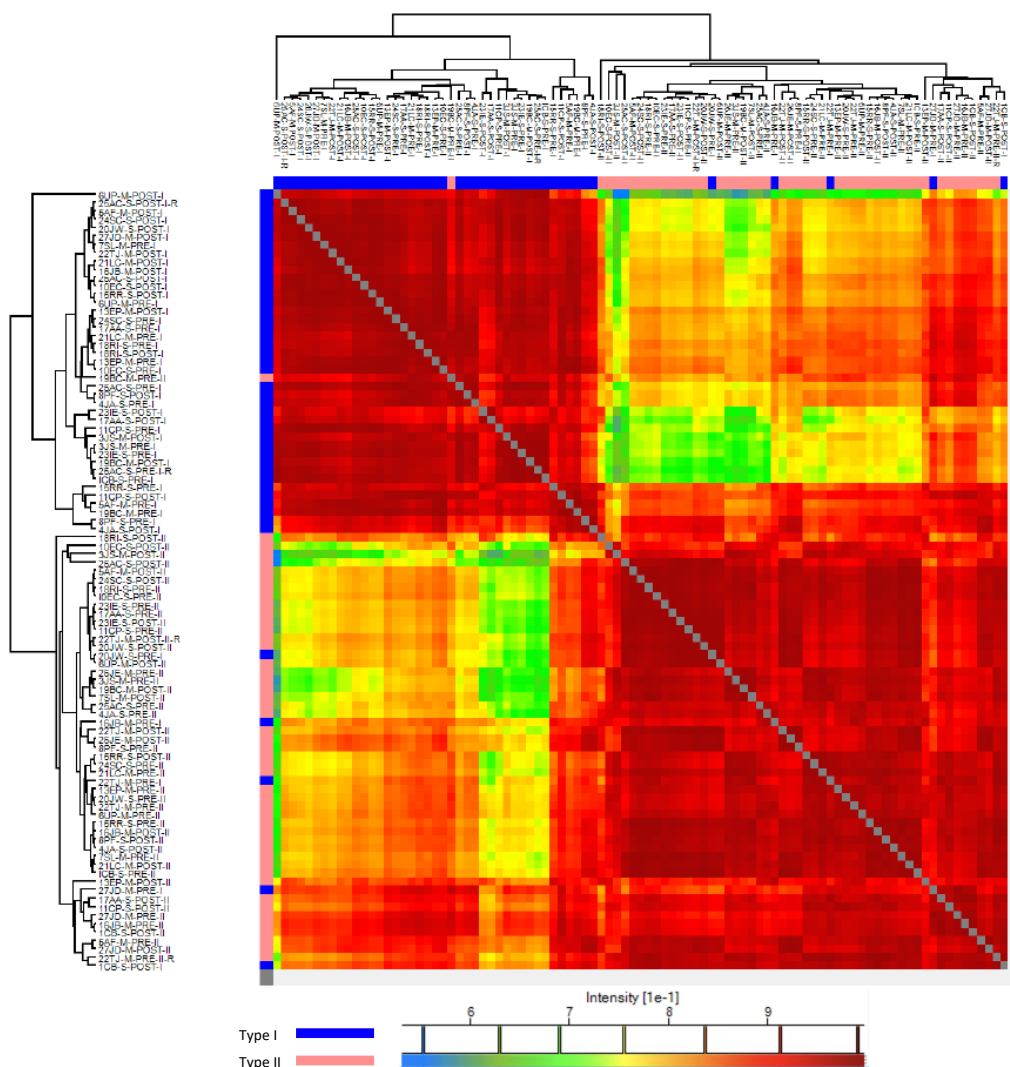


**Figure 4. 4–** Heatmap summarising correlation of all pooled samples in the training study when comparing participants and fibre type. Darkness of the squares reflect the Pearson correlation intensity score.

### 4.2.1 Detection of Mitochondrial Proteins

The proteomic workflow identified 694 annotated known and predicted mitochondrial proteins, with 536 known mitochondrial proteins across all 96 samples for both pre and post samples and all training and fibre types. This represents greater than 45% of the known mitochondrial proteins. This is comparable to a previous single-fibre proteomic study of aged humans, which annotated 634 known mitochondrial proteins across all single fibres (218). Of note, Murgia et al. (216) used categorical annotations based on Uniprot keywords (i.e., mitochondrion), which can give an overrepresentation of mitochondrial proteins identified. For example, the original single fibre study quotes the identification of 654 proteins annotated as mitochondrial; however, when this is annotated with a robust database such as Integrated Mitochondrial Protein Index (293, 294) only 391 proteins are annotated as mitochondrial. This further strengthens the robustness of the methodology presented in Chapter 3 for the identification for mitochondrial proteins.

Of this list of proteins, the most abundant mitochondrial proteins were ATP synthase subunit beta (ATP5B), followed by Aconitate (ACO2), MICOS complex subunit MIC60 (IMMT), and ATP synthase subunit alpha (ATP5A). These observations are supported by recent MS analysis identifying ATP5B, ATP5A, and ACO2 as the three most abundant mitochondrial proteins based on estimates of protein abundance across muscle tissues (8). In addition, a proteomic study of protein composition and function of red and white skeletal muscle mitochondria also found ATP5B to be the most abundant mitochondrial protein in red and white porcine skeletal muscle (92). This overlap with previous research identifying common highly abundant proteins reveals strength in the current methodology to identify both high and lowly abundant proteins. The sum PEP Score is used to rank protein abundance on the basis of the posterior error probability (PEP) values of the peptide spectrum matches (PSMs). Based on the aforementioned, the top 20 mitochondrial proteins in terms of confidence in identification across all samples are presented in Table 4.1.

One of the highly abundant mitochondrial proteins was MICOS complex subunit MIC60 (IMMT), which is part of the mitochondrial contact site and cristae organising system (MICOS). It is also a central player in membrane shaping and crosstalk, and helps shapes

crista junctions and mitochondrial membrane contact sites. These MICOS proteins provide an extended membrane surface for the accumulation of OXPHOS respiratory chain complexes I to V and shape a micro-compartment that is optimised for ATP production (331). IMMT specifically is required to link mitochondrial functions at crista junction and mediates the interaction of MICOS with numerous other protein machineries of the mitochondria (331).

**Table 4. 1– Most Abundant Mitochondrial Proteins Annotated Across All Samples**

<i>Description</i>	<i>Gene Symbol</i>	<i>Functional Class</i>	<i>Sum PEP Score*</i>
<i>ATP synthase subunit beta,</i>	ATP5B	OXPHOS (CV)	797
<i>Aconitate hydratase,</i>	ACO2	TCA	651
<i>MICOS complex subunit MIC60</i>	IMMT	MICOS	650
<i>ATP synthase subunit alpha,</i>	ATP5A	OXPHOS (CV)	636
<i>Heat shock cognate 71 kDa protein</i>	HSPA8	Chaperone	632
<i>Trifunctional enzyme subunit alpha,</i>	HADHA	Fatty Acid Beta-Oxidation	617
<i>60 kDa heat shock protein,</i>	HSPD1	Chaperone	602
<i>Stress-70 protein,</i>	HSPA9	Chaperone	568
<i>Creatine kinase M-type</i>	CKM	Creatine metabolic process/phosphorylation	565
<i>Phosphoglycerate kinase 3</i>	PGK1	Glycogenesis	551
<i>Heat shock 70 kDa protein 1B</i>	HSPA1B	Chaperone	547
<i>Very long-chain specific acyl-CoA dehydrogenase,</i>	ACADVL	Fatty Acid Beta-Oxidation	517
<i>NAD(P) transhydrogenase,</i>	NNT	TCA	515
<i>Heat shock-related 70 kDa protein 2</i>	HSPA2	Chaperone	506
<i>NADH-ubiquinone oxidoreductase 75 kDa subunit</i>	NDUFS1	OXPHOS (CI)	504
<i>2-oxoglutarate dehydrogenase,</i>	OGDH	TCA	481
<i>Acetyl-CoA acetyltransferase,</i>	ACAT1	Fatty Acid Beta-Oxidation	473
<i>Creatine kinase S-type,</i>	CKMT2	Creatine metabolic process/phosphorylation	454
<i>Trifunctional enzyme subunit beta,</i>	HADHB	Fatty Acid Beta-Oxidation	431
<i>3-ketoacyl-CoA thiolase</i>	ACAA2	Fatty Acid Beta-Oxidation	382

\*Sum PEP Score This score is calculated on the basis of the posterior error probability (PEP) values of the peptide spectrum matches (PSMs). A high Sum PEP score indicates a high ratio of abundance for peaks identified for a given peptide.

The large protein list of annotated known mitochondrial proteins was analysed using Database for Annotation, Visualization and Integrated Discovery (DAVID) for functional analysis of the overrepresentation of key gene ontology (GO) biological processes. The key terms are highlighted in the network presented in Figure 4.5. Of the 45% possible mitochondrial proteins identified in single muscle fibres, the dominant pathways identified were associated with electron transport and in particular respiratory chain complex I assembly, followed by mitochondrial translation. Proteins involved with fatty acid beta-oxidation were also highlighted as secondary key processes.

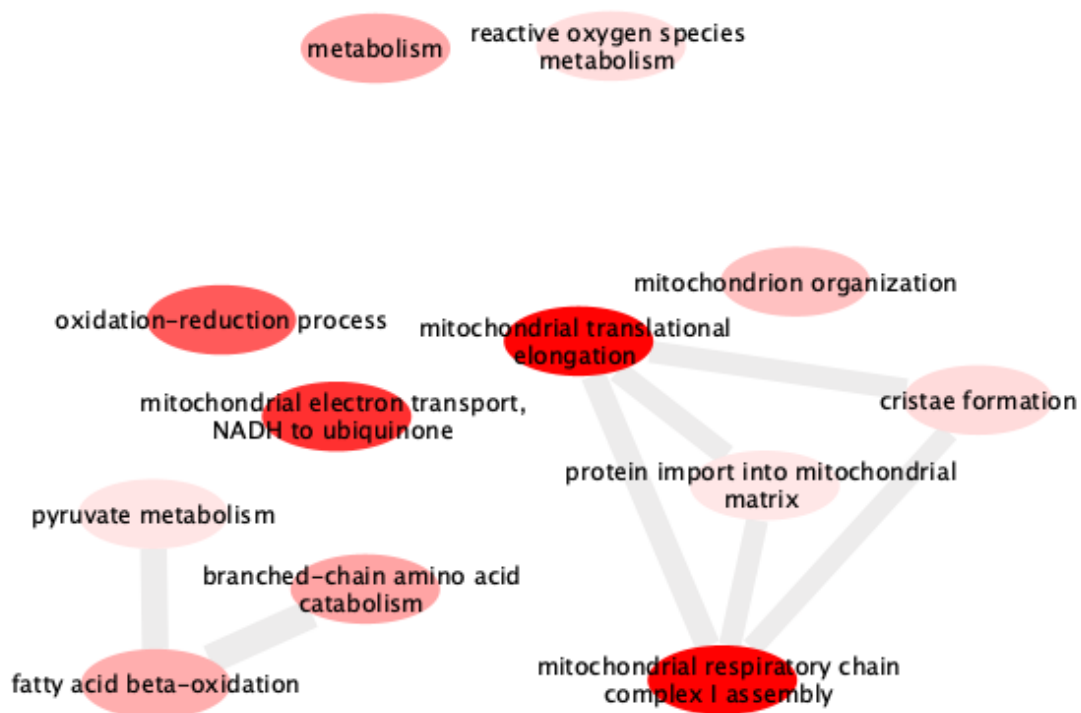


**Figure 4.5-** The gene sets for GO terms were visualised using the Cytoscape 3.8.2 Enrichment Map plugin (287). Each node represents a GO biological process term. The node colour indicates the significance of the term's enrichment. The darker colour (red) indicates more significant enrichment. The edges are related to the relationships between the selected terms, which are defined based on the genes that are shared in a similar way. Gene ontology determined using Database for Annotation, Visualization and Integrated Discovery (DAVID) (137).

### 4.3 Fibre Type Differences

Skeletal muscles are heterogeneous tissues composed of different fibre types, which can be identified by their expression of specific myosin heavy chain (MYH) isoforms (101). The extensive research that has investigated different characteristics, including structural, functional, and metabolic characteristics of these fibre type responses, was reviewed in Chapter 1. However, little is known about possible fibre-type-dependent differences in

the regulation of mitochondrial proteins. Furthermore, the methods for studying mitochondrial protein adaptations in skeletal muscle have mostly been confined to the analysis of whole-muscle samples, where the results may be confounded by the analysis of changes in a mixture of type I and II fibres. Integrating proteomic techniques could provide new information regarding protein regulation and specifically mitochondrial protein adaptations that are divergently regulated in type I & II fibres at the resolution of single muscle fibres. The top enriched proteins were the contractile and sarcomeric titin, myosin (MYH7 > MYH2 > MYH1), and actin. MDS was conducted to determine whether MS analysis of type I and type II fibres reveal distinct protein profiles across all samples. Clear separation of both fibre types was observed in both dimensions, illustrating that there are two distinct protein clusters for types I and II fibres (Figure 4.6).

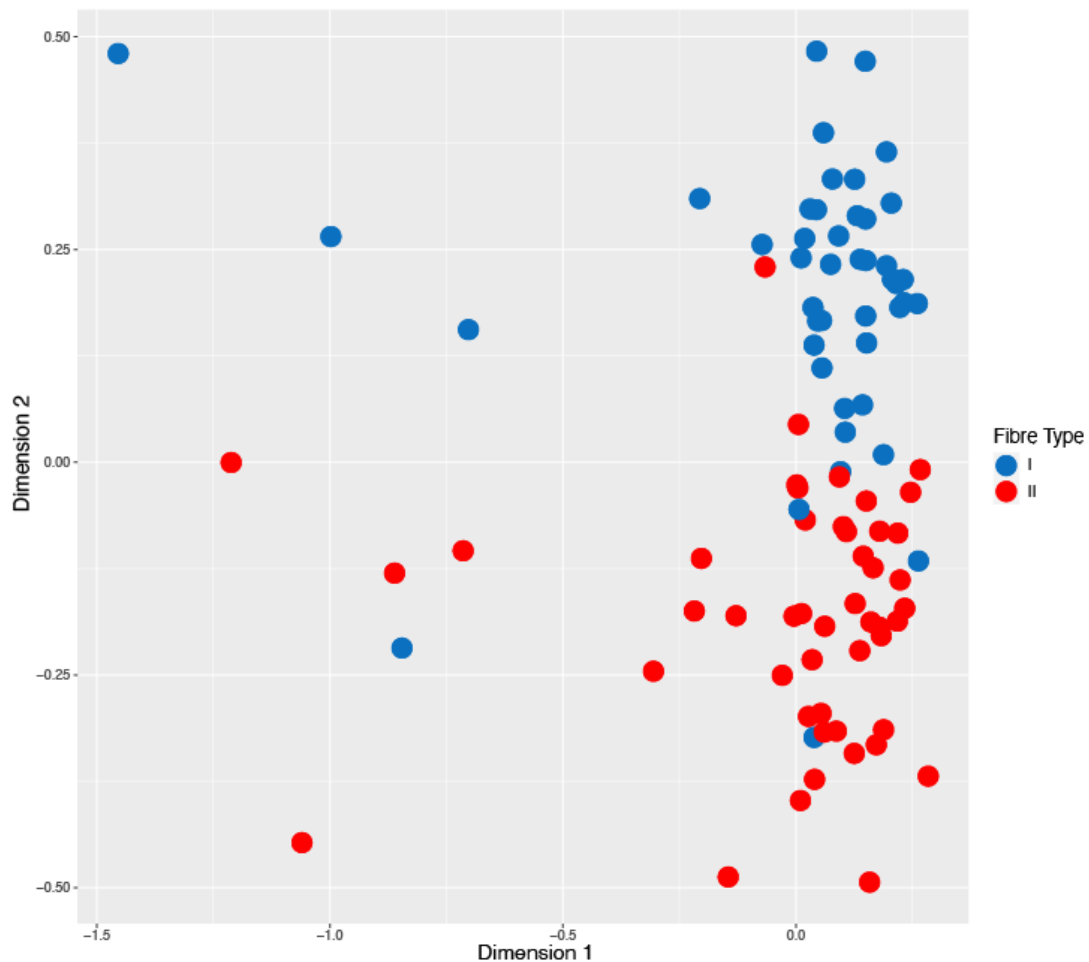


**Figure 4. 6–** Multidimensional scaling (MDS) plot showing variation among samples based on fibre type. Each point represents a participant’s sample, and the distance between the points correlated to the dissimilarity between the samples. The plot highlights the fibre types and illustrates that there are two distinct clusters showing the separation between fibre types I and II.

Proteomic features of the different fibre types pre-exercise are presented in a volcano plot (Figure 4.7). Type I fibres were characterised by an expected clear difference in contractile proteins such as MYH7 and troponin slow skeletal type 1 (TNNT1), whereas type II fibres possessed a greater MYH2, troponin fast skeletal type 3 (TNNT3), and calcium binding proteins calsequestrin (CASQ1). Functionally, notable metabolic differences between fibre types can be demonstrated by the differentially expressed proteins highlighted, where mitochondrial proteins are greater in type I fibres. This includes electron transport chain subunit NDUFB3 (NADH:Ubiquinone Oxidoreductase Subunit B3), and fatty acid proteins such as hydroxyacyl-CoA dehydrogenase trifunctional multienzyme complex for subunit  $\alpha$  and  $\beta$  (HADHA and HADHB). Conversely, more glycolytic proteins, such as glycerol-3-phosphate dehydrogenase 1 and 2 (GPD1 and GPD2), phosphoglycerate kinase (PGK1), and glyceraldehyde-3-phosphate dehydrogenase (GAPDH), had greater differential expression in type II fibres. This is understandable given early studies established that glycolytic enzymes (such as GPD (13)) varied in different skeletal muscle types, with a higher expression observed in type II fibres (13). Most studies on muscle fibre heterogeneity have focused on two main areas within fibre types - contractile response and metabolism (283). However, as confirmed in this single-fibre research, the diversity between muscle fibres is not restricted to contractile proteins (i.e., myosin isoforms) and metabolic enzymes (such as glycolytic or mitochondrial proteins), but extends to a range of subcellular systems, including ionic transport and cellular calcium signalling (283). Fibre-type differences were also observed for lactate dehydrogenase, with the  $\alpha$  unit more expressed in type II fibres and the  $\beta$  unit having greater expression in type I fibres. The response of these proteins has previously been reported in some studies (13) to depend on fibre type and training (40).



capacity to rapidly modulate the rate of energy production and substrate utilisation in response to locomotion powered by actin-myosin cycling (75). The modulation of this is believed to be dependent on training load (193). A comparison of protein responses for pre and post training over 96 samples for two types of training loads (i.e., MICT and SIT) was analysed. The resulting training sample distributions was assessed globally using a MDS of all proteins highlighting any groupings between training types (Appendix 3).

Further to this, proteomic features of the different fibre types post training are presented in volcano plots (Figure 4.8). Overall, an increased number of differentially expressed proteins was observed post MICT (Figure 4.8a) compared to post SIT (Figure 4.8b). Similarly, features observed in different fibre types pre-training (Figure 4.7) remained post-training for both modalities; this was highlighted by increased DE proteins related to slow contractile fibres and fatty acid oxidation in type I fibres and more fast contractile and glycolytic proteins in type II fibres. There was a decreased number of observed mitochondrial proteins post SIT, which is discussed in the subsequent section.

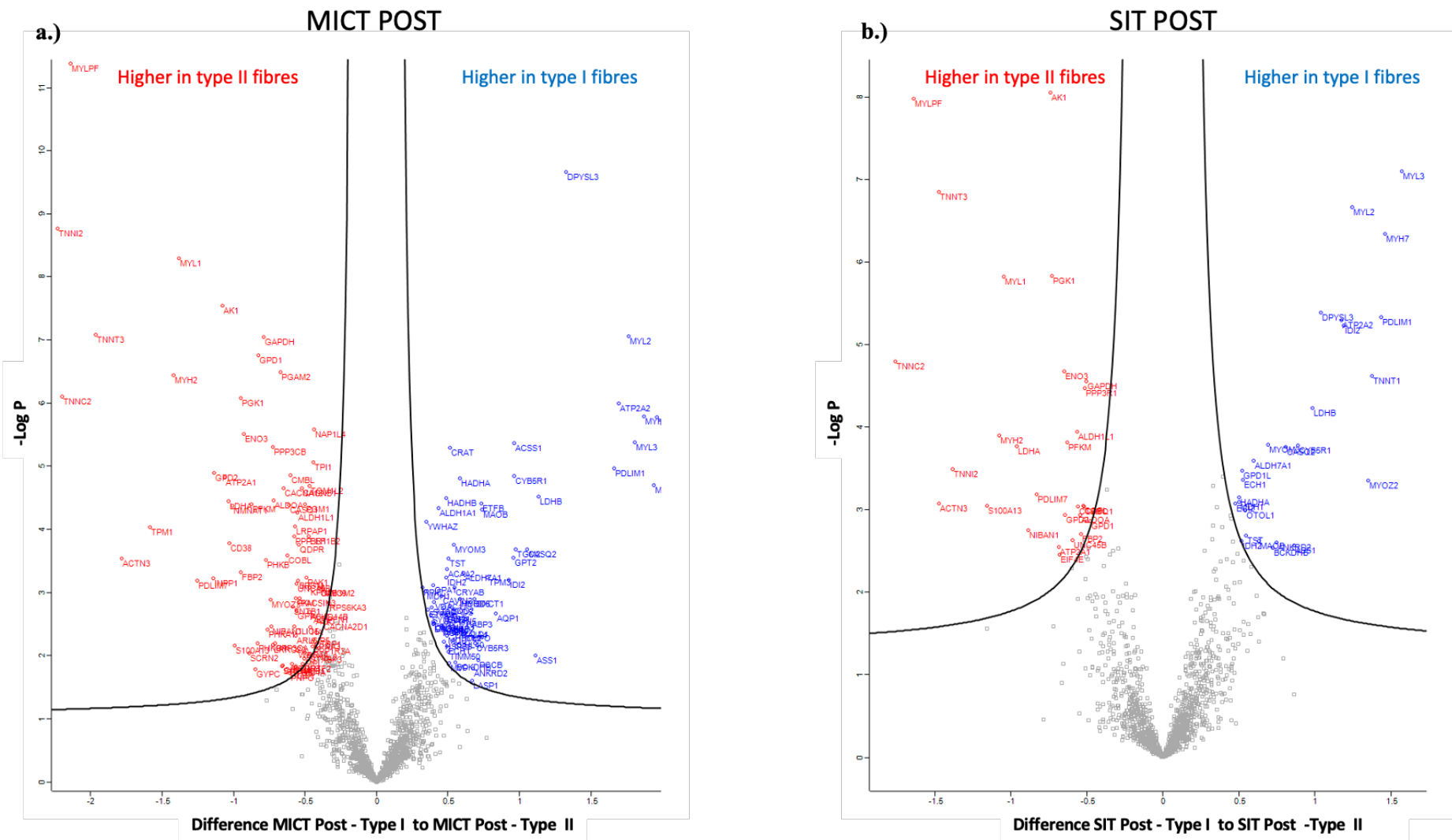


**Figure 4. 8–** Volcano plot of statistical significance (log p) against fold change highlighting the most significantly different proteins between type I (blue) and II (red) fibres a.) Post Moderate Intensity Continuous Training (MICT) b.) Post Sprint Interval Training (SIT).

Further statistical analysis, using Linear Models for Microarray Data (Limma) (295), was conducted to determine the differential expression of proteins in different fibre types. There were 24 proteins differentially expressed between type I and II fibres pre MICT, whereas post MICT there were 101 differentially expressed proteins between type I and II fibres. This suggests MICT led to a greater difference between fibre types following training. Conversely, analysis of differentially expressed proteins pre SIT found 76 proteins differentially expressed pre-training and 73 differentially expressed proteins post-training. This suggests SIT does not have a significant effect on altering the number of differentially expressed proteins between fibre types (Figure 4.9). This observation is further substantiated when comparing all four conditions, where there are 34 unique differentially expressed proteins post MICT, whereas post SIT there are only 14 unique differentially expressed proteins. A table of all differentially expressed proteins in all conditions can be found in Appendix 4.

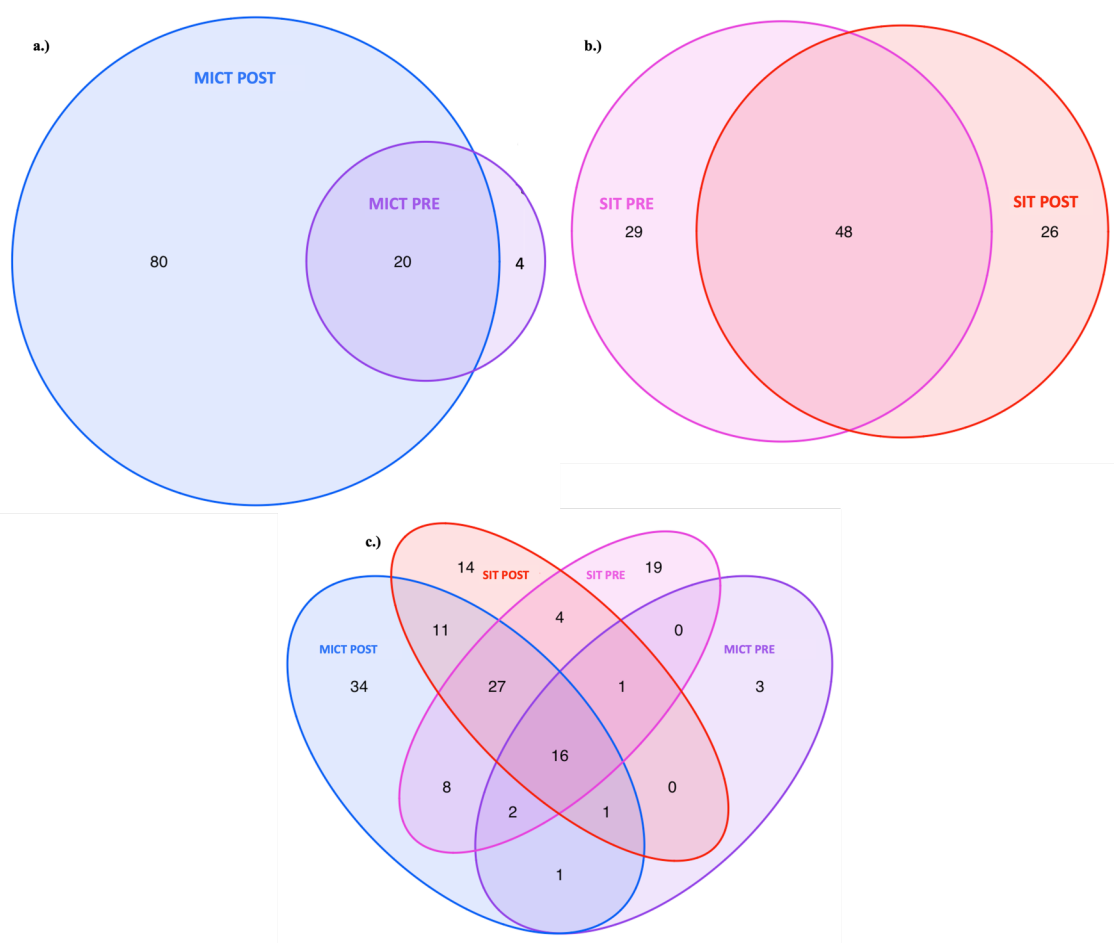


**Figure 4. 9**– Venn diagram showing the differentially expressed (DE) proteins when comparing type I to type II fibres. **a.)** MICT pre and post comparison of overlapping DE proteins. **b.)** SIT pre and post comparison of overlapping DE proteins. **c.)** Overall training comparison of MICT and SIT pre and post for overlapping DE proteins.

Given that exercise training is known to be an important factor in improving cellular adaptations, the question of whether volume or intensity of exercise were more important for training-induced increases in protein responses still remains unclear. Exercise training volume has been suggested to be a primary determinant of the exercise-induced increase in mitochondrial content in humans (27-29). However, as mitochondria can comprise less than 3% of skeletal muscle volume density, it is difficult to discern relative mitochondrial protein expression differences in whole-muscle samples. This leads to the need for single-fibre studies (92). The results provide evidence that training volume has a greater effect on changes in mitochondrial protein expression, with MICT resulting in a greater number of differentially expressed proteins post training compared to SIT.

Research has also shown that skeletal muscle mitochondria regulate substrate metabolism during moderate-intensity exercise, with increased mitochondrial content promoting a greater reliance on fat oxidation and a comparative decrease in carbohydrate utilisation (75, 115, 193). As a result, it is reasonable to hypothesise that proteins, and more specifically mitochondrial proteins, might be present in different amounts depending on the specific energy requirements of each muscle fibre type. Enrichment analysis of Gene Ontology (GO) biological processes for the 80 differentially expressed proteins between fibre types (based on comparisons of type I/type II fibre ratio) pre and post MICT revealed that the top enriched proteins were dominated by muscle and sarcomeric organisation, followed by glycolytic processes and fatty acid beta oxidation (detailed enrichment mapping can be found in the Appendix 5).

#### **4.4.2 Training and Fibre-Specific Responses of Mitochondrial Proteins**

Further examination found 30 differentially expressed mitochondrial proteins between fibre types post MICT. Enrichment analysis was used to map the hierarchical organisation of pathways by GO enriched proteins (Figure 4.10). Conversely, the 24 mitochondrial proteins observed post SIT that were differentially expressed between type I and type II fibres were notably clustered in relation to the tricarboxylic acid cycle (TCA). This aligns with research stating there are relationships with mitochondrial functions and substrate utilisation (115), and provides further divergence of this utilisation between training type and fibre type with the volume of MICT (255).

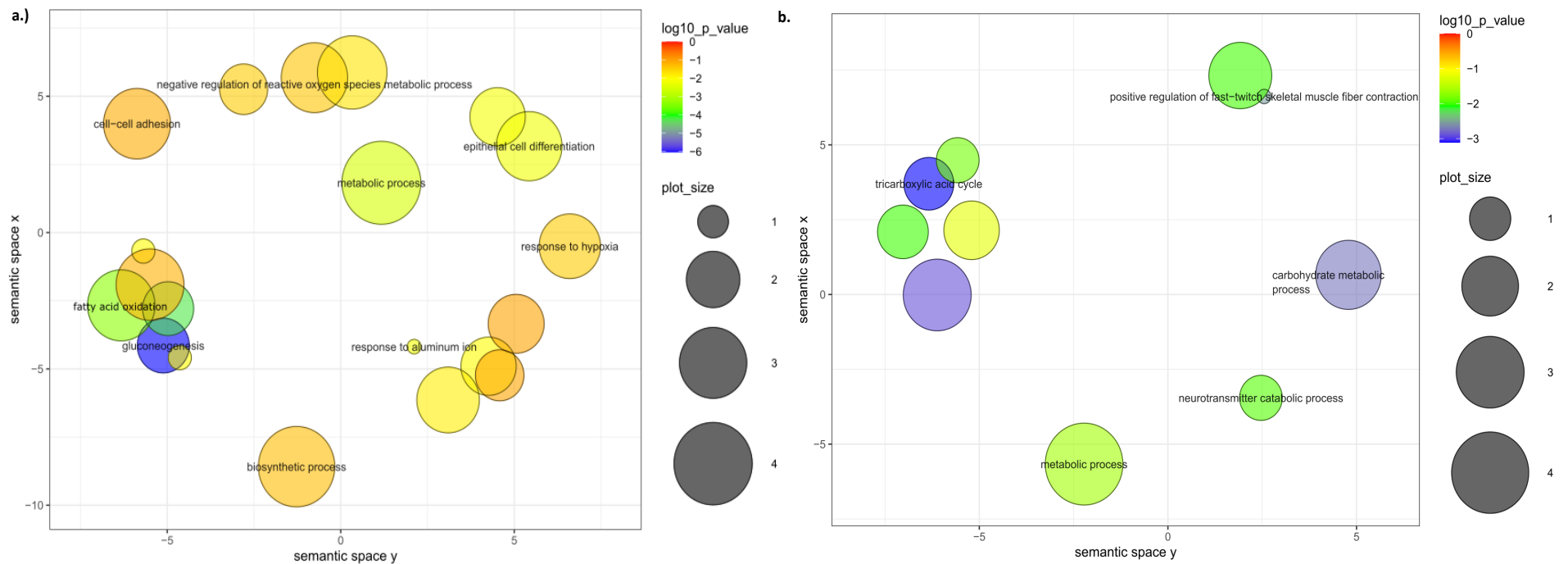


**Figure 4.10-** REVIGO Scatterplot of the Enriched GO Cluster Representatives from mitochondrial protein analysis. Fibre type GO enrichment analysis for differentially expressed proteins with adjusted p-value cut off of 0.05 for type I compared to type II fibres. **a.)** MICT – post **b.)** SIT – post. GO terms along with their p-values were further summarised by REVIGO reduction analysis tool that condenses the GO description by removing redundant terms (306). The remaining terms after the redundancy reduction were plotted in a two dimensional space. using a similarity of 0.7, with SimRel as semantic similarity measure. Colours indicate the p-value (generated from DAVID (137)) of enrichment according to the legend. The size of each bubble reflects the count of each term among the enriched term list. Bubbles of more general terms are larger.

The proteins identified as being significantly changed post MICT (Figure 4.11) and SIT (Figure 4.12) based on comparisons of type I/type II fibre ratio were next determined. Positive numbers indicate proteins that had a greater fold change in type I compared with type II fibres. Of the 54 differentially expressed mitochondrial proteins post training, there were 18 mitochondrial proteins in common between MICT and SIT. Figure 4.11 highlights mitochondrial proteins post MICT that were not observed post SIT. As highlighted with the GO enrichment analysis, it was found that the differentially expressed mitochondrial proteins following MICT that increased in type I compared to type II were related to fatty acid oxidation (i.e., electron transfer flavoprotein subunit beta (ETFB), acyl-CoA synthetase short chain family member 1 (ACSS1), and carnitine O-acetyltransferase (CRAT)). Also noted are mitochondrial proteins related to mitochondrial dynamics (i.e., Parkinsonism associated deglycase (PARK7) and eukaryotic translation elongation factor 1 beta 2 (EEF1B2)). These findings are consistent with the single muscle fibre proteomics of mice, which revealed mitochondrial specialisation amongst fibre types and that type I fibres had the highest protein levels of enzymes responsible for fatty acid beta oxidation - including ETFB, HADHA, and ACSS1 (216, 284). It is generally accepted that tissue-specific functional differences are met with upregulation of protein expression of entire pathways (153), and an increase in the capacity for fat oxidation is a classic metabolic adaptation to endurance training as indicated by higher rates of fat oxidation (20, 197). In a study utilising labelling by isobaric tag for relative and absolute quantitation (iTRAQ), it was found that the most evident difference in mitochondrial pathways was related to fat metabolism and that there was an increased expression of fatty acid beta oxidation proteins in red (typically associated with type I fibres) compared with white muscle mitochondria. These results are also consistent with the main findings of the MICT response in type I compared to type II fibres in this study (92).

A recent study performing immunoblot analysis of pooled single muscle fibres found that type I muscle fibres have a coordinated upregulation of proteins controlling intramuscular lipid storage, mobilisation, and oxidation following endurance training (289). Endurance training and muscle fibre-type-specific abundance of lipid regulatory proteins, including hormone-sensitive lipase (HSL), Perilipin (PLIN) and 3-hydroxyacyl-CoA dehydrogenase (HAD), were found to have a greater expression in type I compared with

type IIa fibres. Although no significant effect of training was detected in pooled single fibres for HSL and PLIN by Shaw et al. (289), a greater abundance of HAD was detected in the endurance-trained group (289). While PLIN and HSL are not considered to reside entirely in the mitochondria (258), the phosphorylation of these proteins are essential for the mobilisation of fats in adipose tissue and demonstrate a preference for type I fibre utilisation for fatty acid oxidation pathways following endurance training. This trend is somewhat in parallel with the observations of the differential expression of specific fatty acid proteins following MICT in type I compared to type II fibres in this single-fibre study. Furthermore, both HAD  $\alpha$  and  $\beta$  subunits were observed post MICT to be differentially expressed in type I to type II fibres. The HADA  $\alpha$  subunit was also observed to be differentially expressed in type I to type II fibres following SIT, while PLIN was observed to be differentially expressed in type I to type II fibres pre training. This also typifies the results observed by Shaw et al. (289) in endurance-trained individuals, where HAD, a key enzyme in beta-oxidation, was also elevated in human type I fibres.

Another protein with greater expression in type I compared to type II fibres following MICT was heat shock chaperone protein  $\alpha$ -crystallin B chain (CRYAB) – a protein that plays a role in skeletal muscle remodelling through induction as a stress response to various stimuli, including contractile activity, and which also plays an important role in sarcomere stability (218). The dysfunction of CRYAB has also been associated with a reduction of mitochondrial mass and respiratory chains deficiencies (42). A previous proteomic training study (74) reported a decrease in CRYAB, which was in contrast to other reports that show increases in this protein after periods of endurance training (210). A study of aged muscle also reported a decline in the expression of this protein (218), yet MICT in the current study appears to reverse this effect, improving the expression level of this protein in type I muscle fibres. The discrepancy in these findings is at present unexplained, but hypothesised to be related to the duration of the exercise training programme (74). Egan's study was 2 weeks, which is of a much shorter duration than the 8-week training study presented here.

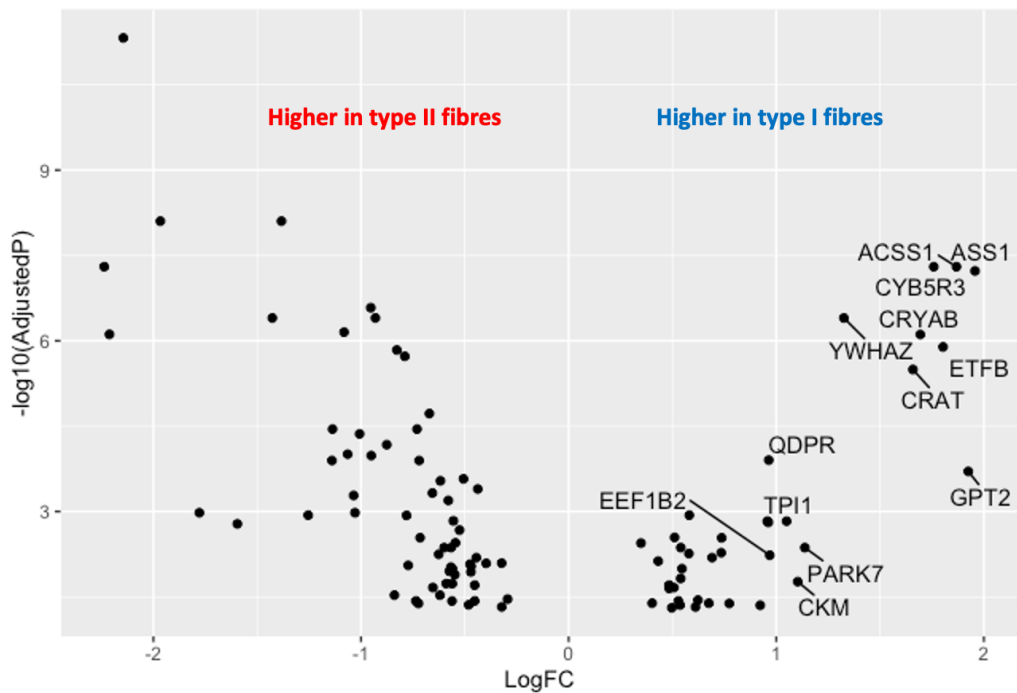


**Figure 4. 11-** Scatterplot showing proteomics data. Points indicate proteins that were differentially expressed (adj. p-value < 0.05) with a positive fold change in type I compared with type II fibres. Mitochondrial proteins that were only identified in POST MICT are labelled.

In the SIT group, mitochondrial proteins that had a greater increase in type I compared to type II fibres were more associated with the TCA cycle - such as isocitrate dehydrogenase 2 (IDH2), succinate-CoA ligase, GDP-forming, beta subunit (SUCLG2), and dihydrolipoamide dehydrogenase (DLD). SIT appears to recapitulate previous observations for type Iix single fibres, where greater abundances in proteins associated with the regulation of pyruvate dehydrogenase and the TCA cycle were also reported (216, 284). Highlighted is IDH2, where it has been proposed that the NADP (Nicotinamide adenine dinucleotide phosphate) dependant IDH2 enzyme works in the reverse direction of the TCA cycle and converts  $\alpha$ -ketoglutarate into citrate as a source for fatty acid synthesis (216). This coincides with the large fold change observed following SIT for IDH2, which has a unique pattern of expression and has previously been shown to be more abundant in type I single fibres (216). This supports the notion that the IDH2 enzyme is a large contributor to the TCA cycle. In particular, it was previously observed that IDH2 levels are very high in type I fibres, slightly lower in IIa, and much lower in Iix fibres ( $p < 0.05$ ) (216, 284). Another hypothesis to explain the high amount of IDH2 protein in type I muscle fibres in response to SIT, is that the forward direction of the TCA cycle generates NADPH to buffer against reactive oxygen species (ROS) produced during mitochondrial respiration. During NADPH generation in

mitochondria, the major proteins involved are IDH2 and the NNT (Nicotinamide nucleotide transhydrogenase) that couples the hydride transfer between NADH and NADP<sup>+</sup> to proton translocation across the inner mitochondrial membrane. Notably, NNT was also one of the most abundant mitochondrial proteins observed overall in this research. Thus, it has been suggested that the continuously active type I fibres have a greater capacity to cope with the higher levels of ROS production. ROS species have been inherently linked to SIT (176, 194).

Another mitochondrial protein of note that was differentially expressed in type I compared to type II fibres following SIT was oxo-isovalerate dehydrogenase subunit beta (BCKDHB). This mitochondrial matrix enzyme complex is involved in the catalysis of the degradation of branched-chain amino acids to generate NADH and carbon dioxide. BCKDH is structurally similar to pyruvate dehydrogenase (PDH) and believed to be regulated in an analogous manner. The mitochondrial PDH catalyses the oxidative decarboxylation of pyruvate, linking glycolysis to the TCA cycle and fatty acid synthesis (30). Interestingly, mono-amine oxidase (MAOB) was observed to be positively differentially expressed in type I fibres following both SIT and MICT. This particular mitochondrial protein is involved in deamination and generating ROS and was previously observed to decrease in the type I fibres of aged humans. This result hints that exercise training reverses this aging effect in type I fibres. In contrast, phosphoglycerate kinase 1 (PGK1) was observed to decrease in type I compared to type II fibres following both MICT and SIT. This enzyme, as part of the glycolytic pathway, was previously found to be higher in type I compared to type II fibres and to have a decreased expression in aged single fibres (218). This provides further evidence that exercise is able to counteract some of the effects of aging.

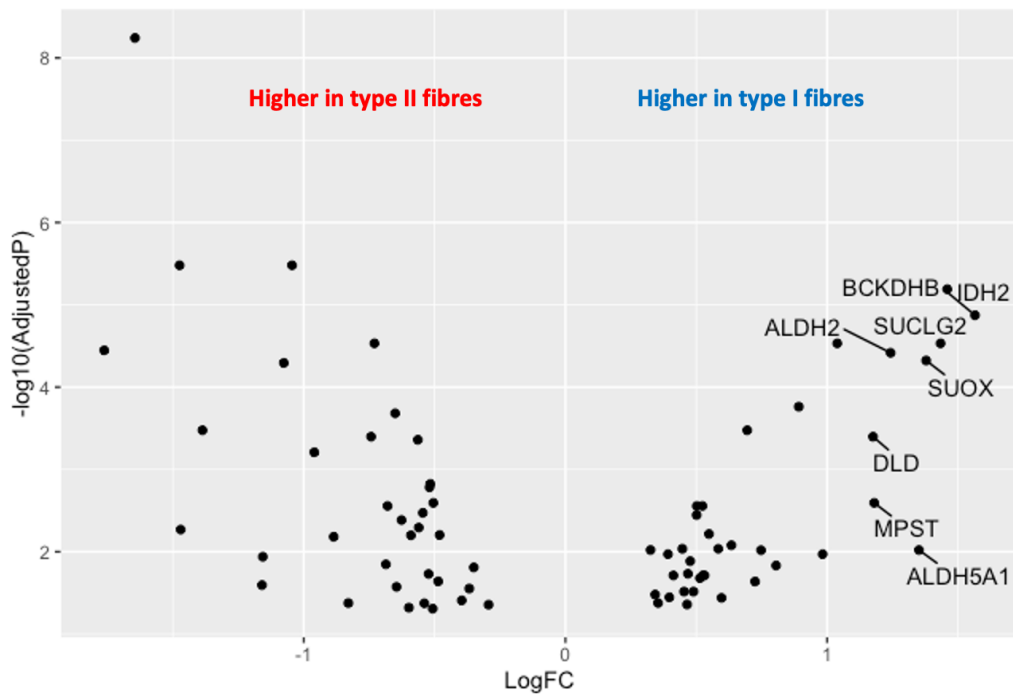


**Figure 4. 12-** Scatterplot showing proteomics data. Points indicate proteins that were differentially expressed (adj. p-value < 0.05) with a positive fold change in type I compared with type II fibres. Mitochondrial proteins that were only identified in POST SIT are labelled.

Pioneering studies in both animals and humans have shown that markers of mitochondrial content increase with training (27, 29, 177, 209). While it has been reported that mitochondrial protein content is greater in type I compared to type II fibres, little is known about the effects of training (92). The overall effect of training on mitochondrial protein abundance in different fibre types was investigated. Known mitochondrial proteins were analysed in both the type I and II fibres and are presented as quantitative proteomic protein plots demonstrating the change between average abundance of mitochondrial proteins pre and post training for each fibre type (Figure 4.13). The mitochondrial fibre type changes are summarised in Table 4.2, whereby the change in mean z-score pre to post training reflects an overall increase or decrease in mitochondrial protein abundance. The gradient of mitochondrial proteins in type I fibres indicates a positive increase following training ( $\nabla \bar{z}\text{-score} = 0.096$ ), whereas overall mitochondrial proteins in type II fibres appears to decrease with training ( $\nabla \bar{z}\text{-score} = -0.090$ ). This suggests training affects mitochondria as suggested in the literature (126, 147, 209); however, more novel is that this change predominantly resides in type I fibres.

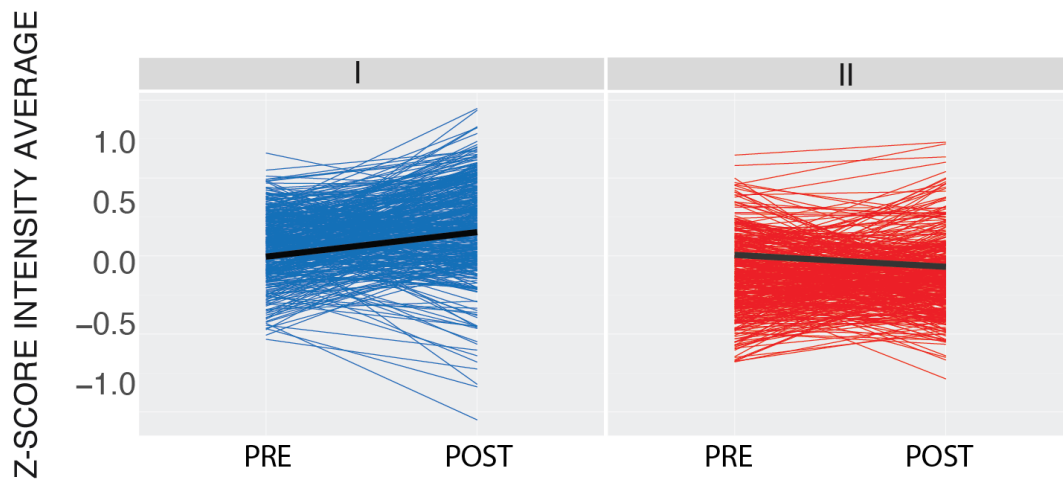


**Figure 4.13– Training and Fibre Type** – Profile plots illustrate the z-score intensity average for all known mitochondrial proteins annotated in type I fibres (blue) and type II fibres (red) for pre and post training for both training types ( $\nabla \bar{z}$ -score represented by the black line).

**Table 4.2– Summary in Changes in Fibre Types in Mitochondrial Proteins of Single Fibre Samples\***

<i>Fibre Type</i>	$\nabla \bar{z}$ -score	$\nabla$ Summary
<i>I</i>	0.096	↑
<i>II</i>	-0.090	↓

\* Increase -  $\uparrow$  ( $z > 0.05$ )  
 No Change -  $\leftrightarrow$  ( $-0.05 > z < 0.05$ )  
 Decrease -  $\downarrow$  ( $z < -0.05$ )  
 $\nabla \bar{z}$ -score – Change in mean z-score

#### 4.5 Functional Pathway Responses

Human and animal single fibre proteomic studies have previously identified that mitochondria from different fibre types have divergent capabilities for substrate utilisation (216, 218). However, given that mitochondria comprise only a small proportion of skeletal muscle, it can be difficult to distinguish changes in mitochondrial proteins in different fibre types. Here I focus on the changes of specific mitochondrial functional groups in different fibre types following different types of training. Exercise training was associated with changes in multiple mitochondrial proteins involved in oxidative phosphorylation, the tricarboxylic acid cycle, and fatty acid oxidation, as well as several components of mitochondrial dynamics.

### 4.5.1 Oxidative Phosphorylation (OXPHOS)

One of the prime functions of mitochondria is its involvement in the oxidative phosphorylation (OXPHOS) system located in the mitochondrial cristae, which is composed of the complexes of the electron transport chain (ETC) and the ATP synthase (139). The protein content of selected subunits of the five complexes of the ETC is routinely used as a biomarker of changes in mitochondrial content following a training intervention (177). Consistent with the previously reported increase in total mitochondrial protein following exercise training, studies have reported increases in the respiratory chain subunits of the mitochondrial ETC complexes (147). In the present study, the content of each ETC complexes subunits has been presented in quantitative proteome profile plots, demonstrating the average abundance from pre to post training in each exercise training and fibre type (Figure 4.14). The global changes are summarised in Figure 4.15, whereby the change in mean z-score pre to post training is reflected by an overall increase ( $\nabla \bar{z}\text{-score} > 0.05$ ) or decrease ( $\nabla \bar{z}\text{-score} < 0.05$ ) of the ETC subunit abundance and subsequently discussed for each complex.

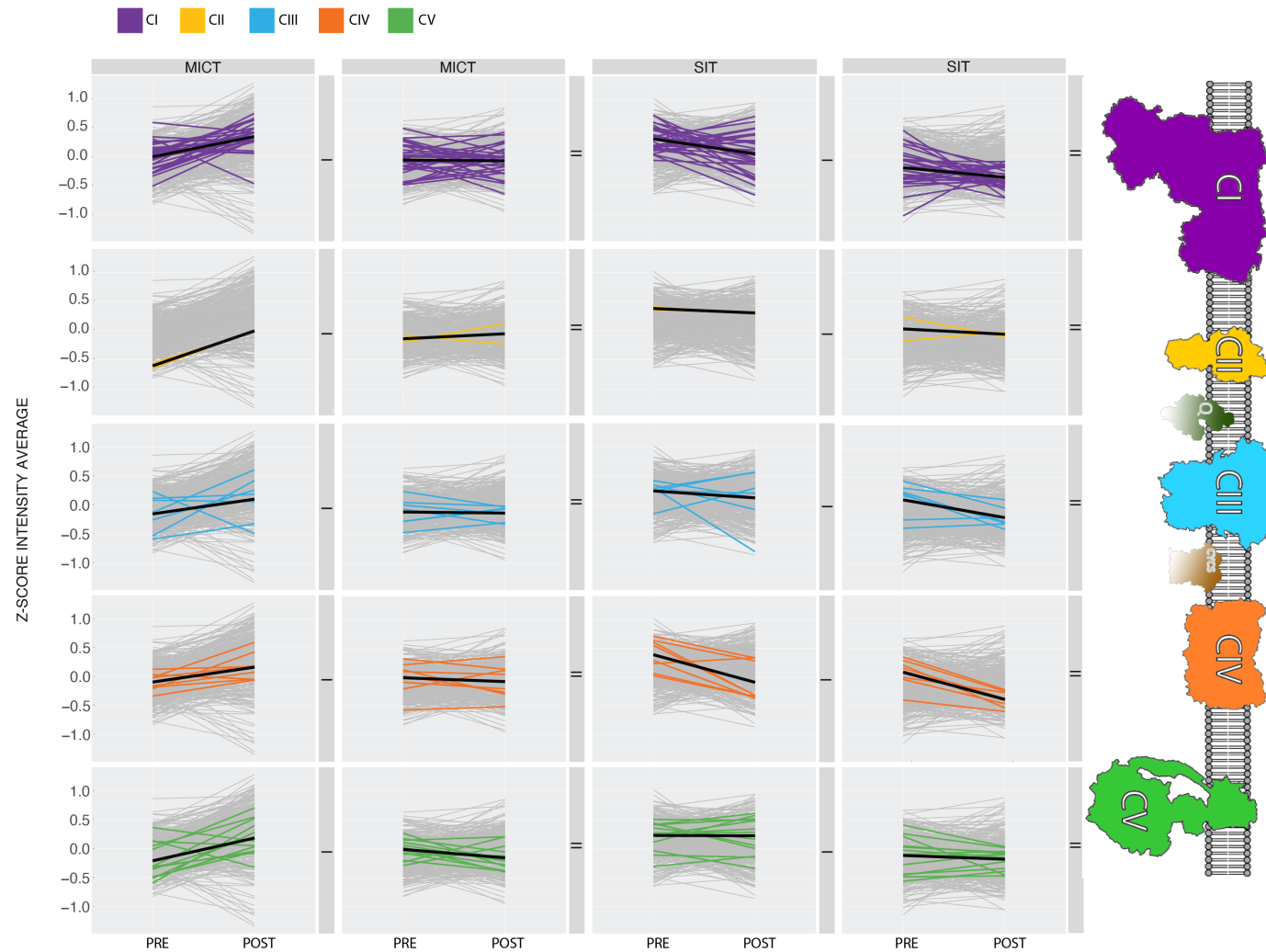


**Figure 4.14- Complex I-V** – Profile plots illustrate the z-score intensity average for all known mitochondrial proteins (grey) along with known subunits of complexes I to V (each complex is depicted by a different colour) pre and post training for both MICT (Moderate Intensity Continuous Training) and SIT (Sprint Interval Training) training in both type I and II fibres ( $\nabla$   $\bar{z}$ -score represented by the black line).

Complex I (CI), NADH:ubiquinone oxidoreductase, is the largest component of the mitochondrial OXPHOS system. As a major entry point for electrons to the respiratory chain, it has been suggested to be an important rate-limiting determinant of overall respiration and to play a central role in energy metabolism. It also has a critical role in apoptosis and cell proliferation, and thus its function in response to exercise perturbations can be a strong indicator of the functional response (109, 288).

The response to training of all annotated subunits of CI proteins in both fibre types can be seen Figure 4.14. Results show a clear fibre-type difference for the protein response to training type. On average, we see a positive gradient trend in type I fibres for MICT ( $\nabla \bar{z}$ -score = 0.348), whereas there is a decrease for SIT ( $\nabla \bar{z}$ -score = -0.261). Conversely, in type II fibres, there is no distinct change in gradient as a consequence of MICT ( $\nabla \bar{z}$ -score = -0.012); there is a slight negative gradient in CI subunits as a consequence of SIT ( $\nabla \bar{z}$ -score = -0.165). These results are somewhat contrary to the findings of the limited single-fibre training studies (employing immunoblotting techniques), where an increase in the CI subunit NDUFA9 was observed for type II fibres, but not type I fibres following high-intensity interval training (HIIT) in older adults (335). A similar study comparing MICT and HIIT in young adults observed no difference for either fibre type (194). Given the current results show significant upregulation of multiple CI subunits following high-volume MICT, this supports that training volumes plays a crucial role in fibre-type dependant response of CI subunits. This finding may help resolve the ongoing discussion on whether volume or intensity are more important for training-induced improvements in mitochondria (27, 194) and provide further insight to the divergent regulatory process within fibre types.

Further investigation of the remaining complexes (II to V) indicates a similar fibre-type dependence on training volume, with similar responses observed to those observed for CI following MICT. There was a positive enrichment ( $\nabla \bar{z}$ -score > 0.05) for the expression of the protein subunits of complexes II, III, IV, & V for type I fibres (Figure 4.15), but little overall change in gradient patterns observed for type II fibres. In type II fibres, complex II increases ( $\nabla \bar{z}$ -score = 0.087), complex III shows no overall change ( $0.05 > \nabla \bar{z}$ -score < -0.05), whereas complex IV and V show a decrease ( $\nabla \bar{z}$ -score = <0.05). As with CI, following SIT there was a decrease for complexes II to IV subunits ( $\nabla \bar{z}$ -score =

<0.05) and no change with complex V ( $\nabla \bar{z}$ -Score = <0.05) in type I fibres and, on average, a negative gradient profile ( $\nabla \bar{z}$ -Score = <0.05) for complex II to V subunits of proteins in type II fibres.

The first single-fibre proteomics study in aged humans reported a decrease in the expression of ETC subunit proteins in both fibre types (218), while our results suggest training reverses some of these changes. In previous studies investigating protein levels of the ETC, changes in whole-muscle have been shown to significantly increase after training. Changes in complex I and complex II have also been shown to positively correlate with changes in complex III and IV, the final acceptors of electrons in the respiratory chain (109). While this study by Greggio et al. (109) showed that training significantly affected the distribution of ETC complexes, this was performed following MICT in the elderly on whole-muscle lysates; thus, the extrapolation of these findings to differing training and/or at the fibre-type level is difficult. Indeed, in this study there was a positive correlation for the responses of CI to V to MICT for type I fibres ( $\nabla \bar{z}$ -score > 0.05), a decrease for type II fibres in complexes IV and V, and little change in complexes I and III. In contrast, following SIT there was generally a negative response of proteins in these complexes in both fibre types ( $\nabla \bar{z}$ -score < 0.05). The differing responses of these complexes suggests the possibility for numerous regulatory pathways of OXPHOS adaptations to physical training (109). Additionally, not only did Greggio et al. (109) observe increases in the individual electron transport chain (ETC) but also of supercomplexes, revealing a novel adaptive mechanism for increased energy demand where complex I was almost exclusively found assembled in supercomplexes in muscle mitochondria, whereas other complexes are redistributed in stoichiometric ratio. While the contribution of supercomplexes is not completely understood, and cannot be discerned specifically by LC-MS based proteomics, the plasticity of these complexes to freely move can play an important contribution to our understanding of OXPHOS adaptations as they also play roles in ROS production by facilitating electron transport across the complexes (1, 87, 99, 109). Another whole-muscle study found no difference in the response to MICT (with the inclusion of sprints) in Complex II, III, IV, and V protein content before and after the training intervention (35). This was more akin to the responses observed in type II fibres in this study, particularly with SIT. The difference observed between our research for MICT in type I fibres compared to that in whole-

muscle samples by Brandt et al. (35) further suggests that protein responses in OXPHOS complexes are divergently regulated in different fibre types.

Other single-fibre immunoblotting studies have also investigated fibre-type responses of complex IV subunit cytochrome oxidase (COXIV) following training. Two of the three single-fibre studies found increases of COXIV protein content in both fibre types following HIIT (312, 335). These responses are similar to our observations for the type I fibre response in complex IV for MICT but differ from the type II fibre trends in both training types. Conversely, one of the single-fibre studies found no difference in COXIV protein content following either MICT or HIIT (194). It is difficult to discern whether the differences in these single-fibre studies are a consequence of population, training type or duration, or quantitative specificity of the analysis method used.

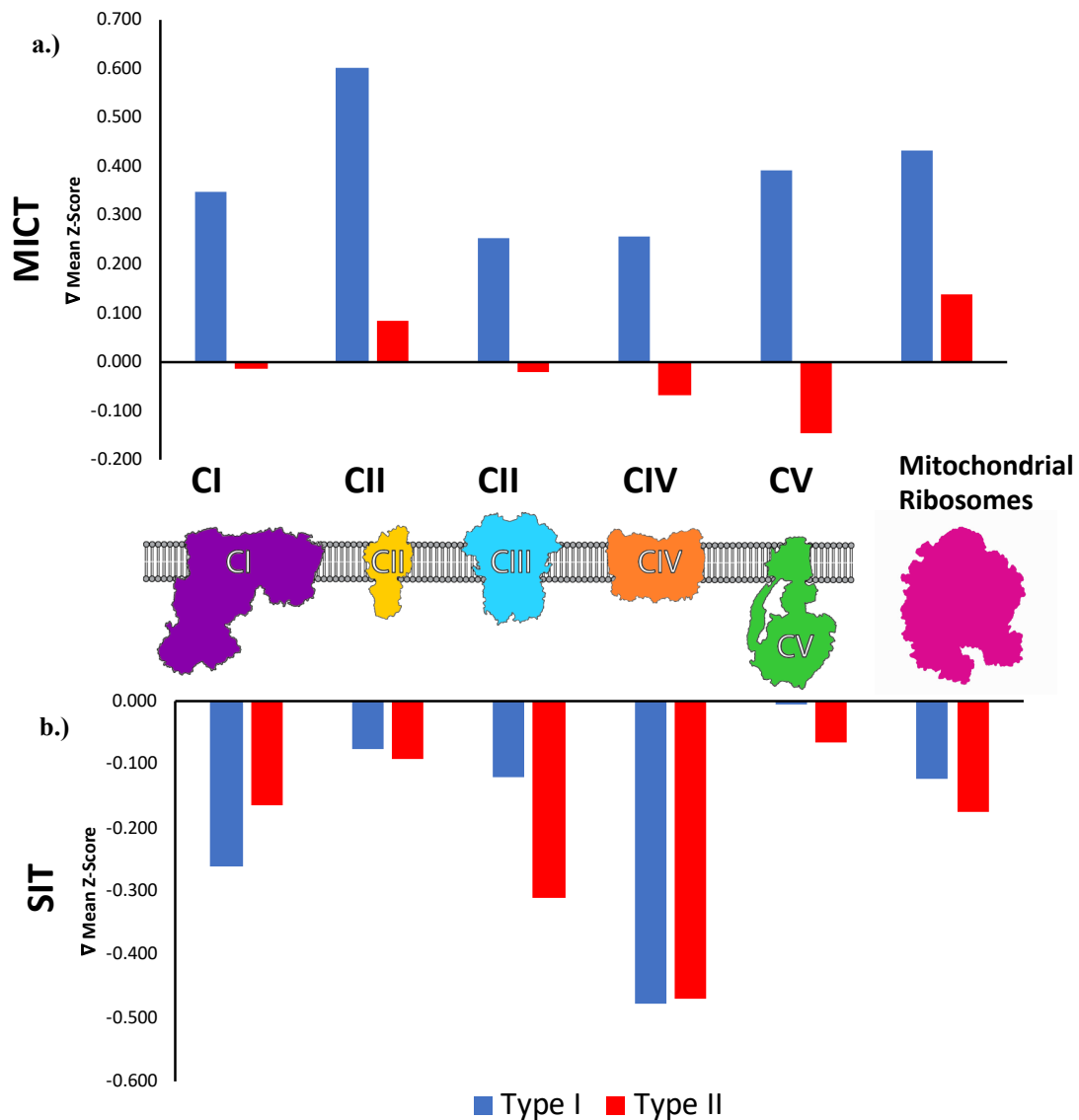


**Figure 4.15-** The respiratory chain complexes, showing the cumulative mean z-score intensity change in fibre type for all proteins identified in each complex shown following a.) Moderate Intensity Continuous Training (MICT) and b.) Sprint Interval Training (SIT). For each complex, the changes are reported in type I (blue bar) and type II fibres (red bar).

Aside from a few single-fibre studies that have used immunoblotting techniques, how these OXPHOS proteins are regulated in different fibre types in response to exercise has remained predominantly limited to whole muscle samples. The size principle states that fibre types are recruited according to intensity, and thus it is reasonable to assume that proteins may respond differently in a single fibres following different training intensities. How individual proteins respond on a fibre-type level remains largely unknown but is fundamentally important to further our knowledge of how skeletal muscles adapt to training. The current results show that OXPHOS proteins are typically upregulated in

type I fibres following training performed at a lower intensity (i.e., MICT). While it was hypothesised that type II fibres would have greater expression following training performed at the higher intensity (i.e., SIT), this does not appear to hold true for mitochondrial proteins involved in OXPHOS.

#### **4.5.2 Individual OXPHOS Protein Trends**

Individual changes in OXPHOS complexes are also summarised in the heatmap displayed in Figure 4.16. The assembly of CI subunits is organised into six modules (N, Q, ND1, ND2, ND4 and ND5) that are involved processes such as catalytic activities, redox active centres, Fe–S clusters, forming the proton channels, and other important assembly and stabilisation operations within the CI (291). As noted in section 4.5.1, complex I appears to display an overall increase in type I fibres following MICT. The biggest changes were reflected by increases in CI subunits associated with Q and ND4 assembly modules (i.e., ND4 module - NDUFB11 & NDUFB4, Q-NDUFA5, and NDUFS7). This is then followed by increases in subunits associated with module ND2 and N. This is reflected by a similar, though less pronounced, increases in type II fibres for Q & ND4 following MICT. The assembly in type II fibres following MICT appears to differ with decreases observed in subunits associated with the ND1 (e.g., NDUFA13) and module N (NDUFA6).

Following SIT the same cluster of subunits responded differently and had the opposite response in type I fibres for Q and ND4 assembly modules, coupled with a more pronounced decrease in type II fibres. Similar to MICT, proteins associated with the other modules (N, ND1, ND2, ND5) increased in type I fibres following SIT and tended to decrease in type II fibres. These results suggests a fibre-type dependence in assembly of CI in response to training. In single fibres at baseline, individual subunits have previously been reported to be higher in type I than type II fibres with a decline in abundance with age (218). The few single-fibre immunoblotting studies that analysed subunit NDUFA9 reported an increase in type II but not type I fibres in older adults following 12 weeks of HIIT (336). Another single-fibre study observed non-significant increases for both fibre types following two weeks of training in MICT and HIIT (194). These findings were contradictory to that observed in this research, where there was a slight decrease in the z-score following both training types for NDUFA9.

Complex III subunits (UQCRCQ and UQCRC1) have previously been reported to be tightly linked with CI subunits (i.e., NDUFA11 and NDUF9) (113). In the current training study, NDUFA11 and UQCRC1 increased in both type I and II following MICT but decreased in both type I and type II fibres following SIT. NDUF9 and UQCRCQ decreased in both type I and II fibres following MICT, whereas, following SIT there were increases in NDUF9 in both type I and II fibres and decrease in both fibres for UQCRCQ.

Complex IV subunits have previously been reported to have a greater abundance in type I than type II fibres in younger adults (218, 336). In the current study, there was an increase in complex IV subunits in type I fibres following MICT and a general decrease in type I fibres following SIT. Interestingly, COX5A increased in all conditions except in type II fibres following MICT. COX4I1 has been previously shown to increase in both type I and II fibres following HIIT (312, 336). This agrees with observations following MICT for type I but not type II fibres but is contrary to the decline observed in both type I and type II fibres following SIT. Additionally, MacInnis et al. (194) observed no training effect on COX4I1 in both type I and II fibres following 2 weeks of MICT and HIIT.

CV is the last enzyme in the OXPHOS system, utilising protons generated by complexes I, III and IV to power ATP synthesis. The assembly of complex V starts with ATP5F1A ( $\alpha$ -subunit) and ATP5F1B ( $\beta$ -subunit) subunits, followed by a series of assembly steps mediated by the assembly factors ATPAF1 and ATPAF2 respectively (124). The analysis of these CV subunits suggest that exercise places an increased demand on the use of ATP; this is particularly observed in type I fibres where  $\alpha$  and  $\beta$  subunits both display an increase following MICT. There was also an increased abundance of these subunits in type I fibres following SIT. The assembly units of CV generally showed increases in type I fibres following both training modalities, and these tended to decrease in type II fibres.

These varying changes in individual subunits of the ETC complexes have previously been suggested to support the concept of possible multiple regulatory layers of respiratory chain adaptations to exercise training (109). In addition, given we have highlighted that individual proteins can respond differently in different fibre types following training, this also further questions the validity of selecting a single protein subunit to be representative

of changes observed in the OXPHOS subunits in different fibre types following training, as is often the case when performing immunoblot analysis.

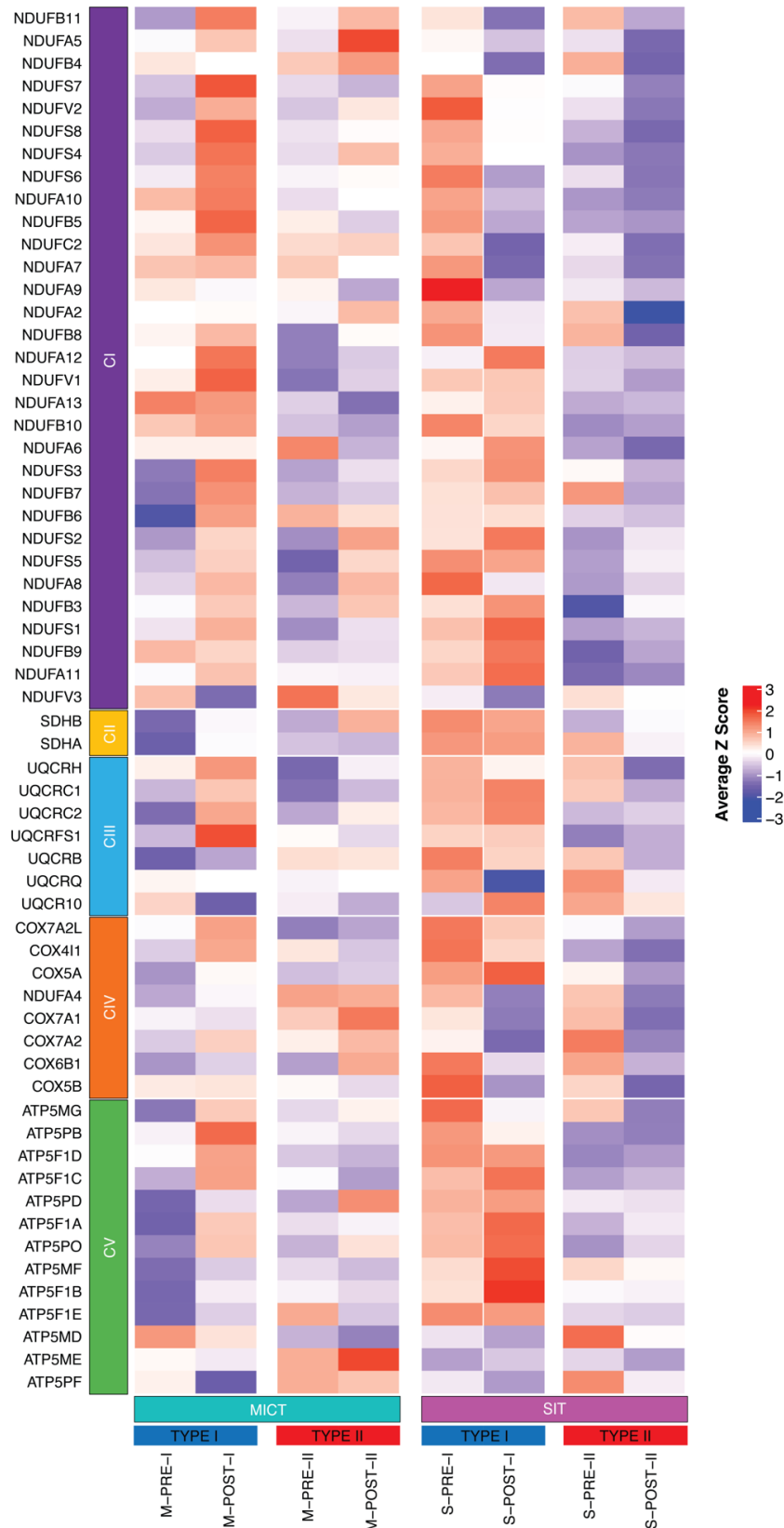


**Figure 4. 16-** Proteomic quantification of individual proteins identified in each complex of the electron transport chain in pooled single human muscle fibres. The expression of the complex subunit is measured by the z-score and subdivided by fibre type (type I & type II) and training type (M/MICT -Moderate Intensity Continuous Training, S/SIT – Sprint

Interval Training). Changes are compared from pre and post training. The colour scale represents Z score as indicated. Complexes are labelled from I-V and the names of the mitochondrial subunits are also included.

### 4.5.3 Mitochondrial Ribosomes

Mitochondrial ribosomes are important for protein synthesis within the mitochondria. Thus, changes in mitochondrial ribosomal proteins were also investigated (Figure 4.17). In response to MICT, profile gradients ( $\nabla \bar{z}$ -score  $> 0.05$ ) increased for both fibre types, whereas the opposite was observed for SIT. This suggests that the volume of MICT was sufficient to induce significant mitochondrial protein synthesis in both fibres whereas SIT does not provide a sufficient stimulus to alter protein synthesis. The MICT results agree with another proteomic study, which revealed larger changes in mitochondrial ribosomal proteins in whole muscle following HIIT (265). This increase in ribosomal proteins also supports the role for greater translational capacity in response to longer training duration. Robinson et. al (265) also hypothesised that translational level regulation is a predominant factor of mitochondrial biogenesis in humans in response to exercise training, which was further substantiated with an increase in ribosomal protein content.

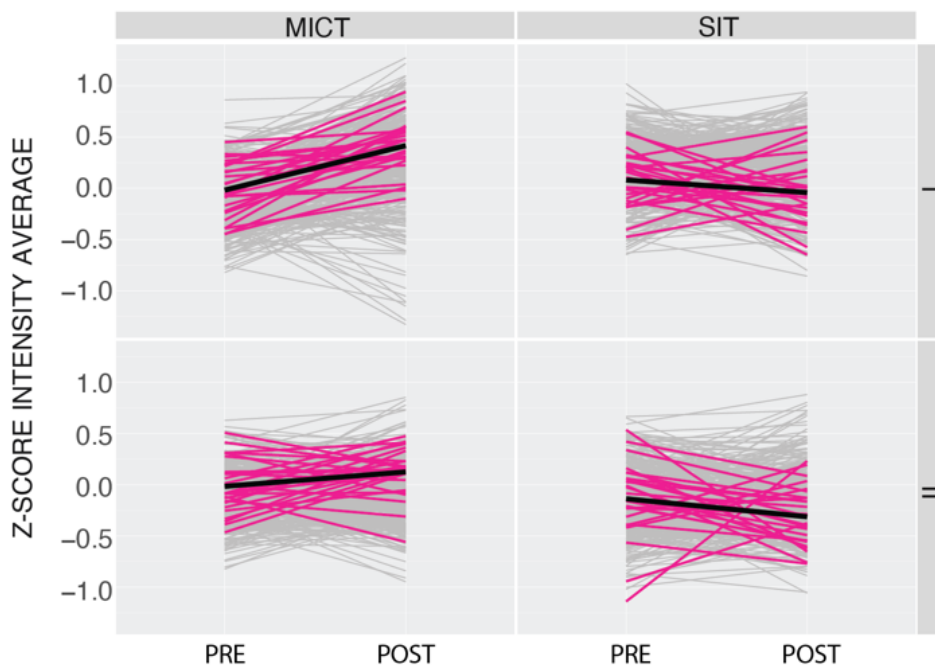


**Figure 4. 17– Mitochondrial Ribosomes** –Profile plots illustrate the z-score intensity average for all known mitochondrial proteins (grey) with mitochondrial ribosome proteins annotated in pink ( $\nabla \bar{z}$ -score -

black), pre and post training for both MICT (Moderate Intensity Continuous Training) and SIT (Sprint Interval Training) in both type I and II fibres.

#### 4.5.4 Other Common Functional Pathways

Three prominent pathways that are known to contribute to the function and generation of energy within the mitochondria are fatty acid (FA) oxidation, mitochondrial dynamics, and the TCA cycle. The content of proteins that are known markers residing within each of these pathways were analysed in both the type I and II fibres and are presented as quantitative proteomic protein plots demonstrating the change between average abundance of these mitochondrial proteins pre and post training for each fibre type (Figure 4.18). The global changes are summarised in Table 4.3, whereby the change in mean z-score pre to post training is reflected by an overall increase or decrease of the protein abundance and subsequently discussed for each functional pathway.

**Table 4. 3– Summary in Changes of Functional Pathways in the Mitochondrial Fraction of Single Muscle Fibre Samples\***

	MICT		SIT		
	∇ $\bar{z}$ -score	∇ Summary	∇ $\bar{z}$ -score	∇ Summary	
TCA	0.624	↑	-0.026	↔	Type I
Fatty Acid Oxidation	0.7761	↑	0.034	↔	
Mitochondrial Dynamics	0.3399	↑	-0.132	↓	
	MICT		SIT		
	∇ $\bar{z}$ -score	∇ Summary	∇ $\bar{z}$ -score	∇ Summary	
TCA	-0.027	↔	0.0076	↔	Type II
Fatty Acid Oxidation	-0.1011	↓	-0.0138	↔	
Mitochondrial Dynamics	0.053	↑	-0.153	↓	
* Increase - ↑( $z > 0.05$ )					
No Change - ↔ (-0.05 > $z < 0.05$ )					
Decrease - ↓ (< 0.05)					
∇ $\bar{z}$ -Score – Change in mean z-score					

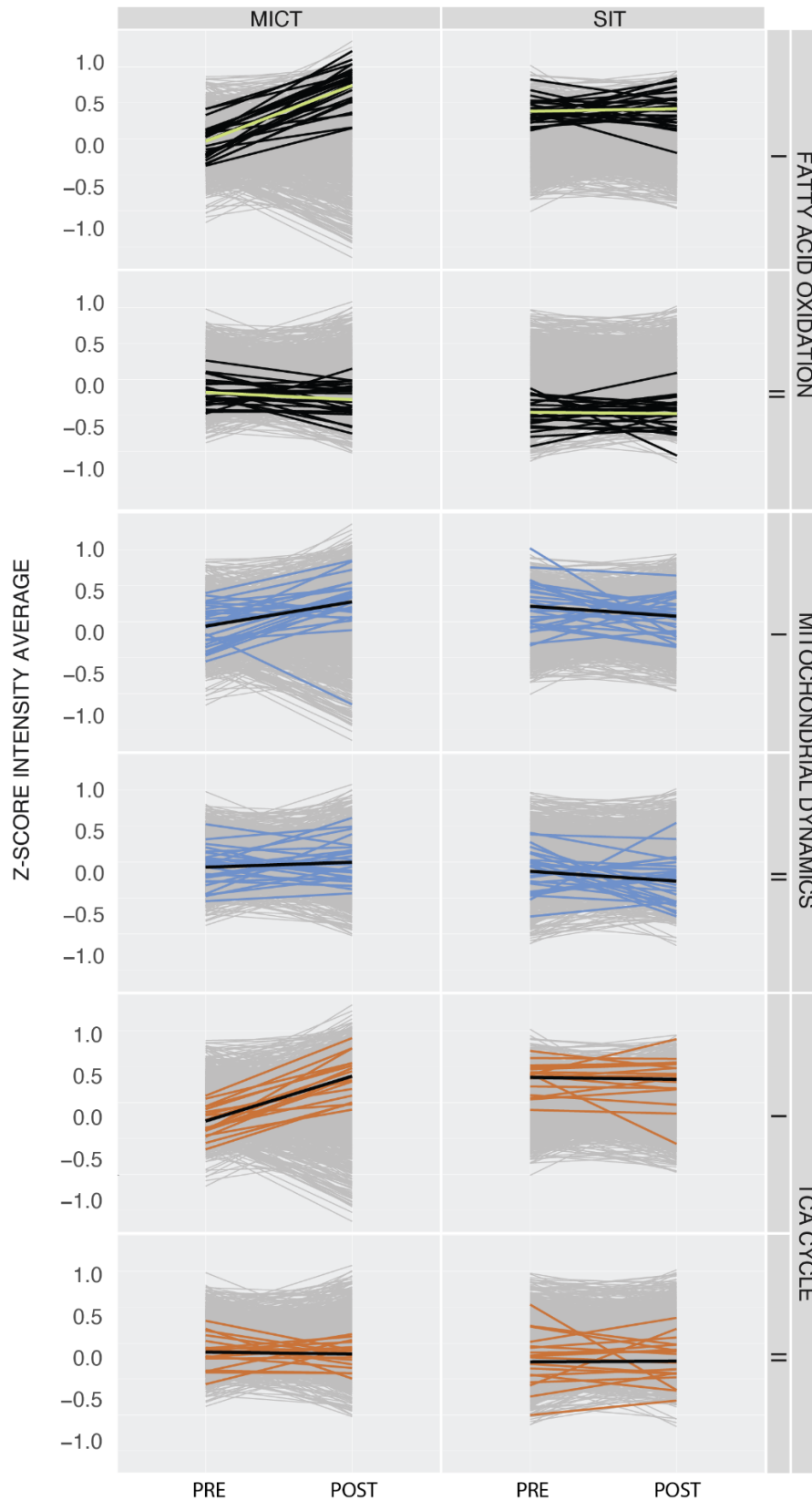


**Figure 4. 18– Common Functional Pathways** – Profile plots illustrate the z-score intensity average for all known mitochondrial proteins (grey), Fatty Acid Oxidation (black profiles,  $\nabla$   $\bar{z}$ -score - yellow), Mitochondrial Dynamics (light blue profiles) and the Tricarboxylic Acid (TCA) Cycle (brown profiles), ( $\nabla$   $\bar{z}$ -score black) pre and post training for both MICT (Moderate Intensity Continuous Training) and SIT (Sprint Interval Training) in both type I and II fibres.

#### 4.5.4.1 Fatty Acid Oxidation

Mitochondrial fatty acid (FA) oxidation is sometimes an under-appreciated pathway that is crucial for mitochondrial function (224). Despite considerable progress during recent years, our understanding of how FA oxidation is controlled during exercise remains incomplete. In general, FA are known to be transported across the mitochondrial membranes and to enter the FA beta-oxidation pathway, which produces acetyl-CoA and reducing equivalents (e.g., NADH). The long-chain nature of fatty acids results in the generation of large amounts of aerobic ATP. At moderate exercise intensities of ~50–70%  $\text{VO}_2$  max, both fat and carbohydrate contribute substrate from stores inside and outside the muscle (115, 192).

Responses of all annotated proteins associated with FA oxidation to training and fibre type against all mitochondrial proteins are presented in Figure 4.18. Results show a clear fibre type variation of protein responses to training type. On average, there was an increased gradient trend in type I fibres for MICT ( $\nabla \bar{z}$ -score= 0.776), whereas these proteins do not appear to change with SIT ( $\nabla \bar{z}$ -score= 0.034). In type II fibres, proteins also appear to be regulated by MICT, with a decrease in gradient ( $\nabla \bar{z}$ -score = -0.1011). On the other hand, FA proteins in type II fibres showed no considerable change pre and post training following SIT ( $\nabla \bar{z}$ -score = -0.034).

One of the key FA mitochondrial proteins that was identified in the dataset was carnitine palmitoyltransferase-1 $\beta$  (CPT1 $\beta$ ), which has previously been reported to be differentially expressed in different fibre types (169). It has also been identified as an important enzyme that controls mitochondrial uptake of FA and functions as the rate-determining step in  $\beta$ -oxidation. Our results provide evidence that the expression of mitochondrial proteins important for FA oxidation depend on fibre type and are enhanced by endurance training. Moreover, we show that mitochondria play distinct metabolic roles in both fibre type-specific and exercise-induced regulation of FA oxidation. These findings support the emerging view that skeletal muscle are inherently unique in different muscle fibre types and display distinct adaptations in response to energy stress (169).

As morphologically dynamic organelles, mitochondria change shape through fusion and fission-related mechanisms that depend on the available energy supply as well as the

levels of stress. Thus, mitochondrial dynamics play an important role in mitochondrial adaptation to cellular metabolic demands (302). The responses of proteins known to be associated with mitochondrial dynamics against all mitochondrial proteins was also investigated and is shown in Figure 4.18. Results show a clear difference for changes in protein abundance in response to MICT, where gradients for both type I and type II fibres increased ( $\nabla \bar{z}\text{-score} = > 0.05$ ). In contrast, gradients for both fibre types decreased in mitochondrial dynamic proteins following SIT ( $\nabla \bar{z}\text{-score} = < 0.05$ ).

Given that the magnitude of change was greater in fibre types following MICT, this suggests that this type of training provides a more potent stimulus to increase these mitochondrial dynamics related proteins. This is consistent with the only other study that has compared MICT and SIT previously (103). At the single-fibre level, an upregulation of mitochondrial dynamics proteins mitofusion 2 (MFN2) and mitochondrial dynamics protein 49 (MiD49) in aged human skeletal muscle was reported following HIIT - with an increased abundance of MFN2 specific to type II muscle fibres (336). This somewhat agrees with our findings following MICT, although we see this increase in both fibre types. This discrepancy may be related to different training and population types, or may indicate that a single protein is not truly reflective of overall changes in proteins associated with mitochondrial dynamics. A single-fibre study in aged humans found a strong decline in the expression of proteins involved in mitochondrial fusions, such as MFN2 and dynamin-like protein OPA1 (218). Again, our results suggests continuous aerobic training has the opposite effect and increases the expression of these proteins in both fibre types.

#### **4.5.4.3 Tricarboxylic Acid (TCA) Cycle**

The TCA cycle is a tightly regulated pathway that constitutes an epicentre in cell metabolism, as multiple substrates can feed into it. In terms of the metabolic pathways, the TCA cycle in the mitochondria is involved in producing reducing equivalents and accepts acetyl-CoA mainly from fatty acid, pyruvate, or amino acid oxidation. During aerobic exercise, increasing mitochondrial calcium concentrations activate the isocitrate and  $\alpha$ -ketoglutarate dehydrogenase enzymes in the TCA cycle and a third enzyme, citrate synthase, controls TCA-cycle flux (115). In addition, the regulation of the TCA cycle and its constant feedback with OXPHOS is critical to keep the cells in a stable state (198).

Responses of all annotated proteins associated with the TCA cycle against all mitochondrial proteins are also presented in Figure 4.18. Results show a clear fibre-type difference for the protein response to different types of training. On average we see a positive gradient trend in type I fibres for MICT ( $\nabla \bar{z}$ -score= 0.624), whereas there was little change following SIT ( $\nabla \bar{z}$ -score= -0.026). Conversely, in type II fibres, there was no distinct change in gradient as a consequence of either MICT or SIT ( $\nabla \bar{z}$ -score= -0.027 & 0.0076 respectively).

Our observations of increased basal TCA cycle proteins following training in single fibres was consistent with prior studies on muscle of endurance-trained individuals, which have reported increases in mitochondrial number and oxidative enzyme content in trained muscle, accompanied by an enhanced capacity for respiration and fatty-acid oxidation (18). The only research on single fibres in aged humans also quantified the expression of all the enzymes of the TCA cycle, with the majority of these enzymes slightly decreased or unchanged in aged fibres regardless of fibre type (218).

#### **4.5.4.4 Glycolysis**

As previously mentioned, type I and type II fibres differ in the relative role of glycolysis and oxidative phosphorylation. Type II fibres rely more upon glycolytic processes to generate ATP at a rapid rate. The differential response in glycolysis from fibre types prompted us to analyse how these glycolytic proteins respond to training. Responses of all annotated proteins associated with glycolysis are presented in Figure 4.19 and summarised in Table 4.4. As expected, the expression of these proteins was higher in type II than in type I fibres. On average we see a negative gradient trend in type I fibres for MICT ( $\nabla \bar{z}$ -score = -0.492) and a marked difference in the response to SIT with higher  $\nabla \bar{z}$ -scores ( $\nabla \bar{z}$ -score= 0.0119). Conversely, in type II fibres, there is no distinct change in gradient as a consequence of SIT ( $\nabla \bar{z}$ = -0.024) and a slight decrease is observed following MICT ( $\nabla \bar{z}$ = -0.153). Though changes are relatively small in type II fibres for glycolytic proteins, it should be noted that the baseline of z-score intensities are higher overall relative to type I (average  $\nabla \bar{z}$ -score= -0.089 for type II compared to  $\nabla \bar{z}$ -score= -0.323 for type I fibres for both training types).

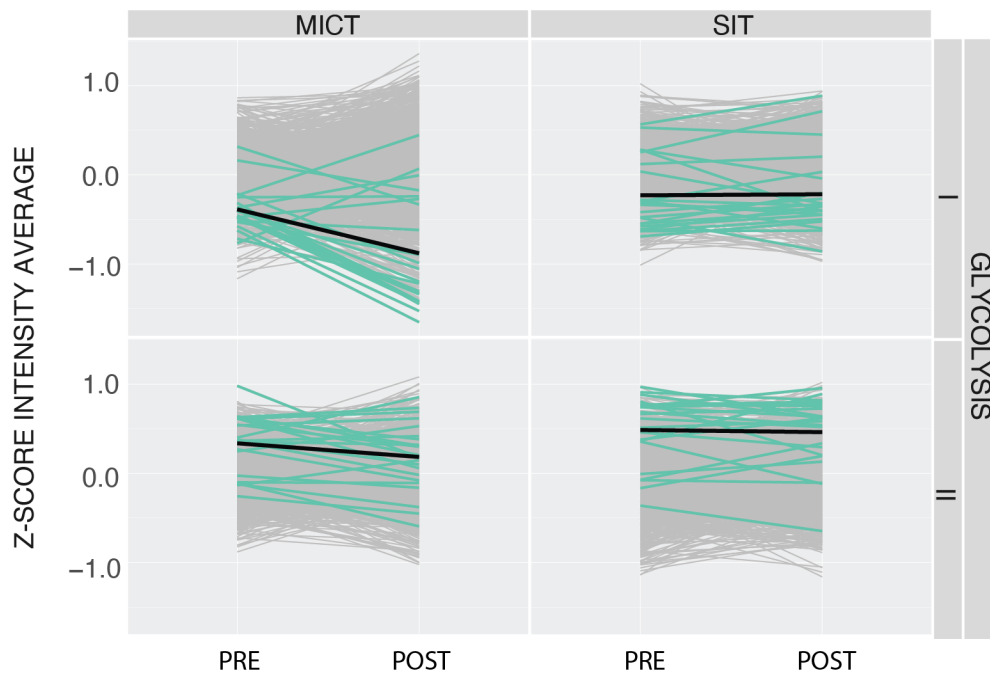


**Figure 4. 19 -Glycolysis** –Profile plots illustrate the z-score intensity average for known mitochondrial proteins (grey) with glycolysis proteins annotated in aqua ( $\nabla \bar{z}$ -score black) pre and post training for both MICT (Moderate Intensity Continuous Training) and SIT (Sprint Interval Training) in both type I and II fibres.

**Table 4. 4 - Summary of Changes of Glycolytic Proteins of Single Muscle Fibre Samples\***

	MICT		SIT	
	$\nabla$ Mean Z-Score	$\nabla$ Summary	$\nabla$ Mean Z-Score	$\nabla$ Summary
Type I	-0.492	↓	0.019	↔
Type II	-0.153	↓	-0.024	↔

\* Increase -  $\uparrow$  ( $z > 0.05$ )  
 No Change -  $\leftrightarrow$  ( $-0.05 > z < 0.05$ )  
 Decrease -  $\downarrow$  ( $z < -0.05$ )  
 $\nabla \bar{z}$ -Score – Change in mean z-score

The expression of glycolytic proteins has previously been explored in single-muscle fibres, with the expression of the majority of glycolytic enzymes reported to be greater in older type I fibres compared to younger type I fibres. In contrast, the same proteins showed a clear decrease in older type II fibres (218). Type II fibres, however, have been extensively reviewed and reported to have the highest glycolytic activity (178, 283), and a greater content of glycolytic enzymes such as glycerophosphate dehydrogenase (GPD) (263, 269). GPD was a protein that was notably identified as being differentially expressed in type II fibres compared to type I fibres (c.f. Figure 4.7 & 4.8). Furthermore, type II fibres having higher z-score intensities overall for all the glycolytic proteins

annotated in both training modalities compared to the type I counterparts (Figure 4.19). The observations in this research show slight to no change overall for these protein in type II fibres in response to either training. A study investigating glycolytic enzyme activity following SIT found no significant change in glycolytic enzyme phosphofructokinase following training except under hypoxic conditions (256), which agrees with the minimal overall change observed in single fibres following SIT in the present study. Another study by Jacobs et al. (149) found an increase in the percentage of type II fibres and PFK enzyme activity following SIT (149).

#### **4.6 Conclusions**

The current study utilised two very different exercise training prescriptions, whereby the MICT group's training volume was ~ 5 fold higher than the SIT group and the intensity was ~ 5 fold higher in SIT versus MICT. This study may further contribute to the ongoing discussion on whether volume or intensity is a more important determinant for improving mitochondrial adaptations to training and delve further into how these adaptations are regulated amongst different fibre types. Overall, greater upregulation of mitochondrial proteins was observed following MICT; this upregulation was predominantly seen in type I fibres. Type II fibres displayed a higher presence of glycolytic proteins. Mitochondrial proteins that were differentially expressed following MICT were more related to fatty acid oxidation, whereas SIT saw differential expression of mitochondrial proteins associated with the TCA cycle. Changes in mitochondrial proteins associated with key functional pathways, including OXPHOS, the TCA cycle, FA oxidation, and mitochondrial dynamics were dominated with observed increase in responses following MICT that were observed mostly in type I fibres. The response to SIT was variable but on average the abundance of proteins related to these pathways was found to decrease following training in both type I and type II fibres. This research has also demonstrated the value of utilising a proteomic approach to explore fibre-specific changes to exercise training in thousands of proteins. The results show that multiple proteins within the same functional pathways change in the same direction. However, some proteins appear to respond differently in the same functional pathways. Utilising a single protein as representative of the changes in a given functional class may not always provide results that are representative of the actual changes occurring.

## **Chapter 5**

### **Conclusions and Future Directions**

The overall goal of this thesis was to develop a proteomic workflow capable of identifying mitochondrial proteins at the resolution of single muscle fibres in healthy humans. This workflow was then used to investigate the effects of both training intensity and volume on mitochondrial proteins in different fibre types, and to ultimately provide new insights into training-induced mitochondrial adaptations at a fibre-specific level. The aim of the first part of the study (described in Chapter 3) was to develop a robust proteomic workflow that could handle a high-detergent matrix, allowing for fibre typing by immunoblotting, in addition to further isotopic labelling for identification of lowly abundant proteins in different fibre types. The purpose of the second part of the study (described in Chapter 4) was to apply the developed proteomic method to examine fibre-specific differences pre and post training between two training types: moderate-intensity-continuous training (MICT) and sprint interval training (SIT) and examining differences between fibre types.

## 5.1 Summary of Key Findings

### Chapter 3:

- A new proteomic methodology was developed that allowed dot blotting for fibre typing and the subsequent analysis of pooled single skeletal muscle fibres via mass spectrometry (MS) in a high-detergent matrix.
- Fibre typing by MS was based on the relative abundance of myosin heavy chain (MYH) isoforms, which was determined by dividing the intensity-based absolute quantification of the respective isoform (MYH1, MYH2, MYH4, MYH7) by the sum of the intensities of all four MYH isoforms. Fibre typing according to proteomic data was consistent ( $p > 0.05$ ) with the dot blotting results in all experiments.
- This methodology can be applied to the analysis of training adaptations in the mitochondrial proteome. More than 35% of mitochondrial proteins were detected in pooled single-fibre samples.
- The key optimisation findings included a reproducible method that utilised suspension trapping (S-Trap) protein extraction for sample processing in combination with styrenedivinylbenzene- reverse phase sulfonate (SDB-RPS) peptide clean-up in 6 single muscle fibre segments.
- A labelling efficiency of >90% was achieved with tandem mass tag (TMT) labelling when combining 1 h of digestion with a combination of trypsin and LysC.
- This enabled identification of over 1000 proteins in a pooled sample of 6 single muscle fibre segments
- The incorporation of TMT labelling allowed for increased identification of lowly abundant proteins using TMTpro-16 plex. This permitted a three-tiered comparison of mitochondrial protein content from different fibre types to be applied to a post vs. pre exercise training study design comparing two different exercise training types from a total of 24 human participants.
- This research also highlights that optimal extraction and processing of protein material is crucial to ensure the highest sensitivity for the downstream detection of proteins.

## Chapter 4:

- Utilising the optimised proteomic workflow described in Chapter 3 enabled a total of 3141 proteins to be identified within all samples, with 66% of these proteins being identified in over 70% of the total samples
- The proteomic workflow identified 536 known mitochondrial proteins across all 96 samples. This represented greater than 45% of the known mitochondrial proteins.
- Clear separation of fibre types was observed, illustrating that there are distinct differences in the mitochondrial proteome of type I and type II fibres. Type I fibres showed a higher presence of mitochondrial proteins notably associated with fatty acid oxidation. Type II fibres displayed a higher presence of glycolytic proteins.
- Mitochondrial proteins that were differentially expressed following MICT were more related to fatty acid oxidation, whereas SIT was associated with the differential expression of mitochondrial proteins associated with the tricarboxylic acid (TCA) cycle.
- Mitochondrial proteins associated with key functional pathways, including oxidative phosphorylation (OXPHOS), the TCA cycle, fatty acid oxidation, and mitochondrial dynamics, were observed to increase following MICT - especially in type I fibres. SIT displayed a more variable response, but on average the abundance of proteins related to these pathways were found to decrease following training in both type I and type II fibres.
- This research has also demonstrated the value of utilising a proteomic approach to explore fibre-specific changes following exercise training in thousands of proteins in a single experiment. The results show that multiple proteins within functional pathways often change in the same direction; however, some proteins behave differently in key regulatory processes (i.e., OXPHOS).

## 5.2 Conclusions & Future Directions

Proteomics applied to exercise training still remains in its infancy. Only a few studies have investigated training-induced changes (74, 107, 129, 134), and until this research there was limited research on changes in mitochondrial proteins at a fibre-specific level (194, 218, 335). The emergence of proteomics has introduced new opportunities to explore the complexity of biological networks underlying the tissue-specific responses (125). It is anticipated that mitochondrial proteomics applied to exercise and training will be a fast-moving area in the coming years. An ‘omics’ approach has the potential to replace the targeted based approaches, such as immunoblotting, that have laid the foundation for our understanding of functional changes that regulate exercise adaptations in humans. This research hopes to be at the forefront of providing an improved understanding of how mitochondrial proteins function together in pathways and complexes within single skeletal muscle fibres in response to training. Hence, it is possible for hundreds of currently uncharacterised protein responses to training to be linked to functional changes with the utilisation of proteomic technology.

Previous research has highlighted that exercise training typically upregulates pathways involving OXPHOS and the TCA cycle (235). This was further observed in this research with a deeper delve into differences in training intensity and fibre types. Many studies observing training-induced changes have been conducted in whole muscle, which has a combination of type I and type II fibres. This research highlights that single fibres display a distinct difference in their proteome characterisation. Following training, increases in the abundance of mitochondrial proteins are predominantly observed in type I fibres. From a functional pathway perspective, there was an increase in mitochondrial proteins related to fatty acid oxidation in type I fibres following MICT. There were also further changes in numerous subunits of OXPHOS. While it was observed that multiple proteins within functional pathways often trend in the same direction, some proteins behave differently to assemble key regulatory processes within complexes of the respiratory chain.

Given the large difference in each group’s training volume and intensity, it was expected that a more divergent response would be observed as a consequence of training. However, most of the changes in differential expression were observed at a fibre-specific level when comparing fibre types as opposed to comparing training. Given skeletal muscle is

dominated by sarcomeric proteins, it was reasonable to investigate the mitochondrial fraction to observe further mitochondrial changes that seemed to respond more to training volume. This study may further contribute to the ongoing discussion on whether volume or intensity is a more important determinant for improving mitochondrial adaptations to training, and how these adaptations are regulated amongst different fibre types. Despite the limited upregulation following SIT, the increased presence of glycolytic proteins in type II fibres and the observed changes in many fatty acid proteins indicates that future research employing other omic approaches in single-fibre cells (e.g., metabolomics and lipidomics) may be warranted to better understand training-induced changes at a fibre-specific level. Given the size principle states that skeletal muscle fibre recruitment is related to exercise intensity, with the extensive proteome data obtained it would be worthwhile investigating changes in contractile proteins with respect to training types to further corroborate the size principle.

### **5.3 Significance and Practical Applications**

This research has helped develop a method that can be applied to investigate fibre-specific changes as a consequence of exercise training. The application of this method to investigate changes following different fibre types of training may help to optimise training-induced adaptations. Lastly, given the many roles of mitochondria and links to some human diseases (51, 248, 328), a better understanding of how mitochondrial proteins adapt to different interventions may provide insights for improving both health and human performance.

## References

1. Acín-Pérez R, Fernández-Silva P, Peleato ML, Pérez-Martos A, and Enriquez JA. Respiratory active mitochondrial supercomplexes. *Mol Cell* 32: 529-539, 2008.
2. Adhihetty PJ, Irrcher I, Joseph AM, Ljubicic V, and Hood DA. Plasticity of skeletal muscle mitochondria in response to contractile activity. *Experimental physiology* 88: 99-107, 2003.
3. Adhihetty PJ, Taivassalo T, Haller RG, Walkinshaw DR, and Hood DA. The effect of training on the expression of mitochondrial biogenesis- and apoptosis-related proteins in skeletal muscle of patients with mtDNA defects. *American Journal of Physiology-Endocrinology and Metabolism* 293: E672-E680, 2007.
4. Aebersold R and Mann M. Mass-spectrometric exploration of proteome structure and function. *Nature* 537: 347-355, 2016.
5. Al Shweiki MR, Mönchgesang S, Majovsky P, Thieme D, Trutschel D, and Hoehenwarter W. Assessment of Label-Free Quantification in Discovery Proteomics and Impact of Technological Factors and Natural Variability of Protein Abundance. *J Proteome Res* 16: 1410-1424, 2017.
6. Alberts B, Johnson A, Lewis J, Raff M, Roberts K, and Walter P. *Molecular Biology of the Cell*. New York: Garland Science, 2002.
7. Armenta JM, Hoeschele I, and Lazar IM. Differential protein expression analysis using stable isotope labeling and PQD linear ion trap MS technology. *J Am Soc Mass Spectrom* 20: 1287-1302, 2009.
8. Arul AB and Robinson RAS. Sample Multiplexing Strategies in Quantitative Proteomics. *Analytical chemistry* 91: 178-189, 2019.
9. Atalay M, Oksala NKJ, Laaksonen DE, Khanna S, Nakao C, Lappalainen J, Roy S, Hänninen O, and Sen CK. Exercise training modulates heat shock protein response in diabetic rats. *Journal of Applied Physiology* 97: 605-611, 2004.

10. Awad D and Brueck T. Optimization of protein isolation by proteomic qualification from *Cutaneotrichosporon oleaginosus*. *Anal Bioanal Chem* 412: 449-462, 2020.
11. Axelrod CL, Fealy CE, Mulya A, and Kirwan JP. Exercise training remodels human skeletal muscle mitochondrial fission and fusion machinery towards a pro-elongation phenotype. *Acta physiologica (Oxford, England)* 225: e13216, 2019.
12. Bąchor R, Waliczek M, Stefanowicz P, and Szewczuk Z. Trends in the Design of New Isobaric Labeling Reagents for Quantitative Proteomics. *Molecules* 24: 701, 2019.
13. Baldwin KM, Winder WW, Terjung RL, and Holloszy JO. Glycolytic enzymes in different types of skeletal muscle: adaptation to exercise. *The American journal of physiology* 225: 962-966, 1973.
14. Barnard RJ, Edgerton VR, Furukawa T, and Peter JB. Histochemical, biochemical, and contractile properties of red, white, and intermediate fibers. *American Journal of Physiology-Legacy Content* 220: 410-414, 1971.
15. Barnard RJ, Edgerton VR, and Peter JB. Effect of exercise on skeletal muscle. I. Biochemical and histochemical properties. *J Appl Physiol* 28: 762-766, 1970.
16. Bass JJ, Wilkinson DJ, Rankin D, Phillips BE, Szewczyk NJ, Smith K, and Atherton PJ. An overview of technical considerations for Western blotting applications to physiological research. *Scandinavian journal of medicine & science in sports* 27: 4-25, 2017.
17. Batth TS, Tollenaere MAX, Rütther P, Gonzalez-Franquesa A, Prabhakar BS, Bekker-Jensen S, Deshmukh AS, and Olsen JV. Protein Aggregation Capture on Microparticles Enables Multipurpose Proteomics Sample Preparation. *Molecular & Cellular Proteomics* 18: 1027, 2019.
18. Befroy DE, Petersen KF, Dufour S, Mason GF, Rothman DL, and Shulman GI. Increased substrate oxidation and mitochondrial uncoupling in skeletal muscle of endurance-trained individuals. *Proceedings of National Academy of Sciences* 105: 6701-6706, 2008.

19. Berchtold MW, Brinkmeier H, and Müntener M. Calcium ion in skeletal muscle: its crucial role for muscle function, plasticity, and disease. *Physiol Rev* 80: 1215-1265, 2000.
20. Bergman BC, Butterfield GE, Wolfel EE, Casazza GA, Lopaschuk GD, and Brooks GA. Evaluation of exercise and training on muscle lipid metabolism. *The American journal of physiology* 276: E106-117, 1999.
21. Bergstrom J. Muscle electrolytes in man. *Scand J Clin Lab Invest* 14: 100-110, 1962.
22. Bergstrom J. Percutaneous needle biopsy of skeletal muscle in physiological and clinical research. *Scandinavian journal of clinical and laboratory investigation* 35: 609-616, 1975.
23. Beyfuss K, Erlich AT, Triolo M, and Hood DA. The Role of p53 in Determining Mitochondrial Adaptations to Endurance Training in Skeletal Muscle. *Scientific Reports* 8: 14710, 2018.
24. Biral D, Betto R, Danieli-Betto D, and Salviati G. Myosin heavy chain composition of single fibres from normal human muscle. *Biochem J* 250: 307-308, 1988.
25. Bisetto E, Comelli M, Salzano AM, Picotti P, Scaloni A, Lippe G, and Mavelli I. Proteomic analysis of F1F0-ATP synthase super-assembly in mitochondria of cardiomyoblasts undergoing differentiation to the cardiac lineage. *Biochimica et Biophysica Acta (BBA) - Bioenergetics* 1827: 807-816, 2013.
26. Bishop D, Jenkins DG, McEniery M, and Carey MF. Relationship between plasma lactate parameters and muscle characteristics in female cyclists. *Medicine and science in sports and exercise* 32: 1088-1093, 2000.
27. Bishop DJ, Botella J, Genders AJ, Lee MJ, Saner NJ, Kuang J, Yan X, and Granata C. High-Intensity Exercise and Mitochondrial Biogenesis: Current Controversies and Future Research Directions. *Physiology (Bethesda, Md)* 34: 56-70, 2019.

28. Bishop DJ, Botella J, and Granata C. CrossTalk opposing view: Exercise training volume is more important than training intensity to promote increases in mitochondrial content. *The Journal of Physiology* 0, 2019.
29. Bishop DJ, Granata C, and Eynon N. Can we optimise the exercise training prescription to maximise improvements in mitochondria function and content? . *Biochimica et Biophysica Acta* 1840: 1266–1275, 2014.
30. Boja ES, Phillips D, French SA, Harris RA, and Balaban RS. Quantitative mitochondrial phosphoproteomics using iTRAQ on an LTQ-Orbitrap with high energy collision dissociation. *J Proteome Res* 8: 4665-4675, 2009.
31. Boluyt MO, Brevick JL, Rogers DS, Randall MJ, Scalia AF, and Li ZB. Changes in the rat heart proteome induced by exercise training: Increased abundance of heat shock protein hsp20. *Proteomics* 6: 3154-3169, 2006.
32. Booth FW, Ruegsegger GN, Toedebusch RG, and Yan Z. Chapter Six - Endurance Exercise and the Regulation of Skeletal Muscle Metabolism. In: *Progress in Molecular Biology and Translational Science*, edited by Bouchard C: Academic Press, 2015, p. 129-151.
33. Bottinelli R and Reggiani C. Human skeletal muscle fibres: molecular and functional diversity. *Prog Biophys Mol Biol* 73: 195-262, 2000.
34. Boyd JC, Simpson CA, Jung ME, and Gurd BJ. Reducing the intensity and volume of interval training diminishes cardiovascular adaptation but not mitochondrial biogenesis in overweight/obese men. *PloS one* 8: e68091-e68091, 2013.
35. Brandt N, Gunnarsson TP, Bangsbo J, and Pilegaard H. Exercise and exercise training-induced increase in autophagy markers in human skeletal muscle. *Physiological reports* 6: e13651, 2018.
36. Brenes A, Hukelmann J, Bensaddek D, and Lamond AI. Multibatch TMT Reveals False Positives, Batch Effects and Missing Values. *Mol Cell Proteomics* 18: 1967-1980, 2019.

37. Brooke MH and Kaiser KK. Three "myosin adenosine triphosphatase" systems: the nature of their pH lability and sulfhydryl dependence. *The journal of histochemistry and cytochemistry : official journal of the Histochemistry Society* 18: 670-672, 1970.
38. Burelle Y and Hochachka PW. Endurance training induces muscle-specific changes in mitochondrial function in skinned muscle fibers. *Journal of applied physiology (Bethesda, Md : 1985)* 92: 2429-2438, 2002.
39. Burgomaster KA, Howarth KR, Phillips SM, Rakobowchuk M, Macdonald MJ, McGee SL, and Gibala MJ. Similar metabolic adaptations during exercise after low volume sprint interval and traditional endurance training in humans. *J Physiol* 586: 151-160, 2008.
40. Burniston JG. Changes in the rat skeletal muscle proteome induced by moderate-intensity endurance exercise. *Biochim Biophys Acta* 1784: 1077-1086, 2008.
41. Cagnin S, Chemello F, Alessio E, and Lanfranchi G. Chapter 13 - Single-Cell Transcriptomics and Proteomics of Skeletal Muscle: Technology and Applications. In: *Single-Cell Omics*, edited by Barh D and Azevedo V: Academic Press, 2019, p. 253-281.
42. Caiozzo VJ, Baker MJ, Huang K, Chou H, Wu YZ, and Baldwin KM. Single-fiber myosin heavy chain polymorphism: how many patterns and what proportions? *American journal of physiology Regulatory, integrative and comparative physiology* 285: R570-580, 2003.
43. Calvo SE, Clauser KR, and Mootha VK. MitoCarta2.0: an updated inventory of mammalian mitochondrial proteins. *Nucleic acids research* 44: D1251-1257, 2016.
44. Calvo SE and Mootha VK. The mitochondrial proteome and human disease. *Annu Rev Genomics Hum Genet* 11: 25-44, 2010.
45. Carpentieri A, Gamberi T, Modesti A, Amoresano A, Colombini B, Nocella M, Bagni MA, Fiaschi T, Barolo L, Gulisano M, and Magherini F. Profiling Carbonylated Proteins in Heart and Skeletal Muscle Mitochondria from Trained and Untrained Mice. *Journal of Proteome Research* 15: 3666-3678, 2016.

46. Chae S, Kim S, Koo YD, Lee JH, Kim H, Ahn BY, Ha Y, Kim Y, Jang MG, 6, Koo K, S, Choi SH, Lim S, Y, Park YJ, Jang HC, Hwang D, Lee S, and Park K. A mitochondrial proteome profile indicative of type 2 diabetes mellitus in skeletal muscles *Experimental & Molecular Medicine* 50: 1-14, 2018.
47. Chandramouli K and Qian P-Y. Proteomics: challenges, techniques and possibilities to overcome biological sample complexity. *Human genomics and proteomics : HGP* 2009: 239204, 2009.
48. Chavanelle V, Boisseau N, Otero YF, Combaret L, Dardevet D, Montaurier C, Delcros G, Peltier SL, and Sirvent P. Effects of high-intensity interval training and moderate-intensity continuous training on glycaemic control and skeletal muscle mitochondrial function in db/db mice. *Sci Rep* 7: 204, 2017.
49. Chen CCW, Erlich AT, and Hood DA. Role of Parkin and endurance training on mitochondrial turnover in skeletal muscle. *Skeletal Muscle* 8: 10, 2018.
50. Cheng L, Pisitkun T, Knepper MA, and Hoffert JD. Peptide Labeling Using Isobaric Tagging Reagents for Quantitative Phosphoproteomics. *Methods in molecular biology (Clifton, NJ)* 1355: 53-70, 2016.
51. Chinnery PF, Howell N, Andrews RM, and Turnbull DM. Clinical mitochondrial genetics. *Journal of medical genetics* 36: 425-436, 1999.
52. Cho Y, Tachibana S, Hazen BC, Moresco JJ, Yates JR, Kok B, Saez E, Ross RS, Russell AP, and Kralli A. *Perm1* regulates CaMKII activation and shapes skeletal muscle responses to endurance exercise training. *Molecular Metabolism* 23: 88-97, 2019.
53. Christiansen D, MacInnis MJ, Zacharewicz E, Frankish BP, and Murphy RM. Dot blotting for fiber type identification of single muscle fibers: a fast, reliable and sample-sparing method, 2017.
54. Christiansen D, MacInnis MJ, Zacharewicz E, Xu H, Frankish BP, and Murphy RM. A fast, reliable and sample-sparing method to identify fibre types of single muscle fibres. *Scientific Reports* 9: 6473, 2019.

55. Cochran AJ, Percival ME, Tricarico S, Little JP, Cermak N, Gillen JB, Tarnopolsky MA, and Gibala MJ. Intermittent and continuous high-intensity exercise training induce similar acute but different chronic muscle adaptations. *Experimental physiology* 99: 782-791, 2014.
56. Cogswell AM, Stevens RJ, and Hood DA. Properties of skeletal muscle mitochondria isolated from subsarcolemmal and intermyofibrillar regions. *The American journal of physiology* 264: C383-389, 1993.
57. Conjard A, Peuker H, and Pette D. Energy state and myosin heavy chain isoforms in single fibres of normal and transforming rabbit muscles. *Pflügers Archiv* 436: 962-969, 1998.
58. Constans A, Pin-Barre C, Molinari F, Temprado J-J, Brioché T, Pellegrino C, and Laurin J. High-intensity interval training is superior to moderate intensity training on aerobic capacity in rats: Impact on hippocampal plasticity markers. *Behavioural Brain Research*: 112977, 2020.
59. Cox J, Hein MY, Luber CA, Paron I, Nagaraj N, and Mann M. Accurate Proteome-wide Label-free Quantification by Delayed Normalization and Maximal Peptide Ratio Extraction, Termed MaxLFQ\* *Molecular and Cellular Proteomics* 13: 2513-2526, 2014.
60. Cox J and Mann M. MaxQuant enables high peptide identification rates, individualized p.p.b.-range mass accuracies and proteome-wide protein quantification. *Nature biotechnology* 26: 1367-1372, 2008.
61. Cravatt BF, Simon GM, and Yates JR. The biological impact of massspectrometry-based proteomics. *Nature* 450: 991-1000, 2007.
62. Dayon L, Hainard A, Licker V, Turck N, Kuhn K, Hochstrasser DF, Burkhard PR, and Sanchez J-C. Relative Quantification of Proteins in Human Cerebrospinal Fluids by MS/MS Using 6-Plex Isobaric Tags. *Analytical chemistry* 80: 2921-2931, 2008.
63. Dent JR, Martins VF, Svensson K, LaBarge SA, Schlenk NC, Esparza MC, Buckner EH, Meyer GA, Hamilton DL, Schenk S, and Philp A. Muscle-specific knockout

of general control of amino acid synthesis 5 (GCN5) does not enhance basal or endurance exercise-induced mitochondrial adaptation. *Mol Metab* 6: 1574-1584, 2017.

64. Deshmukh AS, Murgia M, Nagaraj N, Treebak JT, Cox J, and Mann M. Deep Proteomics of Mouse Skeletal Muscle Enables Quantitation of Protein Isoforms, Metabolic Pathways, and Transcription Factors *Molecular and Cell Proteomics* 14: 841-853, 2015.

65. Desplanches D, Amami M, Dupré-Aucouturier S, Valdivieso P, Schmutz S, Mueller M, Hoppeler H, Kreis R, and Flück M. Hypoxia refines plasticity of mitochondrial respiration to repeated muscle work. *Eur J Appl Physiol* 114: 405-417, 2014.

66. Diaz F and Moraes CT. Mitochondrial biogenesis and turnover. *Cell Calcium* 44: 24-35, 2008.

67. Dilillo M, Pellegrini D, Ait-Belkacem R, de Graaf EL, Caleo M, and McDonnell LA. Mass Spectrometry Imaging, Laser Capture Microdissection, and LC-MS/MS of the Same Tissue Section. *Journal of Proteome Research* 16: 2993-3001, 2017.

68. Dimayacyac-Esleta BR, Tsai CF, Kitata RB, Lin PY, Choong WK, Lin TD, Wang YT, Weng SH, Yang PC, Arco SD, Sung TY, and Chen YJ. Rapid High-pH Reverse Phase StageTip for Sensitive Small-Scale Membrane Proteomic Profiling. *Analytical chemistry* 87: 12016-12023, 2015.

69. Diz AP, Truebano M, and Skibinski DO. The consequences of sample pooling in proteomics: an empirical study. *Electrophoresis* 30: 2967-2975, 2009.

70. Donoghue P, Doran P, Dowling P, and Ohlendieck K. Differential expression of the fast skeletal muscle proteome following chronic low-frequency stimulation. *Biochim Biophys Acta* 1752: 166-176, 2005.

71. Donoghue P, Doran P, Wynne K, Pedersen K, Dunn MJ, and Ohlendieck K. Proteomic profiling of chronic low-frequency stimulated fast muscle. *Proteomics* 7: 3417-3430, 2007.

72. Dudley GA, Abraham WM, and Terjung RL. Influence of exercise intensity and duration on biochemical adaptations in skeletal muscle. *Journal of applied physiology: respiratory, environmental and exercise physiology* 53: 844-850, 1982.
73. Dunn SE and Michel RN. Coordinated expression of myosin heavy chain isoforms and metabolic enzymes within overloaded rat muscle fibers. *American Journal of Physiology-Cell Physiology* 273: C371-C383, 1997.
74. Egan B, Dowling P, O'Connor PL, Henry M, Meleady P, Zierath JR, and O'Gorman DJ. 2-D DIGE analysis of the mitochondrial proteome from human skeletal muscle reveals time coursedependent remodelling in response to 14 consecutive days of endurance exercise training *Proteomics* 11: 1413–1428, 2011.
75. Egan B and Zierath JR. Exercise metabolism and the molecular regulation of skeletal muscle adaptation. *Cell Metab* 17: 162-184, 2013.
76. Ehrlicher SE, Stierwalt HD, Miller BF, Newsom SA, and Robinson MM. Mitochondrial adaptations to exercise do not require Bcl2-mediated autophagy but occur with BNIP3/Parkin activation. *The FASEB Journal* 34: 4602-4618, 2020.
77. Engel WK. The essentiality of histo- and cytochemical studies of skeletal muscle in the investigation of neuromuscular disease. 1962. *Neurology* 51: 655 and 617 pages following, 1998.
78. Essen-Gustavsson B and Henriksson J. Enzyme levels in pools of microdissected human muscle fibres of identified type. Adaptive response to exercise. *Acta Physiol Scand* 120: 505-515, 1984.
79. Fenwick AJ, Wood AM, and Tanner BCW. Effects of cross-bridge compliance on the force-velocity relationship and muscle power output. *PloS one* 12: e0190335-e0190335, 2017.
80. Fiorenza M, Gunnarsson TP, Hostrup M, Iaia FM, Schena F, Pilegaard H, and Bangsbo J. Metabolic stress-dependent regulation of the mitochondrial biogenic molecular response to high-intensity exercise in human skeletal muscle. *The Journal of physiology* 596: 2823-2840, 2018.

81. Fiorenza M, Lemminger AK, Marker M, Eibye K, Marcello Iaia F, Bangsbo J, and Hostrup M. High-intensity exercise training enhances mitochondrial oxidative phosphorylation efficiency in a temperature-dependent manner in human skeletal muscle: implications for exercise performance. *The FASEB Journal* 33: 8976-8989, 2019.
82. Forner F, Foster LJ, Campanaro S, Valle G, and Mann M. Quantitative Proteomic Comparison of Rat Mitochondria from Muscle, Heart, and Liver *Molecular and Cell Proteomics* 5: 608-619, 2006.
83. Franz T and Li X. Step-by-step preparation of proteins for mass spectrometric analysis. *Methods in molecular biology (Clifton, NJ)* 1295: 235-247, 2015.
84. Fritzen AM, Thøgersen FB, Thybo K, Vissing CR, Krag TO, Ruiz-Ruiz C, Risom L, Wibrand F, Høeg LD, Kiens B, Duno M, Vissing J, and Jeppesen TD. Adaptations in Mitochondrial Enzymatic Activity Occurs Independent of Genomic Dosage in Response to Aerobic Exercise Training and Deconditioning in Human Skeletal Muscle. *Cells* 8: 237, 2019.
85. Gandra PG, Valente RH, Perales J, Pacheco AG, and Macedo DV. Proteomic analysis of rat skeletal muscle submitted to one bout of incremental exercise. *Scandinavian journal of medicine & science in sports* 22: 207-216, 2012.
86. Gauthier GF. Ultrastructural identification of muscle fiber types by immunocytochemistry. *The Journal of cell biology* 82: 391-400, 1979.
87. Genova ML and Lenaz G. Functional role of mitochondrial respiratory supercomplexes. *Biochimica et Biophysica Acta (BBA) - Bioenergetics* 1837: 427-443, 2014.
88. Ghosh R, Gilda JE, and Gomes AV. The necessity of and strategies for improving confidence in the accuracy of western blots. *Expert review of proteomics* 11: 549-560, 2014.
89. Gibala MJ, Little JP, van Essen M, Wilkin GP, Burgomaster KA, Safdar A, Raha S, and Tarnopolsky MA. Short-term sprint interval versus traditional endurance training: similar initial adaptations in human skeletal muscle and exercise performance. *J Physiol* 575: 901-911, 2006.

90. Gilda JE, Ghosh R, Cheah JX, West TM, Bodine SC, and Gomes AV. Western Blotting Inaccuracies with Unverified Antibodies: Need for a Western Blotting Minimal Reporting Standard (WBMRS). *PloS one* 10: e0135392-e0135392, 2015.
91. Gillen JB, Martin BJ, MacInnis MJ, Skelly LE, Tarnopolsky MA, and Gibala MJ. Twelve Weeks of Sprint Interval Training Improves Indices of Cardiometabolic Health Similar to Traditional Endurance Training despite a Five-Fold Lower Exercise Volume and Time Commitment. *PLoS One* 11: e0154075, 2016.
92. Glancy B and Balaban RS. Protein composition and function of red and white skeletal muscle mitochondria. *American journal of physiology Cell physiology* 300: C1280-C1290, 2011.
93. Glancy B, Hartnell LM, Malide D, Yu ZX, Combs CA, Connelly PS, Subramaniam S, and Balaban RS. Mitochondrial reticulum for cellular energy distribution in muscle. *Nature* 523: 617-620, 2015.
94. Gollnick PD, Ianuzzo CD, and King DW. Ultrastructural and Enzyme Changes in Muscles with Exercise. In: *Muscle Metabolism During Exercise: Proceedings of a Karolinska Institutet Symposium held in Stockholm, Sweden, September 6–9, 1970 Honorary guest: E Hohwü Christensen*, edited by Pernow B and Saltin B. Boston, MA: Springer US, 1971, p. 69-85.
95. Gollnick PD, Armstrong RB, Saubert CW, Piehl K, and Saltin B. Enzyme activity and fiber composition in skeletal muscle of untrained and trained men. *Journal of Applied Physiology* 33: 312-319, 1972.
96. Gollnick PD and Hodgson DR. The identification of fiber types in skeletal muscle: a continual dilemma. *Exercise and sport sciences reviews* 14: 81-104, 1986.
97. Gomes LC, Di Benedetto G, and Scorrano L. During autophagy mitochondria elongate, are spared from degradation and sustain cell viability. *Nat Cell Biol* 13: 589-598, 2011.
98. Gómez-Pérez Y, Capllonch-Amer G, Gianotti M, Lladó I, and Proenza AM. Long-term high-fat-diet feeding induces skeletal muscle mitochondrial biogenesis in rats in a sex-dependent and muscle-type specific manner. *Nutrition & Metabolism* 9: 15, 2012.

99. Gonzalez-Franquesa A, Stocks B, Chubanava S, Hattel HB, Moreno-Justicia R, Trebak JT, Zierath JR, and Deshmukh AS. Mass-spectrometry based proteomics reveals mitochondrial supercomplexome plasticity. *bioRxiv*: 860080, 2019.
100. Gonzalez-Freire M, Semba RD, Ubaida-Mohien C, Fabbri E, Scalzo P, Højlund K, Dufresne C, Lyashkov A, and Ferrucci L. The Human Skeletal Muscle Proteome Project: a reappraisal of the current literature. *Journal of Cachexia, Sarcopenia and Muscle* 8: 5-18, 2017.
101. Goodman CA, Kotecki JA, Jacobs BL, and Hornberger TA. Muscle fiber type-dependent differences in the regulation of protein synthesis. *PloS one* 7: e37890-e37890, 2012.
102. Granata C. *Effects of different exercise intensity and volume on markers of mitochondrial biogenesis in human skeletal muscle*. Melbourne, Australia: Victoria University, 2015.
103. Granata C, Oliveira RS, Little JP, Renner K, and Bishop DJ. Sprint-interval but not continuous exercise increases PGC-1 $\alpha$  protein content and p53 phosphorylation in nuclear fractions of human skeletal muscle *Scientific Reports* 7:44227: 1-13, 2017.
104. Granata C, Oliveira RS, Little JP, Renner K, and Bishop DJ. Training intensity modulates changes in PGC-1 $\alpha$  and p53 protein content and mitochondrial respiration, but not markers of mitochondrial content in human skeletal muscle. *Faseb j* 30: 959-970, 2016.
105. Granata C, Oliveira RSF, Little JP, and Bishop DJ. High-intensity interval training blunts exercise-induced changes in markers of mitochondrial biogenesis in human skeletal muscle. *bioRxiv*: 580373, 2019.
106. Granata C, Oliveira RSF, Little JP, Renner K, and Bishop DJ. Mitochondrial adaptations to high-volume exercise training are rapidly reversed after a reduction in training volume in human skeletal muscle *The Federation of American Societies for Experimental Biology Journal* 30: 1-11, 2016.
107. Granata C, Stroud D, and Bishop D. Proteomic Analysis of Mitochondrial adaptations to training cycle volume variations in human skeletal muscle

2019.

108. Green DR and Reed JC. Mitochondria and apoptosis. *Science (New York, NY)* 281: 1309-1312, 1998.

109. Greggio C, Jha P, Kulkarni SS, Lagarrigue S, Broskey NT, Boutant M, Wang X, Conde Alonso S, Ofori E, Auwerx J, Canto C, and Amati F. Enhanced Respiratory Chain Supercomplex Formation in Response to Exercise in Human Skeletal Muscle. *Cell Metab* 25: 301-311, 2017.

110. Guan S, Taylor PP, Han Z, Moran MF, and Ma B. DDIA: data dependent-independent acquisition proteomics - DDA and DIA in a single LC-MS/MS run. *bioRxiv*: 802231, 2019.

111. Gundry RL, White MY, Murray CI, Kane LA, Fu Q, Stanley BA, and Van Eyk JE. Preparation of proteins and peptides for mass spectrometry analysis in a bottom-up proteomics workflow. *Curr Protoc Mol Biol* Chapter 10: Unit10.25, 2009.

112. Gunnarsson TP, Brandt N, Fiorenza M, Hostrup M, Pilegaard H, and Bangsbo J. Inclusion of sprints in moderate intensity continuous training leads to muscle oxidative adaptations in trained individuals. *Physiological reports* 7: e13976, 2019.

113. Guo R, Gu J, Zong S, Wu M, and Yang M. Structure and mechanism of mitochondrial electron transport chain. *Biomed J* 41: 9-20, 2018.

114. Han X, Aslanian A, and Yates JR, 3rd. Mass spectrometry for proteomics. *Current opinion in chemical biology* 12: 483-490, 2008.

115. Hargreaves M and Spriet LL. Skeletal muscle energy metabolism during exercise. *Nature Metabolism* 2: 817-828, 2020.

116. Hawley JA, Hargreaves M, Joyner MJ, and Zierath JR. Integrative biology of exercise. *Cell* 159: 738-749, 2014.

117. Hawley JA, Hargreaves M, and Zierath JR. Signalling mechanisms in skeletal muscle: role in substrate selection and muscle adaptation. *Essays Biochem* 42: 1-12, 2006.

118. Henneman E. Relation between Size of Neurons and Their Susceptibility to Discharge. *Science (New York, NY)* 126: 1345, 1957.
119. Henneman E and Olson CB. Relations Between Structure and Function in the Design of Skeletal Muscle. *Journal of Neurophysiology* 28: 581-598, 1965.
120. Henze K and Martin W. Evolutionary biology: essence of mitochondria. *Nature* 426: 127-128, 2003.
121. Hilber K and Galler S. Mechanical properties and myosin heavy chain isoform composition of skinned skeletal muscle fibres from a human biopsy sample. *Pflügers Archiv* 434: 551-558, 1997.
122. Hintz CS, Coyle EF, Kaiser KK, Chi MM, and Lowry OH. Comparison of muscle fiber typing by quantitative enzyme assays and by myosin ATPase staining. *Journal of Histochemistry & Cytochemistry* 32: 655-660, 1984.
123. Hittel DS, Hathout Y, Hoffman EP, and Houmard JA. Proteome analysis of skeletal muscle from obese and morbidly obese women. *Diabetes* 54: 1283-1288, 2005.
124. Hock DH, Robinson DRL, and Stroud DA. Blackout in the powerhouse: clinical phenotypes associated with defects in the assembly of OXPHOS complexes and the mitoribosome. *Biochemical Journal* 477: 4085-4132, 2020.
125. Hoffman NJ. Omics and Exercise: Global Approaches for Mapping Exercise Biological Networks. *Cold Spring Harbor perspectives in medicine* 7: a029884, 2017.
126. Holloszy JO. Biochemical adaptations in muscle. Effects of exercise on mitochondrial oxygen uptake and respiratory enzyme activity in skeletal muscle. *The Journal of biological chemistry* 242: 2278-2282, 1967.
127. Holloszy JO, Oscai LB, Molé PA, and Don IJ. Biochemical Adaptations to Endurance Exercise in Skeletal Muscle. In: *Muscle Metabolism During Exercise: Proceedings of a Karolinska Institutet Symposium held in Stockholm, Sweden, September 6-9, 1970 Honorary guest: E Hohwü Christensen*, edited by Pernow B and Saltin B. Boston, MA: Springer US, 1971, p. 51-61.

128. Holloszy JO, Rennie MJ, Hickson RC, Conlee RK, and Hagberg JM. Physiological consequences of the biochemical adaptations to endurance exercise. *Annals of the New York Academy of Sciences* 301: 440-450, 1977.
129. Holloway KV, O'Gorman M, Woods P, Morton JP, Evans L, Cable NT, Goldspink DF, and Burniston JG. Proteomic investigation of changes in human vastus lateralis muscle in response to interval-exercise training. *Proteomics* 9: 5155-5174, 2009.
130. Hood DA. Mechanisms of exercise-induced mitochondrial biogenesis in skeletal muscle. *Applied physiology, nutrition, and metabolism = Physiologie appliquee, nutrition et metabolisme* 34: 465-472, 2009.
131. Hood DA, Tryon LD, Carter HN, Kim Y, and Chen CC. Unravelling the mechanisms regulating muscle mitochondrial biogenesis. *Biochem J* 473: 2295-2314, 2016.
132. Hoppeler H, Howald H, Conley K, Lindstedt SL, Claassen H, Vock P, and Weibel ER. Endurance training in humans: aerobic capacity and structure of skeletal muscle. *Journal of applied physiology (Bethesda, Md : 1985)* 59: 320-327, 1985.
133. Hostrup M, Gunnarsson TP, Fiorenza M, Mørch K, Onslev J, Pedersen KM, and Bangsbo J. In-season adaptations to intense intermittent training and sprint interval training in sub-elite football players. *Scandinavian journal of medicine & science in sports* 29: 669-677, 2019.
134. Hostrup M, Onslev J, Jacobson GA, Wilson R, and Bangsbo J. Chronic  $\beta$ 2-adrenoceptor agonist treatment alters muscle proteome and functional adaptations induced by high intensity training in young men. *The Journal of Physiology* 596: 231-252, 2018.
135. Howald H, Hoppeler H, Claassen H, Mathieu O, and Straub R. Influences of endurance training on the ultrastructural composition of the different muscle fiber types in humans. *Pflugers Archiv : European journal of physiology* 403: 369-376, 1985.
136. Howlett RA and Willis WT. Fiber-type-related differences in the enzymes of a proposed substrate cycle. *Biochimica et Biophysica Acta (BBA) - Bioenergetics* 1363: 224-230, 1998.

137. Huang DW, Sherman BT, and Lempicki RA. Systematic and integrative analysis of large gene lists using DAVID bioinformatics resources. *Nature protocols* 4: 44-57, 2009.
138. Hubner NC, Ren S, and Mann M. Peptide separation with immobilized pI strips is an attractive alternative to in-gel protein digestion for proteome analysis. *Proteomics* 8: 4862–4872, 2008.
139. Huertas JR, Casuso RA, Agustín PH, and Cogliati S. Stay Fit, Stay Young: Mitochondria in Movement: The Role of Exercise in the New Mitochondrial Paradigm. *Oxidative Medicine and Cellular Longevity* 2019: 7058350, 2019.
140. Hughes CS, Foehr S, Garfield DA, Furlong EE, Steinmetz LM, and Krijgsvelde J. Ultrasensitive proteome analysis using paramagnetic bead technology. *Mol Syst Biol* 10: 757, 2014.
141. Hughes CS, Moggridge S, Müller T, Sorensen PH, Morin GB, and Krijgsvelde J. Single-pot, solid-phase-enhanced sample preparation for proteomics experiments. *Nature protocols* 14: 68-85, 2019.
142. Hussey SE, Sharoff CG, Garnham A, Yi Z, Bowen BP, Mandarino LJ, and Hargreaves M. Effect of exercise on the skeletal muscle proteome in patients with type 2 diabetes. *Medicine and science in sports and exercise* 45: 1069-1076, 2013.
143. Iaia FM, Hellsten Y, Nielsen JJ, Fernstrom M, Sahlin K, and Bangsbo J. Four weeks of speed endurance training reduces energy expenditure during exercise and maintains muscle oxidative capacity despite a reduction in training volume. *Journal of applied physiology (Bethesda, Md : 1985)* 106: 73-80, 2009.
144. Ihsan M, Markworth JF, Watson G, Choo HC, Govus A, Pham T, Hickey A, Cameron-Smith D, and Abbiss CR. Regular postexercise cooling enhances mitochondrial biogenesis through AMPK and p38 MAPK in human skeletal muscle. *American journal of physiology Regulatory, integrative and comparative physiology* 309: R286-294, 2015.
145. Ingjer F. Effects of endurance training on muscle fibre ATP-ase activity, capillary supply and mitochondrial content in man. *The Journal of Physiology* 294: 419-432, 1979.

146. Irrcher I, Adhietty PJ, Joseph A-M, Ljubicic V, and Hood DA. Regulation of Mitochondrial Biogenesis in Muscle by Endurance Exercise. *Sports Medicine* 33: 783-793, 2003.
147. Irving BA, Lanza IR, Henderson GC, Rao RR, Spiegelman BM, and Nair KS. Combined Training Enhances Skeletal Muscle Mitochondrial Oxidative Capacity Independent of Age. *J Clin Endocrinol Metab* 100: 1654–1663, 2015.
148. Jackman MR and Willis WT. Characteristics of mitochondria isolated from type I and type IIb skeletal muscle. *American Journal of Physiology-Cell Physiology* 270: C673-C678, 1996.
149. Jacobs IRA, EsbjÖRnsson M, SylvÉN C, Holm I, and Jansson EVA. Sprint training effects on muscle myoglobin, enzymes, fiber types, and blood lactate. *Medicine & Science in Sports & Exercise* 19, 1987.
150. Jacobs R.A. and Lundby C. Mitochondria express enhanced quality as well as quantity in association with aerobic fitness across recreationally active individuals up to elite athletes. *Journal of Applied Physiology* 114: 344–350, 2013.
151. Jaleel A, Short KR, Asmann YW, Klaus KA, Morse DM, Ford GC, and Nair KS. In vivo measurement of synthesis rate of individual skeletal muscle mitochondrial proteins. *American journal of physiology Endocrinology and metabolism* 295: E1255-E1268, 2008.
152. Jamnick NA, Pettitt RW, Granata C, Pyne DB, and Bishop DJ. An Examination and Critique of Current Methods to Determine Exercise Intensity. *Sports Medicine*, 2020.
153. Johnson DT, Harris RA, Blair PV, and Balaban RS. Functional consequences of mitochondrial proteome heterogeneity. *American Journal of Physiology-Cell Physiology* 292: C698-C707, 2007.
154. Johnson ML, Robinson MM, and Nair KS. Skeletal muscle aging and the mitochondrion. *Trends Endocrinol Metab* 24: 247-256, 2013.
155. Johnson WE, Li C, and Rabinovic A. Adjusting batch effects in microarray expression data using empirical Bayes methods. *Biostatistics* 8: 118-127, 2007.

156. Jonckheere AI, Smeitink JAM, and Rodenburg RJT. Mitochondrial ATP synthase: architecture, function and pathology. *J Inherit Metab Dis* 35: 211-225, 2012.
157. Jones AM, Wilkerson DP, and Fulford J. Muscle [phosphocreatine] dynamics following the onset of exercise in humans: the influence of baseline work-rate. *The Journal of physiology* 586: 889-898, 2008.
158. Ju J-s, Jeon S-i, Park J-y, Lee J-y, Lee S-c, Cho K-j, and Jeong J-m. Autophagy plays a role in skeletal muscle mitochondrial biogenesis in an endurance exercise-trained condition. *The Journal of Physiological Sciences* 66: 417-430, 2016.
159. Kallabis S, Abraham L, Müller S, Dzialis V, Türk C, Wiederstein JL, Bock T, Nolte H, Nogara L, Blaauw B, Braun T, and Krüger M. High-throughput proteomics fiber typing (ProFiT) for comprehensive characterization of single skeletal muscle fibers. *Skeletal Muscle* 10: 7, 2020.
160. Karpievitch YV, Polpitiya AD, Anderson GA, Smith RD, and Dabney AR. Liquid Chromatography Mass Spectrometry-Based Proteomics: Biological and Technological Aspects. *Ann Appl Stat* 4: 1797-1823, 2010.
161. Kiessling KH, Piehl K, and Lundquist CG. Effect of Physical Training on Ultrastructural Features in Human Skeletal Muscle. In: *Muscle Metabolism During Exercise: Proceedings of a Karolinska Institutet Symposium held in Stockholm, Sweden, September 6-9, 1970 Honorary guest: E Hohwü Christensen*, edited by Pernow B and Saltin B. Boston, MA: Springer US, 1971, p. 97-101.
162. Kiessling KH, Pilström L, Bylund AC, Saltin B, and Piehl K. Enzyme Activities and Morphometry in Skeletal Muscle of Middle-Aged Men after Training. *Scandinavian journal of clinical and laboratory investigation* 33: 63-69, 1974.
163. Kim JY, Koves TR, Yu GS, Gulick T, Cortright RN, Dohm GL, and Muoio DM. Evidence of a malonyl-CoA-insensitive carnitine palmitoyltransferase I activity in red skeletal muscle. *Am J Physiol Endocrinol Metab* 282: E1014-1022, 2002.
164. Kim SH, Koh JH, Higashida K, Jung SR, Holloszy JO, and Han DH. PGC-1alpha mediates a rapid, exercise-induced downregulation of glycogenolysis in rat skeletal muscle. *J Physiol* 593: 635-643, 2015.

165. Kim YI and Cho JY. Gel-based proteomics in disease research: Is it still valuable? *Biochim Biophys Acta Proteins Proteom* 1867: 9-16, 2019.
166. Kleinert M, Parker BL, Jensen TE, Raun SH, Pham P, Han X, James DE, Richter EA, and Sylow L. Quantitative proteomic characterization of cellular pathways associated with altered insulin sensitivity in skeletal muscle following high-fat diet feeding and exercise training. *Scientific Reports* 8: 10723, 2018.
167. Kocsis T, Baán J, Müller G, Mendler L, Dux L, and Keller-Pintér A. Skeletal muscle cellularity and glycogen distribution in the hypermuscular Compact mice. *Eur J Histochem* 58: 2353-2353, 2014.
168. Konopka AR, Suer MK, Wolff CA, and Harber MP. Markers of human skeletal muscle mitochondrial biogenesis and quality control: effects of age and aerobic exercise training. *J Gerontol A Biol Sci Med Sci* 69: 371-378, 2014.
169. Koves TR, Noland RC, Bates AL, Henes ST, Muoio DM, and Cortright RN. Subsarcolemmal and intermyofibrillar mitochondria play distinct roles in regulating skeletal muscle fatty acid metabolism. *American Journal of Physiology-Cell Physiology* 288: C1074-C1082, 2005.
170. Krieger DA, Tate CA, McMillin-Wood J, and Booth FW. Populations of rat skeletal muscle mitochondria after exercise and immobilization. *Journal of applied physiology: respiratory, environmental and exercise physiology* 48: 23-28, 1980.
171. Kristensen DE, Albers PH, Prats C, Baba O, Birk JB, and Wojtaszewski JF. Human muscle fibre type-specific regulation of AMPK and downstream targets by exercise. *J Physiol* 593: 2053-2069, 2015.
172. Krusemark CJ, Frey BL, Smith LM, and Belshaw PJ. Complete chemical modification of amine and acid functional groups of peptides and small proteins. *Methods in molecular biology (Clifton, NJ)* 753: 77-91, 2011.
173. Kulak NA, Pichler G, Paron I, Nagaraj N, and Mann M. Minimal, encapsulated proteomic-sample processing applied to copy-number estimation in eukaryotic cells. *Nature Methods* 11: 319, 2014.

174. Lang F, Khaghani S, Turk C, Wiederstein JL, Holper S, Piller T, Nogara L, Blaauw B, Gunther S, Muller S, Braun T, and Kruger M. Single Muscle Fiber Proteomics Reveals Distinct Protein Changes in Slow and Fast Fibers during Muscle Atrophy. *J Proteome Res* 17: 3333-3347, 2018.
175. Lappalainen Z, Lappalainen J, Oksala NKJ, Laaksonen DE, Khanna S, Sen CK, and Atalay M. Diabetes impairs exercise training-associated thioredoxin response and glutathione status in rat brain. *Journal of Applied Physiology* 106: 461-467, 2009.
176. Larsen FJ, Schiffer TA, Ørtenblad N, Zinner C, Morales-Alamo D, Willis SJ, Calbet JA, Holmberg H-C, and Boushel R. High-intensity sprint training inhibits mitochondrial respiration through aconitase inactivation. *The FASEB Journal* 30: 417-427, 2016.
177. Larsen S, Nielsen J, Hansen CN, Nielsen LB, Wibrand F, Stride N, Schroder HD, Boushel R, Helge JW, Dela F, and Hey-Mogensen M. Biomarkers of mitochondrial content in skeletal muscle of healthy young human subjects. *J Physiol* 590: 3349-3360, 2012.
178. Laursen PB and Jenkins DG. The scientific basis for high-intensity interval training: optimising training programmes and maximising performance in highly trained endurance athletes. *Sports medicine (Auckland, NZ)* 32: 53-73, 2002.
179. Leonard AP, Cameron RB, Speiser JL, Wolf BJ, Peterson YK, Schnellmann RG, Beeson CC, and Rohrer B. Quantitative analysis of mitochondrial morphology and membrane potential in living cells using high-content imaging, machine learning, and morphological binning. *Biochimica et Biophysica Acta (BBA) - Molecular Cell Research* 1853: 348-360, 2015.
180. Lexell J, Henriksson-Larsen K, and Sjoström M. Distribution of different fibre types in human skeletal muscles. 2. A study of cross-sections of whole m. vastus lateralis. *Acta Physiol Scand* 117: 115-122, 1983.
181. Li H, Han J, Pan J, Liu T, Parker CE, and Borchers CH. Current trends in quantitative proteomics – an update. *Journal of Mass Spectrometry* 52: 319-341, 2017.

182. Li J, Van Vranken JG, Pontano Vaites L, Schweppe DK, Huttlin EL, Etienne C, Nandhikonda P, Viner R, Robitaille AM, Thompson AH, Kuhn K, Pike I, Bomgardner RD, Rogers JC, Gygi SP, and Paulo JA. TMTpro reagents: a set of isobaric labeling mass tags enables simultaneous proteome-wide measurements across 16 samples. *Nature Methods* 17: 399-404, 2020.
183. Lim MY, Paulo JA, and Gygi SP. Evaluating False Transfer Rates from the Match-between-Runs Algorithm with a Two-Proteome Model. *Journal of Proteome Research* 18: 4020-4026, 2019.
184. Lin J, Wu H, Tarr PT, Zhang CY, Wu Z, Boss O, Michael LF, Puigserver P, Isotani E, Olson EN, Lowell BB, Bassel-Duby R, and Spiegelman BM. Transcriptional co-activator PGC-1 alpha drives the formation of slow-twitch muscle fibres. *Nature* 418: 797-801, 2002.
185. Little JP, Gillen JB, Percival ME, Safdar A, Tarnopolsky MA, Punthakee Z, Jung ME, and Gibala MJ. Low-volume high-intensity interval training reduces hyperglycemia and increases muscle mitochondrial capacity in patients with type 2 diabetes. *Journal of applied physiology (Bethesda, Md : 1985)* 111: 1554-1560, 2011.
186. Little JP, Safdar A, Bishop D, Tarnopolsky MA, and Gibala MJ. An acute bout of high-intensity interval training increases the nuclear abundance of PGC-1alpha and activates mitochondrial biogenesis in human skeletal muscle. *American journal of physiology Regulatory, integrative and comparative physiology* 300: R1303-1310, 2011.
187. Little JP, Safdar A, G, Wilkin GP, Tarnopolsky MA, and Gibala MJ. A practical model of low-volume high-intensity interval training induces mitochondrial biogenesis in human skeletal muscle: potential mechanisms *The Journal of Physiology* 588: 1011–1022, 2010.
188. Liu F, Lössl P, Rabbitts BM, Balaban RS, and Heck AJR. The interactome of intact mitochondria by cross-linking mass spectrometry provides evidence for coexisting respiratory supercomplexes. *Molecular & cellular proteomics : MCP* 17: 216-232, 2018.

189. Liu H, Sadygov RG, and Yates JR, 3rd. A model for random sampling and estimation of relative protein abundance in shotgun proteomics. *Analytical chemistry* 76: 4193-4201, 2004.
190. Losón OC, Song Z, Chen H, and Chan DC. Fis1, Mff, MiD49, and MiD51 mediate Drp1 recruitment in mitochondrial fission. *Molecular Biology of the Cell* 24: 659-667, 2013.
191. Luna VM, Daikoku E, and Ono F. "Slow" skeletal muscles across vertebrate species. *Cell Biosci* 5: 62-62, 2015.
192. Lundby C and Jacobs RA. Adaptations of skeletal muscle mitochondria to exercise training. *Experimental physiology* 101: 17-22, 2016.
193. MacInnis MJ and Gibala MJ. Physiological adaptations to interval training and the role of exercise intensity. *J Physiol* 595: 2915-2930, 2017.
194. MacInnis MJ, Zacharewicz E, Martin BJ, Haikalis ME, Skelly LE, Tarnopolsky MA, Murphy RM, and Gibala MJ. Superior mitochondrial adaptations in human skeletal muscle after interval compared to continuous single-leg cycling matched for total work. *The Journal of Physiology* 595: 2955-2968, 2017.
195. Magdeldin S, Enany S, Yoshida Y, Xu B, Zhang Y, Zureena Z, Lokamani I, Yaoita E, and Yamamoto T. Basics and recent advances of two dimensional-polyacrylamide gel electrophoresis. *Clinical Proteomics* 11: 16, 2014.
196. Mann M. Can Proteomics Retire the Western Blot? *Journal of Proteome Research* 7: 3065-3065, 2008.
197. Martin WH, 3rd, Dalsky GP, Hurley BF, Matthews DE, Bier DM, Hagberg JM, Rogers MA, King DS, and Holloszy JO. Effect of endurance training on plasma free fatty acid turnover and oxidation during exercise. *The American journal of physiology* 265: E708-714, 1993.
198. Martínez-Reyes I and Chandel NS. Mitochondrial TCA cycle metabolites control physiology and disease. *Nature Communications* 11: 102, 2020.

199. Marton O, Koltai E, Takeda M, Koch LG, Britton SL, Davies KJA, Boldogh I, and Radak Z. Mitochondrial biogenesis-associated factors underlie the magnitude of response to aerobic endurance training in rats. *Pflugers Archiv : European journal of physiology* 467: 779-788, 2015.
200. Matoba S, Kang JG, Patino WD, Wragg A, Boehm M, Gavrilova O, Hurley PJ, Bunz F, and Hwang PM. p53 regulates mitochondrial respiration. *Science (New York, NY)* 312: 1650-1653, 2006.
201. Maxwell LC, Faulkner JA, and Murphy RA. Relationship among fibre type, myosin ATPase activity and contractile properties. *Histochem J* 14: 981-997, 1982.
202. Mendell LM. The size principle: a rule describing the recruitment of motoneurons. *Journal of Neurophysiology* 93: 3024-3026, 2005.
203. Miller BF and Hamilton KL. A perspective on the determination of mitochondrial biogenesis. *American journal of physiology Endocrinology and metabolism* 302: E496-E499, 2012.
204. Mishra P, Varuzhanyan G, Pham AH, and Chan DC. Mitochondrial Dynamics is a Distinguishing Feature of Skeletal Muscle Fiber Types and Regulates Organellar Compartmentalization. *Cell Metab* 22: 1033-1044, 2015.
205. Mitchell CR, Harris MB, Cordaro AR, and Starnes JW. Effect of body temperature during exercise on skeletal muscle cytochrome c oxidase content. *Journal of applied physiology (Bethesda, Md : 1985)* 93: 526-530, 2002.
206. Mogensen M and Sahlin K. Mitochondrial efficiency in rat skeletal muscle: influence of respiration rate, substrate and muscle type. *Acta Physiol Scand* 185: 229-236, 2005.
207. Mollica JP, Oakhill JS, Lamb GD, and Murphy RM. Are genuine changes in protein expression being overlooked? Reassessing Western blotting. *Analytical biochemistry* 386: 270-275, 2009.
208. Moore TM, Zhou Z, Cohn W, Norheim F, Lin AJ, Kalajian N, Strumwasser AR, Cory K, Whitney K, Ho T, Ho T, Lee JL, Rucker DH, Shirihai O, van der Blik AM,

Whitelegge JP, Seldin MM, Lusic AJ, Lee S, Drevon CA, Mahata SK, Turcotte LP, and Hevener AL. The impact of exercise on mitochondrial dynamics and the role of Drp1 in exercise performance and training adaptations in skeletal muscle. *Molecular Metabolism* 21: 51-67, 2019.

209. Morgan TE, Cobb LA, Short FA, Ross R, and Gunn DR. Effects of Long-Term Exercise on Human Muscle Mitochondria. In: *Muscle Metabolism During Exercise: Proceedings of a Karolinska Institutet Symposium held in Stockholm, Sweden, September 6-9, 1970 Honorary guest: E Hohwü Christensen*, edited by Pernow B and Saltin B. Boston, MA: Springer US, 1971, p. 87-95.

210. Morton JP, Croft L, Bartlett JD, Maclaren DP, Reilly T, Evans L, McArdle A, and Drust B. Reduced carbohydrate availability does not modulate training-induced heat shock protein adaptations but does upregulate oxidative enzyme activity in human skeletal muscle. *Journal of applied physiology (Bethesda, Md : 1985)* 106: 1513-1521, 2009.

211. Morton JP, Maclaren DP, Cable NT, Campbell IT, Evans L, Kayani AC, McArdle A, and Drust B. Trained men display increased basal heat shock protein content of skeletal muscle. *Medicine and science in sports and exercise* 40: 1255-1262, 2008.

212. Müller T, Kalxdorf M, Longuespée R, Kazdal DN, Stenzinger A, and Krijgsveld J. Automated sample preparation with SP3 for low-input clinical proteomics. *Molecular Systems Biology* 16: e9111, 2020.

213. Murach KA, Bagley JR, McLeland KA, Arevalo JA, Ciccone AB, Malyszek KK, Wen Y, and Galpin AJ. Improving human skeletal muscle myosin heavy chain fiber typing efficiency. *J Muscle Res Cell Motil* 37: 1-5, 2016.

214. Murach KA, Dungan CM, Kosmac K, Voigt TB, Tourville TW, Miller MS, Bamman MM, Peterson CA, and Toth MJ. Fiber typing human skeletal muscle with fluorescent immunohistochemistry. *Journal of Applied Physiology* 127: 1632-1639, 2019.

215. Murakami T, Shimomura Y, Fujitsuka N, Nakai N, Sugiyama S, Ozawa T, Sokabe M, Horai S, Tokuyama K, and Suzuki M. Enzymatic and genetic adaptation of soleus

muscle mitochondria to physical training in rats. *American Journal of Physiology-Endocrinology and Metabolism* 267: E388-E395, 1994.

216. Murgia M, , Nagaraj N, Deshmukh AS, Zeiler M, Cancellara P, Moretti I, Reggiani C, Schiaffino S, and Mann M. Single muscle fiber proteomics reveals unexpected mitochondrial specialization. *EMBO Reports* 16: 387-395., 2015.

217. Murgia M, Tan J, Geyer P, Doll S, Mann M, and Klopstock T. Single fiber proteomics of respiratory chain defects in mitochondrial disorders. *bioRxiv*: 421750, 2018.

218. Murgia M, Toniolo L, Nagaraj N, Ciciliot S, Vindigni V, Schiaffino S, Reggiani C, and Mann M. Single Muscle Fiber Proteomics Reveals Fiber-Type- Specific Features of Human Muscle Aging *Cell Reports* 19: 2396–2409, 2017.

219. Murphy RM. Enhanced technique to measure proteins in single segments of human skeletal muscle fibers: fiber-type dependence of AMPK-alpha1 and -beta1. *Journal of applied physiology (Bethesda, Md : 1985)* 110: 820-825, 2011.

220. Murphy RM and Lamb GD. Important considerations for protein analyses using antibody based techniques: down-sizing Western blotting up-sizes outcomes. *The Journal of Physiology* 591: 5823-5831, 2013.

221. Needham DM. RED AND WHITE MUSCLE. *Physiological Reviews* 6: 1-27, 1926.

222. Nielsen J, Gejl KD, Hey-Mogensen M, Holmberg HC, Suetta C, Krstrup P, Elemans CPH, and Ørtenblad N. Plasticity in mitochondrial cristae density allows metabolic capacity modulation in human skeletal muscle. *J Physiol* 595: 2839-2847, 2017.

223. Nookaew I, Svensson PA, Jacobson P, Jernås M, Taube M, Larsson I, Andersson-Assarsson JC, Sjöström L, Froguel P, Walley A, Nielsen J, and Carlsson LM. Adipose tissue resting energy expenditure and expression of genes involved in mitochondrial function are higher in women than in men. *J Clin Endocrinol Metab* 98: E370-378, 2013.

224. Nowinski SM, Van Vranken JG, Dove KK, and Rutter J. Impact of Mitochondrial Fatty Acid Synthesis on Mitochondrial Biogenesis. *Current Biology* 28: R1212-R1219, 2018.
225. Nunnari J and Suomalainen A. Mitochondria: in sickness and in health. *Cell* 148: 1145-1159, 2012.
226. O'Connell JD, Paulo JA, O'Brien JJ, and Gygi SP. Proteome-Wide Evaluation of Two Common Protein Quantification Methods. *Journal of proteome research* 17: 1934-1942, 2018.
227. Ogata T and Yamasaki Y. Ultra-high-resolution scanning electron microscopy of mitochondria and sarcoplasmic reticulum arrangement in human red, white, and intermediate muscle fibers. *Anat Rec* 248: 214-223, 1997.
228. Ohlendieck K. Proteomics of skeletal muscle differentiation, neuromuscular disorders and fiber aging. *Expert review of proteomics* 7: 283-296, 2010.
229. Ohlendieck K. Skeletal muscle proteomics: current approaches, technical challenges and emerging techniques. *Skeletal Muscle* 1: 1-15, 2011.
230. Olesen J, Kiilerich K, and Pilegaard H. PGC-1alpha-mediated adaptations in skeletal muscle. *Pflugers Archiv : European journal of physiology* 460: 153-162, 2010.
231. Olsen JV, Ong S-E, and Mann M. Trypsin Cleaves Exclusively C-terminal to Arginine and Lysine Residues. *Molecular & Cellular Proteomics* 3: 608, 2004.
232. Ørtenblad N, Nielsen J, Boushel R, Söderlund K, Saltin B, and Holmberg H-C. The Muscle Fiber Profiles, Mitochondrial Content, and Enzyme Activities of the Exceptionally Well-Trained Arm and Leg Muscles of Elite Cross-Country Skiers. *Frontiers in physiology* 9: 1031-1031, 2018.
233. Osellame LD, Blacker TS, and Duchen MR. Cellular and molecular mechanisms of mitochondrial function. *Best Practice & Research Clinical Endocrinology & Metabolism* 26: 711-723, 2012.

234. Overmyer KA, Evans CR, Qi NR, Minogue CE, Carson JJ, Chermiside-Scabbo CJ, Koch LG, Britton SL, Pagliarini DJ, Coon JJ, and Burant CF. Maximal Oxidative Capacity during Exercise Is Associated with Skeletal Muscle Fuel Selection and Dynamic Changes in Mitochondrial Protein Acetylation *Cell Metabolism* 21: 468–478, 2015.
235. Padrao AI, Ferreira R, Amado F, Vitorino R, and Duarte JA. Uncovering the exercise-related proteome signature in skeletal muscle. *Proteomics* 16: 816-830, 2016.
236. Padykula HA and Herman E. The specificity of the histochemical method for adenosine triphosphatase. *The journal of histochemistry and cytochemistry : official journal of the Histochemistry Society* 3: 170-195, 1955.
237. Palacios OM, Carmona JJ, Michan S, Chen KY, Manabe Y, Ward JL, 3rd, Goodyear LJ, and Tong Q. Diet and exercise signals regulate SIRT3 and activate AMPK and PGC-1alpha in skeletal muscle. *Aging (Albany NY)* 1: 771-783, 2009.
238. Pappireddi N, Martin L, and Wühr M. A Review on Quantitative Multiplexed Proteomics. *Chembiochem* 20: 1210-1224, 2019.
239. Perry CG, Heigenhauser GJ, Bonen A, and Spriet LL. High-intensity aerobic interval training increases fat and carbohydrate metabolic capacities in human skeletal muscle. *Applied physiology, nutrition, and metabolism = Physiologie appliquee, nutrition et metabolisme* 33: 1112-1123, 2008.
240. Perry CGR and Hawley JA. Molecular Basis of Exercise-Induced Skeletal Muscle Mitochondrial Biogenesis: Historical Advances, Current Knowledge, and Future Challenges. *Cold Spring Harbor perspectives in medicine* 8, 2018.
241. Perry CGR, Kane DA, Herbst EAF, Mukai K, Lark DS, Wright DC, Heigenhauser GJF, Neuffer PD, Spriet LL, and Holloway GP. Mitochondrial creatine kinase activity and phosphate shuttling are acutely regulated by exercise in human skeletal muscle. *The Journal of Physiology* 590: 5475-5486, 2012.
242. Peter JB, Barnard RJ, Edgerton VR, Gillespie CA, and Stempel KE. Metabolic profiles of three fiber types of skeletal muscle in guinea pigs and rabbits. *Biochemistry* 11: 2627-2633, 1972.

243. Petriz BA, Gomes CP, Rocha LAO, Rezende TMB, and Franco OL. Proteomics applied to exercise physiology: A cutting-edge technology. *Journal of Cellular Physiology* 227: 885-898, 2012.
244. Pette D . , Peuker H, and Staron RS. The impact of biochemical methods for single muscle fibre analysis. *Acta Physiol Scand* 1166: 261-277, 1999.
245. Pette D and Staron RS. Cellular and molecular diversities of mammalian skeletal muscle fibers. *Rev Physiol Biochem Pharmacol* 116: 1-76, 1990.
246. Pette D and Staron RS. Myosin isoforms, muscle fiber types, and transitions. *Microsc Res Tech* 50: 500-509, 2000.
247. Picard M, Hepple RT, and Burelle Y. Mitochondrial functional specialization in glycolytic and oxidative muscle fibers: tailoring the organelle for optimal function. *American journal of physiology Cell physiology* 302: C629-641, 2012.
248. Picard M, Wallace DC, and Burelle Y. The rise of mitochondria in medicine. *Mitochondrion* 30: 105-116, 2016.
249. Picard M, White K, and Turnbull DM. Mitochondrial morphology, topology, and membrane interactions in skeletal muscle: a quantitative three-dimensional electron microscopy study. *Journal of applied physiology (Bethesda, Md : 1985)* 114: 161-171, 2013.
250. Pillai-Kastoori L, Heaton S, Shiflett SD, Roberts AC, Solache A, and Schutz-Geschwender AR. Antibody validation for Western blot: By the user, for the user. *The Journal of biological chemistry* 295: 926-939, 2020.
251. Plubell DL, Wilmarth PA, Zhao Y, Fenton AM, Minnier J, Reddy AP, Klimek J, Yang X, David LL, and Pamir N. Extended Multiplexing of Tandem Mass Tags (TMT) Labeling Reveals Age and High Fat Diet Specific Proteome Changes in Mouse Epididymal Adipose Tissue. *Mol Cell Proteomics* 16: 873-890, 2017.
252. Poole DC and Mathieu-Costello O. Relationship between fiber capillarization and mitochondrial volume density in control and trained rat soleus and plantaris muscles. *Microcirculation* 3: 175-186, 1996.

253. PROTIFI. S-Trap Micro spin column digestion protocol: PROTIFI.
254. Puigserver P and Spiegelman BM. Peroxisome proliferator-activated receptor-gamma coactivator 1 alpha (PGC-1 alpha): transcriptional coactivator and metabolic regulator. *Endocrine reviews* 24: 78-90, 2003.
255. Purdom T, Kravitz L, Dokladny K, and Mermier C. Understanding the factors that effect maximal fat oxidation. *J Int Soc Sports Nutr* 15: 3-3, 2018.
256. Puype J, Van Proeyen K, Raymackers JM, Deldicque L, and Hespel P. Sprint interval training in hypoxia stimulates glycolytic enzyme activity. *Medicine and science in sports and exercise* 45: 2166-2174, 2013.
257. Rappsilber J, Ishihama Y, and Mann M. Stop and go extraction tips for matrix-assisted laser desorption/ionization, nanoelectrospray, and LC/MS sample pretreatment in proteomics. *Analytical chemistry* 75: 663-670, 2003.
258. Rath S, Sharma R, Gupta R, Ast T, Chan C, Durham TJ, Goodman RP, Grabarek Z, Haas ME, Hung WHW, Joshi PR, Jourdain AA, Kim SH, Kotrys AV, Lam SS, McCoy JG, Meisel JD, Miranda M, Panda A, Patgiri A, Rogers R, Sadre S, Shah H, Skinner OS, To T-L, Walker Melissa A, Wang H, Ward PS, Wengrod J, Yuan C-C, Calvo SE, and Mootha VK. MitoCarta3.0: an updated mitochondrial proteome now with sub-organelle localization and pathway annotations. *Nucleic acids research*, 2020.
259. Rauniyar N and Yates JR, 3rd. Isobaric labeling-based relative quantification in shotgun proteomics. *Journal of proteome research* 13: 5293-5309, 2014.
260. Reichmann H and Pette D. A comparative microphotometric study of succinate dehydrogenase activity levels in type I, IIA and IIB fibres of mammalian and human muscles. *Histochemistry* 74: 27-41, 1982.
261. Rivero J-LL, Talmadge RJ, and Edgerton VR. Fibre size and metabolic properties of myosin heavy chain-based fibre types in rat skeletal muscle. *Journal of Muscle Research & Cell Motility* 19: 733-742, 1998.

262. Rivero JL, Talmadge RJ, and Edgerton VR. Correlation between myofibrillar ATPase activity and myosin heavy chain composition in equine skeletal muscle and the influence of training. *Anat Rec* 246: 195-207, 1996.
263. Rivero JL, Talmadge RJ, and Edgerton VR. Fibre size and metabolic properties of myosin heavy chain-based fibre types in rat skeletal muscle. *J Muscle Res Cell Motil* 19: 733-742, 1998.
264. Robinson MD and Oshlack A. A scaling normalization method for differential expression analysis of RNA-seq data. *Genome Biology* 11: R25, 2010.
265. Robinson MM, Dasari S, Konopka AR, Johnson ML, Manjunatha S, Esponda RR, Carter RE, Lanza IR, and Nair KS. Enhanced Protein Translation Underlies Improved Metabolic and Physical Adaptations to Different Exercise Training Modes in Young and Old Humans. *Cell Metab* 25: 581-592, 2017.
266. Rooyackers OE, Adey DB, Ades PA, and Nair KS. Effect of age on in vivo rates of mitochondrial protein synthesis in human skeletal muscle. *Proc Natl Acad Sci U S A* 93: 15364-15369, 1996.
267. Rossi AE, Boncompagni S, and Dirksen RT. Sarcoplasmic reticulum-mitochondrial symbiosis: bidirectional signaling in skeletal muscle. *Exercise and sport sciences reviews* 37: 29-35, 2009.
268. Rossiter HB, Ward SA, Kowalchuk JM, Howe FA, Griffiths JR, and Whipp BJ. Dynamic asymmetry of phosphocreatine concentration and O<sub>2</sub> uptake between the on- and off-transients of moderate- and high-intensity exercise in humans. *J Physiol* 541: 991-1002, 2002.
269. Roy RR, Pierotti DJ, Garfinkel A, Zhong H, Baldwin KM, and Edgerton VR. Persistence of motor unit and muscle fiber types in the presence of inactivity. *The Journal of experimental biology* 211: 1041-1049, 2008.
270. Ruiz-Romero C and Blanco FJ. Mitochondrial proteomics and its application in biomedical research. *Molecular bioSystems* 5: 1130-1142, 2009.

271. Ryan MT and Hoogenraad NJ. Mitochondrial-nuclear communications. *Annual review of biochemistry* 76: 701-722, 2007.
272. Safdar A, Little JP, Stokl AJ, Hettinga BP, Akhtar M, and Tarnopolsky MA. Exercise increases mitochondrial PGC-1alpha content and promotes nuclear-mitochondrial cross-talk to coordinate mitochondrial biogenesis. *The Journal of biological chemistry* 286: 10605-10617, 2011.
273. Sale DG. Influence of exercise and training on motor unit activation. *Exercise and sport sciences reviews* 15: 95-151, 1987.
274. Saleem A, Adihetty PJ, and Hood DA. Role of p53 in mitochondrial biogenesis and apoptosis in skeletal muscle. *Physiological genomics* 37: 58-66, 2009.
275. Saleem A, Carter HN, Iqbal S, and Hood DA. Role of p53 within the regulatory network controlling muscle mitochondrial biogenesis. *Exercise and sport sciences reviews* 39: 199-205, 2011.
276. Samelman TR, Shiry LJ, and Cameron DF. Endurance training increases the expression of mitochondrial and nuclear encoded cytochrome c oxidase subunits and heat shock proteins in rat skeletal muscle. *Eur J Appl Physiol* 83: 22-27, 2000.
277. Saner NJ, Bishop DJ, and Bartlett JD. Is exercise a viable therapeutic intervention to mitigate mitochondrial dysfunction and insulin resistance induced by sleep loss? *Sleep medicine reviews* 37: 60-68, 2018.
278. Saveliev S, Bratz M, Zubarev R, Szapacs M, Budamgunta H, and Urh M. Trypsin/Lys-C protease mix for enhanced protein mass spectrometry analysis. *Nature Methods* 10: i-ii, 2013.
279. Scalzo RL, Peltonen GL, Binns SE, Shankaran M, Giordano GR, Hartley DA, Klochak AL, Lonac MC, Paris HL, Szallar SE, Wood LM, Peelor FF, 3rd, Holmes WE, Hellerstein MK, Bell C, Hamilton KL, and Miller BF. Greater muscle protein synthesis and mitochondrial biogenesis in males compared with females during sprint interval training. *Faseb j* 28: 2705-2714, 2014.

280. Scarpulla RC. Metabolic control of mitochondrial biogenesis through the PGC-1 family regulatory network. *Biochim Biophys Acta* 1813: 1269-1278, 2011.
281. Schiaffino S. Fibre types in skeletal muscle: a personal account. *Acta Physiologica* 199: 451–463, 2010.
282. Schiaffino S, Hanzlíková V, and Pierobon S. Relations between structure and function in rat skeletal muscle fibers. *The Journal of cell biology* 47: 107-119, 1970.
283. Schiaffino S and Reggiani C. Fiber Types in Mammalian Skeletal Muscles. *Physiol Rev* 91: 1447–1531, 2011.
284. Schiaffino S, Reggiani C, Kostrominova TY, Mann M, and Murgia M. Mitochondrial specialization revealed by single muscle fiber proteomics: focus on the Krebs cycle *Scandinavian Journal of Medicine and Science in Sports* 2015: 25 (Suppl 4): 41–48doi: 101111/sms12606 25: 41-48, 2015.
285. Scott W, Stevens J, and Binder–Macleod SA. Human Skeletal Muscle Fiber Type Classifications. *Physical Therapy* 81: 1810-1816, 2001.
286. Scribbans TD, Edgett BA, Bonafiglia JT, Baechler BL, Quadrilatero J, and Gurd BJ. A systematic upregulation of nuclear and mitochondrial genes is not present in the initial postexercise recovery period in human skeletal muscle. *Applied physiology, nutrition, and metabolism = Physiologie appliquee, nutrition et metabolisme* 42: 571-578, 2017.
287. Shannon P, Markiel A, Ozier O, Baliga NS, Wang JT, Ramage D, Amin N, Schwikowski B, and Ideker T. Cytoscape: a software environment for integrated models of biomolecular interaction networks. *Genome Res* 13: 2498-2504, 2003.
288. Sharma LK, Lu J, and Bai Y. Mitochondrial respiratory complex I: structure, function and implication in human diseases. *Curr Med Chem* 16: 1266-1277, 2009.
289. Shaw CS, Swinton C, Morales-Scholz MG, McRae NL, Erftemeyer T, Aldous A, Murphy RM, and Howlett KF. The impact of exercise training status on the fibre type specific abundance of proteins regulating intramuscular lipid metabolism. *Journal of Applied Physiology*, 2020.

290. Sielaff M, Kuharev J, Bohn T, Hahlbrock J, Bopp T, Tenzer S, and Distler U. Evaluation of FASP, SP3, and iST Protocols for Proteomic Sample Preparation in the Low Microgram Range. *Journal of Proteome Research* 16: 4060-4072, 2017.
291. Signes A and Fernandez-Vizarra E. Assembly of mammalian oxidative phosphorylation complexes I-V and supercomplexes. *Essays in biochemistry* 62: 255-270, 2018.
292. Skelly LE and Gillen JB. Finding the metabolic stress 'sweet spot': implications for sprint interval training-induced muscle remodelling. *The Journal of physiology* 596: 4573-4574, 2018.
293. Smith AC, Blackshaw JA, and Robinson AJ. MitoMiner: a data warehouse for mitochondrial proteomics data. *Nucleic acids research* 40: D1160-1167, 2012.
294. Smith AC and Robinson AJ. MitoMiner, an integrated database for the storage and analysis of mitochondrial proteomics data. *Mol Cell Proteomics* 8: 1324-1337, 2009.
295. Smyth GK. limma: Linear Models for Microarray Data. In: *Bioinformatics and Computational Biology Solutions Using R and Bioconductor*, edited by Gentleman R, Carey VJ, Huber W, Irizarry RA and Dudoit S. New York, NY: Springer New York, 2005, p. 397-420.
296. Staron RS. Correlation between myofibrillar ATPase activity and myosin heavy chain composition in single human muscle fibers. *Histochemistry* 96: 21-24, 1991.
297. Staron RS. Human skeletal muscle fiber types: delineation, development, and distribution. *Can J Appl Physiol* 22: 307-327, 1997.
298. Staron RS, Gohlsch B, and Pette D. Myosin polymorphism in single fibers of chronically stimulated rabbit fast-twitch muscle. *Pflügers Archiv* 408: 444-450, 1987.
299. Staron RS, Hagerman FC, Hikida RS, Murray TF, Hostler DP, Crill MT, Ragg KE, and Toma K. Fiber type composition of the vastus lateralis muscle of young men and women. *The journal of histochemistry and cytochemistry : official journal of the Histochemistry Society* 48: 623-629, 2000.

300. Staron RS and Hikida RS. Histochemical, biochemical, and ultrastructural analyses of single human muscle fibers, with special reference to the C-fiber population. *The journal of histochemistry and cytochemistry : official journal of the Histochemistry Society* 40: 563-568, 1992.
301. Stepto NK, Benziane B, Wadley GD, Chibalin AV, Canny BJ, Eynon N, and McConell GK. Short-term intensified cycle training alters acute and chronic responses of PGC1alpha and Cytochrome C oxidase IV to exercise in human skeletal muscle. *PLoS One* 7: e53080, 2012.
302. Stevanović J, Beleza J, Coxito P, Ascensão A, and Magalhães J. Physical exercise and liver “fitness”: Role of mitochondrial function and epigenetics-related mechanisms in non-alcoholic fatty liver disease. *Molecular Metabolism* 32: 1-14, 2020.
303. Stierwalt HD, Ehrlicher SE, Robinson MM, and Newsom SA. Diet and Exercise Training Influence Skeletal Muscle Long-Chain acyl-CoA Synthetases. *Medicine and science in sports and exercise* 52: 569-576, 2020.
304. Stöggl TL and Sperlich B. The training intensity distribution among well-trained and elite endurance athletes. *Frontiers in Physiology* 6: 295, 2015.
305. Stroud DA, Surgenor EE, Formosa LE, Reljic B, Frazier AE, Dibley MG, Osellame LD, Stait T, Beilharz TH, Thorburn DR, Salim A, and Ryan MT. Accessory subunits are integral for assembly and function of human mitochondrial complex I. *Nature* 538: 123-126, 2016.
306. Supek F, Bošnjak M, Škunca N, and Šmuc T. REVIGO summarizes and visualizes long lists of gene ontology terms. *PLoS One* 6: e21800, 2011.
307. Sureda A, Ferrer MD, Tauler P, Romaguera D, Drobic F, Pujol P, Tur JA, and Pons A. Effects of exercise intensity on lymphocyte H<sub>2</sub>O<sub>2</sub> production and antioxidant defences in soccer players. *British Journal of Sports Medicine* 43: 186, 2009.
308. Suttapitugsakul S, Xiao H, Smeekens J, and Wu R. Evaluation and optimization of reduction and alkylation methods to maximize peptide identification with MS-based proteomics. *Molecular bioSystems* 13: 2574-2582, 2017.

309. Swaney DL, Wenger CD, and Coon JJ. Value of using multiple proteases for large-scale mass spectrometry-based proteomics. *Journal of proteome research* 9: 1323-1329, 2010.
310. Takahashi M and Hood DA. Protein import into subsarcolemmal and intermyofibrillar skeletal muscle mitochondria. Differential import regulation in distinct subcellular regions. *The Journal of biological chemistry* 271: 27285-27291, 1996.
311. Talanian JL, Holloway GP, Snook LA, Heigenhauser GJ, Bonen A, and Spriet LL. Exercise training increases sarcolemmal and mitochondrial fatty acid transport proteins in human skeletal muscle. *Am J Physiol Endocrinol Metab* 299: E180-188, 2010.
312. Tan R, Nederveen JP, Gillen JB, Joannis S, Parise G, Tarnopolsky MA, and Gibala MJ. Skeletal muscle fiber-type-specific changes in markers of capillary and mitochondrial content after low-volume interval training in overweight women. *Physiological reports* 6, 2018.
313. Tanner CB, Madsen SR, Hallowell DM, Goring DMJ, Moore TM, Hardman SE, Heninger MR, Atwood DR, and Thomson DM. Mitochondrial and performance adaptations to exercise training in mice lacking skeletal muscle LKB1. *American journal of physiology Endocrinology and metabolism* 305: E1018-E1029, 2013.
314. Taylor EB, Lamb JD, Hurst RW, Chesser DG, Ellingson WJ, Greenwood LJ, Porter BB, Herway ST, and Winder WW. Endurance training increases skeletal muscle LKB1 and PGC-1 $\alpha$  protein abundance: effects of time and intensity. *Am J Physiol Endocrinol Metab* 289: E960-968, 2005.
315. Terada S, Tabata I, and Higuchi M. Effect of high-intensity intermittent swimming training on fatty acid oxidation enzyme activity in rat skeletal muscle. *Jpn J Physiol* 54: 47-52, 2004.
316. Thomas PD, Campbell MJ, Kejariwal A, Mi H, Karlak B, Daverman R, Diemer K, Muruganujan A, and Narechania A. PANTHER: a library of protein families and subfamilies indexed by function. *Genome research* 13: 2129-2141, 2003.
317. Thompson A, Schäfer J, Kuhn K, Kienle S, Schwarz J, Schmidt G, Neumann T, Johnstone R, Mohammed AK, and Hamon C. Tandem mass tags: a novel quantification

strategy for comparative analysis of complex protein mixtures by MS/MS. *Analytical chemistry* 75: 1895-1904, 2003.

318. Tobias IS, Lazauskas KK, Arevalo JA, Bagley JR, Brown LE, and Galpin AJ. Fiber type-specific analysis of AMPK isoforms in human skeletal muscle: advancement in methods via capillary nanoimmunoassay. *Journal of applied physiology (Bethesda, Md : 1985)* 124: 840-849, 2018.

319. Trappe S, Gallagher P, Harber M, Carrithers J, Fluckey J, and Trappe T. Single muscle fibre contractile properties in young and old men and women. *The Journal of physiology* 552: 47-58, 2003.

320. Ubaida-Mohien C, Gonzalez-Freire M, Lyashkov A, Moaddel R, Chia CW, Simonsick EM, Sen R, and Ferrucci L. Physical Activity Associated Proteomics of Skeletal Muscle: Being Physically Active in Daily Life May Protect Skeletal Muscle From Aging. *Front Physiol* 10: 312, 2019.

321. Vaisar T. Thematic review series: proteomics. Proteomic analysis of lipid-protein complexes. *J Lipid Res* 50: 781-786, 2009.

322. Vanhatalo A, Black MI, DiMenna FJ, Blackwell JR, Schmidt JF, Thompson C, Wylie LJ, Mohr M, Bangsbo J, Krstrup P, and Jones AM. The mechanistic bases of the power-time relationship: muscle metabolic responses and relationships to muscle fibre type. *J Physiol* 594: 4407-4423, 2016.

323. Ventura-Clapier R, Moulin M, Piquereau J, Lemaire C, Mericskay M, Veksler V, and Garnier A. Mitochondria: a central target for sex differences in pathologies. *Clin Sci (Lond)* 131: 803-822, 2017.

324. Vilela TC, Effting PS, dos Santos Pedroso G, Farias H, Paganini L, Rebelo Sorato H, Nesi RT, de Andrade VM, and de Pinho RA. Aerobic and strength training induce changes in oxidative stress parameters and elicit modifications of various cellular components in skeletal muscle of aged rats. *Experimental Gerontology* 106: 21-27, 2018.

325. Viswanathan S, Unlu M, and Minden JS. Two-dimensional difference gel electrophoresis. *Nature protocols* 1: 1351-1358, 2006.

326. Vollestad NK and Blom PC. Effect of varying exercise intensity on glycogen depletion in human muscle fibres. *Acta Physiol Scand* 125: 395-405, 1985.
327. Vousden KH and Ryan KM. p53 and metabolism. *Nature Reviews Cancer* 9: 691, 2009.
328. Wallace DC. Mitochondrial diseases in man and mouse. *Science (New York, NY)* 283: 1482-1488, 1999.
329. Walsh B, Tonkonogi M, Söderlund K, Hultman E, Saks V, and Sahlin K. The role of phosphorylcreatine and creatine in the regulation of mitochondrial respiration in human skeletal muscle. *The Journal of physiology* 537: 971-978, 2001.
330. Wiśniewski JR, Zougman A, Nagaraj N, and Mann M. Universal sample preparation method for proteome analysis. *Nature Methods* 6: 359, 2009.
331. Wollweber F, von der Malsburg K, and van der Laan M. Mitochondrial contact site and cristae organizing system: A central player in membrane shaping and crosstalk. *Biochimica et Biophysica Acta (BBA) - Molecular Cell Research* 1864: 1481-1489, 2017.
332. Wright DC, Geiger PC, Han DH, Jones TE, and Holloszy JO. Calcium induces increases in peroxisome proliferator-activated receptor gamma coactivator-1alpha and mitochondrial biogenesis by a pathway leading to p38 mitogen-activated protein kinase activation. *The Journal of biological chemistry* 282: 18793-18799, 2007.
333. Wright DC, Han DH, Garcia-Roves PM, Geiger PC, Jones TE, and Holloszy JO. Exercise-induced mitochondrial biogenesis begins before the increase in muscle PGC-1alpha expression. *The Journal of biological chemistry* 282: 194-199, 2007.
334. Wu Z, Puigserver P, Andersson U, Zhang C, Adelmant G, Mootha V, Troy A, Cinti S, Lowell B, Scarpulla RC, and Spiegelman BM. Mechanisms controlling mitochondrial biogenesis and respiration through the thermogenic coactivator PGC-1. *Cell* 98: 115-124, 1999.
335. Wyckelsma VL, Levinger I, McKenna MJ, Formosa LE, Ryan MT, Petersen AC, Anderson MJ, and Murphy RM. Preservation of skeletal muscle mitochondrial content in

older adults: relationship between mitochondria, fibre type and high-intensity exercise training. *J Physiol* 595: 3345-3359, 2017.

336. Wyckelsma VL, Levinger I, Murphy RM, Petersen AC, Perry BD, Hedges CP, Anderson MJ, and McKenna MJ. Intense interval training in healthy older adults increases skeletal muscle [(3)H]ouabain-binding site content and elevates Na(+),K(+)-ATPase  $\alpha$ (2) isoform abundance in Type II fibers. *Physiological reports* 5: e13219, 2017.

337. Wyckelsma VL, McKenna MJ, Serpiello FR, Lamboleay CR, Aughey RJ, Stepto NK, Bishop DJ, and Murphy RM. Single-fiber expression and fiber-specific adaptability to short-term intense exercise training of Na<sup>+</sup>-K<sup>+</sup>-ATPase  $\alpha$ - and  $\beta$ -isoforms in human skeletal muscle. *Journal of Applied Physiology* 118: 699-706, 2015.

338. Yamaguchi W, Fujimoto E, Higuchi M, and Tabata I. A DIGE proteomic analysis for high-intensity exercise-trained rat skeletal muscle. *Journal of biochemistry* 148: 327-333, 2010.

339. Ydfors M, Hughes MC, Laham R, Schlattner U, Norrbom J, and Perry CGR. Modelling in vivo creatine/phosphocreatine in vitro reveals divergent adaptations in human muscle mitochondrial respiratory control by ADP after acute and chronic exercise. *The Journal of Physiology* 594: 3127-3140, 2016.

340. Yokokawa T, Kido K, Suga T, Isaka T, Hayashi T, and Fujita S. Exercise-induced mitochondrial biogenesis coincides with the expression of mitochondrial translation factors in murine skeletal muscle. *Physiological reports* 6: e13893-e13893, 2018.

341. Zhang L and Elias JE. Relative Protein Quantification Using Tandem Mass Tag Mass Spectrometry. In: *Proteomics: Methods and Protocols*, edited by Comai L, Katz JE and Mallick P. New York, NY: Springer New York, 2017, p. 185-198.

342. Zhao DS, Gregorich ZR, and Ge Y. High throughput screening of disulfide-containing proteins in a complex mixture. *Proteomics* 13: 3256-3260, 2013.

343. Zierath JR and Wallberg-Henriksson H. Looking Ahead Perspective: Where Will the Future of Exercise Biology Take Us? *Cell Metab* 22: 25-30, 2015.

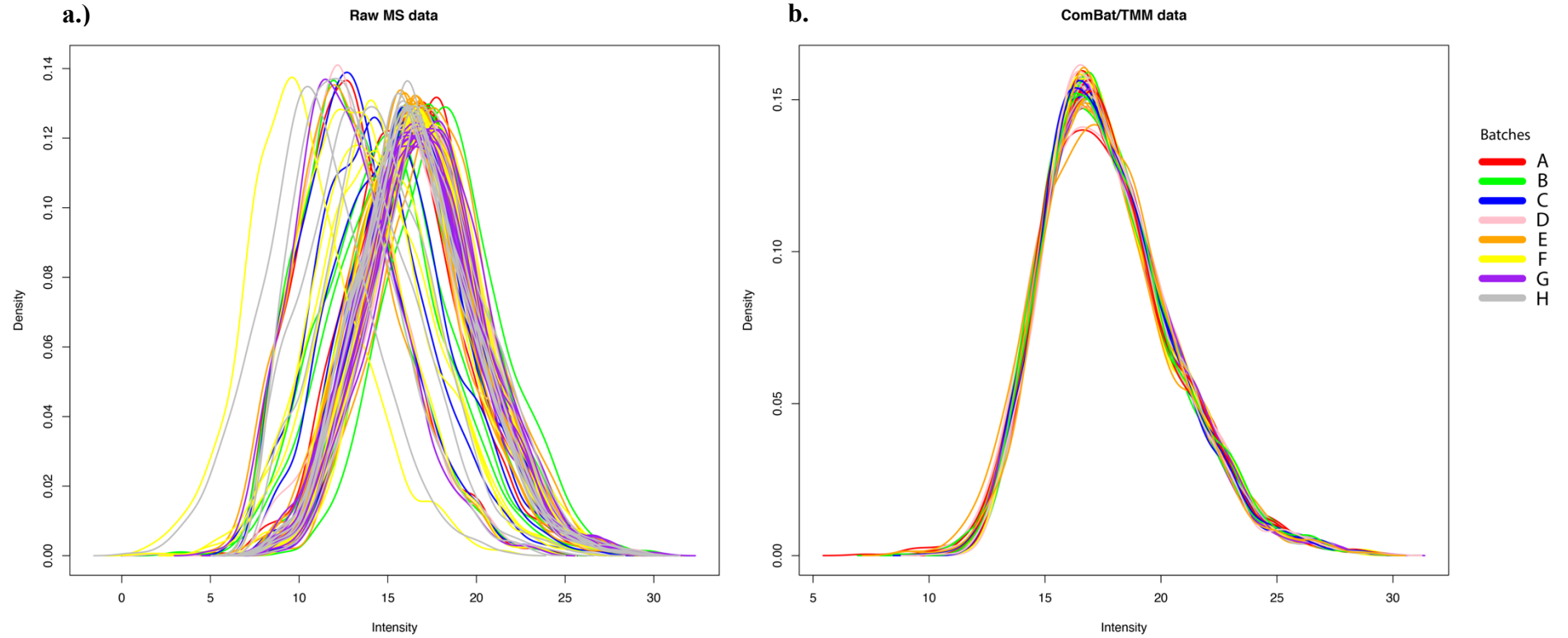
344. Zougman A, Selby PJ, and Banks RE. Suspension trapping (STrap) sample preparation method for bottom-up proteomics analysis. *PROTEOMICS* 14: 1006-1000, 2014.
345. Zubarev RA and Makarov A. Orbitrap Mass Spectrometry. *Analytical chemistry* 85: 5288-5296, 2013.

## **Appendices**

### Appendix 1 – Participant Characteristics and Fibre Types

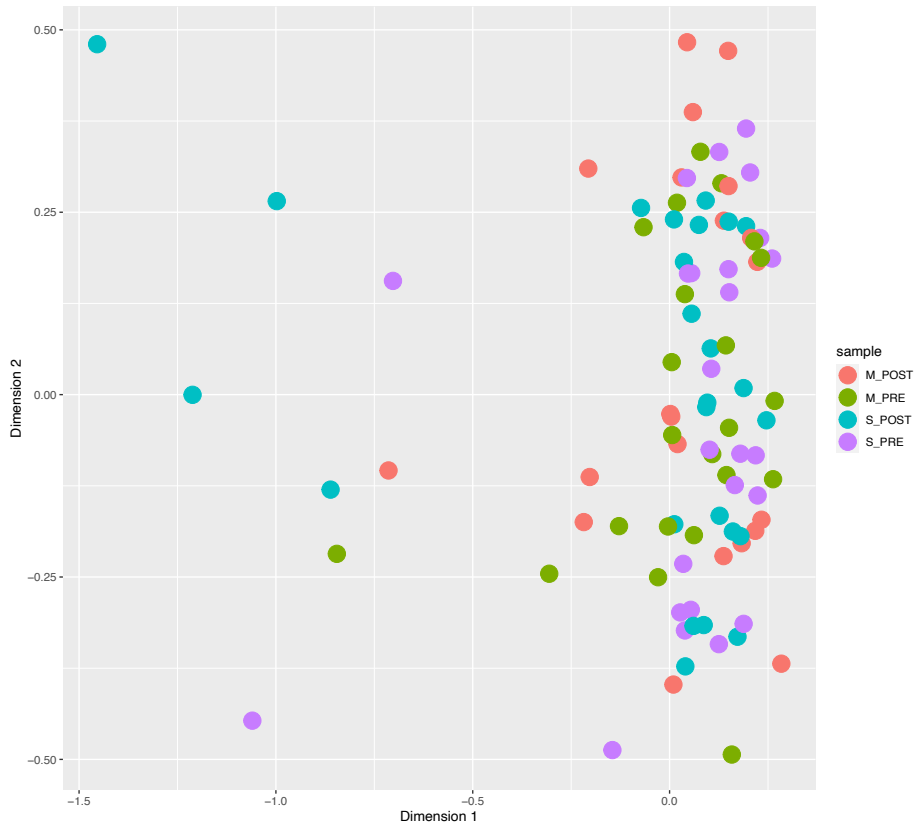
	GROUP	PRE				POST				FIBRE TYPE			
		W <sub>peak</sub>	W/kg	kg	VO <sub>2max</sub>	W <sub>peak</sub>	W/kg	kg	VO <sub>2max</sub>	1 - Type I	1 - Type II	6 - Type I	6 - Type II
1CB	SIT	320	4.27	75	64.21	352	4.76	74	61.85	16	20	21	16
3JS	MICT	320	4.00	80	53.88	368	4.78	77	58.78	14	23	11	32
4JA	SIT	284	3.49	81.4	45.00	294.5	3.57	82.4	43.38	12	21	10	26
5AF	MICT	197	3.03	65	48.21	235	3.65	64.3	51.39	13	20	10	30
6UP	MICT	312.5	4.71	66.4	58.43	330	4.95	66.6	67.63	27	11	22	18
7SL	MICT	297	4.38	67.75	55.44	306	4.65	65.8	55.26	20	20	23	12
8PF	SIT	330	4.95	66.7	52.69	371	5.38	69	58.17	13	26	15	23
10EC	SIT	363	5.24	69.3	63.27	365.5	5.18	70.6	67.68	17	22	18	20
11CP	SIT	333	3.53	94.3	54.38	365	4.05	90.1	56.54	14	23	12	28
13EP	MICT	371	4.25	87.3	53.83	385	4.43	87	53.98	20	20	21	19
15RR	SIT	369	4.85	76.1	54.07	366	4.69	78	49.11	14	25	18	14
16JB	MICT	338	5.20	65	63.60	371	5.70	65.1	61.12	18	14	22	15
17AA	SIT	270	4.05	66.7	46.85	300	4.55	66	47.24	6	13	21	19
18RI	SIT	319	3.84	83.1	48.76	310	3.88	80	47.22	19	13	19	19
19BC	MICT	285	3.03	94.2	36.93	330	3.51	94.1	40.27	9	28	18	21
20JW	SIT	270	3.40	79.5	45.93	300	3.66	81.94	54.42	16	25	19	21
21LC	MICT	320	4.24	75.5	53.82	356	4.73	75.34	54.82	13	27	19	21
22TJ	MICT	270	3.91	69	49.93	285	4.10	69.48	46.61	14	26	8	32
23IE	SIT	484	5.69	85	56.39	495	5.84	84.7	59.12	25	15	18	22
24SC	SIT	198	3.60	55	42.57	213	3.76	56.58	44.41	20	14	21	17
25AC	SIT	300	3.96	75.8	46.09	330	4.32	76.38	47.80	33	7	25	15
26JE	MICT	330	4.10	80.5	47.38	363	4.51	80.5	48.20	18	22	16	24
27JD	MICT	270	4.21	64.2	50.57	309	4.80	64.4	52.21	16	24	18	22
28NS	MICT	415	4.45	93.3						25	15		

## Appendix 2 - Normalisation



**Normalisation** - Distribution density plots visualising the expression values for the batches both **a.)** raw data before normalisation and **b.)** after sample loading (SL), ComBat and trimmed mean of M values (TMM) normalisation have been completed.

### Appendix 3 – Training Type Variation



Multidimensional scaling (MDS) plot showing variation among samples based on training type (M – MICT, S- SIT), for pre and post training. Each point represents a participant sample, and the distance between the points correlates to the dissimilarity between the samples. The plot highlights the training types and illustrates no distinct clusters between MICT & SIT.

## Appendix 4 – Differentially Expressed Proteins based on LIMMA analysis

### Differentially Expressed Proteins Annotated in MICT POST – Type I compared to Type II Fibres

\*Known and predicted mitochondrial proteins are highlighted in red

Description	SYMBOL	logFC	AveExpr	P.Value	adj.P.Val
troponin T1, slow skeletal type	TNNT1	1.957307	23.18153	2.73E-10	5.91E-08
myozenin 2	MYOZ2	1.924706	20.97949	3.76E-06	1.97E-04
myosin heavy chain 7	MYH7	1.868053	27.78824	1.67E-10	4.99E-08
myosin light chain 3	MYL3	1.803415	25.33432	1.27E-08	1.28E-06
myosin light chain 2	MYL2	1.758478	25.67884	1.97E-10	4.99E-08
ATPase sarcoplasmic/endoplasmic reticulum Ca <sup>2+</sup> transporting 2 PDZ and LIM domain 1	ATP2A2	1.693755	22.32439	7.15E-09	7.74E-07
dihydropyrimidinase like 3	PDLIM1	1.65833	19.805	3.78E-08	3.19E-06
lactate dehydrogenase B	DPYSL3	1.325757	19.35748	2.65E-09	3.97E-07
argininosuccinate synthase 1	<b>LDHB</b>	1.137575	20.96691	1.56E-04	4.31E-03
calsequestrin 2	<b>ASS1</b>	1.103258	17.13309	8.46E-04	1.71E-02
transglutaminase 2	CASQ2	1.049838	21.3872	4.21E-05	1.48E-03
cytochrome b5 reductase 1	TGM2	0.968655	16.67703	2.28E-04	5.87E-03
glutamic--pyruvic transaminase 2	<b>CYB5R1</b>	0.963864	21.19349	2.14E-06	1.25E-04
acyl-CoA synthetase short-chain family member 1	<b>GPT2</b>	0.96177	14.25543	4.49E-05	1.55E-03
isopentenyl-diphosphate delta isomerase 2	<b>ACSS1</b>	0.956827	16.46071	4.21E-05	1.48E-03
tropomyosin 3	IDI2	0.922736	18.41265	2.84E-03	4.44E-02
monoamine oxidase B	TPM3	0.77359	26.46363	2.54E-03	4.13E-02
electron transfer flavoprotein beta subunit	<b>MAOB</b>	0.736942	19.1476	9.39E-05	2.90E-03
cytochrome b5 reductase 1	<b>ETFB</b>	0.734874	20.99639	1.96E-04	5.30E-03
ankyrin repeat domain 2	<b>CYB5R3</b>	0.690853	17.79281	2.60E-04	6.47E-03
thymopoietin	ANKRD2	0.675159	21.79186	2.45E-03	4.08E-02
aldehyde dehydrogenase 7 family member A1	TMPO	0.622707	14.8017	2.04E-03	3.60E-02
hydroxyacyl-CoA dehydrogenase/3-ketoacyl-CoA thiolase/enoyl-CoA hydratase	<b>ALDH7A1</b>	0.611049	18.17868	3.11E-03	4.76E-02
myotilin	<b>HADHA</b>	0.581203	23.53946	2.97E-05	1.16E-03
crystallin alpha B	MYOT	0.57911	22.69717	2.07E-04	5.49E-03
DnaJ heat shock protein family myomesin 3	<b>CRYAB</b>	0.546024	23.09548	4.58E-04	1.01E-02
kelch like family member 40	DNAJA4	0.540162	17.69229	1.52E-04	4.31E-03
EH domain containing 2	MYOM3	0.539528	22.16595	7.32E-04	1.50E-02
carnitine O-acetyltransferase	KLHL40	0.536497	18.40065	2.78E-03	4.40E-02
thiosulfate sulfurtransferase	EHD2	0.528316	18.72471	2.21E-03	3.74E-02
enoyl-CoA hydratase 1	<b>CRAT</b>	0.510211	21.37039	8.82E-05	2.85E-03
	<b>TST</b>	0.50706	18.78854	1.16E-03	2.17E-02
	<b>ECH1</b>	0.496938	20.60774	3.25E-03	4.93E-02

hydroxyacyl-CoA dehydrogenase/3-ketoacyl-CoA thiolase/enoyl-CoA hydratase	HADHB	0.484324	22.73727	1.22E-03	2.25E-02
enoyl-CoA delta isomerase 2	ECI2	0.4837	20.33485	1.03E-03	1.97E-02
aldehyde dehydrogenase 1 family member A1	ALDH1A1	0.431194	20.63843	3.04E-04	7.44E-03
voltage dependent anion channel 1	VDAC1	0.40215	22.59442	2.47E-03	4.08E-02
tyrosine 3-monooxygenase/tryptophan 5-monooxygenase activation protein zeta	YWHAZ	0.348561	19.22855	1.21E-04	3.59E-03
Parkinsonism associated deglycase	PARK7	-0.2941	22.39147	1.94E-03	3.46E-02
replication protein A3	RPA3	-0.32242	14.70287	3.07E-03	4.75E-02
creatine kinase, M-type	CKM	-0.32248	26.9748	3.36E-04	8.07E-03
calcium binding protein 39	CAB39	-0.39727	18.32842	3.43E-04	8.13E-03
nucleosome assembly protein 1 like 4	NAP1L4	-0.43774	19.01536	8.49E-06	4.02E-04
triosephosphate isomerase 1	TPI1	-0.44452	25.06695	2.56E-04	6.47E-03
amylase, alpha-1, 6-glucosidase, 4-alpha-glucanotransferase	AGL	-0.4525	23.03362	1.02E-03	1.97E-02
protein phosphatase 1 regulatory subunit 3A	PPP1R3A	-0.45268	20.18666	2.14E-03	3.73E-02
abhydrolase domain containing 14B	ABHD14B	-0.46947	18.20301	4.06E-04	9.19E-03
karyopherin subunit beta 1	KPNB1	-0.47082	17.81223	5.44E-04	1.15E-02
eukaryotic translation elongation factor 1 beta 2	EEF1B2	-0.47465	21.07172	3.60E-04	8.41E-03
phosphorylase, glycogen, muscle	PYGM	-0.48151	24.66872	2.73E-03	4.36E-02
phosphoglucomutase 1	PGM1	-0.50641	23.18993	5.29E-06	2.67E-04
calcium voltage-gated channel auxiliary subunit beta 1	CACNB1	-0.52531	19.0859	6.42E-05	2.12E-03
quinoid dihydropteridine reductase	QDPR	-0.54496	20.10354	1.17E-04	3.55E-03
bisphosphoglycerate mutase	BPGM	-0.54818	16.75452	6.22E-04	1.29E-02
aldehyde dehydrogenase 1 family member L1	ALDH1L1	-0.55509	19.51926	3.95E-05	1.46E-03
WD repeat domain 44	WDR44	-0.55894	15.0234	4.73E-04	1.02E-02
unc-45 myosin chaperone B	UNC45B	-0.55998	20.34457	9.41E-04	1.85E-02
glucose-6-phosphate isomerase	GPI	-0.56186	23.22389	2.22E-03	3.74E-02
LDL receptor related protein associated protein 1	LRPAP1	-0.56668	16.90396	1.56E-04	4.31E-03
pyruvate kinase, muscle	PKM	-0.56706	24.57778	4.25E-04	9.48E-03
chloride intracellular channel 5	CLIC5	-0.57425	17.60242	5.26E-04	1.12E-02
protein phosphatase 3 regulatory subunit B, alpha	PPP3R1	-0.57961	18.75103	1.48E-05	6.39E-04
syntrophin beta 1	SNTB1	-0.58958	18.57457	9.33E-04	1.85E-02
carboxymethylenebutenolidase homolog	CMBL	-0.59946	21.01549	1.49E-04	4.31E-03
calsequestrin 1	CASQ1	-0.61754	23.22241	5.91E-06	2.89E-04
glutaredoxin	GLRX	-0.61982	16.87863	1.64E-03	2.95E-02
cordon-bleu WH2 repeat protein	COBL	-0.62592	16.95584	2.16E-04	5.65E-03
calpain 1	CAPN1	-0.65384	17.63091	1.16E-03	2.17E-02

calcium voltage-gated channel subunit alpha1 S	CACNA1S	-0.6564	16.43761	1.03E-05	4.73E-04
phosphoglycerate mutase 2	PGAM2	-0.67082	25.12976	2.38E-07	1.90E-05
protein phosphatase 3 catalytic subunit alpha	PPP3CA	-0.71534	17.05611	9.15E-05	2.89E-03
aldolase, fructose-bisphosphate A	ALDOA	-0.71992	25.80808	2.35E-06	1.27E-04
leucine rich repeat containing 20	LRRC20	-0.72349	18.53058	2.56E-03	4.13E-02
protein phosphatase 3 catalytic subunit beta	PPP3CB	-0.73023	16.80377	4.94E-07	3.56E-05
myozenin 3	MYOZ3	-0.73578	19.54415	2.17E-03	3.74E-02
phosphorylase kinase regulatory subunit alpha 1	PHKA1	-0.77279	18.86648	3.85E-04	8.83E-03
phosphorylase kinase regulatory subunit beta	PHKB	-0.78076	19.26296	3.09E-05	1.17E-03
glyceraldehyde-3-phosphate dehydrogenase	GAPDH	-0.78917	26.629	2.10E-08	1.87E-06
glycerol-3-phosphate dehydrogenase 1	GPD1	-0.82743	22.51647	1.53E-08	1.45E-06
phosphorylase kinase catalytic subunit gamma 1	PHKG1	-0.83917	18.3265	1.62E-03	2.95E-02
phosphofructokinase, muscle	PFKM	-0.87614	23.30436	1.02E-06	6.70E-05
enolase 3	ENO3	-0.93079	25.86054	2.52E-09	3.97E-07
fructose-bisphosphatase 2	FBP2	-0.95082	21.79191	1.71E-06	1.04E-04
phosphoglycerate kinase 1	PGK1	-0.95297	24.80978	1.38E-09	2.62E-07
nicotinamide nucleotide adenyltransferase 1	NMNAT1	-1.00679	14.91277	6.26E-07	4.32E-05
CD38 molecule	CD38	-1.02909	15.29989	2.51E-05	1.05E-03
lactate dehydrogenase A	LDHA	-1.03565	23.37492	1.17E-05	5.22E-04
ATPase sarcoplasmic/endoplasmic reticulum Ca <sup>2+</sup> transporting 1	ATP2A1	-1.06432	24.334	1.56E-06	9.84E-05
adenylate kinase 1	AK1	-1.08148	23.4138	5.57E-09	7.04E-07
glycerol-3-phosphate dehydrogenase 2	GPD2	-1.13718	17.58765	4.81E-07	3.56E-05
inositol polyphosphate-1-phosphatase	INPP1	-1.13995	15.89397	2.34E-06	1.27E-04
PDZ and LIM domain 7	PDLIM7	-1.25464	18.583	2.93E-05	1.16E-03
myosin light chain 1	MYL1	-1.38316	26.46139	1.56E-11	7.88E-09
myosin heavy chain 2	MYH2	-1.42716	28.55243	2.88E-09	3.97E-07
tropomyosin 1	TPM1	-1.5956	24.99201	4.90E-05	1.65E-03
actinin alpha 3	ACTN3	-1.77867	23.1772	2.56E-05	1.05E-03
troponin T3, fast skeletal type	TNNT3	-1.96642	24.33804	1.22E-11	7.88E-09
myosin light chain, phosphorylatable, fast skeletal muscle	MYLPP	-2.14491	26.16793	3.14E-15	4.75E-12
troponin C2, fast skeletal type	TNNC2	-2.2117	24.14638	6.59E-09	7.69E-07
troponin I2, fast skeletal type	TNNI2	-2.23687	24.16901	1.42E-10	4.99E-08

## Differentially Expressed Proteins Annotated in SIT POST – Type I compared to Type II Fibres

Description	SYMBOL	logFC	AveExpr	P.Value	adj.P.Val
myosin light chain 3	MYL3	1.565172	25.33432	4.42E-08	1.34E-05
myosin heavy chain 7	MYH7	1.458916	27.78824	1.70E-08	6.46E-06
PDZ and LIM domain 1	PDLIM1	1.433388	19.805	1.37E-07	2.94E-05
troponin T1, slow skeletal type	TNNT1	1.378368	23.18153	3.45E-07	4.75E-05
myozenin 2	MYOZ2	1.350951	20.97949	2.57E-04	9.52E-03
myosin light chain 2	MYL2	1.242558	25.67884	2.53E-07	3.83E-05
isopentenyl-diphosphate delta isomerase 2	IDI2	1.180007	18.41265	4.04E-05	2.55E-03
ATPase sarcoplasmic/endoplasmic reticulum Ca <sup>2+</sup> transporting 2	ATP2A2	1.175394	22.32439	4.57E-06	4.00E-04
dihydropyrimidinase like 3	DPYSL3	1.038539	19.35748	1.52E-07	2.94E-05
lactate dehydrogenase B	LDHB	0.982815	20.96691	3.09E-04	1.07E-02
cytochrome b5 reductase 1	CYB5R1	0.891613	21.19349	1.48E-06	1.73E-04
calsequestrin 2	CASQ2	0.804871	21.3872	4.65E-04	1.47E-02
ankyrin repeat domain 2	ANKRD2	0.747395	21.79186	2.65E-04	9.57E-03
branched chain keto acid dehydrogenase E1 subunit beta	BCKDHB	0.724525	12.79514	8.63E-04	2.30E-02
myomesin 3	MYOM3	0.694651	22.16595	3.38E-06	3.34E-04
monoamine oxidase B	MAOB	0.634335	19.1476	2.03E-04	8.33E-03
aldehyde dehydrogenase 7 family member A1	ALDH7A1	0.596441	18.17868	1.55E-03	3.63E-02
carbonic anhydrase 3	CA3	0.58397	24.78727	2.37E-04	9.21E-03
thiosulfate sulfurtransferase coenzyme Q8A	TST	0.548568	18.78854	1.32E-04	6.08E-03
enoyl-CoA hydratase 1	ECH1	0.5252	20.60774	6.87E-04	1.94E-02
glycerol-3-phosphate dehydrogenase 1-like	GPD1L	0.523316	20.20083	4.83E-05	2.78E-03
isocitrate dehydrogenase 2	IDH2	0.513877	23.27245	7.59E-04	2.09E-02
malate dehydrogenase 1	MDH1	0.502002	23.3668	4.82E-05	2.78E-03
hydroxyacyl-CoA dehydrogenase/3-ketoacyl-CoA thiolase/enoyl-CoA hydratase	HADHA	0.50137	23.53946	6.85E-05	3.58E-03
succinate-CoA ligase GDP-forming beta subunit	SUCLG2	0.489348	20.79708	1.23E-03	3.05E-02
enoyl-CoA delta isomerase 2	ECI2	0.47687	20.33485	3.95E-04	1.30E-02
hydroxyacyl-CoA dehydrogenase/3-ketoacyl-CoA thiolase/enoyl-CoA hydratase	HADHB	0.468113	22.73727	6.09E-04	1.85E-02
sulfite oxidase	SUOX	0.46482	16.50016	2.02E-03	4.37E-02
myotilin	MYOT	0.453433	22.69717	1.25E-03	3.05E-02

aldehyde dehydrogenase 5 family member A1	ALDH5A1	0.44682	20.90843	2.34E-04	9.21E-03
voltage dependent anion channel 1	VDAC1	0.412629	22.59442	6.89E-04	1.94E-02
serpin family B member 6	SERPINB6	0.396894	19.52305	1.51E-03	3.58E-02
aldehyde dehydrogenase 1 family member A1	ALDH1A1	0.391702	20.63843	3.06E-04	1.07E-02
	ALDH2	0.354017	20.35776	1.88E-03	4.20E-02
mercaptopyruvate sulfurtransferase	MPST	0.342728	18.46571	1.38E-03	3.31E-02
dihydrolipoamide dehydrogenase	DLD	0.325192	21.45767	2.52E-04	9.52E-03
bridging integrator 1	BIN1	-0.29381	22.28597	2.06E-03	4.40E-02
calcium binding protein 39	CAB39	-0.35026	18.32842	5.01E-04	1.55E-02
phosphoglycerate mutase 2	PGAM2	-0.36746	25.12976	1.11E-03	2.80E-02
protein phosphatase 3 catalytic subunit beta	PPP3CB	-0.39623	16.80377	1.70E-03	3.90E-02
glycerol-3-phosphate dehydrogenase 1	GPD1	-0.48083	22.51647	1.41E-04	6.26E-03
pyruvate kinase, muscle	PKM	-0.48624	24.57778	8.47E-04	2.29E-02
glyceraldehyde-3-phosphate dehydrogenase	GAPDH	-0.50485	26.629	3.88E-05	2.55E-03
glucose-6-phosphate isomerase	GPI	-0.50718	23.22389	2.37E-03	4.92E-02
protein phosphatase 3 regulatory subunit B, alpha	PPP3R1	-0.51658	18.75103	2.08E-05	1.50E-03
calsequestrin 1	CASQ1	-0.51939	23.22241	2.40E-05	1.65E-03
cordon-bleu WH2 repeat protein	COBL	-0.52291	16.95584	6.26E-04	1.86E-02
fructose-bisphosphatase 2	FBP2	-0.53917	21.79191	1.93E-03	4.23E-02
aldolase, fructose-bisphosphate A	ALDOA	-0.54508	25.80808	6.22E-05	3.37E-03
C-terminal binding protein 1	CTBP1	-0.56043	15.54993	1.04E-04	5.09E-03
aldehyde dehydrogenase 1 family member L1	ALDH1L1	-0.56406	19.51926	5.47E-06	4.36E-04
unc-45 myosin chaperone B	UNC45B	-0.59028	20.34457	1.46E-04	6.31E-03
phosphorylase kinase regulatory subunit alpha 1	PHKA1	-0.59825	18.86648	2.27E-03	4.78E-02
phosphofructokinase, muscle	PFKM	-0.62638	23.30436	8.16E-05	4.12E-03
glycerol-3-phosphate dehydrogenase 2	GPD2	-0.64555	17.58765	1.04E-03	2.67E-02
enolase 3	ENO3	-0.65071	25.86054	1.92E-06	2.08E-04
eukaryotic translation initiation factor 4E	EIF4E	-0.67984	16.51946	4.95E-05	2.78E-03
ATPase sarcoplasmic/endoplasmic reticulum Ca <sup>2+</sup> transporting 1	ATP2A1	-0.68616	24.334	4.41E-04	1.42E-02
phosphoglycerate kinase 1	PGK1	-0.73004	24.80978	1.55E-07	2.94E-05
adenylate kinase 1	AK1	-0.74259	23.4138	4.75E-06	4.00E-04
PDZ and LIM domain 7	PDLIM7	-0.82962	18.583	1.88E-03	4.20E-02
	NIBAN1	-0.88572	17.64205	1.56E-04	6.58E-03
lactate dehydrogenase A	LDHA	-0.95981	23.37492	8.17E-06	6.19E-04
myosin light chain 2	MYL1	-1.04476	26.46139	6.46E-09	3.31E-06

myosin heavy chain 1	MYH2	-1.07614	28.55243	4.02E-07	5.08E-05
S100 calcium binding protein A13	S100A13	-1.15649	18.90777	3.40E-04	1.15E-02
tropomyosin 1	TPM1	-1.15951	24.99201	9.70E-04	2.54E-02
troponin I2, fast skeletal type	TNNI2	-1.38703	24.16901	3.53E-06	3.34E-04
actinin alpha 3	ACTN3	-1.47031	23.1772	1.13E-04	5.38E-03
troponin T3, fast skeletal type	TNNT3	-1.47464	24.33804	6.56E-09	3.31E-06
myosin light chain, phosphorylatable, fast skeletal muscle	MYLPF	-1.64495	26.16793	3.78E-12	5.73E-09
troponin C2, fast skeletal type	TNNC2	-1.76253	24.14638	2.12E-07	3.57E-05

## Differentially Expressed Proteins Annotated in SIT PRE– Type I compared to Type II Fibres

Gene Description	SYMBOL	logFC	AveExpr	P.Value	adj.P.Val
myosin light chain 3	MYL3	1.973454	7.548347	3.44E-11	15.18498
mysosin heavy chain 7	MYH7	1.818958	7.73312	1.44E-11	16.01988
myosin light chain 2	MYL2	1.806439	8.117467	2.33E-12	17.76701
ATPase sarcoplasmic/endoplasmic reticulum Ca <sup>2+</sup> transporting 2	ATP2A2	1.761198	7.318743	1.01E-10	14.15319
PDZ and LIM domain 1	PDLIM1	1.698239	6.785573	1.19E-09	11.78771
isopentenyl-diphosphate delta isomerase 2	IDI2	1.439044	5.271312	9.21E-07	5.43212
troponin T1, slow skeletal type	TNNT1	1.431791	5.724213	1.35E-07	7.261297
myozenin 2	MYOZ2	1.326558	3.740826	3.22E-04	-0.08199
lactate dehydrogenase B	LDHB	1.308777	5.002675	2.78E-06	4.383769
dihydropyrimidinase like 3	DPYSL3	1.267036	6.957789	5.38E-10	12.54649
aldo-keto reductase family 1 member C2	AKR1C2	1.132362	3.337241	1.23E-03	-1.31761
cytochrome b5 reductase 1	CYB5R1	0.968462	5.607109	2.23E-07	6.781458
calsequestrin 2	CASQ2	0.929426	4.199702	6.27E-05	1.444541
perilipin 5	PLIN5	0.918884	3.845186	2.24E-04	0.254295
aldehyde dehydrogenase 7 family member A1	ALDH7A1	0.862369	4.723761	8.48E-06	3.32782
glutamic-pyruvic transaminase 2	GPT2	0.685101	3.365764	1.12E-03	-1.2338
NADH:ubiquinone oxidoreductase subunit B3	NDUFB3	0.675446	3.291739	1.42E-03	-1.45016
fatty acid binding protein 3	FABP3	0.643684	3.115874	2.46E-03	-1.94898
carbonic anhydrase 3	CA3	0.569494	3.738563	3.25E-04	-0.08921
cell division cycle 42	CDC42	0.563013	3.371494	1.10E-03	-1.2169
myomesin 3	MYOM3	0.536168	3.828048	2.38E-04	0.198616
cytochrome b5 reductase 3	CYB5R3	0.533064	3.231527	1.72E-03	-1.62337
RAB21, member RAS oncogene family	RAB21	0.528657	3.38366	1.06E-03	-1.18093
acyl-CoA dehydrogenase, C-2 to C-3 short chain	ACADS	0.524439	3.397717	1.01E-03	-1.13926
voltage dependent anion channel 1	VDAC1	0.52413	4.470331	2.27E-05	2.39974
proteasome 26S subunit, non-ATPase 3	PSMD3	0.520437	3.205008	1.87E-03	-1.69887
mercaptopyruvate sulfurtransferase	MPST	0.483612	4.664294	1.07E-05	3.107267
oxoglutarate dehydrogenase	OGDH	0.47506	3.174708	2.05E-03	-1.78452
mitochondrial ribosomal protein S22	MRPS22	0.463594	3.386597	1.05E-03	-1.17224
enoyl-CoA delta isomerase 2	ECI2	0.456854	3.530482	6.56E-04	-0.73917
hydroxyacyl-CoA dehydrogenase/3-ketoacyl-CoA thiolase/enoyl-CoA hydratase	HADHA	0.45127	3.762134	2.99E-04	-0.01387
hydroxyacyl-CoA dehydrogenase/3-ketoacyl-CoA thiolase/enoyl-CoA hydratase	HADHB	0.448915	3.410662	9.72E-04	-1.10076

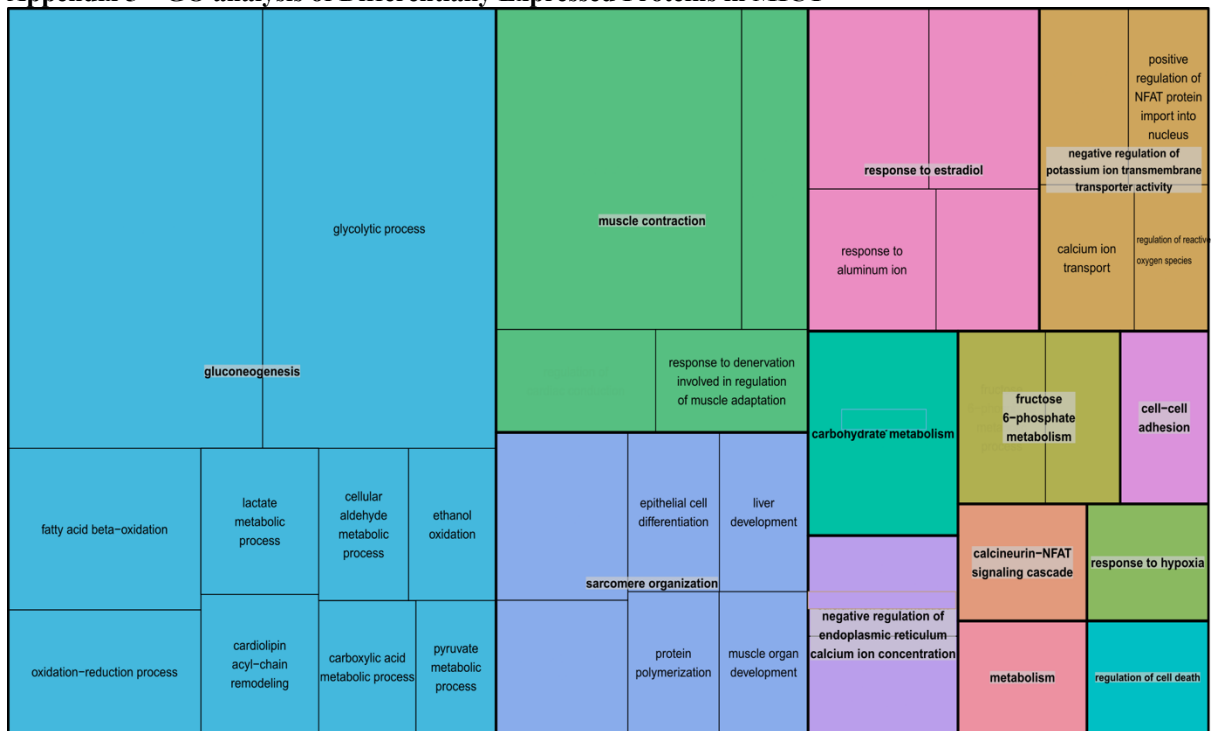
acyl-CoA dehydrogenase, short/branched chain	ACADSB	0.448454	3.721143	3.45E-04	-0.14467
DnaJ heat shock protein family	DNAJA4	0.423049	3.411623	9.69E-04	-1.0979
	ALDH2	0.412766	3.738146	3.25E-04	-0.09054
voltage dependent anion channel 2	VDAC2	0.393893	3.215777	1.81E-03	-1.66827
tyrosine 3-monooxygenase/tryptophan 5-monooxygenase activation protein zeta	YWHAZ	0.375677	4.771634	7.02E-06	3.506574
dihydrolipoamide dehydrogenase	DLD	0.357114	4.190062	6.50E-05	1.411235
LIM and cysteine rich domains 1	LMCD1	0.354511	3.217464	1.80E-03	-1.66347
prolyl endopeptidase	PREP	-0.36333	-3.93186	1.65E-04	0.538565
phosphoglucomutase 1	PGM1	-0.38331	-4.03732	1.13E-04	0.890409
phosphoglycerate mutase 2	PGAM2	-0.41288	-3.79084	2.71E-04	0.07833
pyruvate kinase, muscle	PKM	-0.46074	-3.27521	1.50E-03	-1.49797
protein phosphatase 3 catalytic subunit beta	PPP3CB	-0.46316	-3.78652	2.75E-04	0.064439
calsequestrin 1	CASQ1	-0.46885	-4.02651	1.18E-04	0.854055
protein phosphatase 3 catalytic subunit alpha	PPP3CA	-0.49306	-3.11005	2.51E-03	-1.96514
protein phosphatase 3 regulatory subunit B, alpha	PPP3R1	-0.50066	-4.3593	3.46E-05	2.003202
bisphosphoglycerate mutase	BPGM	-0.50359	-3.58861	5.40E-04	-0.56037
phosphorylase, glycogen, muscle	PYGM	-0.51757	-3.64841	4.42E-04	-0.37419
	PAK1	-0.51803	-3.32733	1.27E-03	-1.34659
coiled-coil domain containing 124	CCDC124	-0.52357	-4.47526	2.23E-05	2.41749
phosphoglycerate kinase 1	PGK1	-0.52808	-4.12124	8.36E-05	1.174965
nicotinamide nucleotide adenylyltransferase 1	NMNAT1	-0.55171	-3.23729	1.69E-03	-1.60689
aldolase, fructose-bisphosphate A	ALDOA	-0.55199	-4.25941	5.03E-05	1.651944
FK506 binding protein 1A	FKBP1A	-0.58087	-3.80438	2.59E-04	0.122004
glycerol-3-phosphate dehydrogenase 1	GPD1	-0.59596	-4.935	3.65E-06	4.124385
phosphorylase kinase regulatory subunit beta	PHKB	-0.61112	-3.78363	2.78E-04	0.055135
fructose-bisphosphatase 2	FBP2	-0.61315	-3.63748	4.58E-04	-0.40837
unc-45 myosin chaperone B	UNC45B	-0.63455	-4.26942	4.84E-05	1.686906
enolase 3	ENO3	-0.63755	-4.99488	2.87E-06	4.353793
glyceraldehyde-3-phosphate dehydrogenase	GAPDH	-0.6537	-5.61055	2.20E-07	6.795483
dynein light chain LC8-type 2	DYNLL2	-0.66645	-4.37434	3.27E-05	2.056543
phosphofructokinase, muscle	PFKM	-0.67073	-4.42471	2.70E-05	2.236041
glycerol-3-phosphate dehydrogenase 2	GPD2	-0.68176	-3.58331	5.50E-04	-0.57679
phosphorylase kinase regulatory subunit alpha 1	PHKA1	-0.73998	-3.89098	1.91E-04	0.403938
adenylate kinase 1	AK1	-0.84236	-5.52977	3.11E-07	6.467081
dimethylarginine dimethylaminohydrolase 1	DDAH1	-0.85285	-3.39414	1.03E-03	-1.14988

lactate dehydrogenase A	LDHA	-0.87674	-4.32809	3.89E-05	1.892872
myosin light chain 1	MYL1	-0.94439	-5.80261	9.61E-08	7.585037
myosin heavy chain 2	MYH2	-0.9984	-5.07892	2.04E-06	4.678304
PDZ and LIM domain 1	PDLIM7	-1.00944	-3.90178	1.84E-04	0.439411
mitochondrial ribosomal protein S22	TPM1	-1.13489	-3.3422	1.21E-03	-1.30308
troponin T3, fast skeletal type	TNNT3	-1.31923	-5.73992	1.26E-07	7.325989
myosin light chain, phosphorylatable, fast skeletal muscle	MYLPF	-1.50852	-7.35819	8.38E-11	14.32994
troponin C2, fast skeletal type	TNNC2	-1.72969	-5.52009	3.24E-07	6.427903
troponin I2, fast skeletal type	TNNI2	-1.73359	-6.18512	1.79E-08	9.191007

## Differentially Expressed Proteins Annotated in MICT PRE– Type I compared to Type II Fibres

Description	SYMBOL	logFC	AveExpr	P.Value	adj.P.Val
myozenin 2	MYOZ2	1.766319	20.97949	1.11E-05	0.008431
troponin T1, slow skeletal type	TNNT1	1.116418	23.18153	6.97E-05	0.015095
myosin heavy chain 7	MYH7	1.073336	27.78824	4.94E-05	0.014967
myosin light chain 3	MYL3	1.049057	25.33432	3.13E-04	0.028009
myosin light chain 2	MYL2	1.035877	25.67884	3.58E-05	0.014456
ATPase sarcoplasmic/endoplasmic reticulum Ca <sup>2+</sup> transporting 2	ATP2A2	0.904193	22.32439	6.99E-04	0.048655
cytochrome b5 reductase 1	CYB5R1	0.8009	21.19349	3.81E-05	0.014456
dihydropyrimidinase like 3	DPYSL3	0.785421	19.35748	1.16E-04	0.020628
kelch like family member 40	KLHL40	0.636395	18.40065	3.07E-04	0.028009
dihydrolipoamide branched chain transacylase E2	DBT	0.594052	17.34607	1.31E-04	0.020628
DnaJ heat shock protein family	DNAJA4	0.489219	17.69229	3.88E-04	0.03174
phosphoglucomutase 1	PGM1	-0.40502	23.18993	1.36E-04	0.020628
protein phosphatase 3 regulatory subunit B, alpha	PPP3R1	-0.43407	18.75103	6.53E-04	0.048655
aldolase, fructose-bisphosphate A	ALDOA	-0.48465	25.80808	7.38E-04	0.048655
aldehyde dehydrogenase 1 family member L1	ALDH1L1	-0.48882	19.51926	1.73E-04	0.021846
glyceraldehyde-3-phosphate dehydrogenase	GAPDH	-0.52399	26.629	6.20E-05	0.015095
pyruvate kinase, muscle	PKM	-0.5905	24.57778	1.71E-04	0.021846
myosin light chain 1	MYL1	-0.6408	26.46139	3.98E-04	0.03174
basigin	BSG	-0.78623	17.65773	2.79E-06	0.004234
myosin light chain, phosphorylatable, fast skeletal muscle	MYLPF	-0.83318	26.16793	2.65E-04	0.028009
troponin T3, fast skeletal type	TNNT3	-0.86238	24.33804	7.11E-04	0.048655
nucleobindin 1	NUCB1	-1.02526	15.80127	3.14E-04	0.028009
troponin C2, fast skeletal type	TNNC2	-1.27084	24.14638	2.72E-04	0.028009

## Appendix 5 – GO analysis of Differentially Expressed Proteins in MICT



The differentially expressed proteins induced by MICT depicted as a treemap of enriched biological processes. The most enriched biological processes (based on statistical likelihood) are shown as larger components within the map and grouped according to common cellular functions. Gene ontology determined using DAVID (137) treemap constructed using REVIGO (306).

## Appendix 6

### Summary in Changes of OXPHOS Complex Proteins in the Mitochondrial Fraction of Single Fibre Samples\*

	MICT		SIT		
	$\nabla \bar{z}$ -Score	$\nabla$ Summary	$\nabla \bar{z}$ -Score	$\nabla$ Summary	
CI	0.348	↑	-0.261	↓	<b>Type I</b>
CII	0.601	↑	-0.076	↓	
CIII	0.254	↑	-0.119	↓	
CIV	0.257	↑	-0.478	↓	
CV	0.392	↑	-0.006	↔	
Mitochondrial Ribosomes	0.434	↑	-0.123	↓	

	MICT		SIT		
	$\nabla \bar{z}$ -Score	$\nabla$ Summary	$\nabla \bar{z}$ -Score	$\nabla$ Summary	
CI	-0.012	↔	-0.165	↓	<b>Type II</b>
CII	0.087	↑	-0.091	↓	
CIII	-0.019	↔	-0.309	↓	
CIV	-0.066	↓	-0.469	↓	
CV	-0.145	↓	-0.065	↓	
Mitochondrial Ribosomes	0.141	↑	-0.175	↓	

- \* Increase - ↑ ( $z > 0.05$ )  
 No Change - ↔ ( $-0.05 > z < 0.05$ )  
 Decrease - ↓ ( $z < -0.05$ )  
 $\nabla \bar{z}$ -Score – Change in mean z-score